12-2023

Feasibility of Using High-Alkali Natural Pozzolans and Reclaimed Fly Ash as Alternative Supplementary Cementitious Materials in Concrete

Weiqi Wang
weiqi@g.clemson.edu

FEASIBILITY OF USING HIGH-ALKALI NATURAL POZZOLANS AND RECLAIMED FLY ASH AS ALTERNATIVE SUPPLEMENTARY CEMENTITIOUS MATERIALS IN CONCRETE

A Dissertation
Presented to
the Graduate School of
Clemson University

In Partial Fulfillment
of the Requirements for the Degree
Doctor of Philosophy
Civil Engineering

by
Weiqi Wang
December 2023

Accepted by:
Dr. Prasad Rangaraju, Committee Chair
Dr. Amir Poursaee
Dr. Qiushi Chen
Dr. Colin McMillen

ABSTRACT

The growing scarcity of conventional supplementary cementitious materials (SCMs) such as Class F and Class C fly ashes and slag has necessitated exploring alternative SCMs that were previously considered suboptimal. In particular, high-alkali SCMs are often avoided because of the potential concern that their alkali content could release into the concrete pore solution, thus exacerbating the potential for alkali-silica reaction (ASR). This study aims to investigate the feasibility of using high-alkali SCMs, such as high-alkali natural pozzolans and reclaimed fly ashes, as alternative SCMs in the concrete industry by characterizing their pozzolanic reactivity and evaluating the potential to mitigate alkali-silica reaction and improve other durability characteristics of concrete.

In this study, the ASR mitigation performance of eight high-alkali SCMs was evaluated using the accelerated mortar bar test (AMBT, ASTM C1567), concrete prism test (CPT, ASTM C1293), and the miniature concrete prism test (MCPT, AASHTO T380). In these tests, a reactive siliceous argillite aggregate was used. Even though specimens containing SCMs lowered ASR expansion significantly compared to the control sample, the results from different tests yielded different outcomes on the level of ASR mitigation offered by these SCMs based on the expansion threshold limits established in the literature. All test specimens containing a 20% dosage of high-alkali SCMs were found to be effective, i.e., passed in the ASTM C1567 test, but all of them failed in the ASTM C1293 test. Also, the majority of the SCMs failed in the AASHTO T380 test. However, compared to control, these SCMs effectively lowered ASR expansion. The study also evaluated the influence of different replacement levels (20%, 30% and 40% cement replacement levels) of SCMs on the ASR mitigation performance, and the results showed that when sufficient dosage of

high-alkali SCMs was used, all the SCMs were found to be effective in mitigating ASR in all the test methods.

In this study, different pozzolanic reactivity test methods were conducted to investigate the pozzolanic reactivity of high-alkali SCMs and identify any mechanism that promoted their ASR mitigation effectiveness. It was found from this study that the reactivity of SCMs, as measured by the strength activity index (ASTM C311) or the R3 test (ASTM C1897), did not correlate well with the ASR mitigation performance of high-alkali SCMs. The calcium hydroxide content obtained from the thermogravimetric analysis (TGA) and the alkali content of pore solution measured using inductively coupled plasma of mixtures containing SCMs showed a significant correlation with the ASR mitigation performance of SCMs. Pore solution analysis also indicated that not all of the alkalies from SCMs were released into the pore solution. Some lower alkali SCMs were found to release more alkali ions into the pore solution than SCMs with high alkali content.

This study also assessed the impact of high-alkali SCMs on other concrete durability properties, including drying shrinkage (ASTM C596), sulfate resistance (ASTM C1012), chloride ion permeability (ASTM C1202), and bulk and surface electrical resistivity (ASTM C1876). The results showed that using high-alkali SCMs improved concrete resistance to sulfate attack, decreased concrete permeability, and increased concrete electrical resistivity. These durability results also strongly correlated with the findings from the TGA study. The study also evaluated the potential impact of high-alkali SCMs on the hydration and early-age behavior of cementitious pastes with high-alkali SCMs using TGA, isothermal calorimetry, Vicat needle setting time, and ultrasonic pulse velocity. In these studies, it was found that the use of high-alkali SCMs did not cause any adverse impact on the setting and early-age strength-gain behavior of test mixtures. It

was also observed that finely ground high-alkali SCMs were found to have a filler effect in cementitious pastes, which accelerated the degree of hydration of cement, as observed from the TGA results.

Based on the results from this study, high-alkali SCMs, such as natural pozzolans and reclaimed fly ashes, are found to be valid alternatives to traditional SCMs for use in concrete, provided the alkalis present in these SCMs are not readily available for release into pore solution of concrete. Based on the findings from this study, it is recommended that pore solution expression and analysis from aged cementitious paste specimens be conducted to ascertain the alkali release nature of high-alkali SCMs at the desired dosage level, as these parameters correlate well with the ASR mitigation efficiency in concrete mixtures. Also, ASTM C1293 and AASHTO T380 test methods were found to be superior in their ability to assess the ASR mitigation performance of high-alkali SCMs, compared to the ASTM C1567 test. Also, the findings from this study confirm that pozzolanic reactivity of high-alkali SCMs as measured by ASTM C311 should not be used as a proxy for assessing the ASR mitigation efficiency of high-alkali SCMs.

Based on the findings from the evaluation of job concrete mixtures using the reactive siliceous argillite aggregate and high-alkali SCMs, this study confirms that an AASHTO T380-based testing protocol can effectively qualify concrete mixtures that are resistant to ASR distress.

DEDICATION

I dedicate this dissertation to my dearest parents, Mrs. Xiajun Lin and Mr. Yonghong Wang, who give me life, raised me, and supported me in chasing my dream. I also dedicate this to my loved girlfriend Zhonglin Feng who is patient to wait for me, and our love spanned the Pacific Ocean for six years. Also, I dedicate this to my cousins, uncle, aunt, and my dear grandma. At the last, I want to dedicate this to my deep love passed away Grandpa Mr. Zhuming Lin, who raised me and gave all his love to me.

ACKNOWLEDGEMENTS

I would like to express my greatest appreciation to all my Ph.D. committee members. My special gratitude goes to my Ph.D. advisor Dr. Prasad Rangaraju for selecting me as his student. Thank him for his training, support, guidance, and encouragement. These experiences have made me a better version of myself and have become a lifelong treasure that motivates me to progress and grow continually. I would also like to express my appreciation to my committee members Dr Amir Poursaee, Dr. Qiushi Chen, and Dr. Colin McMillen, who are willing to serve as my committee members and give me valuable suggestions.

I would also like to express appreciation to my SMaRT team members at Clemson University: Omar Amer, Abdul Basit Peerzada, Harish Konduru, Haripriya Nekkanti, James Roberts, Adam Biehl, Isaiah Conrad, and Kyle Maeger. I cannot make my PhD career work done without their help and support. Here I want to appreciate Omar Amer and James Roberts, especially. Thanks, Omar, for training me to be a qualified lab worker. Thanks, James, for helping me finish lots of research work.

At last, I would like to express my gratitude to every friend in my Clemson life. Thanks for their presence, which has allowed me to have a vibrant life in a foreign country.

TABLE OF CONTENTS

Content **Page**

LIST OF TABLES

Table **Page**

CHAPTER III

CHAPTER IV

CHAPTER V

CHAPTER VI

CHAPTER VII

CHAPTER VIII

APPEXDIX

LIST OF FIGURES

Figures **Page**

CHAPTER IV

CHAPTER V

CHAPTER VI

CHAPTER VII

CHAPTER VIII

CHAPTER I INTRODUCTION

1.1 Background

Fly ash is the primary SCM used in the concrete industry. However, due to global environmental policy changes, much of coal power has transitioned to using clean energy sources to reduce carbon emissions, resulting in the shortage of availability of high-quality fly ash and the resultant product price increases. Therefore, finding a sustainable alternative for the worldwide SCMs industry is urgent. High-alkali SCMs, whose alkali content is generally over 4%, are generally avoided in concrete due to concerns arising from the potential leaching of alkali ions into the pore solution and increase the alkali loading in the concrete pore solution, further exacerbating the ASR. However, some research indicated that alkali content in some SCMs exists as crystal phases, which are not readily released into the concrete pore solution. This finding provided the basis for this research study.

This study evaluated the feasibility of high-alkali SCMs used as alternative traditional SCMs in concrete. The study focused on the impact of high-alkali SCMs on concrete ASR mitigation performance and used different kinds of methods to explain how high-alkali SCMs are involved in the chemical reaction in the concrete matrix. Additionally, to obtain a comprehensive understanding of high-alkali SCMs on concrete, other concrete durability and fresh properties were conducted in this study.

1.2 Objectives

The principal objectives of this study:

- To investigate whether high-alkali natural pozzolans and reclaimed fly ash can be used in concrete as SCMs;
- To evaluate whether high-alkali SCMs can effectively mitigate alkali-silica reaction;
- To assess the correlation between available alkali and total alkali of high-alkali SCMs;
- To evaluate the pozzolanic reactivity of high-alkali SCMs and investigate the correlation between their alkali content and pozzolanic reactivity;
- How high-alkali SCMs impact cement-based matrix hydration performance;
- How high-alkali SCMs impact cement-based matrix durability

1.3 Scope of Research

To investigate the feasibility of using high-alkali SCMs as potential alternative materials to the global SCM market, six natural pozzolans (NPs) and two reclaimed fly ashes (RFAs) with high alkali content (>5%) were studied in this study. Three types of cement were used in this study: ASTM C150 Type I high-alkali cement (Na_2O_{eq} of 1%), ASTM C150 Type I/II low-alkali cement (Na_2O_{eq} of 0.38%), and Type IL cement. The reactive aggregate used in this study is a known reactive aggregate from Goldhill Quarry in North Carolina.

1.4 Summary of Research

To achieve the objectives of the research, the entire process consisted of five stages:

Stage I evaluated the ASR mitigation performance of high-alkali SCMs through various methods, including ASTM C1567 (AMBT), ASTM C1293 (CPT), and AASHTO T380 (MCPT). The parameters considered in this study include different test methods, SCMs replacement levels, and reactive aggregate size.

Stage II shows the evaluation of high-alkali SCMs' pozzolanic reactivity. Based on the preliminary ASR mitigation results conducted in Stage I, SCMs exhibited various performances even though they all have alkali content. Hence, Stage II wanted to explain the difference among SCMs in the ASR mitigation. The evaluation consisted of the materials' natural properties and chemical reaction performance in the cementitious matrix. The natural properties focused on SCMs crystallography, and a cementitious-based test measured chemical performance.

Stage III exhibits the high-alkali SCMs' impact on the other concrete durability properties besides ASR. Except for ASR, other concrete durability properties, such as sulfate resistance and chloride permeability, are also impacted by SCMs.

Stage IV examined the potential influence of high-alkali SCMs on the cementitious matrix's fresh properties and early-age hydration performance.

1.5 Outline of Research

This dissertation is divided into nine Chapters:

1. Chapter I introduces this research, including background, objectives, scope of research, summary of research, and outline of research;
2. Chapter II provides the relevant research related to this study, which was conducted previously;
3. Chapter III presents the materials and test methods employed in this research study.
4. Chapter IV presents the performance of high-alkali SCMs mitigating the alkali-silica reaction and the correlation between SCMs' alkali content measured by X-ray fluorescence and alkali ions concentration of cementitious paste pore solution.
5. Chapter V exhibits the pozzolanic reactivity of high-alkali SCMs measured by various pozzolanic reactivity methods and investigates the correlation between pozzolanic reactivity and their ASR mitigation performance.
6. Chapter VI shows the impact of high-alkali SCMs on concrete durability performance.
7. Chapter VII presents how high-alkali SCMs affect the cementitious-based matrix hydration performance.
8. Chapter VIII exhibits the job concrete mixtures evaluation for ASR by using AASHTO T380 (MCPT) and high-alkali SCMs.
9. Chapter IX presents the summary and conclusions of this research study.

CHAPTER II LITERATURE REVIEW

2.1 What is Supplementary Cementitious Materials

Supplementary cementitious materials (SCMs) are concrete mineral additives to improve fresh and hardened concrete properties. ASTM C618 divides SCMs into two primary categories: natural pozzolans and industrial by-products [1]. Natural pozzolans originate from volcanic activities (e.g., vitreous rhyolites, volcanic ash, pumice, volcanic tuffs) and some sedimentary clays and shales. Some natural pozzolans (e.g., calcined clays) can be used in the concrete directly, but some of them must be preconditioned by thermal activation. Industrial by-products are produced from industrial activities like coal combustion and steelmaking. The typical by-products used in the concrete industry are fly ash, silica fume, and slag.

Generally, SCMs are finely amorphous (less crystallized), siliceous, or aluminous materials, and they can chemically react with calcium hydroxide (CH) at ordinary temperature to form calcium silicate hydrate (C-S-H) and calcium aluminate silicate hydrate (C-A-S-H) [2]. This reaction is also referred to as the pozzolanic reaction, and the ability of SCMs to consume CH is the pozzolanic reactivity [3]. Utilizing pozzolanic reaction has a rich historical legacy dating back to Ancient Rome’s concrete infrastructures like the Pantheon [4]. The significance of pozzolanic reaction for concrete is that it increases the concrete's durability. CH and C-S-H are the two primary cement hydration products [5]. However, in contrast to C-S-H, CH plays a limited role in enhancing compressive strength but is significantly implicated in various deteriorative chemical reactions that can harm the integrity of the concrete [6]–[8]. Therefore, incorporating SCMs into concrete can enhance various properties compared to 100% cement-base concrete, and these improvements encompass [9]:

1. Decrease the permeability;

2. Delay the ettringite formation;
3. Increase resistance to sulfate attacks;
4. Increase resistance to acid attacks;
5. Increase frost resistance;
6. Increase resistance to abrasion;
7. Prevent carbonation;
8. Prevent chloride ingress;
9. Mitigate alkali-silica reaction;
10. Mitigate corrosion

2.2 How SCMs Impact Concrete Properties

2.2.1 Fresh Properties

2.2.1.1 Flow Behavior

SCMs can have a significant impact on the flow behavior of concrete mixes. The flow behavior of concrete mixes, often called workability, is a crucial property that determines how efficiently and effectively the concrete is to be mixed, placed and finished.

Some SCMs indicate the ability to increase the workability of concrete due to their electric charge and microstructure [10]. The Portland cement surface only has negatives, but SCMs could simultaneously have positive and negative charges. The positive end of SCMs can attract the negative charges of cement, preventing cement particles from flocculating. Therefore, the cement particle is widely dispersed in the matrix system and has more surface contact with water. This new hydration matrix phase will reduce the water demand for reaching the required workability. Another mechanism for SCMs to increase workability is the microstructure. Some SCMs have smooth spherical shapes, which reduces the friction force at the interface between cement paste and aggregate. This behavior is also referred to as the " ball-bearing effect [10].

However, some SCMs possess the opposite impact on concrete workability. The primary reason for SCMs to decrease concrete workability is their high amount of loss on ignition (LOI) content. LOI content is the sample's residue mass after being heated to a high temperature, and generally, the LOI content of SCMs is the unburnt carbon content [11]. The high LOI impacts the water demand for concrete: 4% in LOI would require about 5% more water to account for the slump reduction of the concrete [12]. Besides increasing the demand, other risks of utilizing high LOI SCMs in concrete are reducing the strength, increasing the porosity and permeability, and increasing the demand for chemical admixtures, such as air-entraining agents [11], [13].

2.2.2.2 Setting Time

The setting time of cement is the time between the cement paste change from a fluid workable state to a solid rigid state. During the process, the cement paste gradually loses its plasticity as the cement hydration progresses. There are two setting times associated with cement: the initial and final setting times. The initial setting time is defined as when cement starts to harden and lose its plasticity, and the final setting time is when the cement completely loses its plasticity and gains strength.

The substitutions of SCMs in the cementitious mixture can chemically and physically complicate the cement hydration process. It thus can delay or accelerate the setting time cement, which depends on various factors such as the SCMs' chemical composition and particle size distribution. Juenger et al. [14] indicated that the SCMs replacing cement in the concrete delayed the setting time and low early strength. The problem could be intensified by being placed in a cold environment and containing the chemical admixtures. The primary reason some SCMs delay the setting time, especially natural pozzolans, is their high ignition (LOI) content loss. The unburned calcium content of SCMs can retard the cement hydration process. However, this does not mean all the SCMs delay the setting time. Some SCMs, with low LOI content and fine particle sizes, can play the role of the fillers in the mixtures [15]. These SCMs can provide the heterogeneous nucleation of C-S-H on the filler surface, as there is a clear dependence on the surface provided by the SCM particles [16], [17]. The increase in nucleation sites could accelerate the cement hydration rate[18]

2.2.3 Strength

Strength is an essential indicator of evaluating the pozzolanic reactivity of SCMs. The pozzolanic reactivity helps to convert the CH to C-S-H. With more C-S-H appearing in the

concrete, it is expected to give the concrete more strength. However, considering the dilution effect of replacing cement with SCMs, less cement participating in the cement hydration process further produces less C-S-H. Therefore, the strength of concrete that incorporates SCMs depends on the balance of pozzolanic reaction and cement dilution effect.

Also, other factors of SCMs impact the concrete strength values, including the types, chemical composition, and particle sizes of SCMs. For example, GBFS and high calcium FA were regarded as SCMs with high activity; silicate FA and steel slag were seen as SCMs with low activity; quartz and limestone powders were mainly considered inert fillers[19]. Also, the cement blended with high-activity SCMs produces a higher strength than the low-activity SCMs or filler effects.

2.2.4 Durability Properties

2.2.4.1 Drying Shrinkage

Drying shrinkage is one concern of concrete durability issues. The mechanism of drying shrinkage is the volume decrease of hardened concrete due to the loss of moisture from the capillary pore structure, which results in the capillary pressure of inner concrete. When the shrinkage pressure exceeds the tensile strength of the concrete, cracks probably appear. The occurrence of shrinkage cracks increases the risk of deleterious content intrusion into the concrete and further leads to other concrete issues, like alkali-silica reaction, sulfate attack, and corrosion.

Sakthivel et al. [20] studied drying shrinkage tests over 2.5 years on concrete with various mixing proportions, including cement, fly ash, and slag. Their results indicated that there was no significant difference among groups. However, the ultra-high-performance concrete research conducted by Li [21] stated that the addition of fly ash and silica fume increased the drying shrinkage compared to ordinary cement concrete, which was caused by the increased capillary

pressure due to the reined micropore structure [22]. Meanwhile, the binary use of the meta-kaolin and cement decreased the drying shrinkage compared to the control, which was explained by the reduced rate of water loss in the presence of meta-kaolin[23].

2.2.4.2 Sulfate Resistance

Sulfate attack is another concrete durability problem. According to the source of deleterious sulfate, the sulfate attack has two categories: external sulfate attack and internal sulfate attack. The reason for sulfate attack in concrete is the formation of the ettringite ($3CaO \cdot Al_2O_3 \cdot CaSO_4 \cdot 32H_2O$). Ettringite is one of the primary cement hydration products in concrete, which is formed by the reaction between gypsum ($CaSO_4 \cdot 2H_2O$) and calcium aluminate (C_3A). However, ettringite, formed at the early-age cement hydration process, poses no risk to concrete because the phase of this ettringite is “liquid” and flows in the concrete. The real risk is the formation of ettringite after concrete has already finished. The reaction occurs between calcium hydroxide (CH), water, monosulfate hydrate ($C_3A \cdot C\overline{S} \cdot H_{18}$), calcium aluminate hydrate ($C_3A \cdot CH \cdot H_{18}$) react, and sulfate compound ($\overline{S}$) [24]. The formation of ettringite increases the solid volume and further leads to concrete cracks, loss of strength, and disintegration. Additionally, concrete sufferes softening and loss of mass and strength due to the formation of gypsum [25]. Therefore, based on the reactants of the ettringite, the strategies to increase the concrete resistance to sulfate attack are the following: (1) decrease the C_3A content in the cement; (2) lower the w/c ratio for decreasing the amount of water; (3) decrease the amount of calcium hydroxide in the matrix system[3], [26].

As introduced previously, due to the pozzolanic reactivity, SCMs can react with the calcium hydroxide (CH) to form silicate hydrates (C-S-H), which helps to consume the calcium hydroxide (CH) in the system[3]. Furthermore, SCMs densify the interfacial transition zone and thus decrease

the permeability of the concrete [27]. The dense structure of concrete makes external sulfate complicated to enter into concrete. Also, the substitution cement by SCMs reduces the amount of C_3A in the matrix. Therefore, blending SCMs with cement will promote concrete sulfate attack resistance. The comprehensive review by Md Manjur A et al. [28] summarizes various SCMs' performance in sulfate attack resistance, and their summarization indicates that any SCMs, fly ash, slag, metakaolin, and silica fume helps to improve the sulfate resistance. However, they point out that the SCMs with low calcium content perform better than those SCMs with high calcium content.

2.2.4.3 Alkali-Silica Reaction (ASR)

Alkali-silica reaction (ASR) is one kind of alkali-aggregate reaction (AAR). ASR is one of the primary concrete durability problems and causes significant maintenance and reconstruction costs to concrete infrastructure such as buildings, pavements, bridges, dams, and other concrete structures worldwide. The first known ASR case was recognized in the state of California, reported by T.E. Stanton in 1940 [29], and the occurrence of ASR in concrete depends on three indispensable ingredients[30]:

1. High alkali environment (high pH) with alkali ions: Na^+, K^+, and OH^-. The Portland cement hydration process is the primary source of contributing alkalis in concrete. Other sources like aggregates or SCMs provide additional alkali in the concrete pore solution. The equivalent alkalis in concrete is expressed by: $Na_2O_{eq} = Na_2O + 0.658\ K_2O$ (in percentage)

2. Reactive siliceous components from Reactive aggregate. The common reactive aggregates include amorphous silica, cryptocrystalline, microcrystalline quartz, strained quartz, opal, chert, and acidic volcanic glass. The reactivity of aggregates depends on their chemical composition, crystallinity, amorphous structure, and the degree of solubility of the amorphous silicate in the alkaline pore solution[31].

3. Sufficient moisture in the system. Besides the concrete internal mixing water, external moisture sources also probably affect the ASR. Fournier et al.'s [32] report observed that ASR expansion occurs when the relative humidity (RH) is greater than 80%.

ASR is a deleterious chemical reaction with a synergic and multi-stage process. Several works summarized the outlined ASR reaction's mechanism [31], [33]–[35]. Alkali ions in concrete pore solution primarily derived from cement hydration react with reactive silica (SiO_2) from specific siliceous aggregates. The reactive silica, mainly with the structure of siloxane groups (≡ Si-O-Si≡), dissolves by hydroxyl attack. The silanol groups (≡Si-O-Si≡) on the silica surface react with hydroxide ions (OH^-) and generate one negative charge on the silica surface(Si-O^-). Positive alkali ions (Na^+ and K^+) neutralize the silica surface's negative charge, forming the alkali-silica gel (ASR gel) and alkali calcium silicate. The ASR gel has no swelling property but is very hygroscopic [8]. It attracts moisture from the surrounding cement paste, resulting in irreversibility swelling. Due to the expansion confined in the small concrete pore structures, the swelling process will build up an internal osmotic pressure in the concrete. While the internal stress exceeds the concrete's tensile strength, it leads to cracks in the aggregates and cement paste.

Moreover, recent studies report that calcium ions (Ca^{2+}) in the pore solution also play an essential role in the ASR process. Ca^{2+}, primarily from $Ca(OH)_2$, is the prerequisite for ASR gel formation [36]. The chemical formula of gel is calcium-alkali-silicate gels, but their composition is variable. The composition of gels determines whether the gels are deleterious to the concrete. When the gels are highly alkali (Na, K), they act as a flowable liquid and pass through the concrete pore structure without damaging the concrete [37]. However, the gels with high calcium content (i.e., Ca/Si > 0.5 molar ratio) behave more like C-S-H with high stiffness and low expansion properties[38]. Therefore, some researchers estimate that the intermediate Ca content in the

concrete pore solution results in a swelling pressure [39]. ASR affects concrete mechanical properties such as compressive strength, tensile strength, flexural strength, or modulus elasticity [40].

For concrete ASR mitigation, the most effective is to use supplementary cementitious materials (SCMs) by replacing cement in the concrete, which T.E. Stanton first reported in 1950 [41]. The mechanism of SCMs mitigating ASR can be understood in three ways [42], [43]:

1. Portlandite (CH) consumption. Calcium silicate hydrate (C-S-H) and calcium hydroxide (CH: portlandite) are two major cement hydration products. C-S-H is the skeleton of concrete, providing the strength of concrete. CH does not contribute much to concrete strength but is also involved in many deteriorating reactions damaging the concrete and affecting durability, including ASR and sulfate attacks. SCMs have pozzolanic reactivity, defined as the ability to consume CH. The reactive silicate or aluminate in SCMs reacts with CH and transforms it to C-S-H or calcium aluminate hydrate (C-A-H). The pozzolanic reactivity of SCMs depends on the amorphous extent of SCMs[44].

2. Alkali-binding and lowering the pH: The pozzolanic reaction consumes CH and produces a lower Ca/Si ratio of the hydrate. The lower Ca/Si ratio hydrates have a higher alkali binding ability [5] due to the increased amount of acidic silanol (Si-OH) sites in the C-S-H layers. The layer has negative charges [45] and neutralizes with positive alkali ions. Vollpracht et al. [46] reviewed different SCMs in the concrete pore solution, which indicates that SCMs effectively lower the pH of the concrete pore solution.

3. Reduce permeability. Ramezanianpour et al.'s [47] study indicates that SCMs partially replace the cement; even though the compressive strength may not be as good as the 100% cement mixture, permeability is highly improved. The primary reason for reducing permeability is to

densify the interfacial transition zone (ITZ). The study by Nežerka[27] investigated the influence of different SCMs, including fly ash, silica fume, and metakaolin, on the thickness of ITZ. The results suggest that SCMs are sufficient in reducing the ITZ thickness. When the concrete permeability decreases, it is difficult for the alkali ions to migrate inside the concrete; also, it will effectively prevent deleterious compounds from ingressing into the concrete.

2.2.4.4 Permeability (Need to Revise)

The permeability is the key to improving concrete's durability in various aggressive environments. The dense structure prevents the deleterious compound ingress into the concrete. SCMs convert calcium hydroxide to silicate hydrates (C-S-H) and dense the interfacial transition zone, decreasing the concrete's permeability and improving its durability [27].

The most common test related to concrete permeability is the ASTM C1202[79], also called the rapid chloride permeability test (RCPT). Dhanya and Santhanam's study [48] showed that adding SCMs to the concrete improved the concrete's chloride resistance ability. The chloride ions passed through of control with three different ages, 28, 56, and 90 days, were all located in the "Moderate" zone, which was defined that there was 2000 to 4000 Coulombs of charge passing through concrete. The addition of SCMs effectively lowered the amount of charge passed through, they reduced the amount of charge passed through to the "Low" zone (1000 to 2000 Coulombs), and some of them even lowered to the "Very Low" zone (0-1000 Coulombs). Also, with the increasing replacement cement by the SCMs, the charge passed decreased.

2.2.5 Concrete Pore Solution

The pore solution is the liquid phase within the pore structure of concrete, which is a critical property of concrete and plays a significant role in concrete's durability and chemical reactions. The concrete pore solution pH is generally located between 12.5 and 13.8 due to the cement's

alkaline content(Na_2O and K_2O) [49]. Maintaining a relatively high pH helps the steel form the passivation layer and prevent it from corrosion attack [50], but it is an ideal environment for ASR [30]. CH plays an important role in the pH of concrete, whose pH ranges from 9 to 11.5 [51], [52]. The other essential chemical component in the pore solution is alkali ions (Na^+, K^+). Alkali ions are very reactive metal ions because they only have one electron in their outermost shell [53]. The concentration of alkali ions impacts the pH of concrete, and this impact is more significant than CH due to the high solubility of alkali ions [54]. Besides pH, the alkali ions also engage in many chemical reactions. For example, positive alkali ions (Na^+ and K^+) neutralize the silica surface's negative charge, forming the ASR gel [31], [33]–[35].

The addition of SCMs in the concrete matrix decreases CH content due to the pozzolanic reaction. Additionally, after the occurrence of the pozzolanic reaction, the concrete matrix will have a lower Ca/Si ratio due to the formation of C-S-H. The lower Ca/Si ratio hydrates have a higher alkali binding ability due to the increased amount of acidic silanol (Si-OH) sites in the C-S-H layers [5]. The layer has negative charges, which helps to neutralize positive alkali ions [45].

Therefore, the pore solution of concrete is a practical approach to evaluate the SCMs' pozzolanic reactivity and ASR mitigation performance. For example, Shehata et al. evaluated 18 fly ash with various chemical compositions, and they discovered that the specimens' ASR expansion is proportional to their alkali ions concentration [55].

2.3 Factors Affecting the Pozzolanic Reactivity of SCMs

2.3.1 SCMs Crystallinity or Amorphous Level

The amorphous content levels play an important role in the SCM's reactivity. The materials' atomic arrangement determines their amorphous extent, and their reactivity is generally proportional to their amorphous level. Compared to the crystalline atomic structure, the amorphous atomic bond is more liquid and has no long-range atomic structure periodicity [56], so there is less inter-force between the atoms, which makes the amorphous materials more reactive. Much cementitious materials research has proved it as well. Walker and Pavía's study [18] evaluated different SCMs with different amorphous levels, surface area, and chemical compositions. They conclude that compared to other pozzolan properties, SCMs' amorphousness impacts the materials' pozzolan reactivity. Additionally, de Soares et al. [57] compared the pozzolanic behavior of sugar cane bagasse ash with amorphous and crystalline SiO_2. The pozzolanic reactivity of sugar cane bagasse ash is lower, which is very close to the crystalline SiO_2 group but not comparable to the amorphous SiO_2 group.

2.3.2 SCMs Particles Size Distributions

The relatively minor particle size distribution of SCMs will lead to a more extensive surface area, and the larger surface area further increases the reactivity of the SCMs. The research by Van et al. [58] on the reactivity of rice husks with different sizes, it was discovered that the higher the surface area of rice husk ashes, the more the pozzolanic reactivity. Shi et al. [59] conducted the pozzolanic reactivity of the grinding glass powder, and their results indicated that the finer the materials, the higher the pozzolanic reactivity. The particle size of the SCMs also influences the compressive strength. Zhang et al. [60] researched to evaluate the influence of fly ash size on concrete strength. They blended cement with 30% fly ash, which was the same type but with

various size distributions. Their results indicated that the strength increased from 38.0 MPa to 55.0 MPa when the volume median particle size (D50) of FA decreased from 26.4 μm to 1.5 μm. Lawrence et al. [61] discovered the same tendency in using the quartz sand as the SCMs. Their strength values increased from 41.0 MPa to 47.0 MPa as the particle size of QS decreased from 61.0 μm to 2.0 μm. However, Walker et al. [62] indicated that particle size primarily governed the mix's water demand but was not as impactful as the amorphous level on the pozzolanic reactivity. Additionally, Walker also presented that the chemical composition of the pozzolan was not a factor affecting either the pozzolan reactivity or the strength of the paste.

2.3.3 Chemical Compositions of SCMs

The chemical composition of SCMs also determines their pozzolanic reactivity and impacts their alkali-silica mitigation performance. Shehata et al. [55] tested 18 various fly ashes and evaluated whether their chemical compositions influenced their ASR mitigation. According to their results, calcium and alkalis content simultaneously adversely impact SCMs' ASR mitigation performance. Additionally, the pore solution study directly reflected the correlation between the alkali ions content and ASR expansion. Higher alkali ion concentration in the pore solution resulted in a more significant ASR expansion. However, even though mixtures mixed with high-alkali fly ashes had higher alkali content in their pore solution than the control, their ASR expansion was still effectively reduced. Therefore, Shehata et al. suggested the influence of fly ashes on calcium content in the pore solution was also necessary to be studied.

2.4 Methods Used to Evaluate Pozzolanic Reactivity of SCMs

2.4.1 ASTM C311 Standard Test Methods for Sampling and Testing Fly Ash or Natural Pozzolans for Use in Portland-Cement Concrete [63]

ASTM C311 is an essential standard method for evaluating the SCMs used in Portland cement concrete. The document lists the requirements that SCMs must follow when they are applied to the concrete, including the moisture content, loss on ignition (LOI), available alkali, ammonia, density, soundness, air-entrainment of mortar, strength activity index with portland cement, water requirement, and the effectiveness of SCMs in contributing to sulfate resistance.

According to ASTM C618, SCMs are required to pass strength activity index test (SAI) limits. The test mortar mixture with 20% SCMs replacement must reach at least 75% strength of the control mixture at 7- or 28-day. Sanjuán [64] et al. evaluated the effect of silica fume fineness on the improvement of Portland cement strength performance by strength activity index. They discovered that finer silica fumes had a high strength activity index; meanwhile, they also improved their pozzolanic reactivity by consuming more calcium hydroxide (CH).

Available alkali is another indicator to reflect the SCMs pozzolanic reactivity from the converse angle. The alkali contents in concrete are primarily attributed to cement hydration. However, SCMs can also contribute alkali content to the Portland cement matrix, possibly exacerbating the ASR. Therefore, analyzing how much alkali contents are released from SCMs in the concrete pore solution helps to evaluate the SCMs' pozzolanic reactivity.

2.4.2 Isothermal Calorimetry Tests and ASTM C1897 Standard Test Methods for Measuring the Reactivity of Supplementary Cementitious Materials by Isothermal Calorimetry and Bound Water Measurements[65]

Isothermal calorimetry is another excellent tool to monitor cement hydration kinetics and quantify products formed in the initial stage of hydration reactions by measuring the hydration heat. Cement hydration is an exothermic and complex process because cement consists of various compounds like C_3S, C_2S, C_3A, and C_4AF. Different compounds have different reactions, reaction rates, products, and further reactions [66]. The cement hydration kinetics is responsible for the performance of the cement-based matrix. The research [67] investigated the relationship between the hydration heat generation and the compressive strength of standard mortar, and the results indicate that strength development is almost linear with the released heat. However, with the increasing usage of SCMs in the concrete industry, the binary and ternary mixing proportions make the hydration process much more complicated than pure cement because SCMs' composition and pozzolanic reactivity impact the hydration, and the one characteristic of SCMs on cement hydration is lower heat release[68].

ASTM C-1897 R^3 test [65], developed by Karen Scrivener et al. [69] is another new method used in isothermal calorimetry to evaluate the pozzolanic reactivity of SCMs. The test method was initially developed to measure the calcined kaolinitic clays' pozzolanic reactivity and further applied to other SCMs [70], [71]. This test method is used to determine the pozzolanic reactivity of SCMs by measuring the hydrated paste's cumulative heat and bound water. The hydrated paste is mixed with the SCMs, calcium hydroxide, calcium carbonate, potassium sulfate, and potassium hydroxide, which is simulated as concrete pore solution and then cured at 40°C for 3 and 7 days. The pozzolanic reactivity is proportional to the cumulative heat and the chemical-bound water.

2.5.3 Thermogravimetric analysis (TGA)

Thermogravimetric analysis (TGA) is a method of thermal analysis that measures the amount and rate of change in the mass of a sample as a function of temperature and time in a controlled atmosphere. The materials' weight loss results characterize their chemical composition due to ingredients' chemical reactions, including loss of volatiles, decomposition, oxidation, and reduction. Cement hydration is a complex process because various cement reactants have corresponding reactions and products, so correctly identifying and quantifying the hydration reaction products is vital for cement chemistry analysis. XRD is the common approach used for these purposes, but it can only detect crystalline material like ettringite or portlandite. However, partial hydration products are not crystal but exist in the system as amorphous phases, which is why TGA is used as a complementary method for overcoming this limitation of XRD. TGA results generally indicate a thermogravimetric analysis curve (TGA). The other two strategies, differential thermal analysis (DTA) and differential scanning calorimetry (DSC), are also effective for analyzing the results. The difference between these methods is DTA and DSC locate the ranges corresponding to thermal decompositions of different phases in paste, while TGA simultaneously measures the weight loss due to the decomposing. Calcium hydroxide (CH) is the primary product that researchers want to identify, and its decomposing temperature is around 450^{o}C to 500^{o}C[72]. Much research [73]–[75] has been conducted to assess the SCMs' reactivity.

Temperature (°C)	Phase composition	Cement chemist's nomenclature	Temperature (°C)	Phase composition	Cement chem nomenclatu
50-100	$CaSO_4 \cdot 2H_2O$	$C\bar{S}H_2$	250-300	$Al(OH)_3$ [f]	–
100-150	$CaSO_4 \cdot 2H_2O$	$C\bar{S}H_2$	300-350	$Ca_3Al_2O_6 \cdot 6H_2O$	C_3AH_6
	$CaSO_4 \cdot ½H_2O$	$C\bar{S}H_{0.5}$		$Al(OH)_3$ [b, c, g]	–
	–	C–S–H [a]		$Mg_6Al_2O_9CO_3 \cdot 12H_2O$	$M_6A\bar{C}H_1$
	$Ca_3Al_2O_6 \cdot 3CaSO_4 \cdot 26H_2O$ [a, b]	$C_3A \cdot 3C\bar{S} \cdot H_{32}$ [a, b]	350-400	$CaSO_4$ [h]	$C\bar{S}$ [h]
	–	C–S–H	400-450	$Mg(OH)_2$	MH
	$CaAl_2O_4 \cdot 10H_2O$ [b]	CAH_{10} [b]	450-500	$Ca_3Al_2O_6 \cdot CaSO_4 \cdot 12H_2O$ [d]	$C_3A \cdot C\bar{S} \cdot H$
	$Mg_6Al_2O_9 \cdot CO_3 \cdot 12H_2O$	$M_6A\bar{C}H_{12}$		$Ca_3Al_2O_6 \cdot 6H_2O$ [d]	C_3AH_6 [d]
150-200	$CaSO_4 \cdot 2H_2O$	$C\bar{S}H_2$		$Ca(OH)_2$ [a]	CH [a]
	$CaSO_4 \cdot ½H_2O$	$C\bar{S}H_{0.5}$		$Mg_6Al_2O_9 \cdot CO_3 \cdot 12H_2O$	$M_6A\bar{C}H_1$
	$Ca_3Al_2O_6 \cdot CaSO_4 \cdot 12H_2O$	$C_3A \cdot C\bar{S} \cdot H_{12}$	500-550	$Al(OH)_3$ [c, d]	–
	$Ca_2Al_2O_5 \cdot 8H_2O$	C_2AH_8		$Al(OH)_3$ [i]	–
	$Ca_4Al_2O_7 \cdot 13H_2O$	C_4AH_{13}		$CaCO_3$ [j]	$C\bar{C}$ [j]
200-250	$CaSO_4 \cdot ½H_2O$	$C\bar{S}H_{0.5}$	550-800	$CaCO_3$ [k]	$C\bar{C}$ [k]
	$Ca_2Al_2SiO_7 \cdot 8H_2O$	C_2ASH_8		$CaCO_3$ [l]	$C\bar{C}$ [l]
	$Al(OH)_3$ [c]	–		$MgCO_3$	$M\bar{C}$
	$Al(OH)_3$ [c, d, e]	–			

Notes: a - highest rate of loss, b - major loss, c - gibbsite, d - minor loss, e - gibbsite to boehmite transition, f - bayerite, g - gibbsite to alu transition, h - soluble to insoluble anhydrite, i - boehmite to alumina transition, j - calcite, k - vaterite, l - aragonite.

Figure 2- 1 Thermogravimetric analysis of Cement Hydration Products [72]

2.5 The Requirements of SCMs Used in the Concrete Industry

ASTM C618 [1] covers the requirements that the coal fly ash and raw or calcined natural pozzolan must satisfy before applying them in the concrete industry. The specification specifies the materials from physical requirements and chemical compositions. The review primarily introduces the chemical composition requirements of SCMs.

ASTM C618 [1] lists five chemical requirements:

1. The minimum value of the sum of silicon dioxide (SiO_2), aluminum oxide (Al_2O_3), and iron oxide (Fe_2O_3): The SiO_2 and Al_2O_3 are contents for the pozzolanic reaction. Mehta et al. [76] researched to compare the effect of fly ash and silica fume on Portland cement concrete. The higher SiO_2 materials have higher strength values.

2. The amount of calcium oxide (CaO): In the study of Suraneni et al.[77] they discovered that the high CaO content of SCMs weakens the pozzolanic reactivity by measuring the amount of CH consumption.

3. The maximum value of sulfur trioxide (SO_3): the amount of SO_3 delays the cement setting time. Zunino et al. [78] investigated using high SO_3 content fly ash, which exceeds the maximum value in the ASTM C618 [1]. In the research, the setting time delays and 7-day compressive strength decreases. In addition, excess SO3 in the SCMs provides another sulfate source for increasing the sulfate attack risk of concrete.

4. The maximum value of the loss on ignition (LOI): The high LOI increases the water demand for concrete. An increase of 4% in LOI requires about 5% more water to account for the slump reduction of concrete [79]. The high-LOI fly ash also absorbs the air-entraining agents (AEA) that exacerbate the resistance to freeze-thaw [80].

	Class		
	N	F	C
Fineness:			
Amount retained when wet-sieved on 45 μm (No. 325) sieve, max, %	34	34	34
Strength activity index: [A]			
With portland cement, at 7 days, min, percent of control	75[B]	75[B]	75[B]
With portland cement, at 28 days, min, percent of control	75[B]	75[B]	75[B]
Water requirement, max, percent of control	115	105	105
Uniformity requirements:			
The density and fineness of individual samples shall not vary from the average established by the ten preceding tests, or by all preceding tests if the number is less than ten, by more than:			
Density, max variation from average, %	5	5	5
Percent retained on 45-μm (No. 325), max variation, percentage points from average	5	5	5

[A] The *strength* activity index with portland cement is not to be considered a measure of the compressive strength of concrete containing the fly ash or natural pozzolan. The mass of fly ash or natural pozzolan specified for the test to determine the *strength* activity index with portland cement is not considered to be the proportion recommended for the concrete to be used in the work. The optimum amount of fly ash or natural pozzolan for any specific project is determined by the required properties of the concrete and other constituents of the concrete and is to be established by testing. *Strength* activity index with portland cement is a measure of reactivity with a given cement and is subject to variation depending on the source of both the fly ash or natural pozzolan and the cement.
[B] Meeting the 7 day or 28 day *strength* activity index will indicate specification compliance.

Figure 2- 2 Physical Requirements of SCMs used in the concrete [1]

	Class		
	N	F	C
Silicon dioxide (SiO_2) plus aluminum oxide (Al_2O_3) plus iron oxide (Fe_2O_3), min, %	70.0	50.0	50.0
Calcium oxide (CaO), %	report only	18.0 max.	>18.0
Sulfur trioxide (SO_3), max, %	4.0	5.0	5.0
Moisture content, max, %	3.0	3.0	3.0
Loss on ignition, max, %	10.0	6.0[A]	6.0

[A]The use of Class F pozzolan containing up to 12.0 % loss on ignition may be approved by the user if either acceptable performance records or laboratory test results are made available.

Figure 2- 3 Chemical Requirements of SCMs used in the concrete [1]

2.6 SCMs World Market

Fly ash is the principal SCMs used in the concrete industry, so this part primarily investigates and introduces the world fly ash market. Due to most coal-burn plants switching to alternative fuels and some old plants not being equipped with EPA-compliant scrubbers used to capture fly ash, its production has generally decreased [81]. However, fly ash's utilization rate and demand are continually growing. Figure 1-1 presents the fly ashes proceed and recycled used data. The results of the most recent American Coal Ash Association (ACAA) survey presented the production and usage of all coal-combustion products (CCPs) [82]. According to the analyses made by Transparency Market Research [83], the global fly ash market is expected to grow at a compound annual growth rate (CAGR) of 7.1% from 2021 to 2031. Markets and Markets surveyed the fly ash market of various world regions [84]. It reported that the major fly ash market region is the Asia Pacific, including China, India, Japan, Australia, and Indonesia. The second is North America; the reason for the increased usage of fly ash in this area is the growth in construction projects and the high utilization rate. Therefore, SCMs shortage and price increase are predictable.

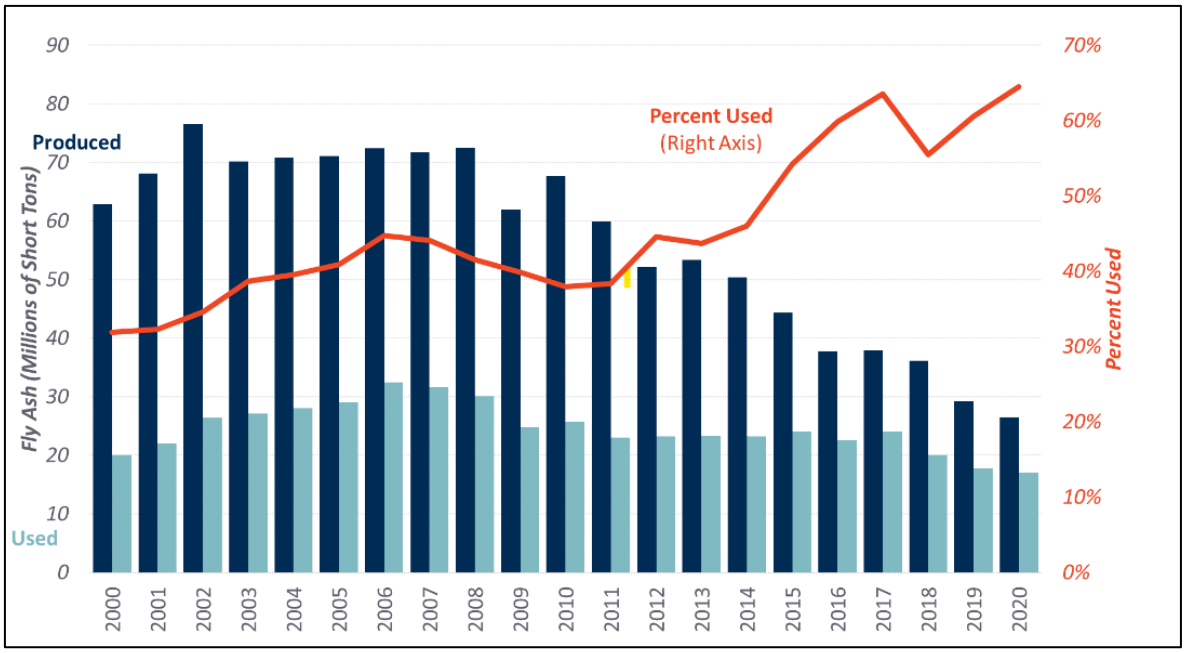

Figure 2- 4 Fly Ash Production & Use (2000–2020) [85]

Another issue for SCMs is the storage of disposed-off materials. Even though the utilization rate of industrial SCMs(e.g., fly ash) is increasing, a significant amount of material is still stored in ash ponds, including impoundments and landfills[86]. Fly ash storage is unsustainable and hazardous to the environment since it contains organic pollutants and probable toxic metals[87]. The aspects influenced by fly ash include air, soil, ground, and underground water[86], [88], [89], consequently affecting human health and agriculture.

Additionally, storing ash costs significant money and space every year. The news report in 2014 [90] reported the issue of Duke Energy's coal ash storage issue in North Carolina. It stated if the state of North Carolina wanted to solve the coal ash storage issue, it could cost more than 10 billion dollars. Therefore, if some disposed-off fly ash can be reclaimed again, it will benefit the economy and environment.

2.7 Why Select High-Alkal SCMs and Concerns for Using this Material

If the alkali content is more than 3% to 4%, they are not recommended to be used because their alkaline is likely to be involved in concrete pore solution exacerbating ASR. However, even though ASTM C618[1] gives the requirements of fly ash for concrete, it does not specify the SCMs' equivalent alkali content (equivalent $Na_2O\%= Na_2O\%+ 0.658K_2O\%$), and the maximum alkaline content value is not clearly defined. Additionally, the correlation between total alkali and available alkali has not been analyzed comprehensively. The total alkali is the entire alkaline content of SCMs, and the available alkali is alkaline content that can engage in concrete pore solution. Generally, most researchers believe that SCMs with total alkalis contribute more alkalis than SCMs with low alkalis. Shehata et al.'s research [91] evaluated the alkali release characteristics of blended cement with high alkali SCMs. Their research indicates that the simulation solution with high total alkali SCMs has a high concentration of alkali ions. However, it also shows that the total alkali contributed from the fly ash depends on its total alkali content and relies on other oxides like calcium oxide (CaO). The results discovered that the high CaO content (CaO>20%) of fly ash provides more alkali ions than the low CaO content of fly ash (CaO<20%). As another kind of SCMs, natural pozzolans contain the alkalis in crystalline phases formed by the volcano activities, and these crystalline phases do not release into the concrete pore solution [92]. Uribe-Afif et al. [93] evaluated the chemical composition of several natural pozzolans. Even though some natural pozzolans had significantly higher alkali content and one of the equivalent alkali contents reached 6.89%, the available alkali content was only 1.09%, which meant only 15% of the total alkalis of this natural pozzolan could release into the pore solution.

Therefore, the SCMs with high alkaline content still have the prospect of being studied in the ASR field. Using SCMs 'alkali content to predict their ASR mitigation performance is insufficient.

More investigations are required to advance understanding of the relationship between SCMs' total and available alkali content.

2.8 Reference

[1] C09 Committee, “ASTM C618-22 Specification for Coal Fly Ash and Raw or Calcined Natural Pozzolan for Use in Concrete,” ASTM International. doi: 10.1520/C0618-22.

[2] S. Gupta and S. Chaudhary, “State of the art review on supplementary cementitious materials in India – II: Characteristics of SCMs, effect on concrete and environmental impact,” *Journal of Cleaner Production*, vol. 357, p. 131945, Jul. 2022, doi: 10.1016/j.jclepro.2022.131945.

[3] P. K. Mehta and P. J. Monteiro, *Concrete: microstructure, properties, and materials*. McGraw-Hill Education, 2014.

[4] “The Pantheon by David Moore.” http://www.romanconcrete.com/docs/chapt01/chapt01.htm (accessed Aug. 31, 2022).

[5] J. D. Birchall, A. J. Howard, and J. E. Bailey, “On the hydration of Portland cement,” *Proceedings of the Royal Society of London. A. Mathematical and Physical Sciences*, vol. 360, no. 1702, pp. 445–453, 1978.

[6] I. G. Richardson, “The calcium silicate hydrates,” *Cement and Concrete Research*, vol. 38, no. 2, pp. 137–158, Feb. 2008, doi: 10.1016/j.cemconres.2007.11.005.

[7] X. Hou, L. J. Struble, and R. J. Kirkpatrick, “Formation of ASR gel and the roles of C-S-H and portlandite,” *Cement and Concrete Research*, vol. 34, no. 9, pp. 1683–1696, Sep. 2004, doi: 10.1016/j.cemconres.2004.03.026.

[8] W. Müllauer, R. E. Beddoe, and D. Heinz, “Sulfate attack expansion mechanisms,” *Cement and Concrete Research*, vol. 52, pp. 208–215, 2013, doi: 10.1016/j.cemconres.2013.07.005.

[9] M. Cyr, “8 - Influence of supplementary cementitious materials (SCMs) on concrete durability,” in *Eco-Efficient Concrete*, F. Pacheco-Torgal, S. Jalali, J. Labrincha, and V. M. John,

Eds., in Woodhead Publishing Series in Civil and Structural Engineering. Woodhead Publishing, 2013, pp. 153–197. doi: 10.1533/9780857098993.2.153.

[10] W. Sun, H. Yan, and B. Zhan, "Analysis of mechanism on water-reducing effect of fine ground slag, high-calcium fly ash, and low-calcium fly ash," *Cement and Concrete Research*, vol. 33, no. 8, pp. 1119–1125, Aug. 2003, doi: 10.1016/S0008-8846(03)00022-X.

[11] L. L. Sutter, "Supplementary Cementitious Materials-Best Practices for Concrete Pavements:[techbrief]," *Supplementary Cementitious Materials-Best Practices for Concrete Pavements:[techbrief]*, no. Journal Article, 2016.

[12] M. Thomas, *Optimizing the use of fly ash in concrete*, vol. 5420. Portland Cement Association Skokie, IL, 2007.

[13] J. C. Hower *et al.*, "Coal-derived unburned carbons in fly ash: A review," *International Journal of Coal Geology*, vol. 179, pp. 11–27, Jun. 2017, doi: 10.1016/j.coal.2017.05.007.

[14] M. C. Juenger, M. C. Won, D. W. Fowler, C. Suh, and A. Edson, "Effects of supplementary cementing materials on the setting time and early strength of concrete," 2008.

[15] M. C. G. Juenger and R. Siddique, "Recent advances in understanding the role of supplementary cementitious materials in concrete," *Cement and Concrete Research*, vol. 78, pp. 71–80, Dec. 2015, doi: 10.1016/j.cemconres.2015.03.018.

[16] S. Garrault-Gauffinet and A. Nonat, "Experimental investigation of calcium silicate hydrate (C-S-H) nucleation," *Journal of Crystal Growth*, vol. 200, no. 3, pp. 565–574, Apr. 1999, doi: 10.1016/S0022-0248(99)00051-2.

[17] T. Oey, A. Kumar, J. W. Bullard, N. Neithalath, and G. Sant, "The Filler Effect: The Influence of Filler Content and Surface Area on Cementitious Reaction Rates," *Journal of the American Ceramic Society*, vol. 96, no. 6, pp. 1978–1990, 2013, doi: 10.1111/jace.12264.

[18] J. J. Thomas, H. M. Jennings, and J. J. Chen, “Influence of Nucleation Seeding on the Hydration Mechanisms of Tricalcium Silicate and Cement,” *J. Phys. Chem. C*, vol. 113, no. 11, pp. 4327–4334, Mar. 2009, doi: 10.1021/jp809811w.

[19] S. Liu, T. Zhang, Y. Guo, J. Wei, and Q. Yu, “Effects of SCMs particles on the compressive strength of micro-structurally designed cement paste: Inherent characteristic effect, particle size refinement effect, and hydration effect,” *Powder Technology*, vol. 330, pp. 1–11, May 2018, doi: 10.1016/j.powtec.2018.01.087.

[20] R. GETTU and R. G. PILLAI, “Drying Shrinkage of Concrete with Blended Cementitious Binders: Experimental Study and Application of Models,” *INDIAN CONCRETE JOURNAL*, 2021.

[21] Z. Li, “Drying shrinkage prediction of paste containing meta-kaolin and ultrafine fly ash for developing ultra-high performance concrete,” *Materials Today Communications*, vol. 6, pp. 74–80, Mar. 2016, doi: 10.1016/j.mtcomm.2016.01.001.

[22] E. Güneyisi, M. Gesoğlu, and E. Özbay, “Strength and drying shrinkage properties of self-compacting concretes incorporating multi-system blended mineral admixtures,” *Construction and Building Materials*, vol. 24, no. 10, pp. 1878–1887, Oct. 2010, doi: 10.1016/j.conbuildmat.2010.04.015.

[23] K. Mermerdaş, E. Güneyisi, M. Gesoğlu, and T. Özturan, “Experimental evaluation and modeling of drying shrinkage behavior of metakaolin and calcined kaolin blended concretes,” *Construction and Building Materials*, vol. 43, pp. 337–347, Jun. 2013, doi: 10.1016/j.conbuildmat.2013.02.047.

[24] P. Monteiro, *Concrete: microstructure, properties, and materials*. McGraw-Hill Publishing, 2006.

[25] M. M. Rahman and M. T. Bassuoni, “Thaumasite sulfate attack on concrete: Mechanisms, influential factors and mitigation,” *Construction and Building Materials*, vol. 73, pp. 652–662, Dec. 2014, doi: 10.1016/j.conbuildmat.2014.09.034.

[26] O. S. Baghabra Al-Amoudi, “Attack on plain and blended cements exposed to aggressive sulfate environments,” *Cement and Concrete Composites*, vol. 24, no. 3, pp. 305–316, Jun. 2002, doi: 10.1016/S0958-9465(01)00082-8.

[27] V. Nežerka, P. Bílý, V. Hrbek, and J. Fládr, “Impact of silica fume, fly ash, and metakaolin on the thickness and strength of the ITZ in concrete,” *Cement and Concrete Composites*, vol. 103, pp. 252–262, Oct. 2019, doi: 10.1016/j.cemconcomp.2019.05.012.

[28] M. M. A. Elahi *et al.*, “Improving the sulfate attack resistance of concrete by using supplementary cementitious materials (SCMs): A review,” *Construction and Building Materials*, vol. 281, p. 122628, Apr. 2021, doi: 10.1016/j.conbuildmat.2021.122628.

[29] T. E. Stanton, “Influence of cement and aggregate on concrete expansion,” *undefined*, 1940, Accessed: Sep. 08, 2021. [Online]. Available: https://www.semanticscholar.org/paper/INFLUENCE-OF-CEMENT-AND-AGGREGATE-ON-CONCRETE-Stanton/9f014d128ed2aea0e6adff0216d34852ea7dc5f1

[30] M. D. A. Thomas, B. Fournier, K. J. Folliard, and Inc. Transtec Group, “Alkali-aggregate reactivity (AAR) facts book.,” FHWA-HIF-13-019, Mar. 2013. Accessed: Aug. 26, 2022. [Online]. Available: https://rosap.ntl.bts.gov/view/dot/26838

[31] P. Léger, P. Côté, and R. Tinawi, “Finite element analysis of concrete swelling due to alkali-aggregate reactions in dams,” *Computers & Structures*, vol. 60, no. 4, pp. 601–611, Jun. 1996, doi: 10.1016/0045-7949(95)00440-8.

[32] B. Fournier, M.-A. Berube, K. J. Folliard, M. Thomas, and United States. Federal Highway Administration. Office of Pavement Technology, “Report on the Diagnosis, Prognosis, and Mitigation of Alkali-Silica Reaction (ASR) in Transportation Structures,” FHWA-HIF-09-004, Jan. 2010. Accessed: Aug. 26, 2022. [Online]. Available: https://rosap.ntl.bts.gov/view/dot/42869

[33] L. S. Dent Glasser and N. Kataoka, “The chemistry of ‘alkali-aggregate’ reaction,” *Cement and Concrete Research*, vol. 11, no. 1, pp. 1–9, Jan. 1981, doi: 10.1016/0008-8846(81)90003-X.

[34] S. Akhtar, “A Critical Assessment to the Performance of Alkali-Silica Reaction (ASR) in Concrete”, doi: DOI:10.13179.

[35] M. Berra, T. Mangialardi, A. E. Paolini, and R. Turriziani, “Critical evaluation of accelerated test methods for detecting the alkali-reactivity of aggregates,” *Advances in Cement Research*, vol. 4, no. 13, pp. 29–37, Jan. 1991, doi: 10.1680/adcr.1991.4.1.29.

[36] F. P. Glasser, “Chemistry of the alkali-aggregate reaction,” in *The Alkali-Silica Reaction in Concrete*, CRC Press, 1991.

[37] M. Kawamura and K. Iwahori, “ASR gel composition and expansive pressure in mortars under restraint,” *Cement and Concrete Composites*, vol. 26, no. 1, pp. 47–56, Jan. 2004, doi: 10.1016/S0958-9465(02)00135-X.

[38] P. J. M. Monteiro, K. Wang, G. Sposito, M. C. dos Santos, and W. P. de Andrade, “Influence of mineral admixtures on the alkali-aggregate reaction,” *Cement and Concrete Research*, vol. 27, no. 12, pp. 1899–1909, Dec. 1997, doi: 10.1016/S0008-8846(97)00206-8.

[39] A. Gholizadeh Vayghan, F. Rajabipour, and J. L. Rosenberger, “Composition–rheology relationships in alkali–silica reaction gels and the impact on the gel’s deleterious behavior,” *Cement and Concrete Research*, vol. 83, pp. 45–56, May 2016, doi: 10.1016/j.cemconres.2016.01.011.

[40] E. O. Fanijo, J. T. Kolawole, and A. Almakrab, “Alkali-silica reaction (ASR) in concrete structures: Mechanisms, effects and evaluation test methods adopted in the United States,” *Case Studies in Construction Materials*, vol. 15, p. e00563, Dec. 2021, doi: 10.1016/j.cscm.2021.e00563.

[41] T. E. Stanton, “Studies of Use of Pozzolans for Counteracting Excessive Concrete Expansion Resulting from Reaction Between Aggregates and The Alkalies in Cement,” *Symposium on Use of Pozzolanic Materials in Mortars and Concretes*, Jan. 1950, doi: 10.1520/STP39409S.

[42] M. Kasaniya, M. D. A. Thomas, and E. G. Moffatt, “Efficiency of natural pozzolans, ground glasses and coal bottom ashes in mitigating sulfate attack and alkali-silica reaction,” *Cement and Concrete Research*, vol. 149, p. 106551, Nov. 2021, doi: 10.1016/j.cemconres.2021.106551.

[43] S.-Y. Hong and F. P. Glasser, “Alkali binding in cement pastes: Part I. The C-S-H phase,” *Cement and Concrete Research*, vol. 29, no. 12, pp. 1893–1903, Dec. 1999, doi: 10.1016/S0008-8846(99)00187-8.

[44] J. Skibsted and R. Snellings, “Reactivity of supplementary cementitious materials (SCMs) in cement blends,” *Cement and Concrete Research*, vol. 124, p. 105799, Oct. 2019, doi: 10.1016/j.cemconres.2019.105799.

[45] J. Duchesne and M. A. Bérubé, “The effectiveness of supplementary cementing materials in suppressing expansion due to ASR: Another look at the reaction mechanisms part 2: Pore solution chemistry,” *Cement and Concrete Research*, vol. 24, no. 2, pp. 221–230, Jan. 1994, doi: 10.1016/0008-8846(94)90047-7.

[46] A. Vollpracht, B. Lothenbach, R. Snellings, and J. Haufe, "The pore solution of blended cements: a review," *Mater Struct*, vol. 49, no. 8, pp. 3341–3367, Aug. 2016, doi: 10.1617/s11527-015-0724-1.

[47] A. A. Ramezanianpour, S. M. Motahari Karein, P. Vosoughi, A. Pilvar, S. Isapour, and F. Moodi, "Effects of calcined perlite powder as a SCM on the strength and permeability of concrete," *Construction and Building Materials*, vol. 66, pp. 222–228, Sep. 2014, doi: 10.1016/j.conbuildmat.2014.05.086.

[48] B. S. Dhanya and M. Santhanam, "Performance evaluation of rapid chloride permeability test in concretes with supplementary cementitious materials," *Mater Struct*, vol. 50, no. 1, p. 67, Aug. 2016, doi: 10.1617/s11527-016-0940-3.

[49] "Development of an accurate pH measurement methodology for the pore fluids of low pH cementitious materials," p. 108.

[50] L. Bertolini, B. Elsener, P. Pedeferri, E. Redaelli, and R. B. Polder, *Corrosion of Steel in Concrete: Prevention, Diagnosis, Repair*. John Wiley & Sons, 2013.

[51] Z. Mohammadi and P. M. H. Dummer, "Properties and applications of calcium hydroxide in endodontics and dental traumatology," *Int Endod J*, vol. 44, no. 8, pp. 697–730, Aug. 2011, doi: 10.1111/j.1365-2591.2011.01886.x.

[52] S. Poorni, R. Miglani, M. R. Srinivasan, and R. Indira, "Comparative evaluation of the surface tension and the pH of calcium hydroxide mixed with five different vehicles: an in vitro study," *Indian J Dent Res*, vol. 20, no. 1, pp. 17–20, Mar. 2009, doi: 10.4103/0970-9290.49050.

[53] "alkali metal | Definition, Properties, & Facts | Britannica." https://www.britannica.com/science/alkali-metal (accessed Sep. 16, 2022).

[54] L. J. Struble and P. W. Brown, *Microstructural Development During Hydration of Cement: Symposium Held December 2-4, 1986, Boston, Massachusetts, U.S.A.* Materials Research Society, 1987.

[55] M. H. Shehata and M. D. A. Thomas, "The effect of fly ash composition on the expansion of concrete due to alkali–silica reaction," *Cement and Concrete Research*, vol. 30, no. 7, pp. 1063–1072, Jul. 2000, doi: 10.1016/S0008-8846(00)00283-0.

[56] Z.-Q. Hu, A.-M. Wang, and H.-F. Zhang, "Chapter 22 - Amorphous Materials," in *Modern Inorganic Synthetic Chemistry (Second Edition)*, R. Xu and Y. Xu, Eds., Amsterdam: Elsevier, 2017, pp. 641–667. doi: 10.1016/B978-0-444-63591-4.00022-7.

[57] M. M. N. S. de Soares, D. C. S. Garcia, R. B. Figueiredo, M. T. P. Aguilar, and P. R. Cetlin, "Comparing the pozzolanic behavior of sugar cane bagasse ash to amorphous and crystalline SiO2," *Cement and Concrete Composites*, vol. 71, pp. 20–25, Aug. 2016, doi: 10.1016/j.cemconcomp.2016.04.005.

[58] V.-T.-A. Van, C. Rößler, D.-D. Bui, and H.-M. Ludwig, "Pozzolanic reactivity of mesoporous amorphous rice husk ash in portlandite solution," *Construction and Building Materials*, vol. 59, pp. 111–119, May 2014, doi: 10.1016/j.conbuildmat.2014.02.046.

[59] C. Shi, Y. Wu, C. Riefler, and H. Wang, "Characteristics and pozzolanic reactivity of glass powders," *Cement and Concrete Research*, vol. 35, no. 5, pp. 987–993, May 2005, doi: 10.1016/j.cemconres.2004.05.015.

[60] T. Zhang, Q. Yu, J. Wei, and P. Zhang, "Effect of size fraction on composition and pozzolanic activity of high calcium fly ash," *Advances in Cement Research*, vol. 23, no. 6, pp. 299–307, Dec. 2011, doi: 10.1680/adcr.2011.23.6.299.

[61] P. Lawrence, M. Cyr, and E. Ringot, “Mineral admixtures in mortars effect of type, amount and fineness of fine constituents on compressive strength,” *Cement and Concrete Research*, vol. 35, no. 6, pp. 1092–1105, Jun. 2005, doi: 10.1016/j.cemconres.2004.07.004.

[62] R. Walker and S. Pavía, “Physical properties and reactivity of pozzolans, and their influence on the properties of lime–pozzolan pastes,” *Mater Struct*, vol. 44, no. 6, pp. 1139–1150, Jul. 2011, doi: 10.1617/s11527-010-9689-2.

[63] C09 Committee, “ASTM C311-22 Test Methods for Sampling and Testing Fly Ash or Natural Pozzolans for Use in Portland-Cement Concrete,” ASTM International. doi: 10.1520/C0311_C0311M-22.

[64] M. Á. Sanjuán, C. Argiz, J. C. Gálvez, and A. Moragues, “Effect of silica fume fineness on the improvement of Portland cement strength performance,” *Construction and Building Materials*, vol. 96, pp. 55–64, Oct. 2015, doi: 10.1016/j.conbuildmat.2015.07.092.

[65] C09 Committee, “ASTM C1897-20 Standard Test Methods for Measuring the Reactivity of Supplementary Cementitious Materials by Isothermal Calorimetry and Bound Water Measurements,” ASTM International. [Online]. Available: https://www.astm.org/c1897-20.html

[66] K. Scrivener, A. Ouzia, P. Juilland, and A. Kunhi Mohamed, “Advances in understanding cement hydration mechanisms,” *Cement and Concrete Research*, vol. 124, p. 105823, Oct. 2019, doi: 10.1016/j.cemconres.2019.105823.

[67] L. Frølich, L. Wadsö, and P. Sandberg, “Using isothermal calorimetry to predict one day mortar strengths,” *Cement and Concrete Research*, vol. 88, pp. 108–113, Oct. 2016, doi: 10.1016/j.cemconres.2016.06.009.

[68] A. Schöler, B. Lothenbach, F. Winnefeld, M. B. Haha, M. Zajac, and H.-M. Ludwig, “Early hydration of SCM-blended Portland cements: A pore solution and isothermal calorimetry study,”

Cement and Concrete Research, vol. 93, pp. 71–82, Mar. 2017, doi: 10.1016/j.cemconres.2016.11.013.

[69] F. Avet, R. Snellings, A. Alujas Diaz, M. Ben Haha, and K. Scrivener, "Development of a new rapid, relevant and reliable (R3) test method to evaluate the pozzolanic reactivity of calcined kaolinitic clays," *Cement and Concrete Research*, vol. 85, pp. 1–11, Jul. 2016, doi: 10.1016/j.cemconres.2016.02.015.

[70] R. Snellings, X. Li, F. Avet, and K. Scrivener, "A Rapid, Robust, and Relevant (R3) Reactivity Test for Supplementary Cementitious Materials," *ACI Materials Journal*, vol. 116, no. 4, Jul. 2019, doi: 10.14359/51716719.

[71] F. Avet *et al.*, "Report of RILEM TC 267-TRM phase 2: optimization and testing of the robustness of the R3 reactivity tests for supplementary cementitious materials," *Mater Struct*, vol. 55, no. 3, p. 92, Mar. 2022, doi: 10.1617/s11527-022-01928-6.

[72] N. C. Collier, "Transition and decomposition temperatures of cement phases–a collection of thermal analysis data," *Ceramics-Silikaty*, vol. 60, no. 4, 2016.

[73] G. De Schutter, "Hydration and temperature development of concrete made with blast-furnace slag cement," *Cement and Concrete Research*, vol. 29, no. 1, pp. 143–149, Jan. 1999, doi: 10.1016/S0008-8846(98)00229-4.

[74] W. Deboucha, N. Leklou, A. Khelidj, and M. N. Oudjit, "Hydration development of mineral additives blended cement using thermogravimetric analysis (TGA): Methodology of calculating the degree of hydration," *Construction and Building Materials*, vol. 146, pp. 687–701, Aug. 2017, doi: 10.1016/j.conbuildmat.2017.04.132.

[75] J. I. Bhatty, “Hydration versus strength in a portland cement developed from domestic mineral wastes — a comparative study,” *Thermochimica Acta*, vol. 106, pp. 93–103, Sep. 1986, doi: 10.1016/0040-6031(86)85120-6.

[76] P. K. Mehta and O. E. Gjørv, “Properties of portland cement concrete containing fly ash and condensed silica-fume,” *Cement and Concrete Research*, vol. 12, no. 5, pp. 587–595, Sep. 1982, doi: 10.1016/0008-8846(82)90019-9.

[77] P. Suraneni, A. Hajibabaee, S. Ramanathan, Y. Wang, and J. Weiss, “New insights from reactivity testing of supplementary cementitious materials,” *Cement and Concrete Composites*, vol. 103, pp. 331–338, Oct. 2019, doi: 10.1016/j.cemconcomp.2019.05.017.

[78] F. Zunino, D. P. Bentz, and J. Castro, “Reducing setting time of blended cement paste containing high-SO3 fly ash (HSFA) using chemical/physical accelerators and by fly ash pre-washing,” *Cement and Concrete Composites*, vol. 90, pp. 14–26, Jul. 2018, doi: 10.1016/j.cemconcomp.2018.03.018.

[79] J. C. Hower *et al.*, “Coal-derived unburned carbons in fly ash: A review,” *International Journal of Coal Geology*, vol. 179, pp. 11–27, Jun. 2017, doi: 10.1016/j.coal.2017.05.007.

[80] M. D. A. Thomas, *Optimizing the use of fly ash in concrete*, vol. 5420. Portland Cement Association Skokie, IL, USA, 2007.

[81] T. M. Research, “Fly Ash Market is Expected to be Valued at US$ 13.8 Bn by 2031, States TMR Study,” *GlobeNewswire News Room*, Apr. 05, 2022. https://www.globenewswire.com/en/news-release/2022/04/05/2416875/0/en/Fly-Ash-Market-is-Expected-to-be-Valued-at-US-13-8-Bn-by-2031-States-TMR-Study.html (accessed May 05, 2022).

[82] “2020-Production-and-Use-Survey-Results-FINAL.pdf.” Accessed: May 05, 2022. [Online]. Available: https://acaa-usa.org/wp-content/uploads/2021/12/2020-Production-and-Use-Survey-Results-FINAL.pdf

[83] R. and Markets, “Global Fly Ash Market Report 2021: Increasing Focus on Infrastructure and Road Paving & Use of Environment-Friendly Products - Forecast to 2026,” *GlobeNewswire News Room*, Dec. 15, 2021. https://www.globenewswire.com/news-release/2021/12/15/2352442/28124/en/Global-Fly-Ash-Market-Report-2021-Increasing-Focus-on-Infrastructure-and-Road-Paving-Use-of-Environment-Friendly-Products-Forecast-to-2026.html (accessed May 05, 2022).

[84] “Fly Ash Market by Type (Type F, Type C), Application (Portland Cement & Concrete, Bricks & Blocks, Road Construction, Agriculture), and Region (Asia Pacific, Europe, North America, Middle East & Africa, South America) - Global Forecast to 2023.” Markets and Markets. [Online]. Available: https://www.marketsandmarkets.com/Market-Reports/fly-ash-market-76345803.html?gclid=CjwKCAjwx7GYBhB7EiwA0d8oewjHac48Eoh1oWzQoJyVvj9llAeO3FAI5t4EWTzWpGoLfz2yaAriQxoC-LcQAvD_BwE

[85] “Production & Use Reports – ACAA.” https://acaa-usa.org/publications/production-use-reports/ (accessed May 05, 2022).

[86] J. S. Harkness, B. Sulkin, and A. Vengosh, “Evidence for Coal Ash Ponds Leaking in the Southeastern United States,” *Environ. Sci. Technol.*, vol. 50, no. 12, pp. 6583–6592, Jun. 2016, doi: 10.1021/acs.est.6b01727.

[87] H. P. Jambhulkar, S. M. S. Shaikh, and M. S. Kumar, “Fly ash toxicity, emerging issues and possible implications for its exploitation in agriculture; Indian scenario: A review,” *Chemosphere*, vol. 213, pp. 333–344, Dec. 2018, doi: 10.1016/j.chemosphere.2018.09.045.

[88] Z. T. Yao *et al.*, "A comprehensive review on the applications of coal fly ash," *Earth-Science Reviews*, vol. 141, pp. 105–121, Feb. 2015, doi: 10.1016/j.earscirev.2014.11.016.

[89] L. B and A. K. Dikshit, "Behaviour of Metals in Coal Fly Ash Ponds," *APCBEE Procedia*, vol. 1, pp. 34–39, Jan. 2012, doi: 10.1016/j.apcbee.2012.03.007.

[90] A. Larson, "Duke Energy's Coal Ash Solution Could Cost More Than $10 Billion," *POWER Magazine*, Apr. 24, 2014. https://www.powermag.com/duke-energys-coal-ash-solution-could-cost-more-than-10-billion/ (accessed Aug. 29, 2022).

[91] M. H. Shehata and M. D. A. Thomas, "Alkali release characteristics of blended cements," *Cement and Concrete Research*, vol. 36, no. 6, pp. 1166–1175, Jun. 2006, doi: 10.1016/j.cemconres.2006.02.015.

[92] P. K. Mehta, "Natural pozzolans: Supplementary cementing materials," in *Proc., Int. Symp. on Advances in Concrete Technology*, CANMET, Athens, Greece, 1987, pp. 407–430.

[93] R. E. Rodríguez-Camacho and R. Uribe-Afif, "Importance of using the natural pozzolans on concrete durability," *Cement and Concrete Research*, vol. 32, no. 12, pp. 1851–1858, Dec. 2002, doi: 10.1016/S0008-8846(01)00714-1.

CHAPTER III EXPERIMENTAL PROGRAM

3.1 Materials

3.1.1 Cement

Two types of ordinary Portland cement (OPC) meeting ASTM C150 [1] were used in this study: A Type I/II OPC (Na_2Oeq = 0.38%) that was obtained from Argos cement company, SC, and a Type I high alkali portland cement (Na2Oeq = 1.00%) that was provided by Lehigh Hanson, Inc. The Type I/II OPC was used for most of the tests, while the high alkali cement was used only in tests related to ASR, i.e., the miniature concrete prism test (MCPT) as per AASHTO T380 [2] and concrete prism test (CPT) as per ASTM C1293 [3]. The chemical compositions and physical properties of portland cement are presented in Table 2-1.

Table 2- 1 Cement Chemical Compositions

Material	Specific Gravity	LOI	Chemical Composition								
			SiO_2	Al_2O_3	Fe_2O_3	CaO	MgO	Na_2O	K_2O	SO_3	Alkali eq.
Low alkali cement	3.15	3.6%	19.93	4.77	3.13	63.27	3.70	0.06	0.48	3.95	0.38
High alkali cement	3.15	--	19.00	4.99	3.11	63.45	3.84	0.31	1.05	4.05	1.00

3.1.2 Fine Aggregate

3.1.3.1 Non-reactive Fine Aggregate

This was used in a non-reactive siliceous natural river sand from Glasscock Co. in Sumter, SC, with an oven-dry specific gravity of 3.63, an absorption ratio of 0.35% and a fineness modulus of 3.6 study.

3.1.3.2 Reactive Fine Aggregate

Highly reactive aggregate, produced by North Carolina, was used for testing ASR. This aggregate's specific gravity and percent absorptions were 3.6 and 1%, respectively. This reactive aggregate was used for ASTM C1260[4], ASTM C1567 [5], and AASHTO T380[2].

3.1.3 Coarse Aggregate

3.1.3.1 Non-reactive Coarse Aggregate

Coarse non-reactive is obtained from Anderson, SC. This aggregate was used for AASHTO T380[2] and ASTM C1202 RCPT test [6].

3.1.3.2 Reactive Coarse Aggregate

Highly reactive aggregate, produced by North Carolina, was used for testing ASR. This aggregate's specific gravity and percent absorptions were 3.6 and 1%, respectively. This reactive aggregate was used for ASTM C1293[3] and AASHTO T380[2].

3.1.4 High-Alkali SCMs Physical and Chemical Properties

All the SCMs were provided by the National Pozzolan Association (NPA). The SCMs included six types of natural pozzolans (NP) and two types of reclaimed fly ashes (RFA). In order to indicate the products conveniently, the materials were labeled from NP 1 to NP 8. The chemical composition provided by product companies is shown in the following Table 2- 2. All these high alkalies SCMs were evaluated by various experiments in this study.

3.1.4.1 Chemical Composition measured by X-Ray Fluorescence (XRF)

Determining the chemical composition of SCMs helps to evaluate their reactivity. X-ray fluorescence (XRF) is an analytical technique that uses the interaction of X-rays with material to qualitatively and quantitatively analyze its elemental composition.

The mechanism of XRF is to use X-rays to irradiate a substance, and the substance absorbs some X-rays. The absorbed X-rays knock out an electron from one of the orbitals surrounding the

nucleus within an atom of the material. A hole is produced in the orbital, resulting in a high energy, unstable configuration for the atom. To restore equilibrium, an electron from a higher energy, outer orbital falls into the hole. Since this is a lower energy position, the excess energy is emitted in the form of fluorescent X-rays. The energy difference between the expelled and replacement electrons is characteristic of the element atom in which the fluorescence process is occurring – thus, the energy of the emitted fluorescent X-ray is directly linked to a specific element being analyzed.

There are two common XRF measuring methods: energy dispersive X-Ray fluorescence (EDXRF) analysis and wavelength dispersive X-Ray fluorescence (WDXRF). This study used the WDXRF to assess the chemical composition of high alkalis SCMs, and compared to the EDXRF, WDXRF can get more accurate and higher-resolution data. The following Table indicates the chemical composition of the high alkalis SCMs.

Table 2- 2 SCMs Chemical Compositions

	Sample Type							
Chemical Composition	NP 1	NP 2 (RFA 1)	NP 3	NP 4	NP 5	NP 6	NP 7	NP 8 (RFA 2)
Silicon Dioxide (SiO2)	68.620%	53.060%	73.420%	65.480%	71.950%	71.210%	71.910%	56.810%
Aluminum Oxide (Al2O3)	13.140%	15.130%	12.300%	11.190%	12.260%	12.990%	11.680%	14.200%
Iron Oxide (Fe2O3)	1.910%	6.880%	1.410%	1.750%	1.500%	0.901%	2.180%	2.690%
Sum (SiO2+Al2O3)	81.760%	68.190%	85.720%	76.670%	84.210%	84.200%	83.590%	71.010%
Sum (SiO2+Al2O3+Fe2O3)	83.670%	75.070%	87.130%	78.420%	85.710%	85.101%	85.770%	73.700%
Calcium Oxide (CaO)	1.730%	13.700%	0.791%	2.990%	0.928%	0.561%	0.317%	10.130%
Magnesium Oxide (MgO)	1.430%	4.530%	0.229%	0.326%	0.39%	0.130%	0.090%	1.410%
Sodium Oxide (Na2O)	2.740%	3.430%	2.850%	3.600%	3.900%	3.880%	5.500%	2.790%
Potassium Oxide (K2O)	3.160%	1.910%	4.190%	3.420%	3.960%	4.080%	4.230%	2.690%
Sodium Oxide Equivalent (Na2O+0.658K2O)	4.819%	4.687%	5.607%	5.850%	6.506%	6.565%	8.283%	4.560%
P2O5	0.035%	0.191%	0.009%	0.014%	0.025%	0.003%	0.003%	0.257%
TiO2	0.139%	0.528%	0.050%	0.166%	0.133%	0.062%	0.065%	0.430%
MnO	0.070%	0.061%	0.032%	0.030%	0.072%	0.241%	0.102%	0.166%
V2O5	0.001%	0.021%	0.001%	0.001%	0.002%	0.001%	0.001%	0.013%
Loss on Ignition	7.180%	0.550%	4.720%	10.870%	4.880%	5.950%	3.940%	8.420%

3.1.4.2 Loss on Ignition (LOI) ASTM D7348 [7]

LOI value represents the amount of unburned carbon in the materials. In this study, SCMs samples were heated to a high temperature, then measured their weight loss. The reason for

evaluating the LOI is to investigate whether the SCMs can be used in the concrete industry because high LOI ashes require a higher water-to-binder ratio to get acceptable workability, thus reducing strength and increasing porosity. Also, ASTM C618 [8] gives the LOI requirements for fly ashes and natural pozzolans, which are 6% and 10%, respectively. The materials' LOI values are shown in Table 2-3.

3.1.4.3 Particle Size Distribution measured by Laser-Diffraction

Particle size is another indicator for evaluating the SCMs' reactivity. Generally, the finer the materials, the higher their reactivity. However, due to increased surface area, the finer materials require more water demand for capable workability. In this study, laser diffraction conducted the SCMs' particle size distribution. Laser diffraction measures the particle size distribution by using the laser beam passing through the test samples, then assessing the intensity of scattered light caused by materials' angular variation. Generally, the large particles scatter light results from the smaller angles relative to the laser beam, and small particles scatter light at large angles.

3.1.4.4 X-ray diffraction (XRD)

X-ray diffraction (XRD) used in this study was to qualitative and quantitative the crystal structure of SCMs. XRD's mechanism is X-ray interference, and the detector detects crystal constructive X-rays interference at certain incident angles. The incident X-ray irradiates the substance with incident angles Θ. Based on the crystal's unique lattice structure, different crystal phases lead to different X-rays with various wavelengths and diffraction angles 2Θ between the X-ray source and detector. "Bragg-Brentano" geometry $n\lambda = 2d\sin\Theta$ is the primary basis for the XRD test, where d is crystal atoms' distance, λ is the wavelength of diffracted X-rays.

The XRD test in this study was run by Rigaku automated multipurpose X-ray diffraction and analyzed by SmartLab XRD analyzer software. The raw SCMs were delivered to XRD analysis directly without other additional pretreatments. This experiment assessed the SCMs' crystallinity

(or amorphous level) and primary crystal phase, which helped evaluate the SCMs' pozzolanic reactivity.

3.1.5 Chemicals

3.1.5.1 Deionized Water

Deionized water was used to prepare the chemical solutions in this study.

3.1.5.2 Sodium Hydroxide (NaOH)

NaOH pellets used in this study are the product of Fisher Science Lab Supplies. The NaOH was used to mix NaOH solution and concrete for the ASR test methods. Also, 0.3 N NaOH solution was prepared for the rapid chloride penetration test.

3.1.5.3 Sodium Sulfate (Na2SO4)

Na_2SO_4 was used in ASTM C1012 sulfate resistance test [9].

3.1.5.4 Saturated-lime

Saturated lime was used to cure the samples.

3.1.5.5 Isopropanol

Isopropanol, used in this study, is produced by the Alliance Chemical Company. The concentration is 99.9%. Isopropanol was used for the thermogravimetric test (TGA), and its function was to stop the cement hydration by solvent exchange.

3.1.5.6 Diethyl ether

Diethyl ether, used in this study, is an anhydrous product produced by Lab Chemical Supply. The TGA test used this chemical to remove the residue of isopropanol on the sample's surface.

3.1.5.7 Calcium hydroxide (Ca(OH)2)

Fisher Science Lab Supplies provide $Ca(OH)_2$, and in this test, $Ca(OH)_2$ was used in the ASTM C1897 [10] R^3 test for mixing and simulating the concrete pore solution

3.1.5.8 Calcium carbonate (CaCO3)

$CaCO_3$ was used in the ASTM C1897 [10] for mixing and simulating the pore solution.

3.1.5.9 Potassium sulfate (K2SO4)

K2SO4 was used in the ASTM C1897 [10] for mixing and simulating the pore solution.

3.1.5.10 Potassium hydroxide (KOH)

Fisher Science Lab Supplies provide calcium hydroxide, and in this test, calcium hydroxide was used in the ASTM C1897 R^3 test [10] for mixing and simulating the concrete pore solution

3.1.5.11 Sodium chloride (NaCl)

NaCl solution was prepared for the rapid chloride penetration test.

3.1.5.12 Nitric acid (HNO_3)

2% Nitric acid was used for diluting the pore solution, which was diluted from 68% Nitric acid

3.2 Fresh Properties

3.2.1 ASTM C311 -22 Water Demand [11]

The flowability of test mixtures was measured and compared to the control mixture. Three SCMs replacement levels were evaluated by this test, which were 20%, 30%, and 40%, respectively. 20% mixtures' mixing proportions and test procedures were according to ASTM C311[11] for determining the water demand and strength activity index. 30% and 40% were mixed with 0.485 water-cementitious ratios and 3.25 sand-cementitious ratios.

3.2.2 Ultrasonic Pulse Velocity

Ultrasonic pulse velocity test (UPV) was conducted to monitor changes in volume pores and moisture content within pores with the cement hydration process. For the test, Ultrasonic Tester BP-700 series was employed. The pastes were prepared by blending low-alkali cement with 20% SCMs by mass of cement at a water-to-binder ratio of 0.42. To ensure precise results, the paste mixture underwent vacuum mixing to eliminate the influence of air bubbles. The test configuration involved positioning the sensors 40mm apart, with data collection occurring at one-minute intervals. After casting, the specimens were stored in the air chamber at 23^{o}C and 50% RH for 24 hours.

3.2.3 ASTM C191 - 21 Test Methods for Time of Setting of Hydraulic Cement by Vicat Needle --- Automatic Setting Time [12]

This test aimed to assess the effect of substituting SCMs for a portion of cement on the length of time cement paste sets. The setting time was measured according to ASTM C191[12] using the Automatic Vicat consistency apparatus with the hard rubber conical mold.

Different from the standard Vicat mix proportion, all the mixtures were mixed by a 0.42 water-to-cementitious ratio. Two SCMs replacement levels were evaluated, which were 20% and 40%, respectively.

3.2.4 Isothermal Calorimetry Study

The heat flow of the investigated paste mixtures, with 0.42 water-binder- ratio, containing 20% SCMs, was determined at 23oC with a four-channel Isothermal Calorimeter. After casting, 100 g of mixtures was placed in the measuring bottle, and the heat flow of each specimen was recorded for 7 days.

3.3 SCMs Reactivity Experiments

3.3.1 ASTM C311-22 Standard Test Methods for Sampling and Testing Fly Ash or Natural Pozzolans for Use in Portland-Cement Concrete[11]

The strength activity index (SAI) is the ratio of the 2in×2in×2in cube strength of the 80% cement and 20% SCMs mixtures to the strength of the control (100% cement) at 7 & 28-day. The rate of strength development can reflect how the SCMs influence the cement hydration process. Also, the SAI results indicate the SCMs' pozzolanic reactivity.

The control mixture was mixed with 500 g of portland cement, 1375 g of graded standard sand, and 242 mL of water, and the test mixture was mixed with 400 g of portland cement, 100 g of the test sample, 1375 g of graded standard sand and the amount of water resulting the flow as ±5% of control mixture. After casting, the specimens were placed in moist rooms for 24 hours with the proper protection from the dripping water. Then the specimens were demolded from the mold and placed in the curing in lime-saturated water. The strength activity index was calculated by the average compressive strength of test mixture cubes divided by the average compressive strength of control mix cubes. All eight SCMs were evaluated.

3.3.2 Thermogravimetric analysis (TGA)

Thermogravimetric analysis (TGA) is a widely applied technique to evaluate and reactivity of SCMs. The mechanism of TGA is measuring the weight loss of hydrate or anhydrate materials caused by high temperatures. High temperatures can result in several thermal reactions: dehydration, dehydroxylation, decarbonation, oxidation, decomposition, phase transition, or melting. Therefore, weight loss at certain temperature intervals can determine the exact phase of products. For example, as the ASR hazardous compound, calcium hydroxide (Portlandite) decomposes at a temperature between 400 and 500 Celcius. The TGA common analysis

approaches are differentiation of the thermogravimetric (TG), differential thermogravimetry (DTG), differential scanning calorimetry (DSC), and differential thermal analysis (DTA). This study used TGA to determine hydration products' phase change influenced by specimens' age and various SCMs applied.

This study used the AutoTGA Q5000 instrument for running TGA analysis from 0 to 1000°C. Test specimens were paste, with the 0.42 w/c ratio, and 50g of binder materials with 20% SCMs replacement. The specimens' test age was 12-hour, 1 day, 3-day, 7-day, 28-day, and 56-day, respectively. The specimens were sealed in the test tubes and stored in the air chamber at 23°C and 50% RH before usage. In addition, there are pretreatment procedures before running the TGA:

1. Crush and grind the specimens by using the pestle.
2. The powder was placed in the 50ml isopropanol for 15 minutes. The purpose of this step was to remove the pore solution with isopropanol.
3. Using Büchner funnel, filter the solution.
4. Removing the isopropanol by using 10 mL diethylene ether. Pumped the specimens until their color turned a lighter color.
5. Stored the specimens and run the TGA tests immediately to avoid carbonation.

3.3.3 ASTM C1897-20 Standard Test Methods for Measuring the Reactivity of Supplementary Cementitious Materials by Isothermal Calorimetry and Bound Water Measurements (R^3 test) Conducted by Isothermal Calorimetry [10]

The study ran the R^3 test to assess the SCM's pozzolanic reactivity, which followed the ASTM C1897-20 method A. In the R^3, all eight SCMs were evaluated. The isothermal calorimetry conducted this test, which helped to determine the mixtures' heat of hydration. The paste was mixed with the SCM, calcium hydroxide, calcium carbonate, potassium sulfate, and potassium

hydroxide, which was simulated as the Portland cement pore solution. Heat hydration was directly used to determine the chemical reactivity of the SCMs.

The mass ratio of SCMs to calcium hydroxide and calcium carbonate was 1 to 3 and 2 to 1, respectively. The potassium solution was prepared by dissolving 4.00 g of potassium hydroxide and 20.0 g of potassium sulfate in 1.00 L of reagent water conditioned at 23±3 °C. The mass ratio of potassium to the solids blended by SCMs, calcium hydroxide, and calcium carbonate was 1.3. Before mixing, all the materials, including solution and solids, were required to the precondition in the storage environment at 40±2 °C. After all the materials' temperatures reached 40±2 °C, they were mixed at 1600 ± 50 r/min for 2 min using the high-shear blender to get the homogeneous paste. Then the mixtures were placed in the isothermal calorimetry, which was also set at 40±0.5 °C for at least 16h. Additionally, all the other mixing tools like specimen containers, lids, and pipettes were also required to precondition at 40±0.5 °C. The test lasted 7 consecutive days and kept measuring the rate of hydration and cumulative heat.

3.4 Alkali-Silica Reaction (ASR) Experimental Program

3.4.1 ASTM C1260-21 Standard Test Method for Potential Alkali Reactivity of Aggregates (Mortar-Bar Method) [4]

This test method evaluates the potential for aggregates' deleteriousness to the alkali-silica reaction but is not used to assess the aggregates' combinations with other supplementary cementitious materials(SCMs). Four 1in×1in ×11.25in mortar bars were cast for each mixture and then placed in the sodium hydroxide (NaOH) solution for 16-day, and their expansion was recorded at specific time intervals. In order to keep the consistency of the results, the standard required the specific fine aggregate particle size distribution, shown in Table 1. The mass proportion of the cement and aggregate in this test was 1:3.25 when the aggregate's relativity density was at or above 3.45. For the aggregate with a relative density below 3.45, the previous mass ratio did not work, and it needed to be recalculated. The detailed information can be checked in the ASTM C1260-21[4]. In addition, the water-cement ratio was 0.47 by mass in this test.

The concentration of NaOH solution was 1N, which was 1 mol of NaOH (40g) dissolved in the 1-liter solution. NaOH was dissolved in 900 ml water first after powder or pellets of NaOH are mixed and dissolved completely, then using the water diluted and obtained the 1-L solution. The volume of the mortar bar was 184 mL, and the volume proportion of sodium hydroxide solution to mortar bars must be 4±0.5 volumes of solution to 1 volume of mortar bars. Due to the specimens exposed to the NaOH solution, the alkali content of cement did not influence the ASR expansion a lot.

The standard also lists the conditioning requirements for the steps:

1. Specimens were cast and demold in the room with a temperature of 20 to 27.5ºC and relative humidity(RH) not less than 50%.

2. After casting, the specimens were moved to the moist room for 24±2-hour moist curing, and the moist room should conform to ASTM C511[13], which had a temperature of 23 ±2 °C and over 95% RH. The moist room prevented the specimens from shrinkage caused by the evaporation process.
3. Next, the specimens were stored in the water at 80 ± 2 °C for 24 hours. Sufficient water was required to immerse the specimens in the sealed container. In addition, the water needed to be preconditioned in the oven for 24 hours to reach the temperature of 80 °C.
4. Then moved, the specimens to the NaOH solution, and the solution had the same temperature and precondition requirements as the water.

Table 2- 3 Aggregate Size Distribution for ASTM C1260 [4]

Sieve Size		Mass, %
Passing	Retained on	
4.75 mm (No. 4)	2.36 mm (No. 8)	10
2.36 mm (No. 8)	1.18 mm (No. 16)	25
1.18 mm (No. 16)	600 µm (No. 30)	25
600 µm (No. 30)	300 µm (No. 50)	25
300 µm (No. 50)	150 µm (No. 100)	15

Zero reading was recorded at the time after 24-hour water bathing and before storing in NaOH. The time between removal and return to the curing solution should not exceed 10 mins. Before measuring the bar length, use a towel to dry the surface. Three subsequent intermediate readings were taken in the following 14-day, which should be at the same time each day.

The threshold values of ASTM C1260 for 14-day exposure to 1N NaOH solution used for evaluating the ASR deleterious extent of aggregate are the following:

1. expansion<0.1% innocuous;
2. 0.1%<expansion<0.2% inconclusive;

3. expansion>0.2% reactive.

3.4.2 ASTM C1567-21 Standard Test Method for Potential Alkali Reactivity of Aggregates (Mortar-Bar Method) --- Accelerated Mortar Bar Test (AMBT) -- [5]

This test method allows for detection within 16 days of the potential for the deleterious alkali-silica reaction of combinations of SCMs and aggregate in mortar bars. The SCMs include pozzolans, fly ash, and ground granulated blast furnace slag.

This test's preparations and operation procedures were the same as the ASTM C1260. However, when the SCMs used in this test, the mixed flow needed to conform ± 7.5 percentage points of a control mortar without SCMs. If the mixture was too dry, a high-range water reducer should be used to increase the workability. The evaluation criteria are the same as ASTM C1260 as well:

1. expansion<0.1% innocuous;
2. 0.1%<expansion<0.2% inconclusive;
3. expansion>0.2% reactive.

In this study, eight SCMs were used for mixing the mortar bars with 20% replacement levels.

3.4.3 ASTM C1293-20a Standard Test Method for Determination of Length Change of Concrete Due to Alkali-Silica Reaction --- Concrete Prisms Test (CPT) [3]

This test method is used to determine the susceptibility of an aggregate or combination of an aggregate with pozzolan or slag for participation in expansive alkali-silica reaction by measurement of length change of 3in×3in×11.25in concrete prisms.

The cementitious materials content is 420 ±10 kg/$m^{3,}$ and the water-cementitious ratio ranged from 0.42 to 0.45. If the mixture was too dry to cast high-quality specimens, using a high-range water reducer increases workability. The total alkali content of the cement used in this test method

should have a Na_2O_{eq} content of 0.90 ± 0.10 percent. NaOH dissolved in the mixing water maintained the alkali content of the concrete mixture to 1.25% by mass of cement. The dry mass of coarse aggregate per unit volume of concrete was 0.70±0.02 of its dry-rodded bulk density. The fine aggregate should meet Specification ASTM C33[14] with a fineness modulus of 3.7±0.2, and the gradation of coarse aggregate is indicated in Table 2-4. Both reactive coarse and fine aggregates can be conducted in this experimental work. If the study evaluates the reactivity of coarse aggregates work, the coarse aggregates needed to mix with non-reactive aggregates and vice versa

Table 2- 4 Aggregate Size Distribution for ASTM C1293[3]

Passing Sieve Size	Retained on Sieve Size	Mass,%
19.5mm	13.5mm	1/3
13.5mm	9.5mm	1/3
9.5mm	4.75mm	1/3

The cast specimens were stored in a moist room for curing 1-day, and then zero readings were recorded. The specimens were placed in sealed buckets with perforated racks. The perforated racks acted as the role of a platform for supporting the concrete specimens, which let specimens 30 to 40 mm above the bottom. Below the racks, there was a 20±5mm depth of water. The function of this water was to guarantee high relative humidity in the bucket. The buckets were stored in the room at 38.0±2°C.

Subsequent readings were taken at -day, 28-day, 56-day, 3-month, 6-month, 9-month, and 12-month. If additional readings were required, measure them at six months intervals. Additionally, the buckets were removed from the curing room to the ambient temperature room at 23.0±2°C for 18±6 hours before each measurement. The expansion criteria of ASTM C1293 without SCMs are the following:

1. Expansion<0.04% at one-year, non-reactive
2. 0.04%<expansion<0.12% at one-year, marginal

3. Expansion>0.12% at one-year, highly reactive

When evaluating the SCMs ASR mitigation performance, if the ASR expansion is less than 0.04 at 1 year, the test SCM is considered effective for mitigating ASR. In this test, two different SCMs replacement levels were conducted to evaluate the high alkali SCMs ASR mitigation performance, which was 20%, and 30% by the mass to cement. All eight SCMs were used in the 20% replacement levels test. Five SCMs, including NP2, NP3, NP5, NP6, and NP 8, were also selected for the 30%.

3.4.4 AASHTO T380 Standard Method of Test for Potential Alkali Reactivity of Aggregates and Effectiveness of ASR Mitigation --- Miniature Concrete Prism Test (MCPT) [2]

This test method allows the detection of the potential for the deleterious alkali-silica reaction of aggregate in 2in×2in×11.25in miniature concrete prisms within 56 days (8 weeks) for most of the aggregates. An additional 28 days (4 weeks) may be necessary in the case of low/slow reacting aggregates to assess their potential reactivity. To evaluate the effectiveness of mitigation measures of SCMs, the test method is conducted for 56 days. MCPT is developed from the existing test methods and combines their advantages. Compared to ASTM C1260, MCPT improves the accuracy and is able to evaluate the coarse aggregate. Meanwhile, MCPT promotes efficiency compared to ASTM C1293, which only yields results in 8-week but ASTM C1293 needs a 2-year duration.

The cement content in the concrete mixture was 420 kg/m^3, and the total alkali content of cement used in this study should meet the Na_2O_{eq} content of 0.90 ± 0.10 percent. The fineness modulus of fine aggregates conformed to 3.6 ± 0.3, and coarse aggregates' size distribution needed to follow Table.2-5. Water to-cementitious ratio was 0.45 by mass, and NaOH dissolved in the

mixing water maintained the alkali content of the concrete mixture to 1.25% by cement mass. If SCMs replaced cement in the concrete mixture, the NaOH added to the mixture should be adjusted to maintain the ratio of 1.25%. Use a dry mass of coarse aggregate per unit volume of concrete equal to 0.65 of its dry-rodded bulk density.

Table 2- 5 Aggregate Size Distribution for AASHTO T380[2]

Passing Sieve Size	Retained on Sieve Size	Mass,%
13.5mm (1/2 in.)	9.5mm(3/8in.)	57.5
9.5mm (3/8 in.)	4.75mm(No.4)	43.5

The specimens are cast and cured in the following steps:

1. Specimens were cast and stayed in the molds for 24 hours. During the initial 24 hours, specimens were stored in a moist room, preventing moisture evaporation.
2. Next, the specimens were stored in the water at 60 ± 1.7 °C for 24 hours. Sufficient water was required to immerse the specimens in the sealed container. In addition, the water needed to be preconditioned in the oven for 24 hours to reach the temperature of 60 °C.
3. Then the specimens were moved to the NaOH solution, which was also mandatory for preconditioning. The concentration of NaOH was 1N, and the amount of NaOH should be sufficient to immerse the specimens. After all the steps, specimens were immersed in the NaOH in the 60 °C oven.

The zero reading was measured after the water bath, and the subsequent readings were collected periodically at 3, 7, 10, 14, 21, 28, 42, and 56 days. Some aggregates reacted slowly so additional measurements may be needed at 70 and 84 days. During the period, the mass of the container should be measured as well because the moisture content of the NaOH solution can evaporate due to the container's bad sealed condition, which further increases the NaOH solution's concentration. The high-concentration solution exacerbated the ASR expansion and resulted in

misleading results. Therefore, if the mass of the container was smaller than the previous measurement, extra moisture should be added to the solution to calibrate the concentration.

The criteria for evaluating whether SCMs are effective in mitigating ASR in the MCPT method at 56-day are the following:

1. Expansion<0.020% Effective;
2. 0.020%<Expansion<0.025% Uncertain
3. Expansion>0.025% Not effective.

For the specimens aged between 56-day to 84-day (8 weeks to 12 weeks), the average expansion should be controlled less than 0.010% per 2 weeks. In this test, three different SCMs replacement levels were conducted to evaluate the high alkali SCMs ASR mitigation performance, which was 20%, 30%, and 40% by the mass to cement. All eight SCMs were used for the 20% replacement levels test, and five SCMs, including NP2, NP3, NP5, NP6, and NP 8, were selected for the 30% and 40% replacement levels as well.

3.5 Other Concrete Durability Test

3.5.1 ASTM C596-18 Standard Test Method for Drying Shrinkage of Mortar Containing Hydraulic Cement --- Drying Shrinkage [15]

Mortar bars were prepared and cured for all the test mixtures according to ASTM C596 [8] to evaluate whether the mortar drying shrinkage behavior was affected by blending with high alkali SCMs. Five SCMs, including NP2, NP3, NP5, NP6, and NP 8, were conducted in this test. The standard suggested the mixture was mixed with 750 g of cement and 1500 g of sand and water, which was designed to achieve a similar flow (110 ± 5 %). Due to the research purpose difference, the mixture in this study was 0.485 water to cementitious ratio, 3.25 sand to cementitious ratio, and test groups with 20% SCMs replacement by mass.

The mortar bars were placed in the moist room for 24 hours after molding, then moved to lime-saturated water for 48 hours. The zero reading was recorded after the standard curing. Then specimens were kept in the air chamber at 23 °C and 50% relative humidity. The length change of mortar bars was continuously monitored unit no further shrinkage occurred.

3.5.2 ASTM C1012-18b Test Method for Length Change of Hydraulic-Cement Mortars Exposed to a Sulfate Solution --- Sulfate Resistance Test [9]

This test aimed to determine the length change of mortar bars with different SCMs immersed in the sulfate solution. Five SCMs, including NP2, NP3, NP5, NP6, and NP 8, were conducted in this test.

The mortar bars were mixed with the 0.485 water-cementitious and 3.75 sand-cementitious ratios, and the test groups had 20% SCMs replacement of cement. Six bars and 21 cubes were cast, respectively. After molding, the specimens were placed in the curing container on top of the risers.

The container was covered by lids, which prevented the specimens from evaporating. Then the containers were placed into the oven at 35±3°C for 24 hours before demolding.

After demolding, all the specimens were stored in saturated limewater. Cubes were used for measuring the compressive strength of the mixture. Two cubes were measured each time, and their average values were calculated. When the average values reached 20 MPa [2850 psi], the zero readings were recorded, and then mortar bars were stored in the sodium sulfate solution (Na_2SO_4). In order to keep the consistency of the results, all groups were not immersed in Na_2SO_4 solution until the last groups reached target strength. The Na_2SO_4 solution was firstly mixed by dissolving 50.0g of Na_2SO_4 in 900 mL water. The initial solution was diluted with additional water till obtaining 1 L solution. The solution was measured pH by the pH meter after preparation. If the pH did not in the range of 6.0 to 8.0, the solution had to be re-prepared. In addition, the volume proportion of solution and mortar bars was 4.0 ± 0.5.

The subsequent length change measurements were at 1, 2, 3, 4, 8, 13, and 15 weeks after the bars were placed in the sulfate solution. The 4, 6, 9, and 12 month length changes were also collected. Furthermore, the solution was discarded after each measurement.

3.5.3 ASTM C1202-22 Test Method for Electrical Indication of Concretes Ability to Resist Chloride Ion Penetration --- Rapid Chloride Penetration Test (RCPT) [6]

This method was applied to determine the influence of high alkali SCMs on the electrical conductance of concrete. Five SCMs, including NP2, NP3, NP5, NP6, and NP 8, were conducted in this test.

The 4in×8in (diameter × height) concrete cylinders were cast with the 20% SCMs replacement by mass and stored in a moist room for 56-day. Then the cylinders were cut into 4in×2in by the water-cooled diamond saw. The small cylinders were placed in the ambient room

for several hours, which allowed the samples completely dry. Then use the epoxy-sealed cylinders' side surface and let the two-ends surfaces be exposed. When the epoxy was no longer sticky, the specimens were placed in the desiccator and pumped for 3 hours. Next, the stopcock was opened, which drained sufficient water into the desiccator. When specimens were completely immersed in the water, close the stopcock and let the vacuum pump run for another 1 hour. After this, turn off the pump and allow the air to enter the desiccator. The specimens were kept in the water for around 18 h ± 2h. After all the preparation procedures, the specimens were placed in the cell immediately, and 3.0 % sodium chloride (NaCl) solution and 0.3 N sodium hydroxide (NaOH) solution were filled into the side of the cell. 3% NaCI was prepared by the mass ratio of NaCI to distilled water. 0.3 N NaOH was 0.3 mol of NaOH in the 1 L solution. After checking the cell was assembled properly and no leakage happened, connect the wire to the cell posts, and turn on the equipment. The voltage was kept at 60V constantly. The ion penetration was collected for the following 6 hours every half an hour.

3.6 Compressive Strength

The standard ASTM C39 / C39M-21[16] test method and ASTM C109/109M -21[17] were used to evaluate the compressive strength of cylindrical concrete specimens and hydraulic cement mortar cubes.

After reaching testing age, the cured concrete specimens were capped with neoprene pads and placed vertically in a compression testing machine. A relatively constant load was applied to the specimens based on the specimens' diameter till the specimens failed. The maximum failure load applied was recorded, and the compressive strength was calculated using the cross-sectional area of the concrete specimen. Mortar cubes had the same procedures, but there was no need for capping the neoprene pads.

3.7 Chemical Analysis

3.7.1 Pore Solution Analysis

Pore solution analysis used in this study was to determine the impact of SCMs on the concentration of alkali ions in the cementitious mixture pore solution. The cement paste was cast in 2 Oz plastic jars with a 0.5 water-to-cementitious ratio. The test specimens were mixed with 20% and 40% SCMs replacement as well. After casting, the specimens were sealed with 53 mm caps and stored in a moist room. The specimens were measured at different ages, which were 1 day, 7-day, and 14-day, respectively.

The method used for extracting pore solution was pore water expressions. Before extracting process, using the dry graphite lube sprayed on the piston and inner hole of the expression set-up to decrease the friction when applying the load. The plastic plate was placed in the set-up hole, and then the samples were placed in the hole. Next, the piston was alignment to the hole and the pressure by the compressive machine. A straw was used to connect the small hole at the bottom of the expression set-up and the pore solution collector. After each collection, the set-up was cleaned with 70% alcohol. In addition, the extracted pore solution was sealed in the stored ambient chamber. The pore solution was diluted by 2% HNO_3 and analyzed by inductively coupled plasma optical-emission spectrometry (ICP-OES).

Due to this study still being in the preliminary stage, only three SCMs, NP 2, NP3, and NP 5, were selected for the pore solution analysis. The cementitious mixture evaluated in this test was the paste with a 0.5 w./c ratio.

3.7.2 Scanning Electron Microscope (SEM) and Energy Dispersive X-ray Spectroscopy (EDX)

The microstructure characteristics of concrete were examined through scanning electron microscopy (SEM) and energy-dispersive X-ray spectroscopy (EDX) assessments. The water saw cut the concrete samples to the proper cross-section size. Then, the obtained samples were rinsed for a few minutes with isopropanol in an ultrasonic bath to remove residue paste on the surface. After cleaning, the samples were immersed in the isopropanol for at least seven days to stop the cement hydration.

Before impregnating samples in the epoxy, the samples were placed in the vacuum drying in the desiccator for at least two hours. Then, the cross-section concrete samples were embedded in the mold with epoxy and dried in the desiccator with vacuum conditions for 24 hours. The epoxy was mixed with resin and hardener, and the ratio of resin and hardener was 0.1. Once the sample was removed from the mold, both the top side of the embedded sample (opposite the sample's surface) and the bottom (where the sample is) were pre-polished using SiC paper and isopropanol as lubricant. In sequence, the bottom side was polished using 80-grade, 500-grade, and 1200-grade diamond/SiC to remove epoxy and let the bottom surface be exposed. After the precondition polishing, the samples were polished by the diamond spray of 9 μm, 3 μm, and 1 μm in order. Hitachi 3400 SEM was used to evaluate concrete samples with conditions of 20 kV and 30Pa.

3.8 Reference

[1] "ASTM C150/C150M-21 Standard Specification for Portland Cement," American Society for Testing and Materials, Aug. 2021.

[2] "AASHTO T380 Standard Method of Test for Potential Alkali Reactivity of Aggregates and Effectiveness of ASR Mitigation Measures (Miniature Concrete Prism Test, MCPT)," American Association of State HIghway and Transportation Officials.

[3] C09 Committee, "ASTM C1293-20a Standard Test Method for Determination of Length Change of Concrete Due to Alkali-Silica Reaction," ASTM International, Jul. 2020.

[4] C09 Committee, "ASTM C1260-21 Standard Test Method for Potential Alkali Reactivity of Aggregates (Mortar-Bar Method).pdf," ASTM International.

[5] C09 Committee, "ASTM C1567-21 Test Method for Determining the Potential Alkali-Silica Reactivity of Combinations of Cementitious Materials and Aggregate (Accelerated Mortar-Bar Method)," ASTM International. doi: 10.1520/C1567-13.

[6] C09 Committee, "ASTM C1202-22 Test Method for Electrical Indication of Concretes Ability to Resist Chloride Ion Penetration," ASTM International. doi: 10.1520/C1202-22.

[7] D05 Committee, "ASTM D7348-21Test Methods for Loss on Ignition (LOI) of Solid Combustion Residues," ASTM International. doi: 10.1520/D7348-21.

[8] C09 Committee, "ASTM C618-22 Specification for Coal Fly Ash and Raw or Calcined Natural Pozzolan for Use in Concrete," ASTM International. doi: 10.1520/C0618-22.

[9] C01 Committee, "ASTM C1012-18b Test Method for Length Change of Hydraulic-Cement Mortars Exposed to a Sulfate Solution," ASTM International. doi: 10.1520/C1012_C1012M-18B.

[10] C09 Committee, “ASTM C1897-20 Standard Test Methods for Measuring the Reactivity of Supplementary Cementitious Materials by Isothermal Calorimetry and Bound Water Measurements,” ASTM International. [Online]. Available: https://www.astm.org/c1897-20.html

[11] C09 Committee, “ASTM C311-22 Test Methods for Sampling and Testing Fly Ash or Natural Pozzolans for Use in Portland-Cement Concrete,” ASTM International. doi: 10.1520/C0311_C0311M-22.

[12] C01 Committee, “ASTM C191-21 Test Methods for Time of Setting of Hydraulic Cement by Vicat Needle,” ASTM International. doi: 10.1520/C0191-21.

[13] “ASTM C511-19 Standard Specification for Mixing Rooms, Moist Cabinets, Moist Rooms, and Water Storage Tanks Used in the Testing of Hydraulic Cements and Concretes,” American Society for Testing and Materials, Jul. 2019.

[14] C09 Committee, “ASTM C33/C33M-18 Specification for Concrete Aggregates,” ASTM International. doi: 10.1520/C0033_C0033M-18.

[15] “ASTM C596-18 Standard Test Method for Drying Shrinkage of Mortar Containing Hydraulic Cement,” American Society for Testing and Materials, Dec. 2018.

[16] C09 Committee, “ASTM C39-21 Test Method for Compressive Strength of Cylindrical Concrete Specimens,” ASTM International. doi: 10.1520/C0039_C0039M-21.

[17] C01 Committee, “ASTM C109/109M -21 Test Method for Compressive Strength of Hydraulic Cement Mortars (Using 2-in. or [50mm] Cube Specimens),” ASTM International. doi: 10.1520/C0109_C0109M-21.

CHAPTER IV IMPACT OF HIGH ALKALI NATURAL POZZOLANS and RECLAIMED FLY ASH ON ALKALI-SILICA REACTION MITIGATION

Abstract

Due to the shortage of proper supplementary cementitious materials (SCMs) in the concrete industry, seeking a new alternative is necessary. High-alkali supplementary cementitious materials (SCMs) is generally avoided in concrete because of potentially exacerbating the alkali-silica reaction (ASR). This study investigates the feasibility of materials with this characteristic using different ASR methods, including ASTM C1567 (AMBT), C1293 (CPT), and AASHTO T380 (MCPT), for evaluating high-alkali SCMs' performance in controlling ASR expansion. The paste pore solution analysis was conducted to determine the alkali ions concentration and further explain high-alkali SCMs ASR mitigation performance. Thermogravtrimc analysis (TGA) was used in this study to evaluate the performance of high-alkali SMCs on consuming calcium hydroxide (CH). The findings showed that high-alkali SCMs effectively lowered the ASR expansion compared to the control, and the extent of mitigation improved with the SCMs replacement level increasing. Not all alkali content of SCMs was released into the pore solution during the reaction, and there was no direct correlation between the alkali content of SCMs and their ASR mitigation performance or alkali ions concentration. High-alkali SCMs effectively consumed CH in the paste matrix, and the amount of CH consumed increased with sample age raising. Pore solution and TGA analysis support results obtained from ASR experiments. According to the results, high-alkali SCMs have the potential to be the alternative option for the current SCMs market.

Keywords: Alkali-silica reaction; High-alkali supplementary cementitious materials; Alkali-silica evaluation method; Pore solution Analysis; Thermogravtrimc Analysis (TGA)

4.1 Introduction

Alkali–silica reaction (ASR) is an acknowledged concrete durability problem that results from deleterious reactions between alkali hydroxides in the pore solution of concrete and reactive forms of silica, typically present in the interface between aggregates and cement paste. ASR reaction is a multi-stage process [1]–[4]. Alkali ions in concrete pore solution primarily derived from cement hydration react with reactive silica from specific siliceous aggregates. The reactive silica, mainly with the structure of siloxane groups (≡Si-O-Si≡), dissolves by hydroxyl attack. The silanol groups (≡Si-O-Si≡) on the silica surface react with hydroxide ions (OH^-) and generate one negative charge on the silica surface(Si-O^-). Positive alkali ions (Na^+ and K^+) neutralize the silica surface's negative charge, forming the alkali-silica gel (ASR gel) and alkali calcium silicate. Formation ASR gel is not expansive but is very hygroscopic[8], which attracts moisture from the surrounding cement paste, resulting in irreversible swelling. Due to the expansion confined in the small concrete pore structures, the swelling process will build up an internal osmotic pressure in the concrete, further resulting in cracks in the aggregates and cement paste.

The occurrence of ASR in concrete depends on three indispensable ingredients[5]: 1) a high alkali environment (high pH) with alkali ions; 2) reactive siliceous components from aggregate; 3) sufficient moisture in the system. Therefore, to avoid ASR in the concrete, using low-alkali cement, lowering the moisture content in the mixture, and using non-reactive aggregate are the strategies. However, due to the water requirements of mixed proportions and local material selection limitations, using supplementary cementitious materials (SCMs) as mineral additives in concrete

is the most effective and practical method to mitigate ASR, which T.E. Stanton first discovered in 1950 [6]. The mechanism of SCMs mitigating ASR can be understood from three aspects [7], [8]:

1) Calcium hydroxide consumption. The primary cement hydration products are calcium silicate hydrate (C-S-H) and calcium hydroxide (CH) [9]. Compared to the C-S-H, CH not only does not contribute much to concrete strength [10] but also involves many deteriorating reactions damaging the concrete and affecting durabilities like ASR and sulfate attacks [11], [12], [5], [13]. SCMs can consume CH, which is also known as pozzolanic reactivity. The reactive silicate or aluminate in SCMs reacts with CH and transforms it to C-S-H or calcium aluminate hydrate (C-A-H) [6].
2) Alkali-binding and lowering the pH. The pozzolanic reaction consumes CH and lowers the Ca/Si ratio of the hydrate. The lower Ca/Si ratio hydrates have a higher alkali binding ability [5] due to the increased amount of acidic silanol (Si-OH) sites in the C-S-H layers. The layer with negative charges [14] neutralizes with positive alkali ions. For the pH, Vollpracht et al.[15] reviewed the impact of different SCMs on the concrete pore solution, which indicates that SCMs effectively lower the pH of the concrete pore solution.
3) Reduce permeability. Replacing cement with SCMs decreases the concrete permeability [16] due to densifying the interfacial transition zone (ITZ) [17]. With permeability decreasing, it prevents deleterious compounds from ingressing into the concrete.

SCMs' efficiency in suppressing ASR can be evaluated by measuring ASR expansion in the laboratory with several experimental methods. ASTM C1567 accelerated mortar bar test (AMBT) is the most widely used method to evaluate the SCMs' ASR mitigation ability. The method has the efficiency advantage of only needing a 14-day test duration, but the accuracy is unreliable. ASTM C1293 concrete prism test (CPT) is the most reliable method for assessing aggregate reactivity,

both coarse and fine, and SCMs' ASR mitigating ability. Opposite to AMBT's high efficiency, CPT requires two years duration. AASHTO T380 miniature Concrete Prisms Test (MCPT) is the most recently developed method, combining the advantages of AMBT's efficiency and CPT's accuracy. MCPT's experimental duration is 56 days, but in the case of low/slow reacting aggregates, an additional four weeks are necessary and a maximum of 84 days.

Fly ash is the principal SCMs used in the concrete industry. However, due to the global environmental policy changes, lots of power industry burning coal has switched to using clean energy to reduce carbon footprint emissions, resulting in the shortage of availability of industrial by-products and product price increases [18], [19]. Therefore, searching for new substitutes for the worldwide SCMs industry is urgent. Natural pozzolans, such as volcanic tuffs or pumices, are natural materials that have pozzolanic properties. Some researchers have proved that natural pozzolans blended with cement can suppress ASR expansion [20], [21]. However, the previous study focused mainly on using natural pozzolans with low alkali content. There is currently limited research on applying natural pozzolans with high alkali content in concrete.

The primary concern for using high-alkali SCMs, whose alkali content is generally over 4%, is that the materials could exacerbate ASR distress because the alkali ions in SCMs could release into and increase the alkali loading in the concrete pore solution. Shehata et al.'s research [22] evaluated the alkali release characteristics of blended cement with high alkali SCMs. Their research indicated that the simulation solution with high total alkali SCMs has a high alkali ions concentration. However, P. K. Mehta's research [23] indicated that some alkali content of natural pozzolans existed as the crystal phase, which can not release into the pore solution. Also, Uribe-Afif et al. [24] evaluated the chemical composition of several natural pozzolans. Even though some natural pozzolans had significantly higher alkali content and one of the equivalent alkalis contents

reached 6.89%, the available alkali content was only 1.09%, which meant only 15% of the total alkalis of this natural pozzolan could release into the pore solution. Additionally, Kim et al.'s research [25] indicated that using the change of alkalis ion concentration in the pore solution directly predicted the ASR expansion process.

This paper evaluates the performance of high-alkali SCMs in mitigating ASR by various accelerated ASR expansions in the laboratory. Pore solution analysis was used to quantify the alkali ions concentration and further discovered whether the alkalis ions of SCMs impacted the alkalinity of the pore solution. Based on the results, make a preliminary judgment that high-alkali SCMs potentially be an alternative for the SCMs global market, which relieves the SCMs shortage problem.

4.2 Materials and Method

4.2.1 Materials

Two types of ordinary Portland cement (OPC) meeting ASTM C150 [23] were used in this study: A low-alkali Type I/II Portland cement (Na_2O_e = 0.38%) from Argos cement company, Harleyville, SC, and a high-alkali Type I Portland cement (Na_2O_e = 1.00%) from Lehigh Hanson Inc. The chemical composition and physical properties of both Portland cements are presented in Table 4- 1.

This study tested six natural pozzolans and two reclaimed fly ashes provided by the Natural Pozzolan Association (NPA) and its member companies. The natural pozzolans and reclaimed fly ashes were labeled from NP 1 to NP 5 and RFA 1 to RFA 2. The materials' chemical compositions and particle size distribution are presented in Table 4- 1 and Figure 4- 1, measured by wavelength X-ray fluorescence and laser diffraction, respectively.

The reactive aggregate used in this study is a known reactive aggregate from the Goldhill Quarry in North Carolina, which consists of reactive metatuff–argillite. The aggregate's reactivity was evaluated by ASTM C1260 [26], shown in Figure 4- 2. The aggregate's specific gravity and percent absorptions were 2.6 and 1%, respectively.

Table 4- 1 SCMs Chemical Composition

		SiO_2	Al_2O_3	Fe_2O_3	S+Al+Fe	CaO	MgO	Na_2O	K_2O	Na_2O_e	LOI	SG	Amorphous Level (%)
	Low-alkali Portland cement	19.93	4.77	3.13	27.83	62.27	2.70	0.06	0.48	0.37	2.6	3.15	NA
	High-alkali Portland cement	19.00	4.99	2.11	26.1	62.45	2.84	0.31	1.05	1.0	NA	3.15	NA
Volcanic rhyolitic tuff	NP 1	68.62	13.14	1.91	83.67	1.73	1.43	2.7	3.2	4.82	7.18	2.53	37.67
Pumice	NP 2	73.42	12.30	1.41	87.13	0.79	0.23	2.9	4.2	5.61	4.72	2.35	98.55
Pumice	NP 3	65.48	11.19	1.75	78.42	2.99	0.33	3.6	3.4	5.85	10.87	2.26	3.38
Volcanic rhyolitic tephra	NP 4	71.95	12.26	1.50	85.71	0.93	0.39	3.9	4.0	6.51	4.88	2.35	87.76
Volcanic glass	NP 5	71.21	12.99	0.90	85.1	0.56	0.13	3.9	4.1	6.57	5.95	2.40	100
Pumice	NP 6	71.91	11.68	2.18	85.77	0.32	0.09	5.5	4.2	8.28	3.94	2.34	91.17
Reclaimed fly ash	RFA 1	53.06	15.13	6.88	75.07	13.70	4.53	3.4	1.9	4.69	0.55	2.56	82.48
Reclaimed fly ash	RFA 2	56.81	14.20	2.69	73.7	10.13	1.41	2.8	2.7	4.56	8.42	2.42	88.88

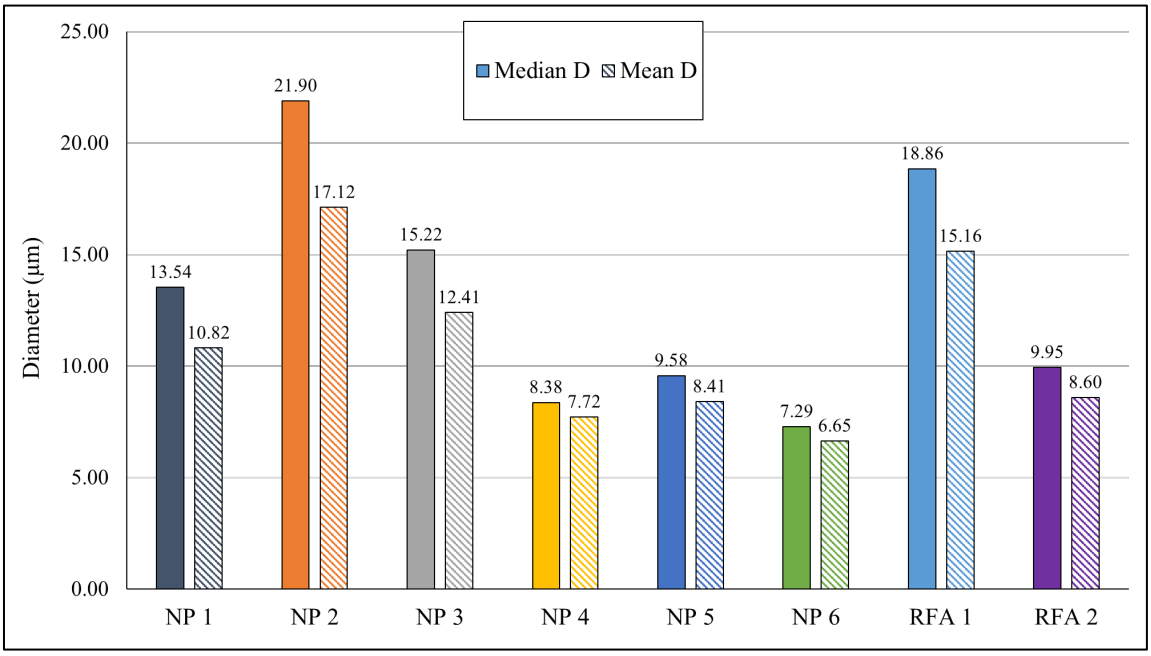

(a)

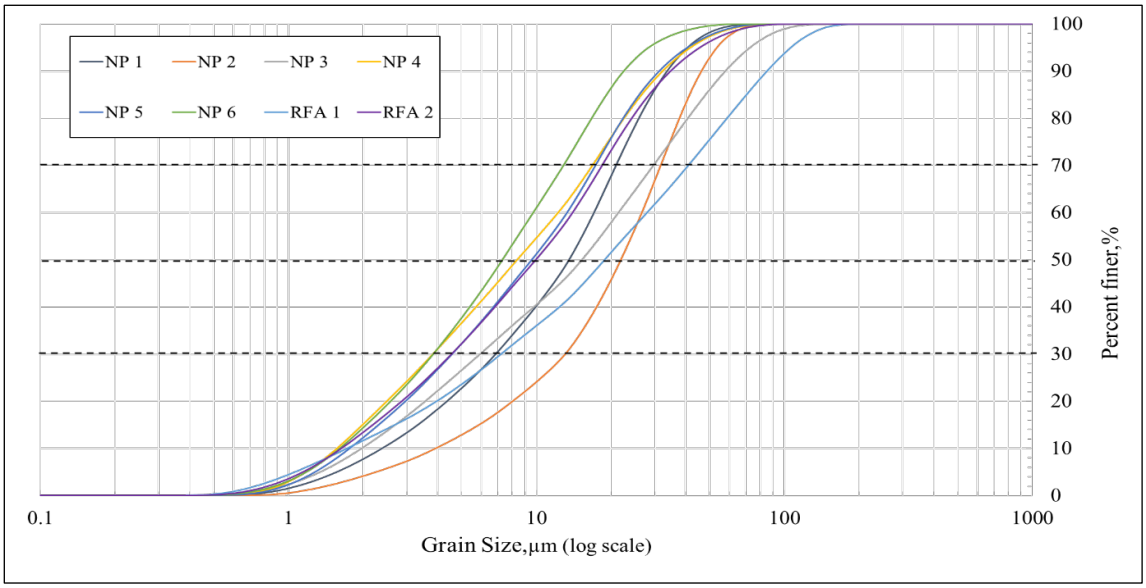

Figure 4- 1(a)SCMs' Particle Size; (b)Particle Size Distribution of Natural Pozzolans

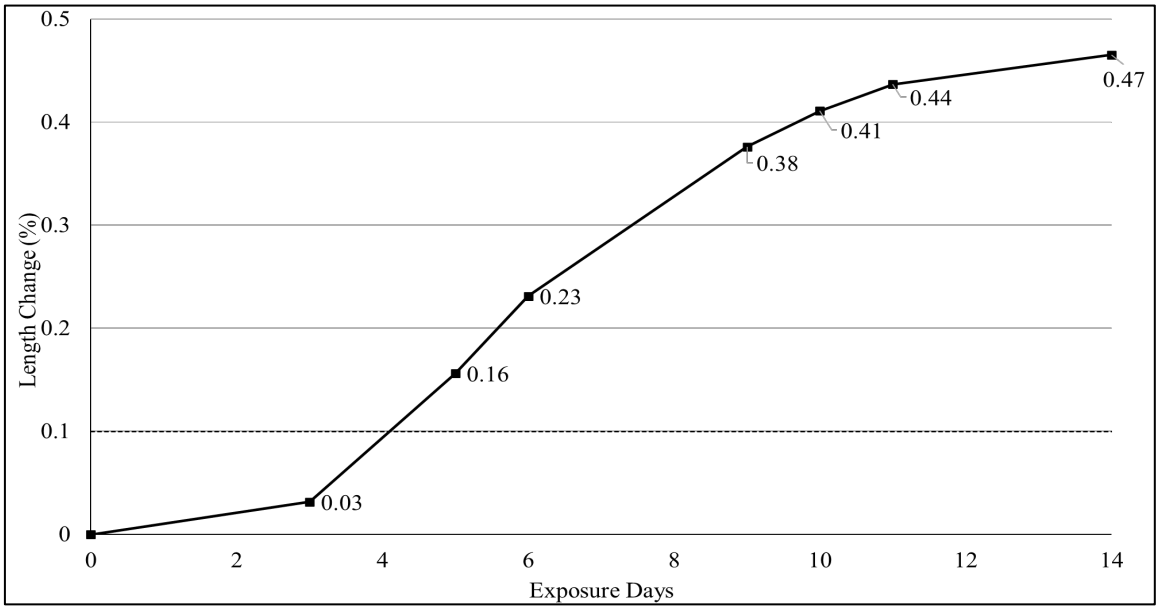

Figure 4- 2 ASTM C1260

4.2.2 ASTM C1567-21 Accelerated Mortar Bar Test (AMBT) [27]

The mortar mixtures were prepared according to ASTM C1567 [27], using fine reactive aggregate and a mixture of ordinary Portland cement (OPC) and SCMs as the binder. For each mixture, four 1 in. x 1 in. x 11.25 in. (25 mm × 25 mm × 285 mm) mortar prisms were cast with 0.47 water-binder ratio (w/b) and 2.25 sand-binder ratio (s/c). Also, the gradation of fine aggregate followed ASTM C1260 [26], shown in Table 4- 2. SCMs were used at 20% dosage levels by mass of cement.

The specimens were cast in the ambient temperature room with relative humidity(RH) not less than 50%, then cured in the moist room for 24±2-h. The lengths of the prisms were measured periodically for 14 days. The water and soak solution of 1N NaOH must be preconditioned in the oven to reach 80 ± 2 °C before use. The specifications for evaluating the ASR mitigation performance of test materials are shown in the following:

4. Expansion<0.1% innocuous;
5. 0.1%<expansion<0.2% inconclusive;

6. Expansion>0.2% reactive.

Table 4- 2 ASTM C1260 Fine Aggregate Gradation

Sieve Size		Mass, %
Passing	Retained on	
4.75 mm (No.4)	2.36 mm (No.8)	10
2.36 mm (No.8)	1.18 mm (No.16)	25
1.18 mm (No.16)	600 μm (No.30)	25
600 μm (No.30)	300 μm (No.50)	25
300 μm (No.50)	150 μm (No.100)	15

4.2.3 ASTM C1293-20a Concrete Prisms Test (CPT) [28]

Concrete prisms were prepared by mixing non-reactive aggregate, coarse reactive aggregate, and binder mixtures of high-alkali Type I cement and SCMs. In this method, cementitious material content was 420 ±10 kg/m^3, with w/b of 0.45. SCMs were used at 20% dosage levels by mass of cement. The coarse aggregate had a dry mass per unit volume of concrete of 0.70, and its gradation followed the requirement of ASTM C1293, shown in Table 4- 3. Reagent-grade NaOH pellets were dissolved in the mixing water to boost the alkali content of the concrete to 1.25% by the mass of cement. After demolding, the concrete was stored in the room at 38.0±2°C and 100% RH. The zero reading was taken after demolding, and the subsequent readings were measured at 7-day, 28-day, 56-day, 3-month, 6-month, 9-month, 12-month, 15-month, 18-month, 21-month, and 24-month. The expansion criteria of ASTM C1293 without SCMs are the following:

4. Expansion<0.04% at one-year, non-reactive
5. 0.04%<expansion<0.12% at one-year, marginal
6. Expansion>0.12% at one-year, highly reactive

However, for the concrete mixed with fly ashes or other SCMs, the mineral additives effectively mitigate the ASR when the ASR expansion is less than 0.04% in two years.

Table 4- 3 ASTM C1293 Coarse Aggregate Gradation

Passing Sieve Size	Retained on Sieve Size	Mass,%
19.5mm	12.5mm	1/3
12.5mm	9.5mm	1/3
9.5mm	4.75mm	1/3

4.2.4 AASHTO T380 Miniature Concrete Prism Test (MCPT) [29]

AASHTO T380 (MCPT) was used to evaluate the high-alkali SCMs to mitigate ASR in this study. In this method, the cementitious materials content of concrete mixtures was maintained at 420 kg/m^3, with a w/b ratio of 0.45. The dry mass of coarse aggregate per unit volume of concrete was maintained at 0.65, and the coarse aggregates' gradation followed the recommended gradation per AASHTO T380, shown in Table 4- 4. The fineness modulus of fine aggregates conformed to 2.60 ± 0.3. Reagent-grade NaOH pellets were dissolved in the mixing water to boost the alkali content of the concrete to 1.25% by the mass of cement. SCMs were used at dosage levels of 20%, 30%, and 40% by mass of cement.

The test specimens were cast and cured at ambient temperature and 100% RH for 24 hours. After demolding, the specimens were placed in water at 60°C for another 24 hours. The zero-day reading was taken at the end of 24 hours of water bath curing. Then, the specimens were transferred into a sealed container with 1N NaOH maintained at 60°C. The prism length changes were recorded periodically at 0, 3, 7, 10, 14, 21, 28, 42, 56, 70, and 84 days. The criteria for evaluating the efficacy of SCMs in mitigating ASR in the MCPT method at 56-days are as follows per AASHTO T380:

4. Expansion < 0.020% - Effective ASR Mitigation;
5. 0.020% < expansion < 0.025% Uncertain ASR Mitigation

6. Expansion > 0.025% Not effective ASR mitigation

If the samples exhibit expansion between 0.20 and 0.25 at 56 days, the average expansion between 56-day to 84-day (8 weeks to 12 weeks), should be less than 0.010% per 2 weeks for the mitigation measure to be considered effective.

Table 4- 4 AASHTO T380 Coarse Aggregate Gradation

Passing Sieve Size	Retained on Sieve Size	Mass,%
12.5mm (1/2 in.)	9.5mm(3/8in.)	57.5
9.5mm (3/8 in.)	4.75mm(No.4)	42.5

4.2.5 Pore Solution Analysis

Pore solution extraction and analysis were performed on binder paste specimens at different ages to determine the pore solution chemistry. The samples were mixed with binders consisting of high-alkali cement and SCMs, and deionized water. The w/b ratio for this study was maintained at 0.60 for all samples in this experiment. The method used to extract pore solution in this study was using a pore solution expression die based on Barneyback and Diamond [30]. Maximum stress of about 260 MPa was applied to extract the pore solution from samples. The load rate was maintained between 1 and 1.8 kN/s. The pore solution was collected into centrifuge tubes, preventing potential contamination from carbonation, and they were stored at 4°C in a refrigerator before testing.

Inductively coupled plasma optical emission spectroscopy (ICP-OES) was used to analyze the pore solution to determine the concentration of alkalis ions (Na^+&K^+). Before running ICP, the pore solution was centrifuged for 10 mins to separate any solids and the liquid. One ml pore solution was extracted from the storage tubes and diluted with 2% Nitric acid (HNO_3) based on

mass. The pore solution's dilution factor was 100, meaning a 100 ml mixture solution contained 1 ml of pore solution. All water used in this study was deionized water.

4.2.6 Thermogravimetric Analysis (TGA) for Determining Calcium Hydroxide (CH) Consumption

Thermogravimetric analysis (TGA) was conducted to determine the calcium hydroxide (CH) amount in the cement paste. For this testing, AutoTGA Q5000 instrument was employed. The pastes were prepared by blending low-alkali cement with SCMs at a 20% mass replacement of cement, at a water-to-binder ratio of 0.42. The prepared paste samples were stored in a sealed container and were tested at the ages 7-day, 28-day, and 56-days. After casting, the specimens were sealed in air-tight test tubes to avoid potential carbonation and stored in an air chamber maintained at 23°C and 50% RH. Before testing, the samples were de-molded from the tubes and ground using an agate mortar and pestle to pass the No.100 sieve (150 μm). Then, the powder samples were immersed in 50ml isopropanol for 15 minutes to remove moisture from the powder. The suspension was filtered by using Büchner funnel to obtain the dehydrated powder, and 10 ml diethylene was added to the powder to remove extra isopropanol. After preparation, the sample was immediately stored in air-tight vials and tested. The weight loss observed in the samples between the temperatures of 400°C and 500°C was recorded, and the amount of calcium hydroxide ($Ca(OH)_2$) per gram of cement in the mixture was calculated using **Equation 2:**

$$Ca(OH)_2 = \frac{(Mass_{400^oC} - Mass_{500^oC}) \times (Ca(OH)_2 \text{ Molor mass})}{H_2O \text{ Molar mass}} \quad (2)$$

4.2.7 Scanning Electron Microscopy (SEM) / Energy Dispersive X-ray Spectroscopy (EDX)

The microstructure characteristics of concrete were examined through scanning electron microscopy (SEM) and energy-dispersive X-ray spectroscopy (EDX) assessments. The concrete selected in this experiment was ASTM C1293 samples after finishing two years of length measurement. The cross-section concrete samples were embedded in epoxy, and the samples' surface was exposed by polishing. The SEM/EDX was conducted by Hitachi 3400 SEM under 20 kV and 30Pa conditions.

4.3. Results

4.3.1 ASTM C1567 Accelerated Mortar Bar Test (AMBT)

Figure 4- 3 shows the length changes of ASTM C1567 mortar bars with 20% SCMs replacement. Without SCMs replacement, the control indicated the highest ASR expansion, as expected, of 0.49%. The considerable ASR expansion of control occurred from the 3rd to the 7th day; the expansion rate of this period was much higher than the other measuring time intervals. The specimens still showed an intense expansion tendency after 14 days.

All the SCMs effectively mitigated the ASR expansion compared to the control by limiting expansion lower than 0.10% at 14 days. The NPs indicated a better performance than RFAs in this test. NPs limited the ASR expansion from around 0.02% to 0.03%, but two RFAs were over 0.04%, especially RFA 1, which reached 0.07% on the 14th day. In order to avoid the potential problem of cement hydration reaction delayed by mixing with natural pozzolans, the specimens were still measured until 56 days. Even though specimens continuously expanded with time and some groups passed the threshold limit, all materials lowered the ASR expansion by at least 85% compared to the control. Therefore, AMBT results indicate that the high natural pozzolans could effectively mitigate the ASR expansion.

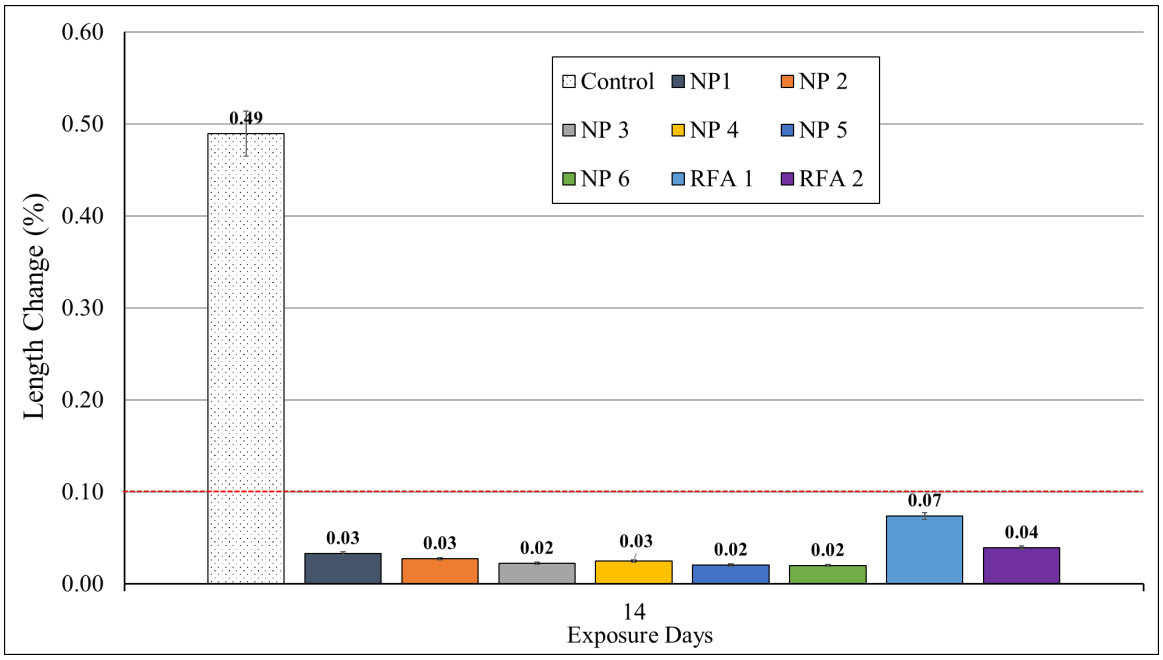

Figure 4- 3 ASTM C1567 Mortar Bar Length Change at 14 days

4.3.2 ASTM C1293 Concrete Prisms Test (CPT) [28]

Figure 4- 4 and Figure 4- 5 show the 2-year length changes of ASTM C1293 concrete prisms with 20% SCMs replacement stored in the 100% RH environment at 38 ◦C. All the mixtures shrank initially because chemical shrinkage occurred. As the degree of cement hydration increased, the absolute internal volume of initial hydration components decreased [31]. The control indicated the highest expansion of 0.169% at 2 years. The other mixtures incorporating SCMs lowered the ASR expansion compared to the control, but the extent of reduction was not as substantial as shown in the AMBT. For instance, NP 1 effectively lowered 94% ASR expansion compared to control in the AMBT, but the expansion reduction was only 30% in the CPT. Additionally, all materials were considered effective in mitigating the ASR in AMBT. However, according to the specification of ASTM C1293, none of them passed the test, as they all exceeded the threshold limit of 0.04% within two years, and most even failed less than one year. Furthermore, the expansion tendency between the control and mixtures mixed with natural pozzolans also behaved differently. The

control exhibited a much faster expansion rate in the first year compared to the second year. The net expansion values of the control group over the two years were 0.16% and 0.01%, respectively. In contrast, the test groups showed a stable expansion rate, and even after two years, the specimens still exhibited a tendency to expand.

Among the mixtures with SCMs, RFA 1 behaved weakly in mitigating ASR expansion. Even though compared to the control, RFA 1 lowered a certain extent of ASR expansion, the extent was only 17%. Additionally, RFA 1 had the worst performance in AMBT as well. In Table 4- 1, the alkali content of RFA 1 was 4.69%, and compared to other materials, the value was relatively lower, but RFA 1's expansion was the most, which indicated that the SCMs' amount of alkali content was not the direct factor to determine the ASR mitigation performance. In contrast to RFA 1, NP 4 had the best ASR mitigation performance, and it only expanded by 0.059% in two years, whose reduction reached 65%. However, NP 5's alkali content was the third the most, 6.51%. NP 5 was the second in this test, and its expansion was slightly over NP 4, which was 0.065%. For the rest of the NPs and RFAs, their results were around 0.1%.

The findings from comparing the results between AMBT and CPT indicated that only using AMBT to evaluate high-alkali SCMs was not comprehensive, and 20% of high-alkali SCMs replacement was inadequate to mitigate ASR expansion caused by this reactive aggregate. Therefore, three natural pozzolans, NP 2, NP 4, and NP 5, and two RFAs, RFA and RFA 2, were selected to run the high SCMs replacement, which increased the SCMs replacement level to 30%. This test aimed to evaluate whether increasing the replacement level could improve the ASR mitigation performance. The mixtures with the 30% replacement level were tested for one year, and the comparison results between the two replacement levels are presented in Figure 4- 6. Based on Figure 4- 6, the 30% SCMs replacement level suppressed ASR expansion compared to 20%,

with the reduction level of ASR mitigation being at least around 50%. The expansion of NP 2 at one year was 0.070% and 0.037% for 20% and 30% replacement levels, respectively. However, 30% of RFA 1 has already failed, and its expansion was 0.069% in one year. Compared to 20%of RFA 1, there was a certain extent of improvement in lowering expansion, but the value was still too high. NP 4 also performed the best in this 30%; till the latest measurement, the concrete prisms of 30% NP4 have not expanded compared to the zero reading. Additionally, RFA 2 opposed the highest expansion reduction, 0.55%, among all the mixtures, which decreased by 78% expansion.

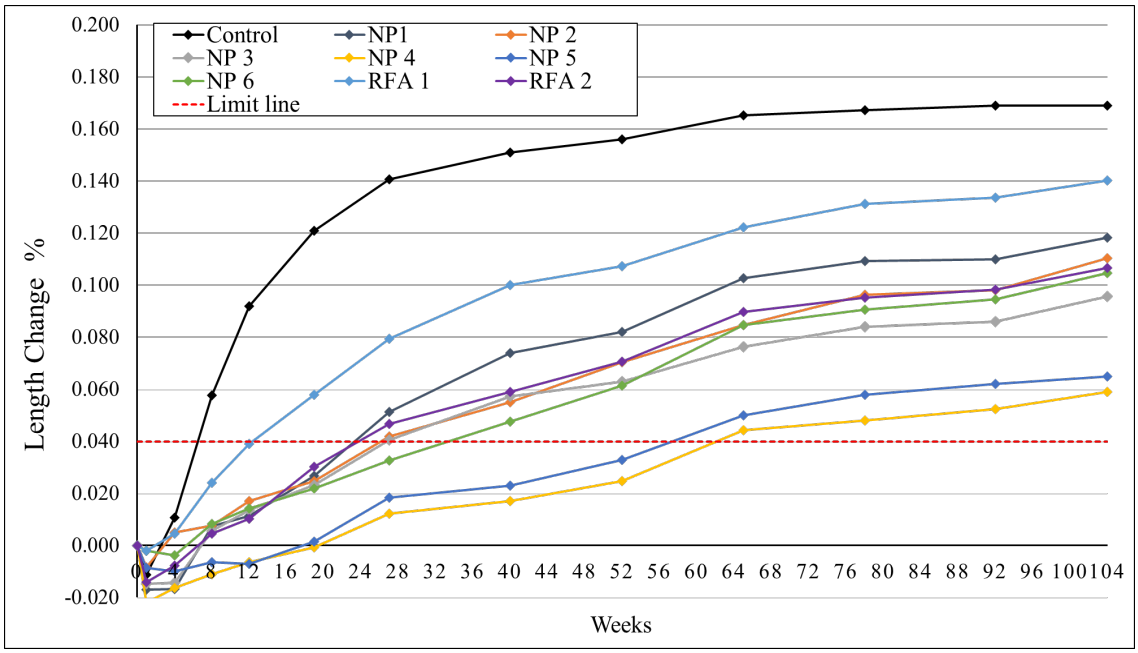

Figure 4- 4 ASTM C1293 Length Change of Concrete Prisms with 20% SCMs Replacement

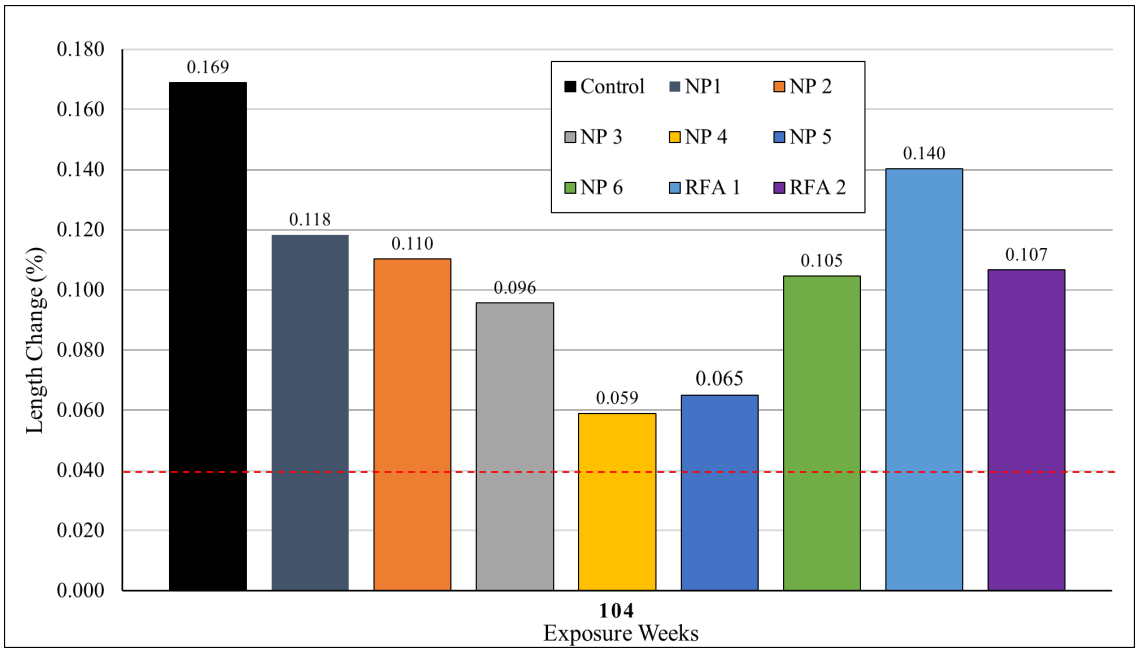

Figure 4- 5 ASTM C1293 Concrete Prisms Length Change at 2 years

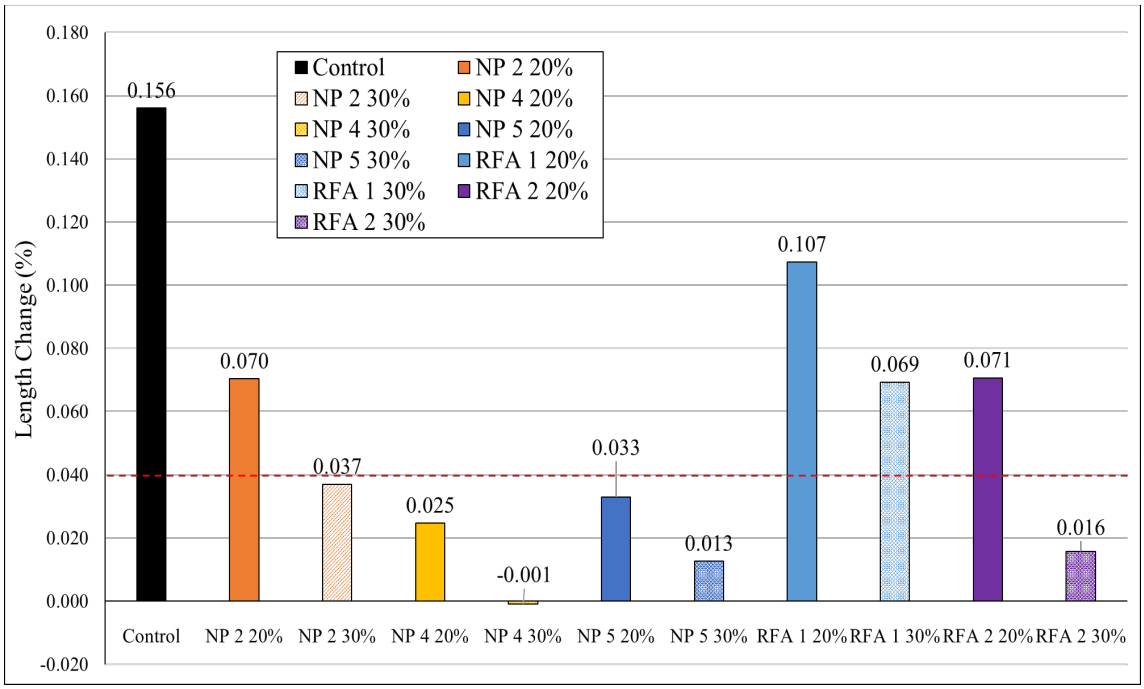

Figure 4- 6 ASTM C1293 Replacement Level 1-Year Comparison

4.3.3 AASHTO T380 Miniature Concrete Prism Test (MCPT) [29]

Figure 4- 7 and Figure 4- 8 exhibited the length change of concrete prisms in AASHTO T380 (MCPT) with 20% SCMs. In MCPT, SCMs are considered to effectively mitigate ASR when expansion is below 0.020% at 56 days, and the expansion rate should not exceed 0.010% every two weeks from day 56 to day 84.

Except for NP 2 and RFA 1, the rest of the materials were able to limit the ASR expansion to approximately or lower than 0.020% at 56 days. The expansion of NP 2 and RFA 1 was 0.026% and 0.035%, respectively. RFA 1 performed the worst in this MCPT, which kept consistent with the previous ASR experiments. Additionally, NP 2 and RFA 1 also failed to satisfy the requirement of expansion rate, and both expansion rates exceeded 0.010% per two weeks. Even though NP 1's 56^{th}-day expansion was 0.019%, less than 0.020%, meeting the requirement, its expansion rate was over 0.010%; therefore, NP 1 was not considered successful in mitigating ASR expansion. NP 4 had the lowest expansion on the 56^{th} day, but on the 84^{th} day, NP 7 performance exceeded NP 4 because NP 4 expanded a lot during the 56^{th} to 84^{th} day. During the interval, from the 56^{th} to the 84^{th} day, the rest mixtures, except NP 7, continued to expand, and their expansion values exceeded 0.020% at 84 days.

The same materials selected in CPT were conducted for the replacement level tests, and in this test, the replacement levels were increased to 30% and 40%, respectively. The comparison results are presented in Table 4-1. The results indicated that with the SCMs replacement level increasing, the ASR expansion became lower. Apart from RFA 1, the 30% replacement level was adequate for the rest of the materials to control ASR expansion of less than 0.02% on the 56^{th} and even the 84th days. 30% of RFA 1 still failed, and its expansion on the 56^{th} day was 0.035%, much

higher than the threshold of 0.020%. However, 40% of RFA 1 successfully controlled the expansion below the limit; even on the 84th day, its expansion was only 0.018%.

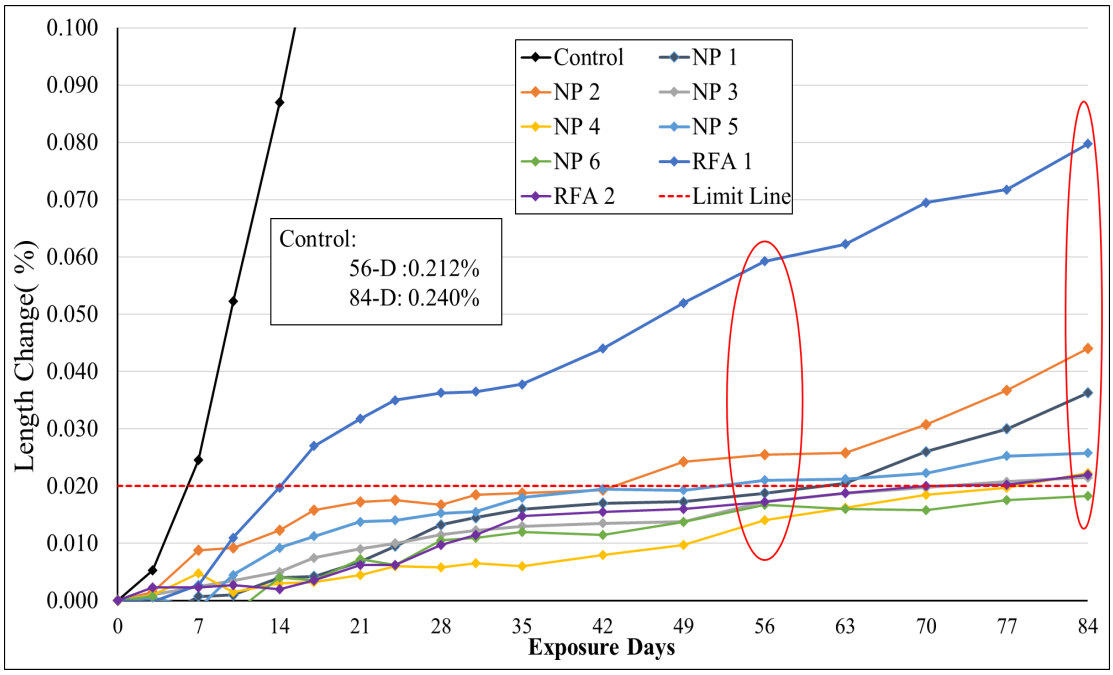

Figure 4- 7 AASHTO T380 Length Change of Concrete Prisms with 20% SCMs Replacement

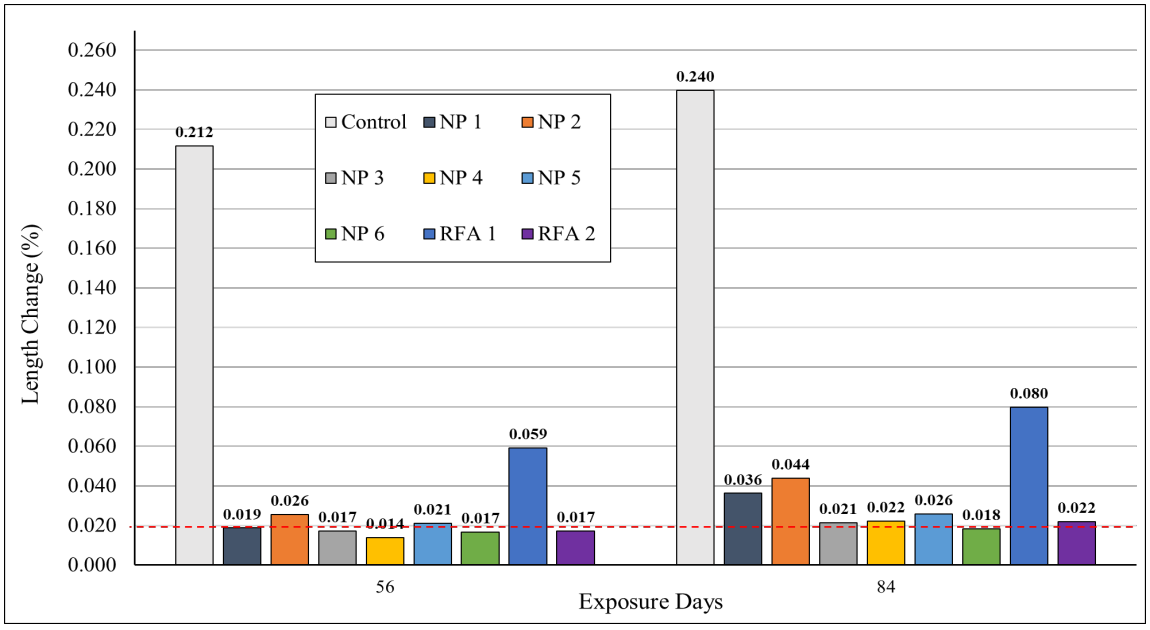

Figure 4- 8 AASHTO T380 56-D & 84-D Expansion Value with 20% SCMs Replacement

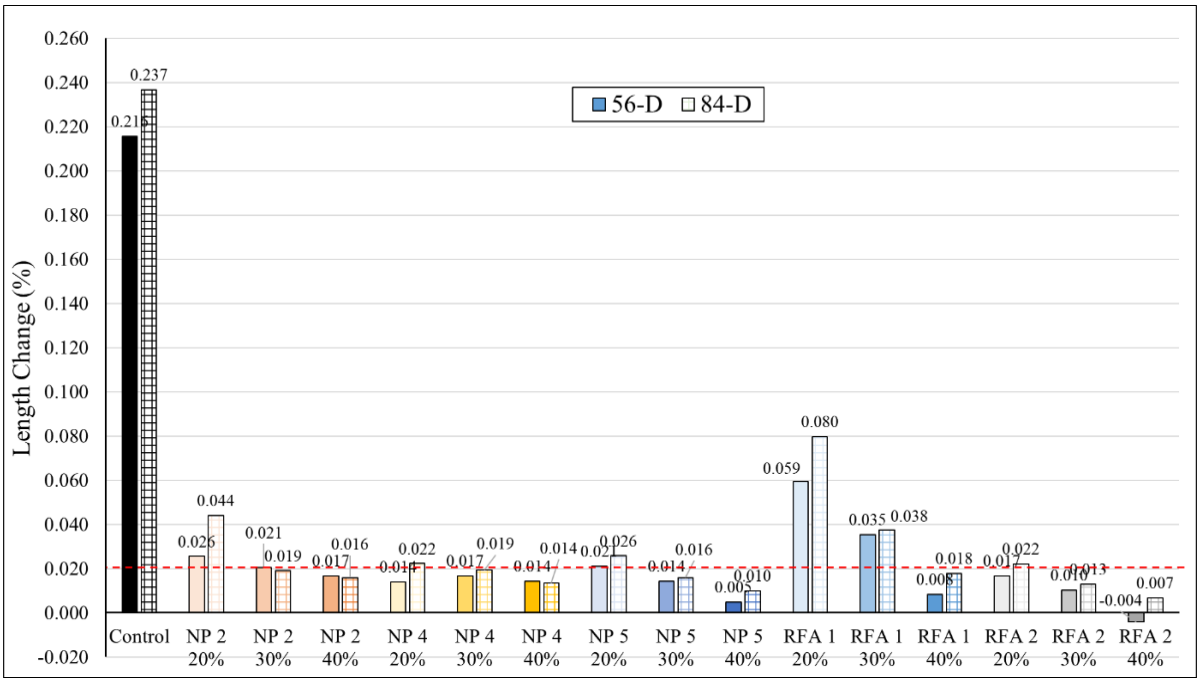

Figure 4- 9 AASHTO T380 Replacement Level Results Comparison

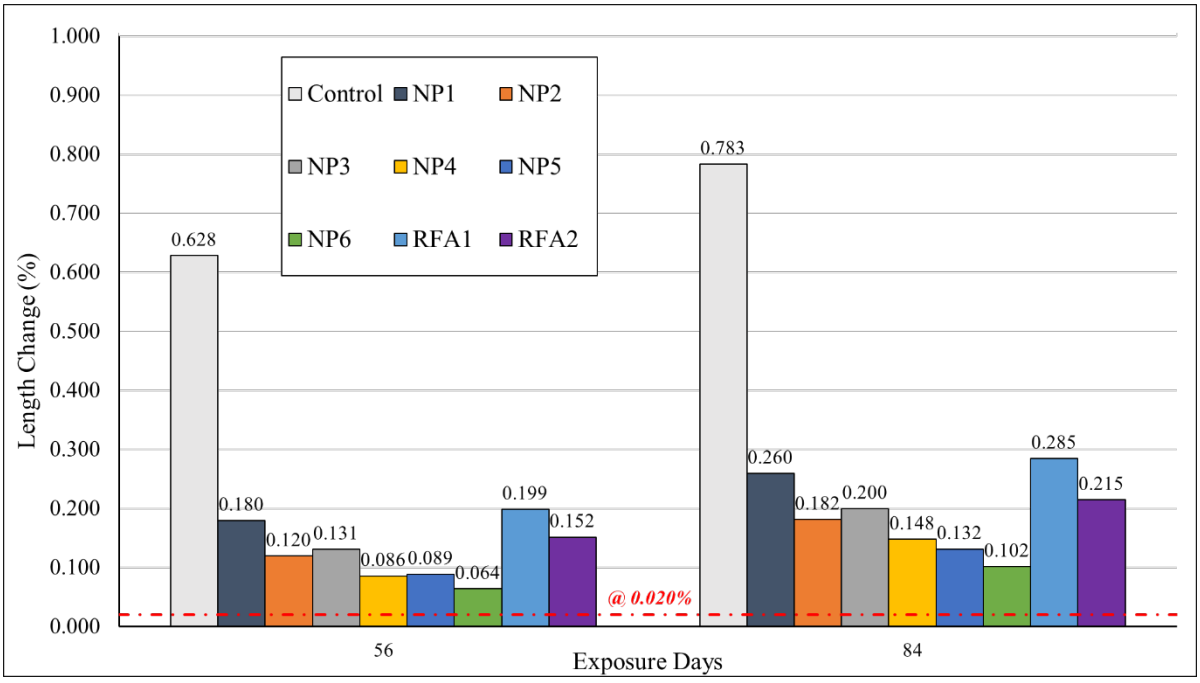

Figure 4- 10 AASHTO T380 56-D & 84-D expansion Value with 20% SCMs Replacement with Fine reactive aggregate

Figure 4- 10 shows the high-alkali SCMs ASR mitigation performance when MCPT's aggregate combination was reactive fine aggregate and non-reactive coarse aggregate. Based on the comparison between Figure 4- 8 and Figure 4- 10, fine reactive aggregate exacerbated ASR expansion because fine reactive aggregate possessed more surface area, which let more reactive silica be involved in the reaction. Even though high-alkali SCMs significantly lowered the ASR expansion compared to the control, their extent of relief was far from sufficient to pass the experiment.

4.3.4 Pore Solution Analysis

Figure 4- 11 and Figure 4- 12 show the potassium (K^+) and sodium (Na^+) concentrations of pore solution expressed from cement paste at 28 and 84-day test durations, and Figure 4- 13 indicates the sum of alkalis ions concentration ($K^+ + Na^+$). Due to all the mixtures with 20% SCMs, the red dash line was labeled in the Figures, representing the 80% alkali ions concentration. According to the results, K^+ concentration was much higher than Na^+, and the chemical composition of cement caused it. The amount of K_2O content of high-alkali cement was three-time than the Na_2O. Control's alkali ions concentration did not change much between the 28th day and the 84th day, and the reason was that cement had completely hydrated and released all alkali ions.

In Figure 4- 11, all test mixtures were below the 80% line. NP 3 had the lowest K^+ but increased significantly from the 28th to the 84th day, from 0.127 to 0.172 mmol/L. For the rest materials, they tended to decrease K^+ concentration with sample age increasing. RFA 1 indicated a slight decrease from the 28th to the 84th day, but the decrease was not evident. Additionally, the K+ concentration of RFA 1 was much higher than in other groups. The change in K+ concentration revealed the occurrence of a pozzolanic reaction.

Na^+ concentration behaved differently from K^+. Other mixtures, except for NP 1 and NP 2, indicated higher concentrations than the 80% control, especially NP 3. NP 3's Na+ concentration was highest, 0.242 and 0.235 mmol/L, respectively, for the 28th and 84th days, but 80% control was only about 0.145 mmol/L. RFA 1 still did not perform well. On the 28th day, RFA 1's Na+ concentration was about 0.188 mmol/L, the second highest, and it increased the most between the two measurements, 0.043, and reached 0.231 on the 84th day. The Na^+ concentration increment of mixtures compared to the control indicated that the high-alkali SCMs also released alkali ions into the pore solution during the pozzolanic reaction.

It was observed that the mixtures with RFA 1 had the highest total alkalis ions concentration among all the mixtures, which was also higher than the 80% of the control. NP 1 showed the lowest total alkali ions concentration, and NP 2 lowered the evident alkalis ions with the time increasing. NP 4, NP 5, NP 6, and RFA 2 maintained a similar level between the 28th and the 84th day's measurements. NP 3 and RFA 2, their alkali ions concentration raised significantly between the two measurements.

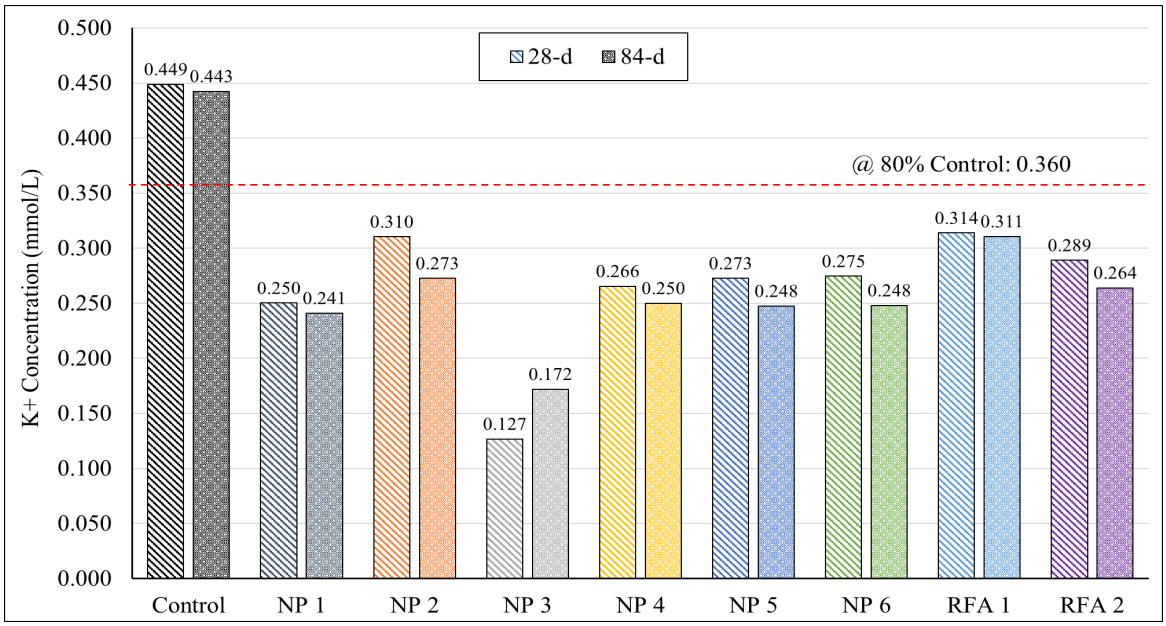

Figure 4- 11 K^+ Concentration

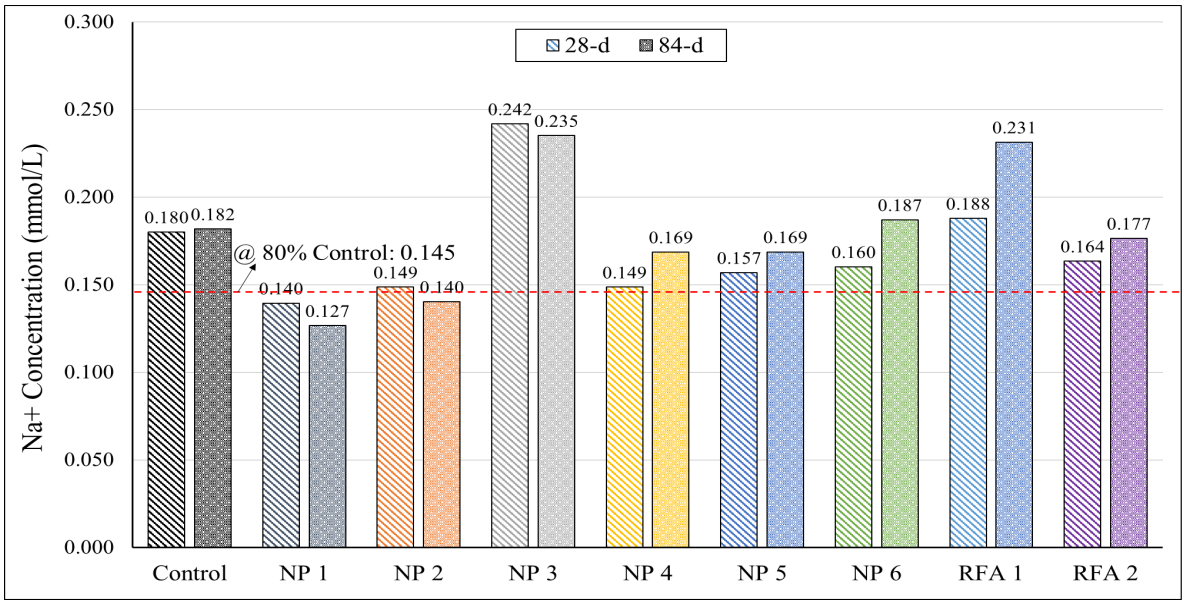

Figure 4- 12 Na^+ Concentration

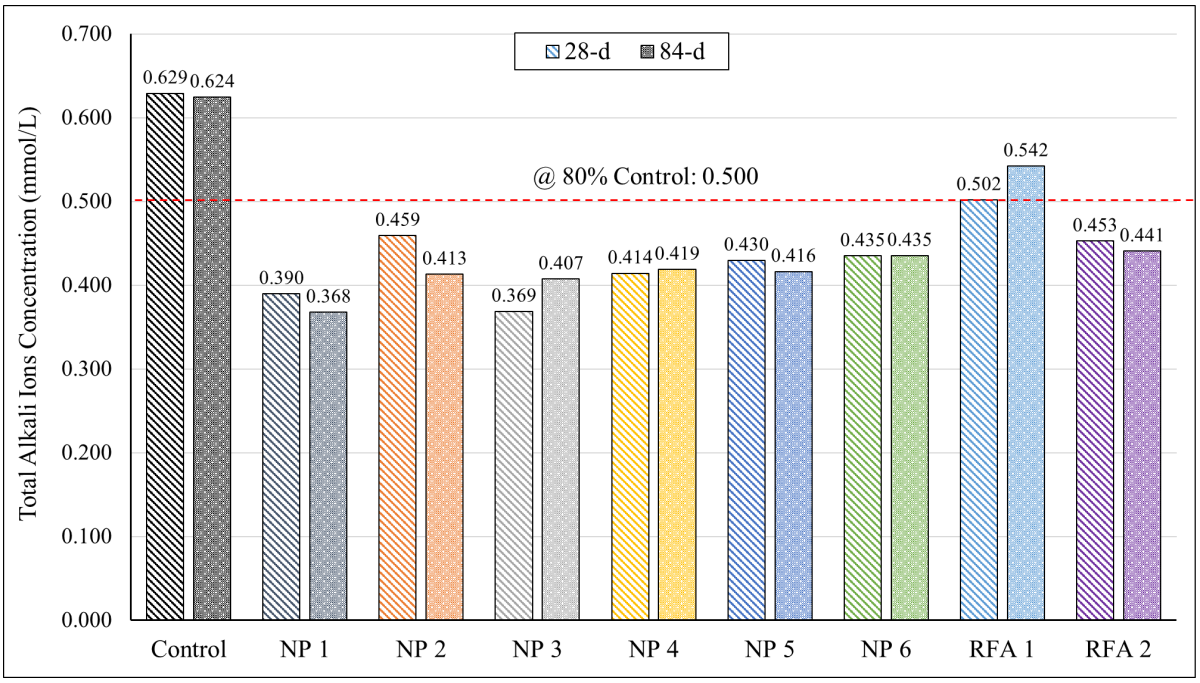

Figure 4- 13 Total Alkali Ions Concentration with 20% High-alkali SCMs Replacement

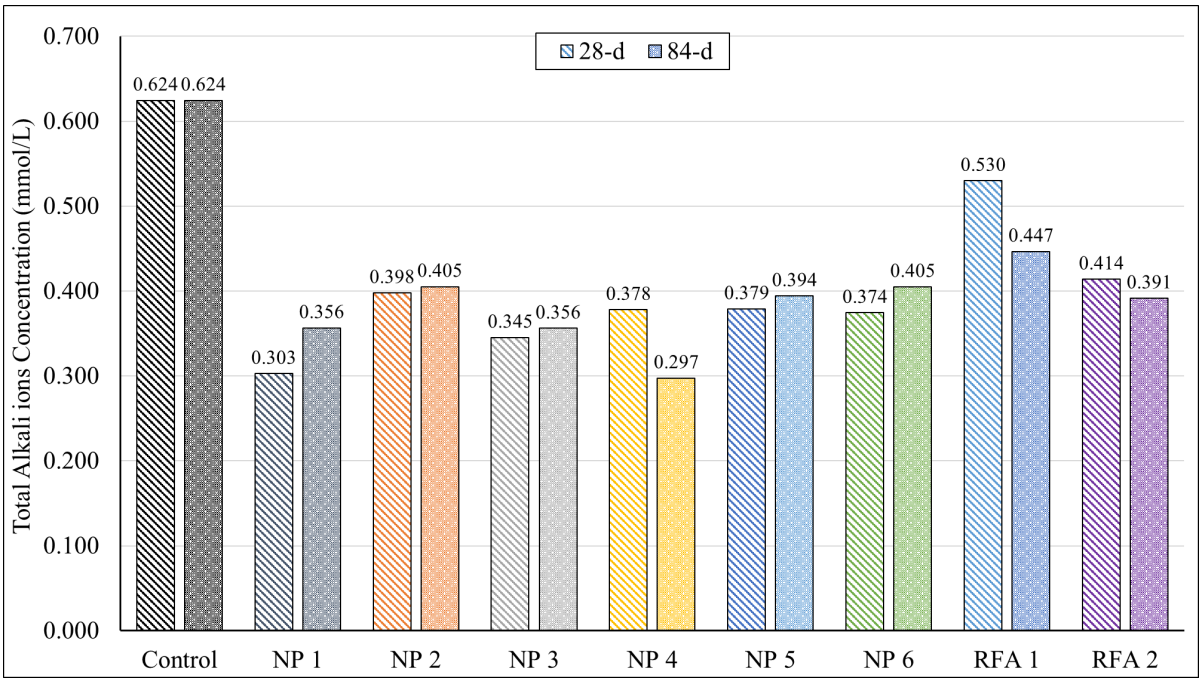

Figure 4- 14 Total Alkali Ions Concentration with 30% High-alkali SCMs Replacement

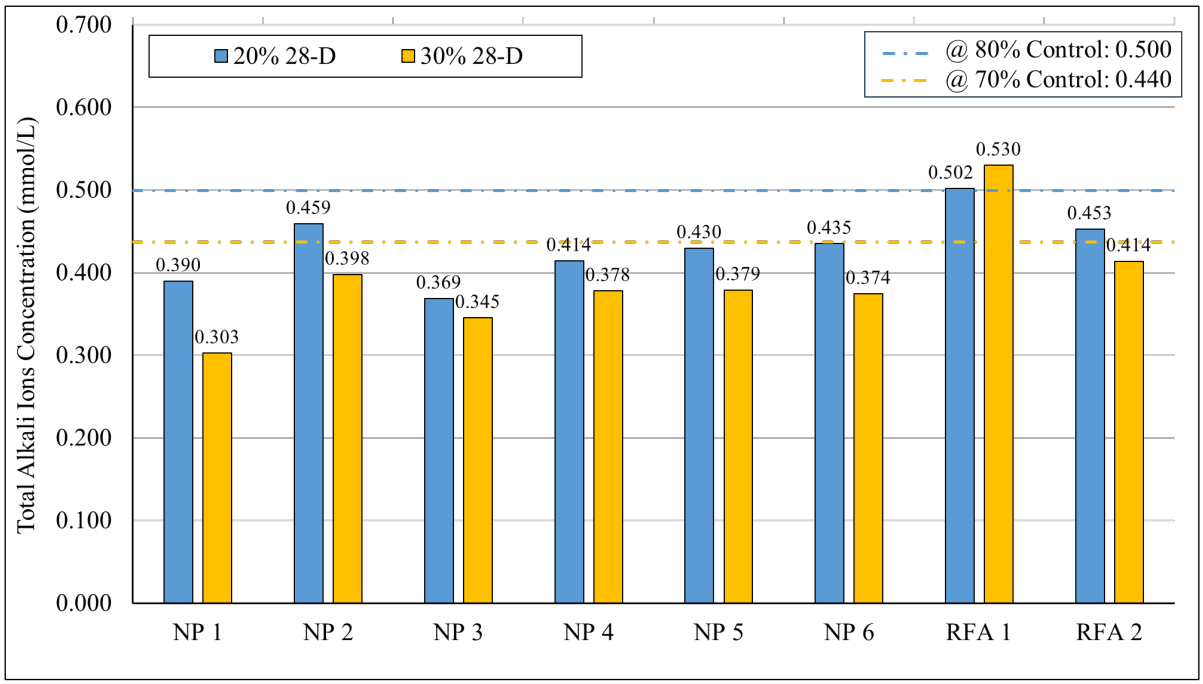

Figure 4- 15 28 Days Total Alkali Ions Concentration Comparison between 20% and 30% Replacement Levels

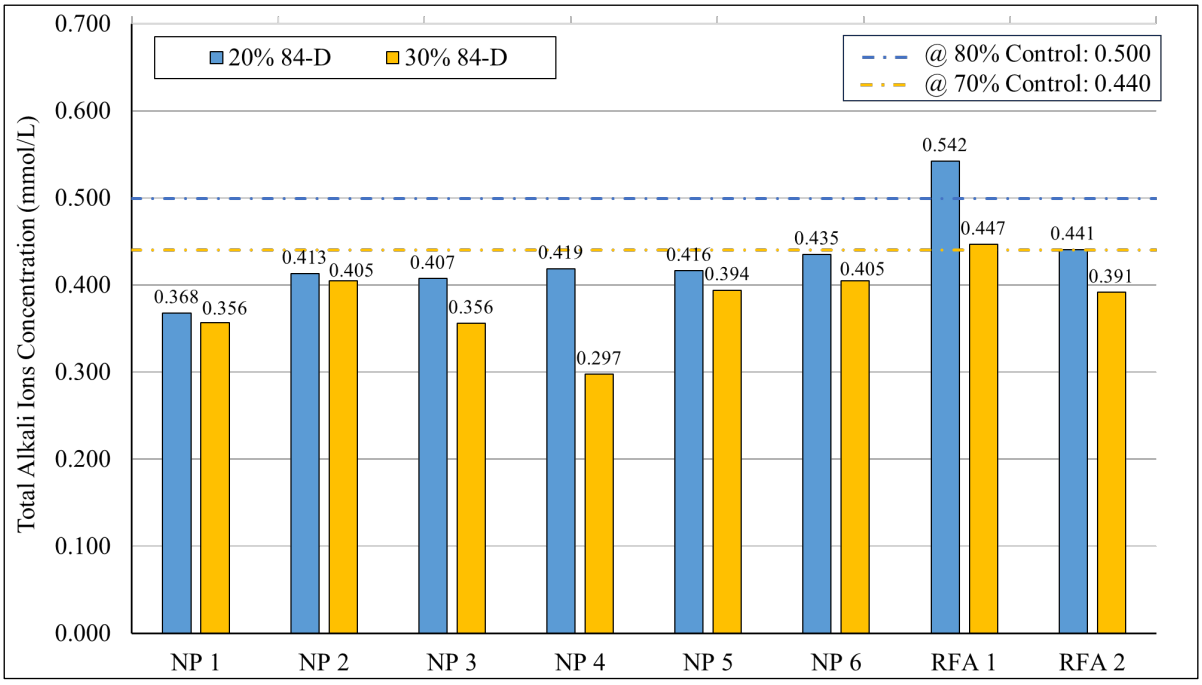

Figure 4- 16 Days Total Alkali Ions Concentration Comparison between 20% and 30% Replacement Levels

The study also analyzed the impact of 30% SCMs replacement on the pore solution's total alkali ions concentration, and the results are shown in Figure 4- 14. Considering the dilution factor of the SCMs, the concentration results were compared to 70% of the control, which was 0.440%. Except for the RFA 1, the rest of the materials were lower than 0.440%. Additionally, some materials' 84-day value increased compared to 28-day, especially NP 5 and NP 6. Also, 30% 84-day RFA 1 decreased significantly compared to its 30% 28-day rather than the decrease shown in Figure 4- 13. Figure 4- 15 and Figure 4- 16 show the comparison of total alkali ion concentration between 20% and 30% replacement levels. The blue and yellow dash line represents 80% and 70% of the total alkali ions concentration of the control, respectively. The results showed that high SCMs replacement possessed less total alkali ions than the low replacement level. Therefore, from the pore solution perspective, increasing high-alkali SCMs replacement level effectively controlled the total alkali concentrations.

4.3.5 TGA Analysis

4- 17 indicates the relative CH contents in the paste. Considering the cement dilution that occurs when cement is replaced with 20% SCM, the calcium hydroxide (CH) content of the test mixtures was divided by 0.8 to correct for the dilution. The calibrated high-alkali SCMs CH consumption values were compared to the control, expressed as % control, and the results are shown in Figure 4- 17.

At early ages, before 7 days, it is clear that all the high-alkali SCMs increased the CH content in the mixtures, which resulted from the filler effect of SCMs. The filler effect increased nucleation sites, further accelerating the cement hydration process [32]. With the sample age increasing and pozzolanic reactivity, the CH content of mixtures with SCMs started to decrease, and some groups were lower than the control, indicating the occurrence of pozzolanic reactions caused by high-

alkali SCMs. NP 2 and RFA 1 did not effectively lower the CH content in the mixtures compared to the control, and their CH content level was maintained at a constant level between 28 days and 56 days. It could result from the larger particle size of NP 1 and RFA 1. These two materials have larger particle sizes than the rest. For the rest of the materials, they decreased the CH content by at least 5% compared to the control.

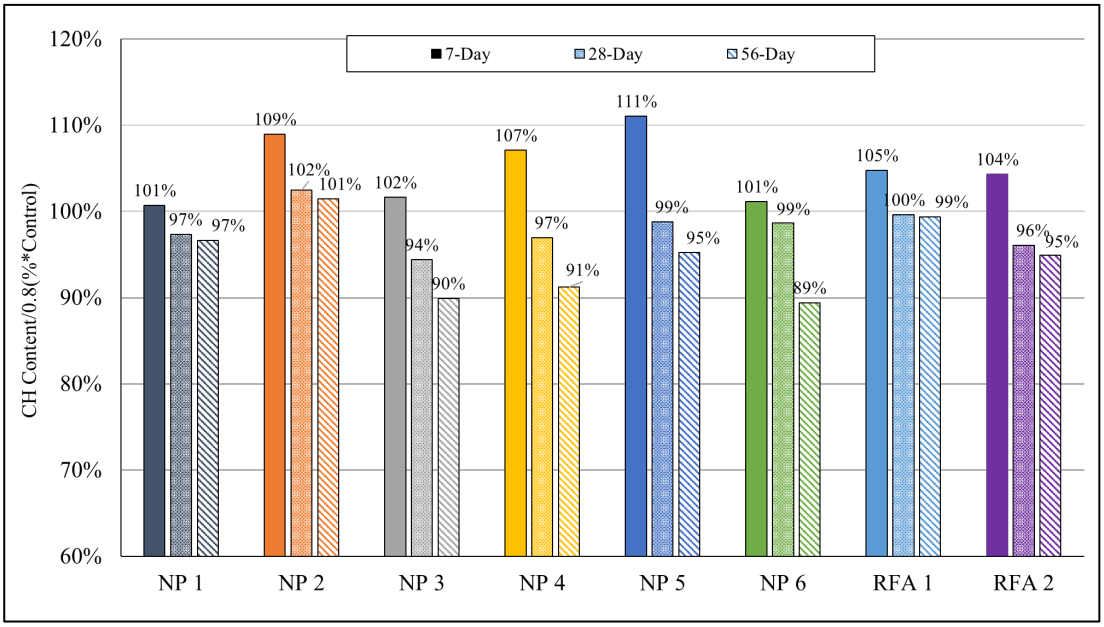

Figure 4- 17 Relative CH Contents in Pastes Containing 20% High-Alkali SCMs Replacement

4.3.6 SEM/EDX

Figure 4- 18 shows the SEM figure of ASTM C1293 control. The substantial dark region corresponds to the coarse aggregate, while the diminutive dark sections symbolize the fine aggregate. Furthermore, the cement paste is depicted by the grey area. According to the figure, coarse reactive aggregate indicated many inner cracks, these cracks originated from the interior of the aggregate and then gradually extended out to cement paste. Some fillers were also observed in the cracks.

In this sample, five spectrum points were selected for EDX. Spectrum 1 and 5, were selected within the crack for the EDX, and they aimed to evaluate the chemical composition of filler and crack, respectively. Spectrum 2, 3, and 4 were located in the coarse aggregate, cement paste, and un-hydrated cement, respectively. From the chemical composition results of Spectrum 1 and 5 shown in Figure 4- 19 and Figure 4- 23, the fillers in the crack were ASR gel, because they had a very high amount of Na and K elements compared to the rest of the points. As for the rest of the spectrum points, different points had different characteristics depending on the material type. For example, Spectrum 2 on coarse aggregate was abundant in O and Si.

In order to make a comparison between the control and SCMs group, NP 4 was conducted in SEM/EDX as well, and its result is shown in Figure 4- 24. Even though NP 4 had the lowest ASR expansion results in ASTM C1293, ASR cracks were still observed. Additionally, EDX also discovered ASR gels in the cross-section sample, which are shown in Figure 4- 25 and Figure 4- 26.

Based on the results obtained in SEM/EDX, 20% high-alkali SCMs replacement was not effective in controlling the concrete inner ASR crack. Even though the difference in concrete prisms' length change between groups blended with SCMs and control was very significant, the best group in controlling ASR still exhibited inner ASR cracks and ASR gel.

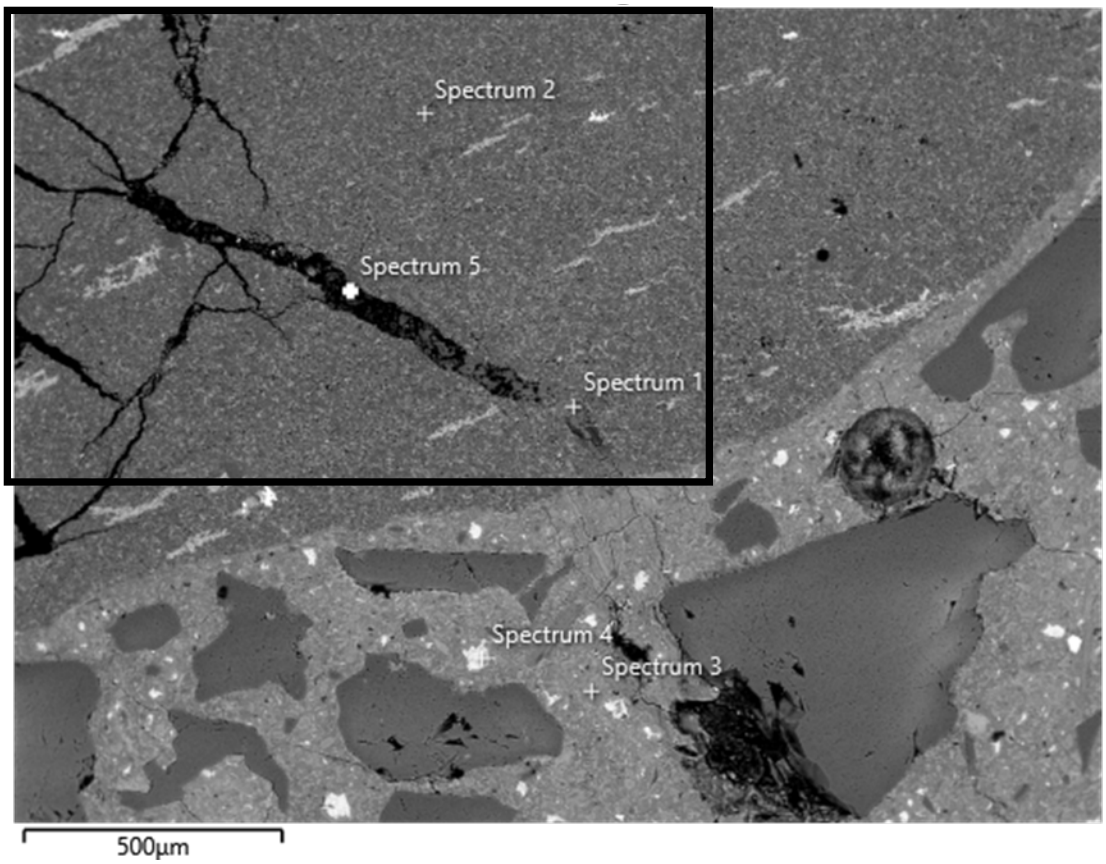

Figure 4- 18 Control CPT SEM

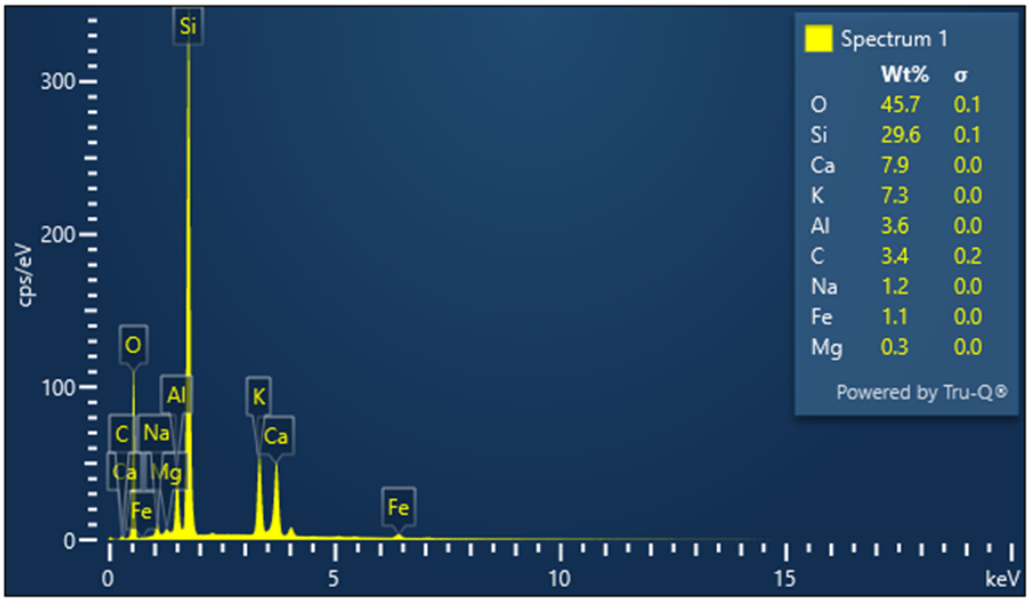

Figure 4- 19 Spectrum 1 of Control EDX

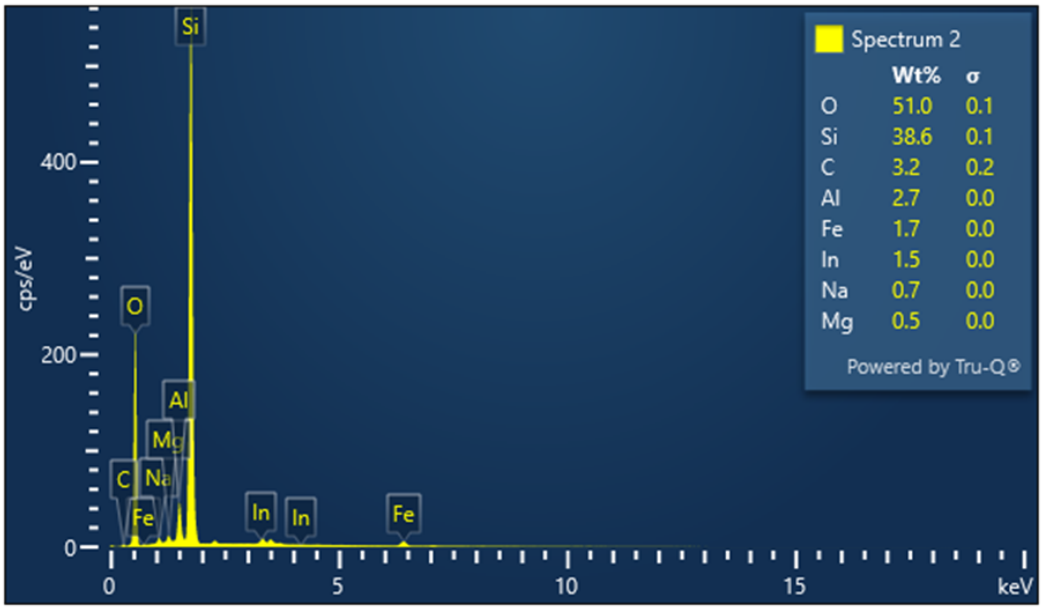

Figure 4- 20 Spectrum 2 of Control EDX

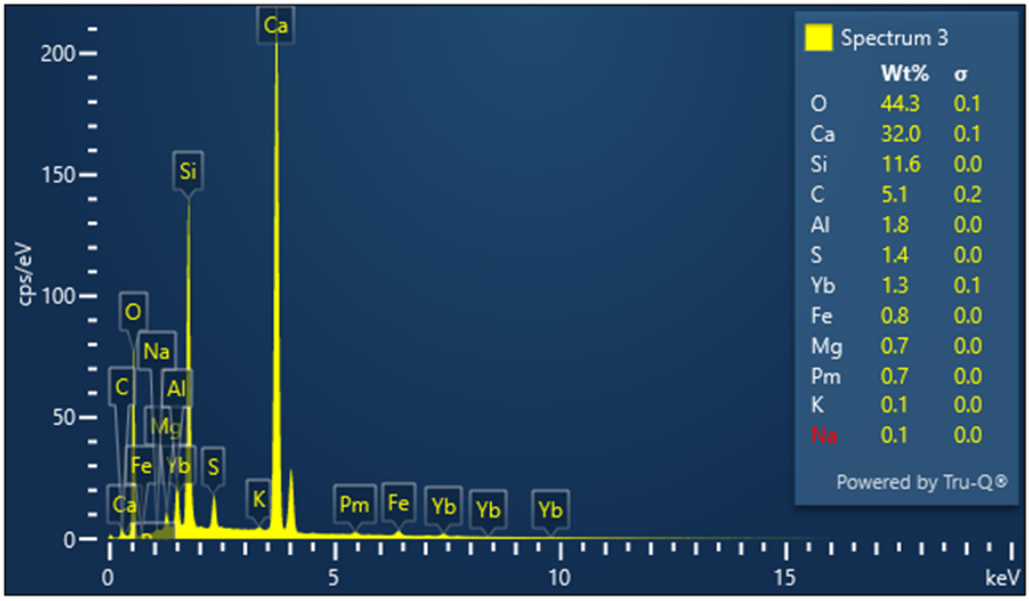

Figure 4- 21 Spectrum 3 of Control EDX

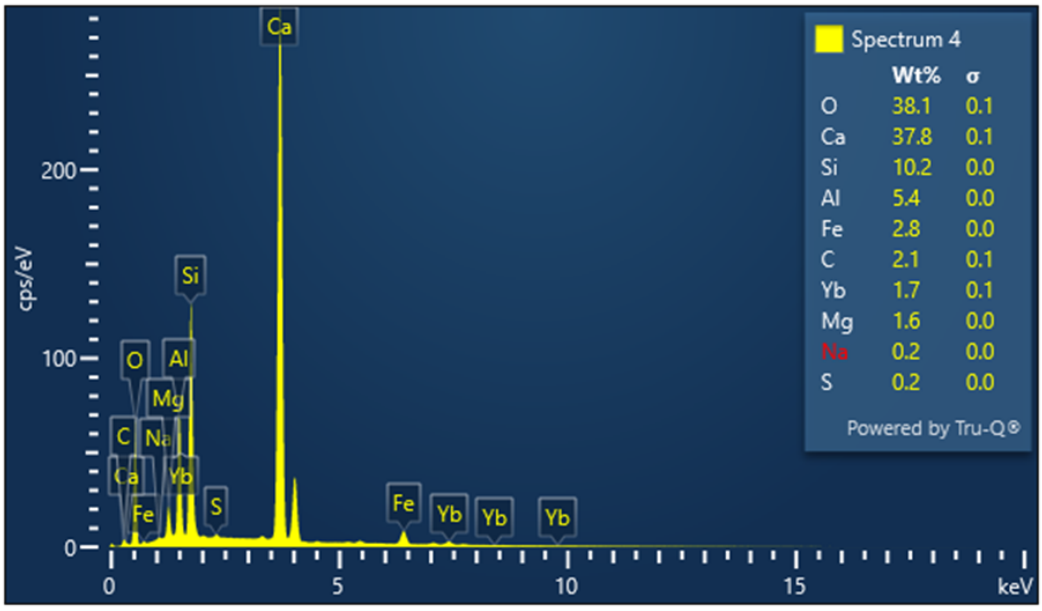

Figure 4- 22 Spectrum 4 of Control EDX

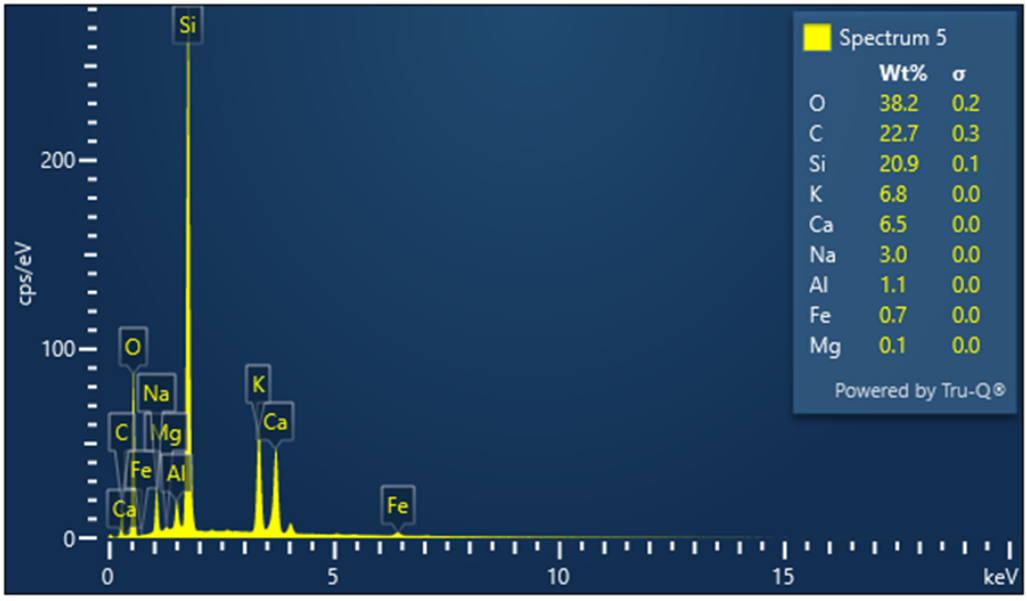

Figure 4- 23 Spectrum 5 of Control EDX

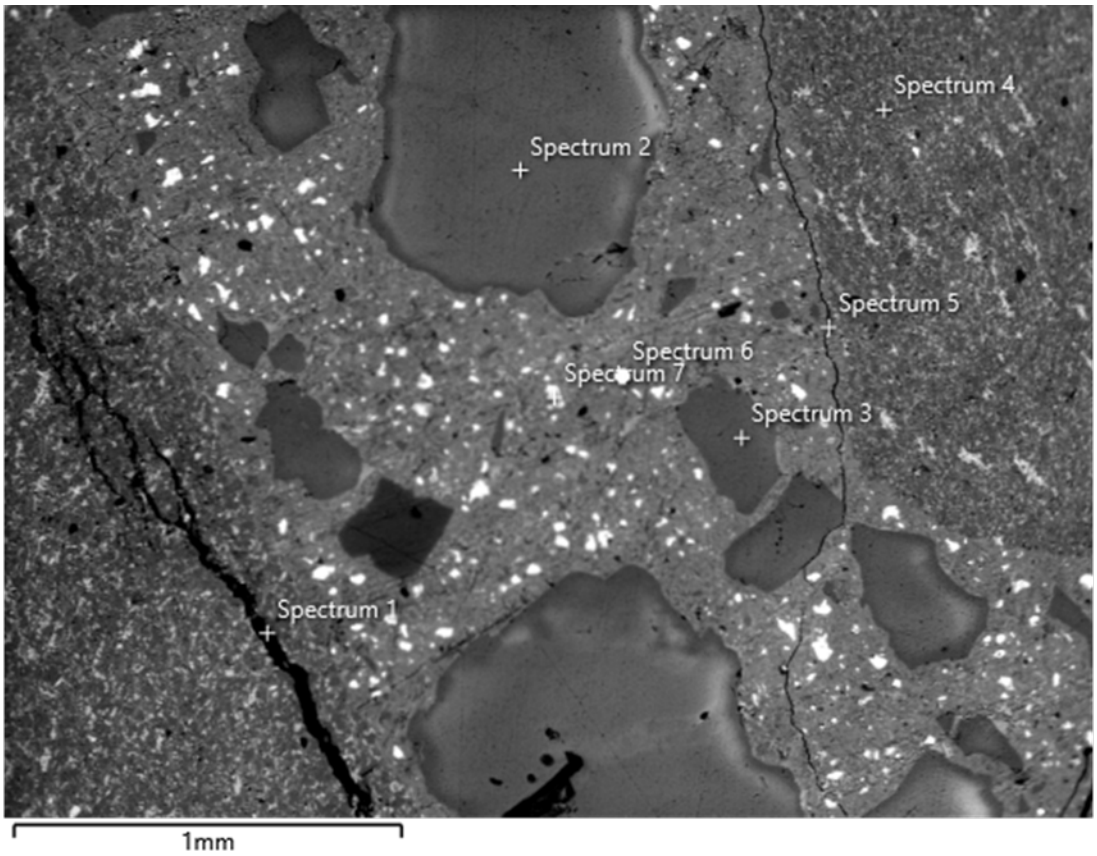

Figure 4- 24 NP 4 CPT SEM

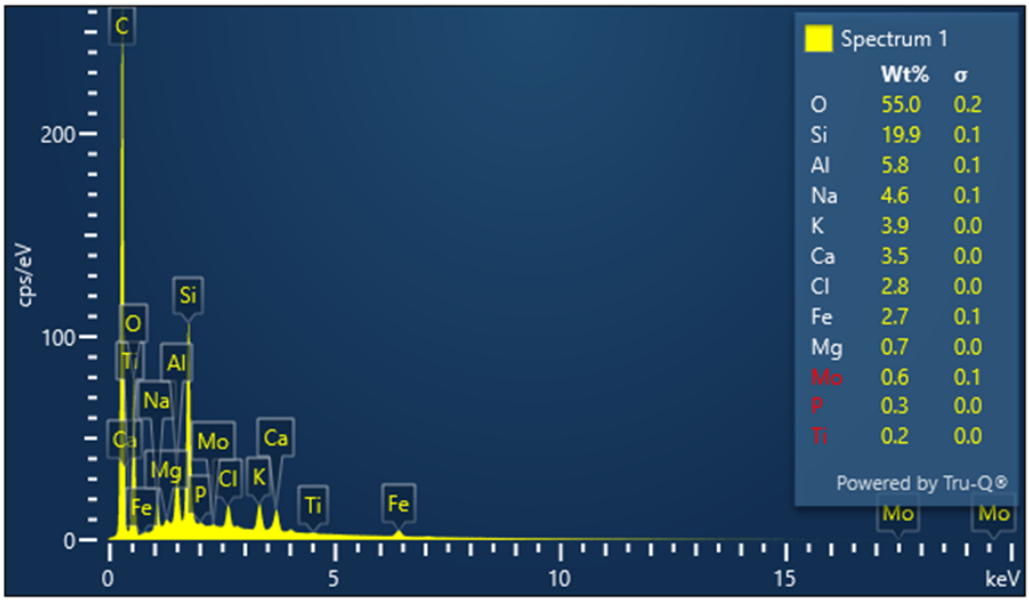

Figure 4- 25 Spectrum 1 of NP 4 EDX

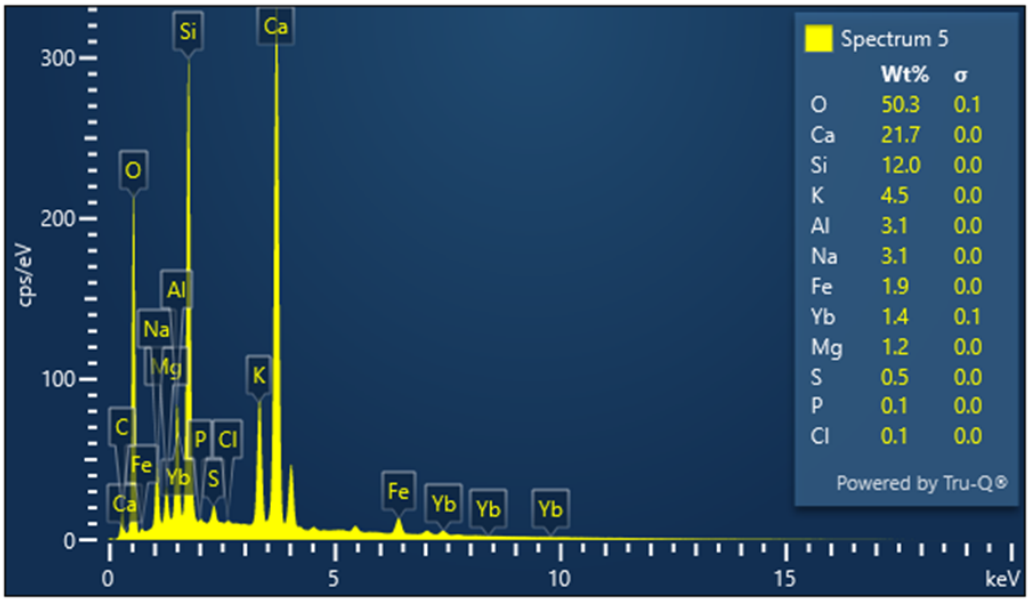

Figure 4- 26 Spectrum 5 of NP 4 EDX

4.4 Discussion

Correlations between ASR Expansion in the various evaluating methods and the high-alkali SCMs' alkali levels were explored and shown in Figure 4- 27. The R^2 values were only 0.2448, 0.1675, and 0.2740, respectively, which corresponded to the alkali level vs. ASTM C1293 2-year, AASHTO T380 56-D, and AASHTO T380 84-D, respectively. The results showed no correlations between the SCMs' alkali level and ASR expansion. For example, compared to the other materials, RFA 1 had the weakest performance in mitigating ASR expansion in all ASR experiments; however, its alkali content was not the highest, which was even the second lowest, 4.69%. On the contrary, NP 6, with the highest alkali content, still behaved very well in the ASR mitigation tests, and in MCPT, it performed the best. Figure 4- 28 shows the correlation between high-alkali SCMs' alkali levels and the alkali concentration of 84-D pore solution. The low R^2 value, 0.0342, also indicates that the alkali level can not directly determine the alkali concentration in the pore solution. These findings prove that using the alkali level of SCMs to predict their ASR mitigation performance is not comprehensive, and some alkali content in the SCMs is not available to release into concrete pore solution during the pozzolanic reaction.

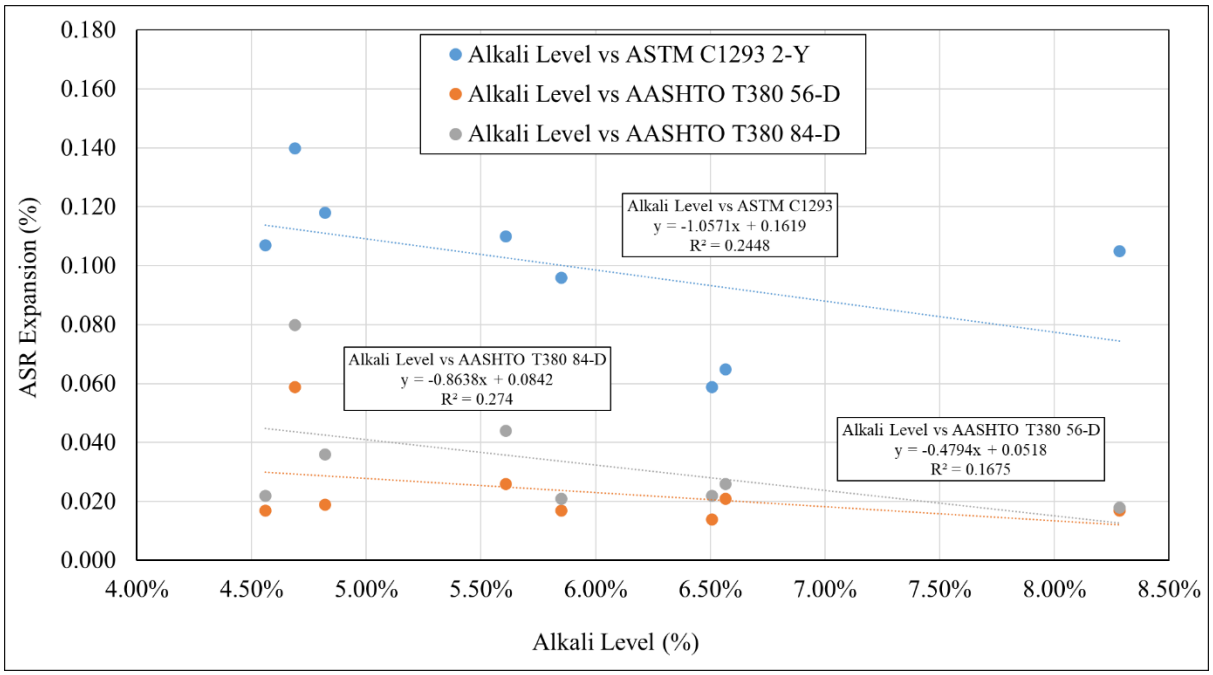

Figure 4- 27 Correlation between High-Alkali SCMs' Alkali Level and ASR Expansion

Figure 4- 29 shows the correlations between the ASR expansion of all ASR methods and the alkalis concentration of the pore solution. The pore solution did not correlate well with the ASTM C1293, whose R^2 value was 0.5562. However, the pore solution results indicated a strong correlation with AASHTO T380, the R^2 between alkalis concentration to 56-D and 84-D was 0.8052 and 0.7961, respectively. The reason for the weak correlation between pore solution and ASTM C1293, the researcher thinks, could be caused by inconsistent test duration. The maximum curing age of pore solution samples was 84-D, but the ASTM C1293 was two years. However, compared to using SCMs' alkali content as an indicator for evaluating SCMs' ASR mitigation performance, using alkali ions concentration of pore solution is more persuasive and reasonable.

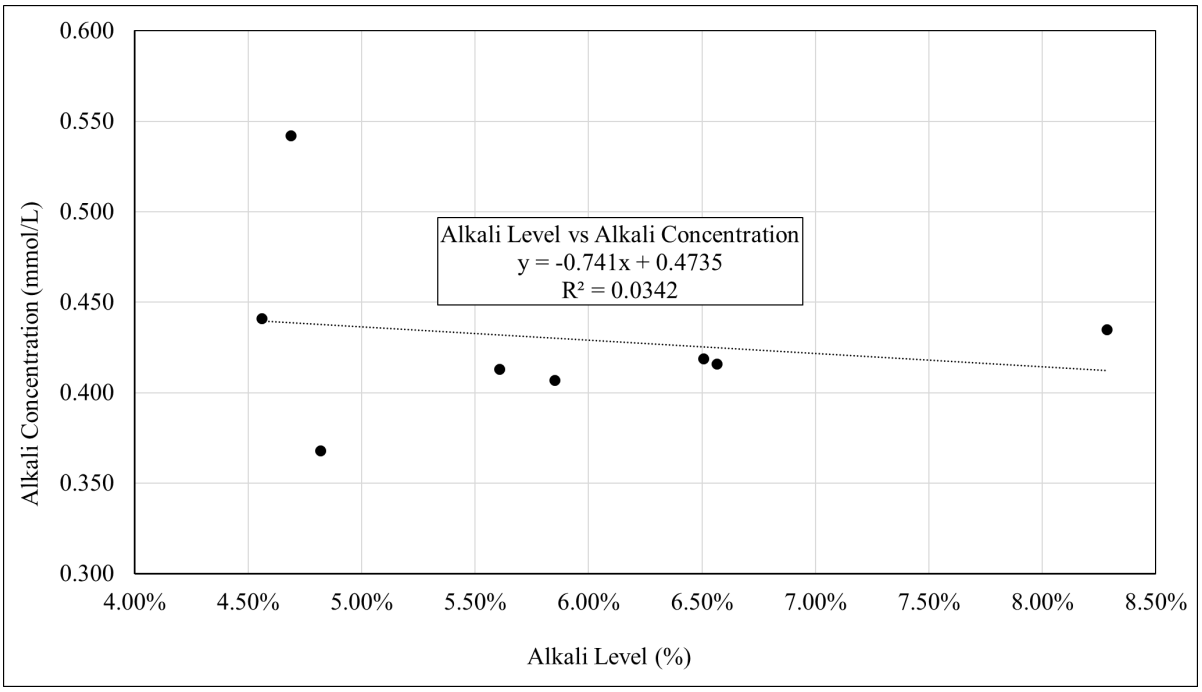

Figure 4- 28 Correlation between High-Alkali SCMs' Alkali Level and Alkali Concentration of Pore Solution

Figure 4- 30 shows the correlation between ASR results and TGA weight loss during 400-500^{o}C, and results indicate that TGA significantly supports the ASR results conducted by AASHTO T380 and ASTM C1293. R^2 of TGA with AASHTO T380 56-D and 84-D was 0.9092 and 0.935, respectively. Additionally, the R2 of TGA against ASTM C1293 2-Y was 0.6705. Contrasted to the pore solution analysis shown in Figure 4- 29, the TGA results offered more substantial support for ASR expansion."

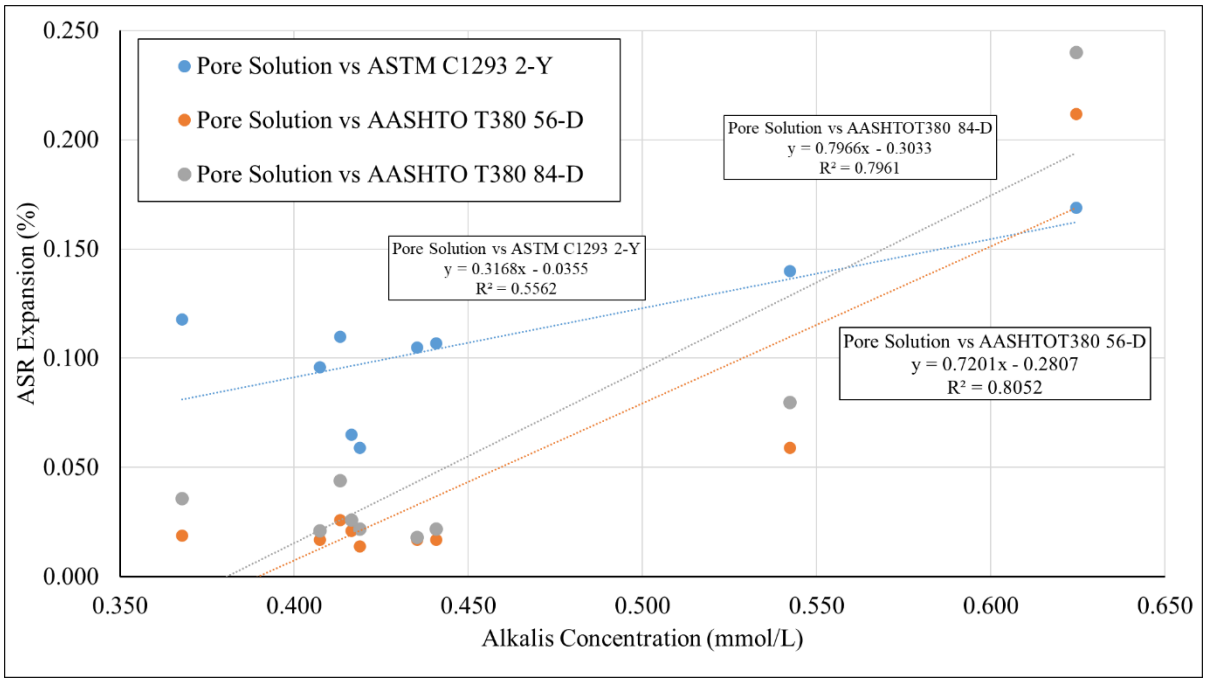

Figure 4- 29 Correlation between 20% Replacement Level ASR Experiments and Pore Solution

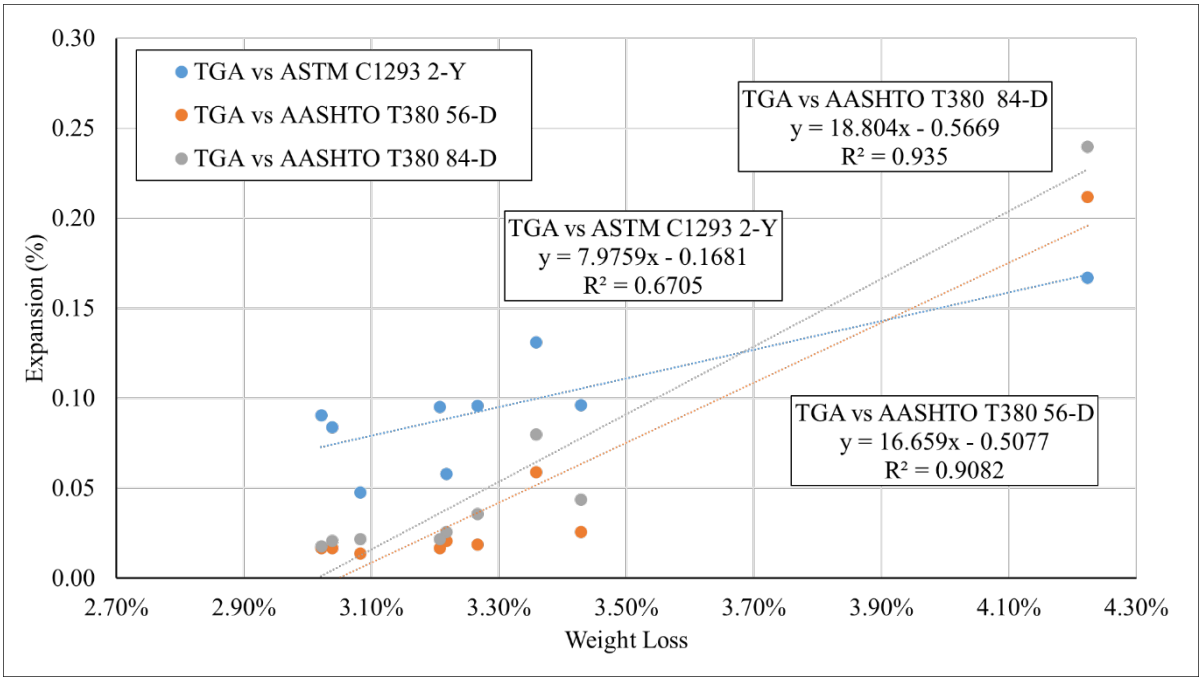

Figure 4- 30 Correlation between 20% Replacement Level ASR Experiments and TGA Weight Loss during 400-500ºC

4.5 Conclusion

From the data obtained in this study, some conclusions are drawn:

1. Compared to the control, high-alkali SCMs effectively reduce the ASR expansion. RFA 1 did not perform as well as the rest but reduced ASR-induced expansion at the 20% replacement level compared to the control.
2. Different ASR test methods yield different characterizations of high-alkali SCMs. Per ASTM C1567, all the high-alkali SCMs materials passed the test, but all SCMs failed in ASTM C1293 during the two-year, and some of them failed to pass in AASHTO T380 tests (84 days) at a 20% dosage level, respectively. Preliminary results indicate that at higher replacement levels (30% and 40%), high-alkali SCMs are performing much more effectively in mitigating ASR.
3. High-alkali SCMs effectively lower the alkali concentration in the pore solution compared to the control. Increasing the high-alkali SCMs replacement level helped to decrease the alkali ions further.
4. Using high-alkali SCMs' alkali content to evaluate their ASR mitigating abilities or the potential alkali release is inadequate. Materials with low alkalis content may release more alkali ions into the pore solution and increase the challenge of controlling the ASR expansion. Also, no strong correlation exists between the SCMs' alkali content and the alkali ions concentration of the pore solution. Evaluating the pore solution's alkali ions concentration is more persuasive than directly using SCMs' alkali content.
5. High-alkali SCMs effectively consumed CH. The amount of CH consumed by SCMs increased with the sample age increasing. The materials indicated the filler effect at an

early age, increasing the degree of hydration. Additionally, TGA results significantly correlated with ASR results conducted by AASHTO T380 and ASTM C1293.

6. Even though the difference in concrete prisms' length change between groups blended with SCMs and control was very significant, inner ASR cracks and ASR gel were still observed in the best group in controlling ASR.
7. Above all, high-alkali SCMs can potentially be the new alternative SCMs for the concrete industry for mitigating ASR.

4.4 Reference

[1] P. Léger, P. Côté, and R. Tinawi, "Finite element analysis of concrete swelling due to alkali-aggregate reactions in dams," *Computers & Structures*, vol. 60, no. 4, pp. 601–611, Jun. 1996, doi: 10.1016/0045-7949(95)00440-8.

[2] L. S. Dent Glasser and N. Kataoka, "The chemistry of 'alkali-aggregate' reaction," *Cement and Concrete Research*, vol. 11, no. 1, pp. 1–9, Jan. 1981, doi: 10.1016/0008-8846(81)90003-X.

[3] S. Akhtar, "A Critical Assessment to the Performance of Alkali-Silica Reaction (ASR) in Concrete", doi: DOI:10.13179.

[4] M. Berra, T. Mangialardi, A. E. Paolini, and R. Turriziani, "Critical evaluation of accelerated test methods for detecting the alkali-reactivity of aggregates," *Advances in Cement Research*, vol. 4, no. 13, pp. 29–37, Jan. 1991, doi: 10.1680/adcr.1991.4.1.29.

[5] M. D. A. Thomas, B. Fournier, K. J. Folliard, and Inc. Transtec Group, "Alkali-aggregate reactivity (AAR) facts book.," FHWA-HIF-13-019, Mar. 2013. Accessed: Aug. 26, 2022. [Online]. Available: https://rosap.ntl.bts.gov/view/dot/26838

[6] T. E. Stanton, "Studies of Use of Pozzolans for Counteracting Excessive Concrete Expansion Resulting from Reaction Between Aggregates and The Alkalies in Cement," *Symposium on Use of Pozzolanic Materials in Mortars and Concretes*, Jan. 1950, doi: 10.1520/STP39409S.

[7] M. Kasaniya, M. D. A. Thomas, and E. G. Moffatt, "Efficiency of natural pozzolans, ground glasses and coal bottom ashes in mitigating sulfate attack and alkali-silica reaction," *Cement and Concrete Research*, vol. 149, p. 106551, Nov. 2021, doi: 10.1016/j.cemconres.2021.106551.

[8] S.-Y. Hong and F. P. Glasser, “Alkali binding in cement pastes: Part I. The C-S-H phase,” *Cement and Concrete Research*, vol. 29, no. 12, pp. 1893–1903, Dec. 1999, doi: 10.1016/S0008-8846(99)00187-8.

[9] J. D. Birchall, A. J. Howard, and J. E. Bailey, “On the hydration of Portland cement,” *Proceedings of the Royal Society of London. A. Mathematical and Physical Sciences*, vol. 360, no. 1702, pp. 445–453, 1978.

[10] I. G. Richardson, “The calcium silicate hydrates,” *Cement and Concrete Research*, vol. 38, no. 2, pp. 137–158, Feb. 2008, doi: 10.1016/j.cemconres.2007.11.005.

[11] X. Hou, L. J. Struble, and R. J. Kirkpatrick, “Formation of ASR gel and the roles of C-S-H and portlandite,” *Cement and Concrete Research*, vol. 34, no. 9, pp. 1683–1696, Sep. 2004, doi: 10.1016/j.cemconres.2004.03.026.

[12] K. E. Kurtis, P. J. M. Monteiro, J. T. Brown, and W. Meyer-Ilse, “Imaging of ASR Gel by Soft X-Ray Microscopy,” *Cement and Concrete Research*, vol. 28, no. 3, pp. 411–421, Mar. 1998, doi: 10.1016/S0008-8846(97)00274-3.

[13] W. Müllauer, R. E. Beddoe, and D. Heinz, “Sulfate attack expansion mechanisms,” *Cement and Concrete Research*, vol. 52, pp. 208–215, 2013, doi: 10.1016/j.cemconres.2013.07.005.

[14] J. Duchesne and M. A. Bérubé, “The effectiveness of supplementary cementing materials in suppressing expansion due to ASR: Another look at the reaction mechanisms part 2: Pore solution chemistry,” *Cement and Concrete Research*, vol. 24, no. 2, pp. 221–230, Jan. 1994, doi: 10.1016/0008-8846(94)90047-7.

[15] A. Vollpracht, B. Lothenbach, R. Snellings, and J. Haufe, “The pore solution of blended cements: a review,” *Mater Struct*, vol. 49, no. 8, pp. 3341–3367, Aug. 2016, doi: 10.1617/s11527-015-0724-1.

[16] A. A. Ramezanianpour, S. M. Motahari Karein, P. Vosoughi, A. Pilvar, S. Isapour, and F. Moodi, “Effects of calcined perlite powder as a SCM on the strength and permeability of concrete,” *Construction and Building Materials*, vol. 66, pp. 222–228, Sep. 2014, doi: 10.1016/j.conbuildmat.2014.05.086.

[17] V. Nežerka, P. Bílý, V. Hrbek, and J. Fládr, “Impact of silica fume, fly ash, and metakaolin on the thickness and strength of the ITZ in concrete,” *Cement and Concrete Composites*, vol. 103, pp. 252–262, Oct. 2019, doi: 10.1016/j.cemconcomp.2019.05.012.

[18] T. M. Research, “Fly Ash Market is Expected to be Valued at US$ 13.8 Bn by 2031, States TMR Study,” *GlobeNewswire News Room*, Apr. 05, 2022. https://www.globenewswire.com/en/news-release/2022/04/05/2416875/0/en/Fly-Ash-Market-is-Expected-to-be-Valued-at-US-13-8-Bn-by-2031-States-TMR-Study.html (accessed May 05, 2022).

[19] M. C. G. Juenger, R. Snellings, and S. A. Bernal, “Supplementary cementitious materials: New sources, characterization, and performance insights,” *Cement and Concrete Research*, vol. 122, pp. 257–273, Aug. 2019, doi: 10.1016/j.cemconres.2019.05.008.

[20] E. Menéndez, M. Á. Sanjuán, R. García-Roves, C. Argiz, and H. Recino, “Sustainable and Durable Performance of Pozzolanic Additions to Prevent Alkali-Silica Reaction (ASR) Promoted by Aggregates with Different Reaction Rates,” *Applied Sciences*, vol. 10, no. 24, Art. no. 24, Jan. 2020, doi: 10.3390/app10249042.

[21] R. Chihaoui, H. Siad, Y. Senhadji, M. Mouli, A. M. Nefoussi, and M. Lachemi, “Efficiency of natural pozzolan and natural perlite in controlling the alkali-silica reaction of cementitious materials,” *Case Studies in Construction Materials*, vol. 17, p. e01246, Dec. 2022, doi: 10.1016/j.cscm.2022.e01246.

[22] M. H. Shehata and M. D. A. Thomas, “Alkali release characteristics of blended cements,” *Cement and Concrete Research*, vol. 36, no. 6, pp. 1166–1175, Jun. 2006, doi: 10.1016/j.cemconres.2006.02.015.

[23] P. K. Mehta, “Natural pozzolans: Supplementary cementing materials,” in *Proc., Int. Symp. on Advances in Concrete Technology*, CANMET, Athens, Greece, 1987, pp. 407–430.

[24] R. E. Rodríguez-Camacho and R. Uribe-Afif, “Importance of using the natural pozzolans on concrete durability,” *Cement and Concrete Research*, vol. 32, no. 12, pp. 1851–1858, Dec. 2002, doi: 10.1016/S0008-8846(01)00714-1.

[25] T. Kim, J. Olek, and H. Jeong, “Alkali–silica reaction: Kinetics of chemistry of pore solution and calcium hydroxide content in cementitious system,” *Cement and Concrete Research*, vol. 71, pp. 36–45, May 2015, doi: 10.1016/j.cemconres.2015.01.017.

[26] “ASTM C1260-21 Standard Test Method for Potential Alkali Reactivity of Aggregates (Mortar-Bar Method).pdf.”

[27] C09 Committee, “ASTM C1567-21 Test Method for Determining the Potential Alkali-Silica Reactivity of Combinations of Cementitious Materials and Aggregate (Accelerated Mortar-Bar Method),” ASTM International. doi: 10.1520/C1567-13.

[28] C09 Committee, “ASTM C1293-20a Standard Test Method for Determination of Length Change of Concrete Due to Alkali-Silica Reaction,” ASTM International, Jul. 2020.

[29] “AASHTO T380 Standard Method of Test for Potential Alkali Reactivity of Aggregates and Effectiveness of ASR Mitigation Measures (Miniature Concrete Prism Test, MCPT),” American Association of State HIghway and Transportation Officials.

[30] R. S. Barneyback and S. Diamond, “Expression and analysis of pore fluids from hardened cement pastes and mortars,” *Cement and Concrete Research*, vol. 11, no. 2, pp. 279–285, Mar. 1981, doi: 10.1016/0008-8846(81)90069-7.

[31] M. Wyrzykowski, S.-I. Igarashi, P. Lura, and V. Mechtcherine, “Recommendation of RILEM TC 260-RSC: using superabsorbent polymers (SAP) to mitigate autogenous shrinkage,” *Mater Struct*, vol. 51, no. 5, p. 135, Oct. 2018, doi: 10.1617/s11527-018-1241-9.

[32] E. Berodier and K. Scrivener, “Understanding the Filler Effect on the Nucleation and Growth of C-S-H,” *Journal of the American Ceramic Society*, vol. 97, no. 12, pp. 3764–3773, 2014, doi: 10.1111/jace.13177.

CHAPTER V POZZOLANIC REACTIVITY OF HIGH-ALKALI SUPPLEMENTARY CEMENTITIOUS MATERIALS AND ITS IMPACT ON MITIGATION OF ALKALI-SILICA REACTION

Abstract

The growing scarcity of conventional supplementary cementitious materials (SCMs) such as Class F, Class C fly ashes, and slag has necessitated exploring alternative SCMs previously considered suboptimal. In particular, high-alkali SCMs are often avoided because of the potential concern that their alkali content could release into the concrete pore solution, thus exacerbating the potential for alkali-silica reaction (ASR). However, preliminary research indicates that not all high-alkali SCMs are deleterious, and some can effectively suppress the ASR expansive reaction when used in sufficient dosage levels. This study evaluates the feasibility of using high-alkali SCMs, such as high-alkali natural pozzolans and reclaimed fly ashes, focusing on their pozzolanic reactivity and the correlation between the reactivity and their ASR mitigation performance. The pozzolanic reactivity of the SCMs was evaluated by the R^3 test per ASTM C1897 and the strength activity index (SAI) test per ASTM C311. Thermogravimetric analysis (TGA) was used to determine the calcium hydroxide consumption by the SCMs. ASR mitigation performance of SCMs was evaluated in accordance with AASHTO T380 (MCPT). Additionally, pore solution expression and analysis of paste specimens were conducted to determine the correlation between the total alkali and the released alkali levels in the pore solution. Based on the results of this study, all SCMs indicated high pozzolanic reactivity—however, individual performance varied by test

method. Ultimately, the high-alkali SCMs, particularly natural pozzolans, did not appear to release any significant levels of alkalis into the pore solution readily and, therefore show potential for ASR mitigation when used in sufficient dosage levels.

Keywords: High-Alkali Supplementary Cementitious Materials(SCMs), Pozzolanic Reactivity Tests, Alkali-Silica Reaction (ASR), Pore Solution Analysis, Thermogravimetric analysis,

5.1. Introduction

Supplementary cementitious materials (SCMs), as mineral additives in concrete, have been widely used throughout the concrete industry [1]. ASTM C618 recognizes two primary categories of SCMs: natural pozzolans and industrial by-products [2]. Natural pozzolans include volcanic ash, pumice, volcanic tuffs, and calcined clays such as metakaolin. Industrial by-products such as fly ashes are derived from activities such as coal combustion for power generation. Other SCMs, such as slag and silica fume, are derived from iron and silicon metal production, respectively.

Concrete is the second most widely used material behind water and is responsible for at least 8% (36.3 billion tons) of global CO_2 emissions [3]–[5]. Using SCMs as a partial replacement for cement in concrete is a sustainable approach that reduces the overall carbon footprint of concrete by not only aiding in the sustainable disposal of industrial residues that otherwise would need to be landfilled but also improves the durability of the Portland cement-based binder matrix. Also, replacing Portland cement with SCMs will lead to using less clinker in the concrete, which reduces the overall carbon footprint of concrete[6]–[8]. Typical SCMs are finely ground siliceous and alumino-siliceous materials that are amorphous in nature and are reactive with calcium hydroxide (CH) in the presence of water at ambient temperature [9]. These characteristics allow SCMs to react with the hydration product of cement (CH), thus producing the calcium silicate hydrate (C-S-H) [10]. This process is also called the pozzolanic reaction, and the ability of SCMs to consume

CH is the pozzolanic reactivity [1]. The pozzolanic reaction improves concrete durability by decreasing permeability[11]. In addition, the pozzolanic reaction can produce CSH / CASH gel that can serve to sequester alkali ions from the pore solution. This process can help to reduce the hydroxyl ion concentration in pore solution and thus improve the mitigation of durability problems such as alkali-silica reaction [12]. The pozzolanic reactivity of SCMs depends on various factors, such as the amorphous content, particle size distribution, and chemical composition. High amorphous content, smaller particle size, and high amounts of silica and alumina can lead to higher pozzolanic reactivity of SCMs [13]–[15].

Among all the test methods to evaluate the pozzolanic reactivity of SCMs, the ASTM C311 strength activity index test (SAI) is the most common method used, wherein the compressive strength of the test sample containing SCMs is measured and compared to that of a control sample at 7 and 28 days [16]. ASTM C618 requires the SCM-containing mixtures to gain at least 75% of the compressive strength of the control mixture at 7 days or 28 days to qualify as an effective pozzolan [2]. ASTM C1897 R^3 test [17], developed by Karen Scrivener et al. [18] employs isothermal calorimetry to evaluate the pozzolanic reactivity of SCMs. This test method determines the pozzolanic reactivity of SCMs by measuring the cumulative heat generated in mixtures, wherein SCMs are mixed with a simulated pore solution made of calcium hydroxide (CH), calcium carbonate, potassium sulfate, and potassium hydroxide.

Thermogravimetric analysis (TGA) is a method of thermal analysis that measures the amount and rate of change in the mass of a sample as a function of temperature and time in a controlled atmosphere. The mass loss that occurs at a specific temperature range can be attributed to a specific compound, and this parameter can be used to quantify the compound in the matrix. Several studies have shown the effective use of TGA in quantifying the CH content in the mixture, and this, in

turn, can be used to assess the pozzolanic reactivity of an SCM [19], [20]. Typically, CH decomposes between 450^{o}C to 500^{o}C[21]. With active pozzolanic reaction, CH in a cementitious matrix is consumed and converted to CSH gel, and the decrease in the CH content, as measured by the TGA method, can be used to gauge the pozzolanic reactivity of SCMs.

Fly ash is the primary SCM used in the concrete industry. However, due to global environmental policy changes, much of coal power has transitioned to using clean energy sources to reduce carbon emissions, resulting in the shortage of availability of high-quality fly ash and the resultant product price increases [22], [23]. Therefore, finding a sustainable alternative for the worldwide SCMs industry is urgent. High-alkali SCMs, whose alkali content is generally over 4%, are generally avoided in concrete due to concerns arising from the potential leaching of alkali ions into the pore solution and increase the alkali loading in the concrete pore solution, further exacerbating the ASR. ASR is a common concrete deterioration mechanism that results from the reaction of reactive amorphous silica found in some natural aggregates with alkali hydroxides (OH^-, Na^+, and K^+) present in the concrete pore solution. This reaction produces ASR gel, which is hygroscopic in nature and has a tendency to absorb moisture and expand. When the ASR gel is restrained from expansion within the concrete matrix, tensile stresses are generated in concrete that leads the concrete to crack. The presence of CH in the matrix plays a significant role in determining the expansive nature of the ASR gel [24]. SCMs are the most common and effective method for controlling ASR, as the pozzolanic reactions consume CH and further develop the C-S-H binder [25]. This mechanism will further increase the alkali-binding ability of CSH gel, lowering the pH of the pore solution and refining the pore structure to decrease the permeability [11], [26], [27]. Also, reducing the readily available CH content in the matrix will inhibit the formation of a more expansive ASR gel. Therefore, SCMs' ASR mitigation performance can also

be viewed as an indirect method to evaluate the pozzolanic reactivity of SCMs. The common test methods that are used to evaluate the effectiveness of SCMs in mitigating ASR are ASTM C1567, ASTM C1293, and AASHTO T380 [28], [29], [29].

Pore solution analysis is the typical method used to evaluate the impact of SCMs' alkali release mechanism, which is also used to predict the ASR expansion process based on the concentration of alkali ions [30]. Shehata et al.'s research [22] evaluated the alkali release characteristics of blended cement with high alkali SCMs, and their research indicated that some SCMs with high total alkali content released alkali ions into the pore solution, which increased alkali concentration in the pore solution. However, Mehta's research [32] indicated that alkali content in some natural pozzolans exists as crystal phases, which are not readily released into the concrete pore solution. The same finding was discovered by Uribe-Afif et al. [33]. In their study, one of the SCMs had a total alkali content of 6.89% Na_2O_{eq}, but the available alkali content was only 1.09% Na_2O_{eq} thus only 15% of the total alkalis were available to be released into the pore solution. These findings provide the potential feasibility of using high-alkali SCMs in concrete without concerns for ASR.

This study investigates the pozzolanic reactivity and ASR mitigation performance of selected high-alkali SCMs. For this purpose, six natural pozzolans and two reclaimed fly ash were studied. The SCMs were characterized for their mineralogy and particle size distribution using X-ray diffraction (XRD) and laser diffraction, respectively. X-ray fluorescence (XRF) was conducted to study the chemical composition of the materials. The pozzolanic reactivity of the SCMs was assessed in accordance with ASTM C311 and ASTM C1897 [16], [17]. TGA was conducted on paste specimens to quantify the amount of CH consumed by SCM pozzolanic reactions at various ages. Pore solution analysis was conducted on paste specimens to study alkali release and alkali-

binding in mixtures with high-alkali SCMs at different sample ages. ASR mitigation performance of mixtures with SCMs was investigated using the AASHTO T380 (MCPT) test method [34]. Finally, the results of pozzolanic reactivity experiments and ASR mitigation studies were compared and analyzed and correlations between these performance measures were evaluated.

5.2. Materials and Method

5.2.1 Materials

Two types of ordinary Portland cement (OPC) meeting ASTM C150 [23] were used in this study: A low-alkali Type I/II Portland cement (Na_2O_e = 0.38%) from Argos cement company, Harleyville, SC, and a high-alkali Type I Portland cement (Na_2O_e = 1.00%) from Lehigh Hanson Inc. The chemical composition and physical properties of both Portland cement are presented in Table 5- 1Chemical Composition.

In this study, five natural pozzolans and two reclaimed fly ashes were investigated. The natural pozzolans are identified as NP 1 through NP 6 and reclaimed fly ashes as RFA 1 and RFA 2. The material chemical compositions and particle size distributions were measured by X-ray fluorescence and laser diffraction, respectively. These results are presented in Table 5- 1 and Figure 5- 1. XRD data of high-alkali SCMs were collected using the Rigaku X-ray diffractor. Measurements were made in flat-plate Bragg–Brentano θ–2θ geometry, and their angular range was from 10° to 80° 2θ values with a 0.02° 2θ step size. The scan rate for the test was 1° 2θ per minute. The amorphous level, i.e.the amount of non-crystallinity, was determined by the Rietveld analysis, which used the integrated surface area of the crystal compared to the total surface area [35]. In this study, XRD results are shown in Figure 5- 3. The SCMs' amorphous content is shown in Table 5- 1, which indicates that all the materials have a high amorphous content except NP 3.

NP 3 did not exhibit a significant amorphous hump, and rather it had many crystal peaks that often overlapped.

The reactive aggregate used in this study is a known reactive aggregate from the Goldhill Quarry in North Carolina, which consists of reactive metatuff–argillite. The aggregate's specific gravity and water percent absorptions were 2.6 and 1%, respectively.

Table 5- 1Chemical Composition

		SiO_2	Al_2O_3	Fe_2O_3	S+Al+Fe	CaO	MgO	Na_2O	K_2O	Na_2O_e	LOI	SG	Amorphous Level (%)
	Low-alkali Portland cement	19.93	4.77	3.13	27.83	62.27	2.70	0.06	0.48	0.37	2.6	3.15	NA
	High-alkali Portland cement	19.00	4.99	2.11	26.1	62.45	2.84	0.31	1.05	1.0	NA	3.15	NA
Volcanic rhyolitic tuff	NP 1	68.62	13.14	1.91	83.67	1.73	1.43	2.7	3.2	4.82	7.18	2.53	37.67
Pumice	NP 2	73.42	12.30	1.41	87.13	0.79	0.23	2.9	4.2	5.61	4.72	2.35	98.55
Pumice	NP 3	65.48	11.19	1.75	78.42	2.99	0.33	3.6	3.4	5.85	10.87	2.26	3.38
Volcanic rhyolitic tephra	NP 4	71.95	12.26	1.50	85.71	0.93	0.39	3.9	4.0	6.51	4.88	2.35	87.76
Volcanic glass	NP 5	71.21	12.99	0.90	85.1	0.56	0.13	3.9	4.1	6.57	5.95	2.40	100
Pumice	NP 6	71.91	11.68	2.18	85.77	0.32	0.09	5.5	4.2	8.28	3.94	2.34	91.17
Reclaimed fly ash	RFA 1	53.06	15.13	6.88	75.07	13.70	4.53	3.4	1.9	4.69	0.55	2.56	82.48
Reclaimed fly ash	RFA 2	56.81	14.20	2.69	73.7	10.13	1.41	2.8	2.7	4.56	8.42	2.42	88.88

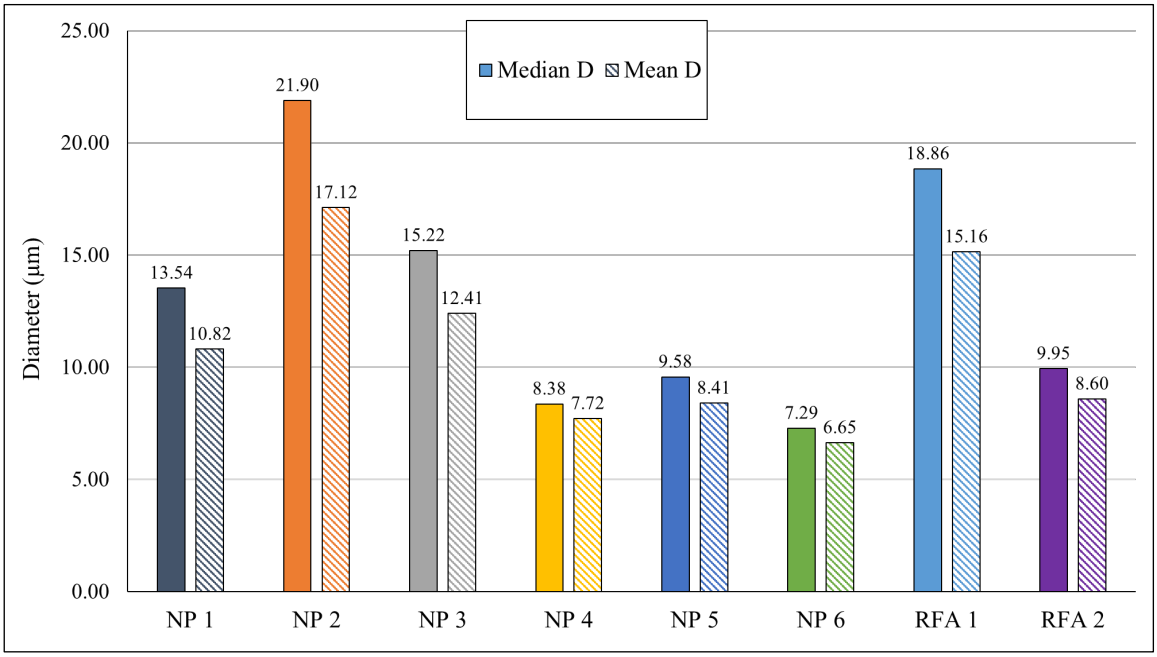

(a)

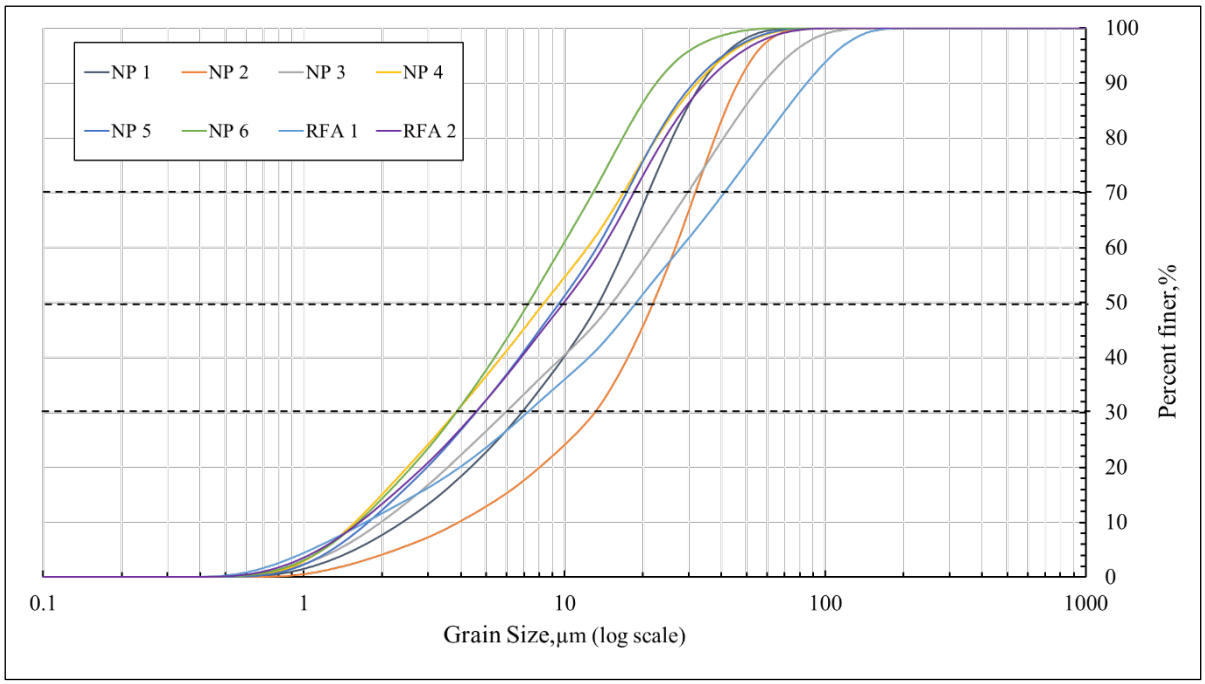

Figure 5- 1(a)SCMs' particle size; (b)Particle size distribution of natural pozzolans

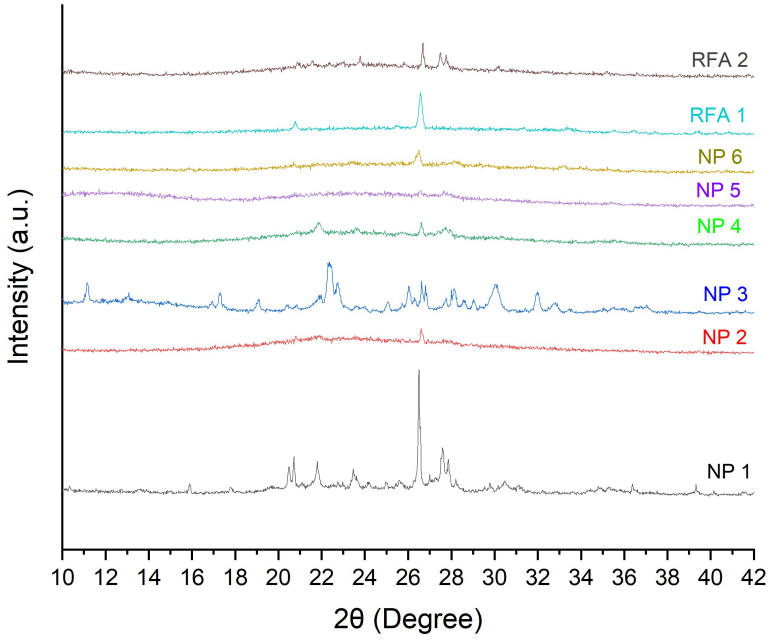

Figure 5- 2 XRD Pattern

5.2.2 ASTM C311 Strength Activity Index (SAI)

The strength activity index test (SAI) was used to evaluate the pozzolanic activity of SCMs in mixtures blended with low-alkali cement, and the mixture proportions were followed in accordance with ASTM C311. In this test, eight mixtures with six samples were prepared for 7-day and 28-day strength measurements. After casting, the specimens were placed in the standard curing room for 24 hours. After demolding, the samples were cured at ambient temperature in lime-saturated water. Compressive strength was measured using the TEST MARK CM-3000 SD compression testing machine at a loading rate of 50 psi/s. The SAI was calculated using **Equation (1)**:

$$\boldsymbol{SAI} = \frac{\boldsymbol{Average\ compressive\ strength\ of\ test\ mixtures}}{\boldsymbol{Average\ compressive\ strength\ of\ control}} \times 100\% \quad (1)$$

5.2.3 ASTM C1897 R^3

Pozzolanic reactivity of SCMs was evaluated using the R^3 test per ASTM C1897-20 method A. Isothermal calorimetry was used in this test to quantitatively determine the heat signature. The mixtures consisted of SCMs, calcium hydroxide (CH), calcium carbonate (CaCO3), potassium sulfate (K_2SO_4), and potassium hydroxide (KOH). The mass ratio of SCMs to CH and $CaCO_3$ was 1 to 3 and 2 to 1, respectively. The potassium solution was prepared by dissolving 4.00 g of KOH and 20.0 g of K_2SO_4 in 1.00 L of reagent water. The mass ratio of potassium to the solids, i.e., blend of SCMs, CH, and CaCO3, was 1.2. The cumulative heat was measured at 40°C for 7 days. All the materials were mixed at 1600 ± 50 r/min for 2 min using the high-shear blender to achieve a homogeneous paste.

5.2.4 Thermogravimetric Analysis (TGA) for Determining Calcium Hydroxide (CH) Consumption

Thermogravimetric analysis (TGA) was conducted to determine the amount of calcium hydroxide (CH) in the cement paste. For this testing, AutoTGA Q5000 instrument was employed. The pastes were prepared by blending low-alkali cement with SCMs at a 20% mass replacement of cement, at a water-to-binder ratio of 0.42. The prepared paste samples were stored in a sealed container and were tested at the ages 12-hours, 1 day, 3-day, 7-day, 28-day, and 56-days. After casting, the specimens were sealed in air-tight test tubes to avoid potential carbonation and stored in an air chamber maintained at 23°C and 50% RH. Before testing, the samples were de-molded from the tubes and ground using an agate mortar and pestle to pass the No.100 sieve (150 μm). Then, the powder samples were immersed in 50ml isopropanol for 15 minutes to remove moisture from the powder. The suspension was filtered by using Büchner funnel to obtain the dehydrated powder, and 10 ml diethylene was added to the powder to remove extra isopropanol. After preparation, the sample was immediately stored in air-tight vials and tested. The weight loss observed in the samples between the temperatures of 400°C and 500°C was recorded and the amount of calcium hydroxide ($Ca(OH)_2$) per gram of cement in the mixture was calculated using **Equation 2:**

$$\boldsymbol{Ca(OH)_2} = \frac{(\boldsymbol{Mass_{400^oC} - Mass_{500^oC}}) \times (\boldsymbol{Ca(OH)_2\ Molor\ mass})}{\boldsymbol{H_2O\ Molar\ mass}} \quad (2)$$

5.2.5 Pore Solution Analysis

Pore solution extraction and analysis were performed on binder paste specimens at different ages to determine the pore solution chemistry. The samples were mixed with binders consisting of high-alkali cement and SCMs, and deionized water. The w/b ratio for this study was maintained at 0.60 for all samples in this experiment. The method used to extract pore solution in this study was using a pore solution expression die based on Barneyback and Diamond [36] . Maximum stress of about 260 MPa was applied to extract the pore solution from samples. The load rate was maintained between 1 and 1.8 kN/s. The pore solution was collected into centrifuge tubes, preventing potential contamination from carbonation, and they were stored at 4°C in a refrigerator before testing.

Inductively coupled plasma optical emission spectroscopy (ICP-OES) was used to analyze the pore solution to determine the concentration of alkalis ions (Na^+&K^+). Before running ICP, the pore solution was centrifuged for 10 mins to separate any solids and the liquid. One ml pore solution was extracted from the storage tubes and diluted with 2% Nitric acid (HNO_3) based on mass. The pore solution's dilution factor was 100, meaning a 100 ml mixture solution contained 1 ml of pore solution. All water used in this study was deionized water.

5.2.6 AASHTO T380 Miniature Concrete Prism Test (MCPT)

AASHTO T380 (MCPT) was used to evaluate the high-alkali SCMs to mitigate ASR in this study. In this method, the cementitious materials content of concrete mixtures was maintained at 420 kg/m^3, with a w/b ratio of 0.45. The dry mass of coarse aggregate per unit volume of concrete was maintained at 0.65, and the coarse aggregates' gradation followed the recommended gradation per AASHTO T380. The fineness modulus of fine aggregates conformed to 2.60 ± 0.3. Reagent-grade NaOH pellets were dissolved in the mixing water to boost the alkali content of the concrete

to 1.25% by the mass of cement. SCMs were used at dosage levels of 20%, 30%, and 40% by mass of cement.

The test specimens were cast and cured at ambient temperature and 100% RH for 24 hours. After demolding, the specimens were placed in water at 60°C for another 24 hours. The zero-day reading was taken at the end of 24 hours of water bath curing. Then the specimens were transferred into a sealed container with 1N NaOH maintained at 60°C. The prism length changes were recorded periodically at 0, 3, 7, 10, 14, 21, 28, 42, 56, 70, and 84 days. The criteria for evaluating the efficacy of SCMs in mitigating ASR in the MCPT method at 56-days are as follows per AASHTO T380:

7. Expansion < 0.020% - Effective ASR Mitigation;
8. 0.020% < expansion < 0.025% Uncertain ASR Mitigation
9. Expansion > 0.025% Not effective ASR mitigation

If the samples exhibit expansion between 0.20 and 0.25 at 56 days, the average expansion between 56-day to 84-day (8 weeks to 12 weeks), should be less than 0.010% per 2 weeks for the mitigation measure to be considered effective.

5.3. Results and Discussion

5.3.1 Strength Activity Index (SAI)

Figure 5- 3 shows the strength activity index (SAI) results, expressed as a percent of the Portland cement control. At 7 days, except NP 3 and RFA 1, the rest of the test materials had a strength activity index of approximately 85%. NP 3 indicated a greater value than other materials and was very close to that of control mixture at 99%. However, the strength activity index of RFA 1 was only 70%, lower than the requirement of ASTM C618 of 75%. At 28 days, apart from NP 2, the other SCMs showed a significant increase in SAI compared to the corresponding value at 7 days, especially RFA 2, which increased from 85% to 112%. The pozzolanic reaction is the predominant reason for the relative increase in the strength activity index at this age [37]–[39]. The 28-day SAI of NP 4, 5, and 6 increased by around 10% from 7-day, reaching around 95%. However, NP 2's 28-day SAI stayed constant at 86%.

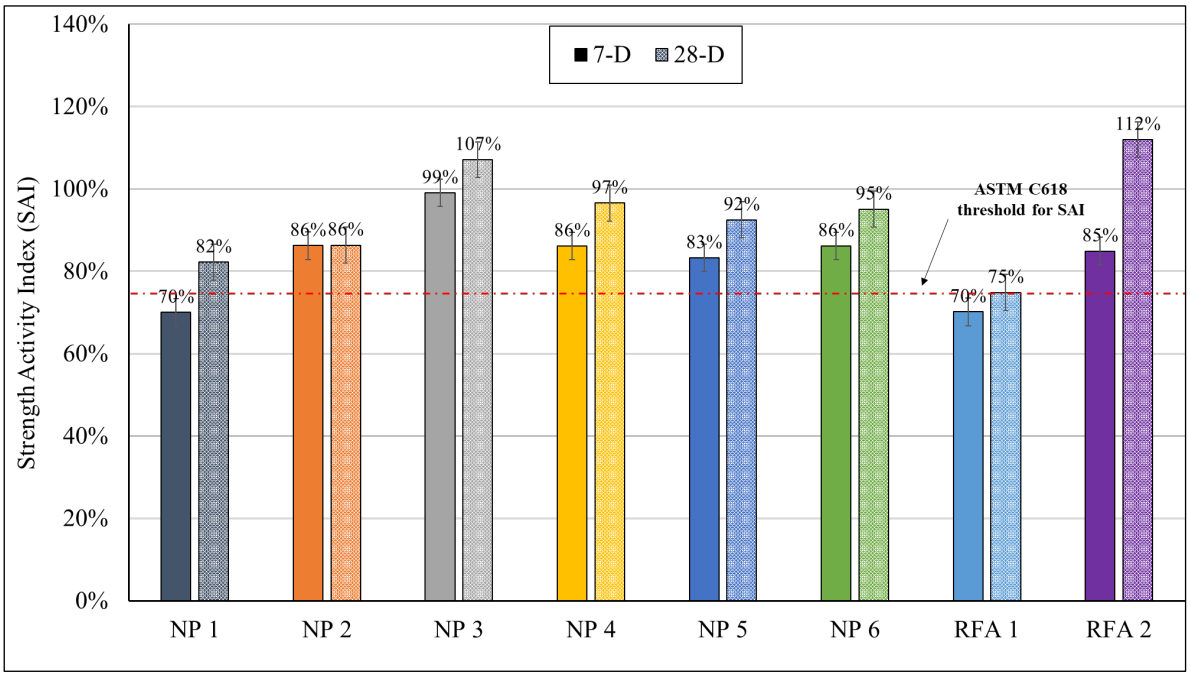

Figure 5- 3 High-Alkali SCMs Strength Activity Index Results (SAI)

5.3.2 ASTM C1897 - R3

Figure 5- 4 indicates the 7-day cumulative heat release for the R^3 results. All the paste specimens with SCMs investigated in this study showed a 7-day cumulative heat above 300 J/g. A previous study concluded that the if the material's 7-day cumulative heat exceeded 200 J/g, it was a highly pozzolanic material; on the contrary, if the cumulative heat was below 100 J/g, it indicated an inert material [40]. Therefore, all the high-alkali SCMs in this test are highly pozzolanic materials. Two reclaimed fly ash had the highest cumulative heat in this test, with RFA 1 and RFA 2 leading other natural pozzolans. The cumulative heat of NP 4 and NP 5 was around 350 J/g, and NP 2 and NP 3 were about 300 J/g.

The results from R^3 test did not correlate well with SAI results. For example, RFA 1 was highly pozzolanic material with the highest cumulative heat release at 7-day in the R^3 test. However, in the SAI test, it had the lowest strength activity index at both 7-days and 28-days. Additionally, NP 3 had very high strength activity index, only second to RFA 2, but its cumulative heat release was moderate among all materials in the R^3 test.

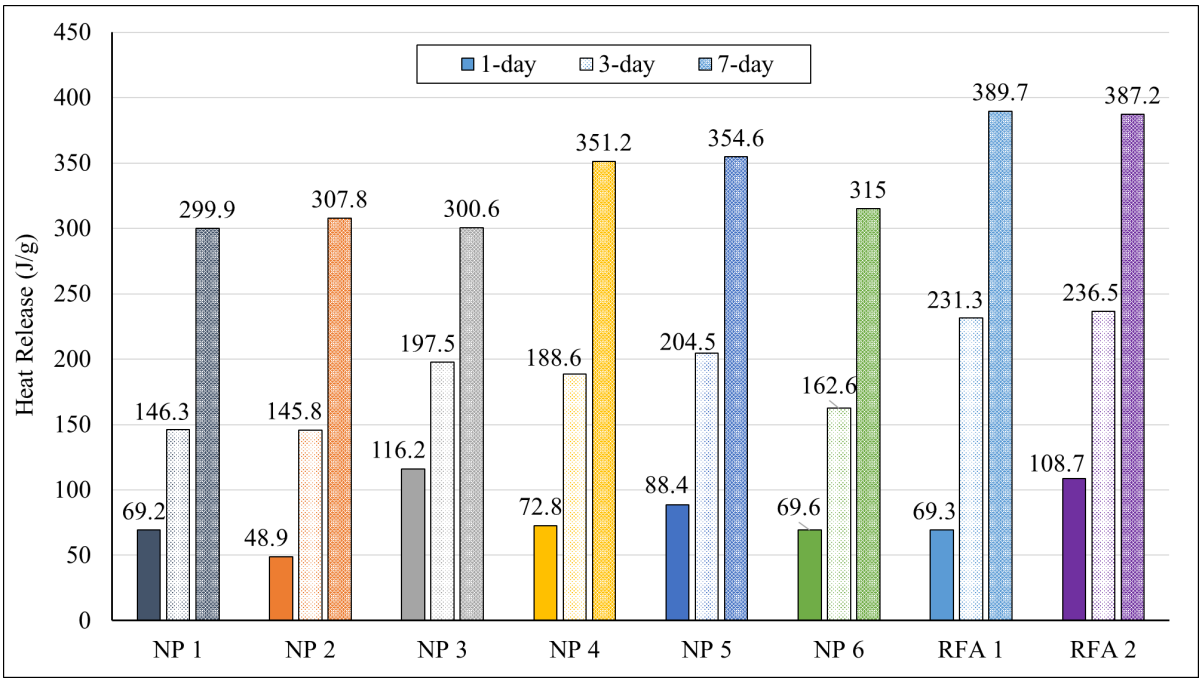

Figure 5- 4 Heat Release of High-Alkali SCMs in R^3 test

5.3.3 Thermogravimetric analysis (TGA)

Figure 5- 5 indicates the relative CH contents in the paste. Considering the cement dilution that occurs when cement is replaced with 20% SCM calcium hydroxide (CH) content of the test mixtures was divided by 0.8 to correct for the dilution. The calibrated high-alkali SCMs CH consumption values were compared to the control, expressed as % control, and the results are shown in Figure 5- 5.

At early ages, before 7 days, it is clear that all the high-alkali SCMs increased the CH content in the mixtures, which resulted from the filler effect of SCMs. The filler effect increased nucleation sites, further accelerating the cement hydration process [41]. With the sample age increasing and pozzolanic reactivity, the CH content of mixtures with SCMs started to decrease, and some groups were lower than the control, indicating the occurrence of pozzolanic reactions caused by high-alkali SCMs. NP 2 and RFA 1 did not effectively lower the CH content in the mixtures compared to the control, and their CH content level was maintained at a constant level between 28 days and

56 days. It could result from the larger particle size of NP 2 and RFA 1. These two materials have larger particle sizes than the rest. For the rest of the materials, they decreased the CH content by at least 5% compared to the control.

The CH consumption in the TGA was inconsistent with the R^3 test results. The materials indicated as highly pozzolanic materials in R^3 did not effectively consume CH in the mixtures such as the RFA 1 and NP 2. The potential reason for the results was the different test environments. The R^3 test's environment was highly alkaline and high temperature (40°C), potentially increasing high-alkali SCMs' reactivity and reducing the impact of particle size; this tendency was also observed in a previous study [42].

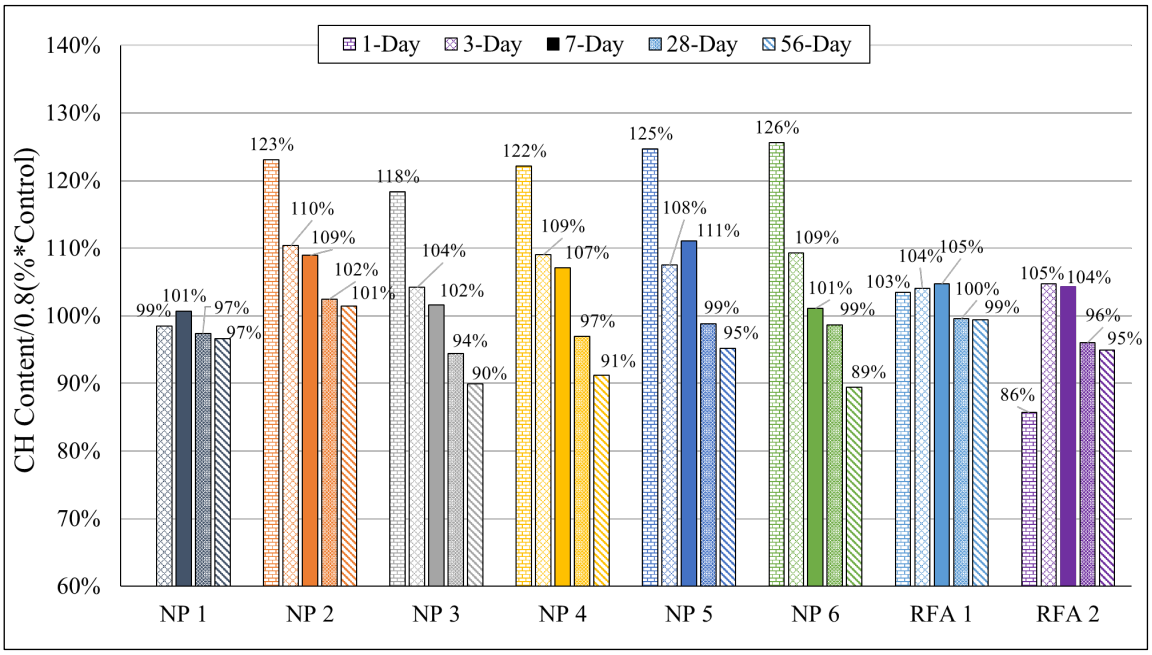

Figure 5- 5 Relative CH Contents in Pastes Containing 20% High-Alkali SCMs Replacement

5.3.4 Pore Solution Analysis

Figure 5- 6 and Figure 5- 7 show the potassium (K^+) and sodium (Na^+) concentrations of pore solutions expressed from various paste specimens containing SCMs at 28 and 84-day test durations. Figure 5- 8 indicates the sum of alkalis ions concentration ($K^+ + Na^+$) in the same paste specimens.

Since mixtures with SCMs contain only 80% cement, the red line in the figure is included to represent the 80% alkali ions concentration, resulting directly from the Portland cement. The pore solution analysis results indicate K^+ concentration was much higher than Na^+ in all the mixtures, with exception of NP 2, and this is due to the fact that K_2O is the principal alkali oxide in Portland cement. The alkali ions concentration in control mixture remained constant from 28 days to 84 days, as majority of Portland cement hydrations occurs during this period and all alkalies are essentially released during this period.

In Figure 5- 6, the K^+ concentration of all test mixtures with SCMs was below the 80% line at 28 days and 84 days. NP 3 had the lowest K^+ but increased significantly from the 28^{th} to the 84^{th} day, from 0.127 to 0.172 mmol/L. For the rest of the mixtures with other SCMs, the K^+ concentration decreased with increasing sample age. RFA 1 indicated only a slight decrease from the 28^{th} to the 84^{th} day. Additionally, the K+ concentration of RFA 1 was much higher compared to mixtures with other SCMs. The change in K+ concentration strongly suggests the alkali binding by the pozzolanic reaction products.

Na^+ concentration behaved differently from K^+. Other mixtures, except for NP 1, indicated higher concentrations than the 80% control, especially NP 3. The Na^+ ion concentration of NP 3 was highest at both 28 days and 84 days, with 0.242 and 0.235 mmol/L, respectively. while that of the control was only about 0.145 mmol/L. RFA 1 still did not perform well. On the 28^{th} day, RFA 1's Na+ concentration was about 0.188 mmol/L, the second highest, and it increased by 0.04 mmol/L to reach 0.231 on the 84^{th} day. The increase in Na^+ concentration of all mixtures compared to the 80% of the control mixture indicated that the majority of the high-alkali SCMs released Na^+ ions into the pore solution during the pozzolanic reaction, although these values were lower than that of K^+ ion concentrations.

It was observed that the mixtures with RFA 1 had the highest total alkalis ions concentration among all the mixtures, which was also higher than the 80% of the control. NP 2 showed the lowest total alkali ions concentration, and NP 2 lowered the alkalis ions from 28 days to 84 days. The total alkali content of pore solution in mixtures with NP 4, NP 5, NP 6, and RFA 2 remained constant between the 28 and 84-day measurements. Both NP 2 and RFA 2 showed an increase in total alkali concentration in pore solution from 28 days to 84 days.

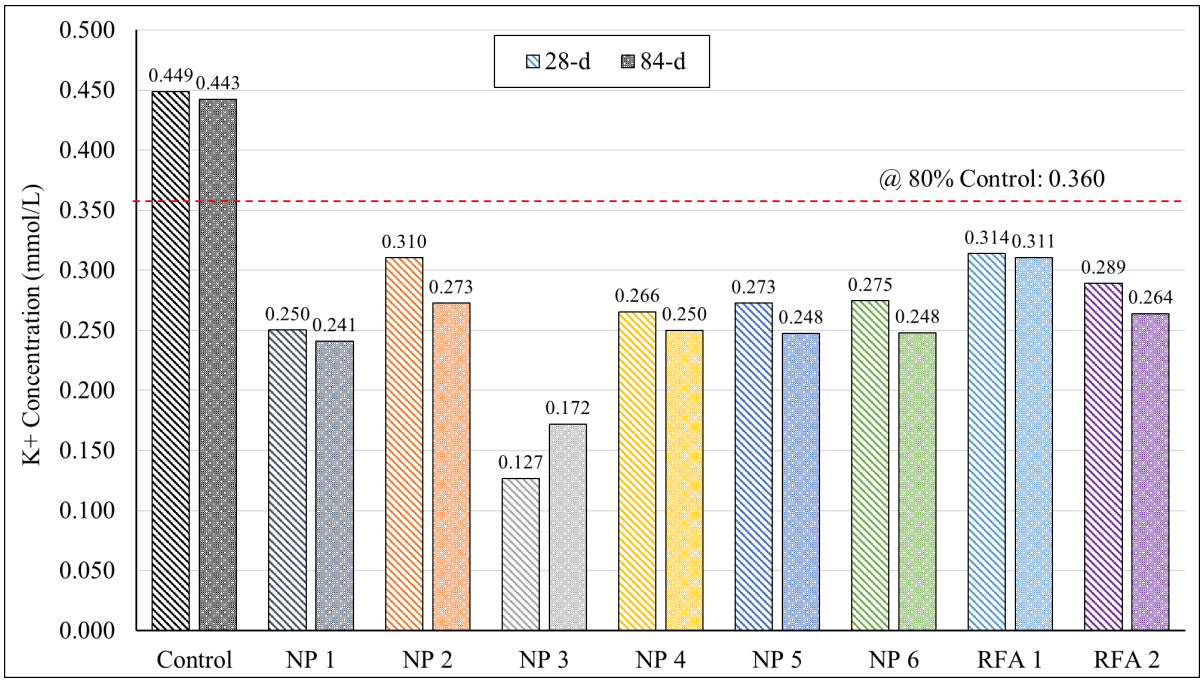

Figure 5- 6 K^+ Concentration

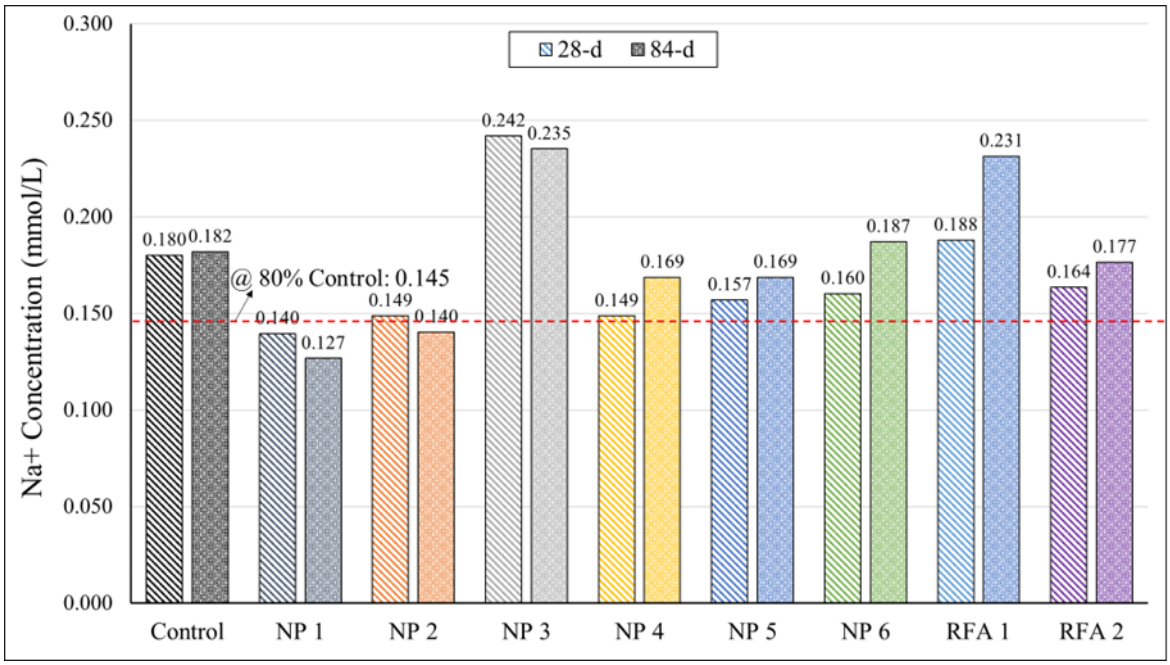

Figure 5- 7 Na^+ Concentration

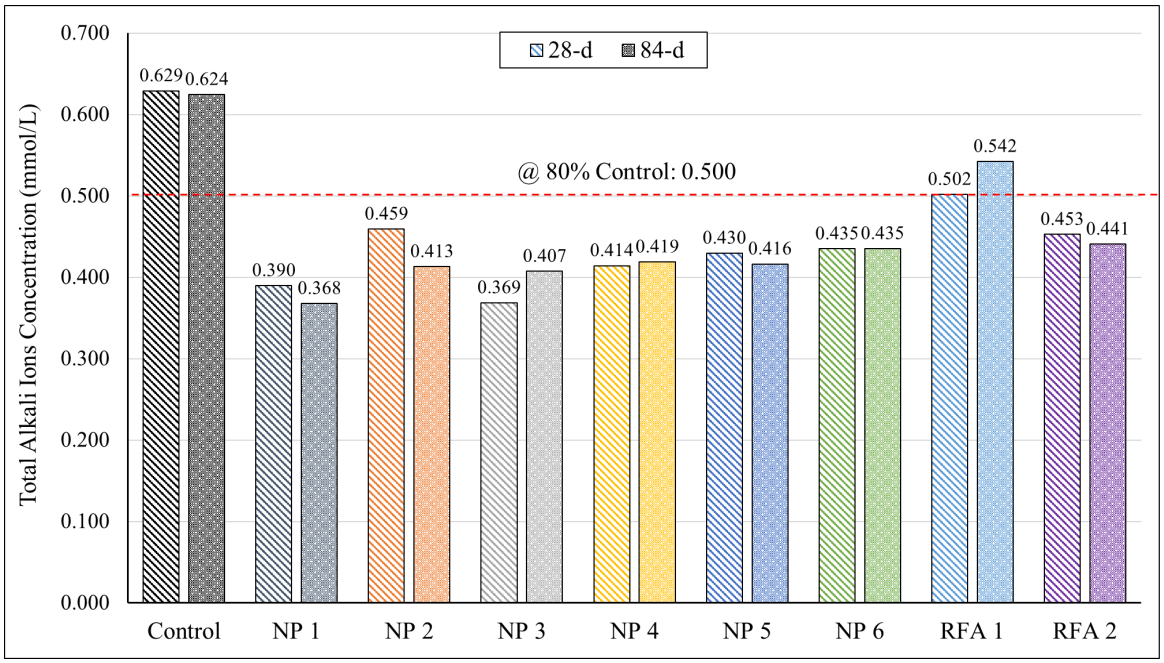

Figure 5- 8 Total Alkali Ions Concentration

5.3.5 AASHTO T380 Miniature Concrete Prism Test (MCPT)

Figure 5- 9 and Figure 5- 10 exhibited the length change of concrete prisms in AASHTO T380 (MCPT) with 20% SCMs. In MCPT, SCMs are considered to effectively mitigate ASR when expansion is below 0.020% at 56 days, and the expansion rate should not exceed 0.010% every two weeks from day 56 to day 84.

Except for NP 2 and RFA 1, other materials effectively limited the ASR expansion to lower than 0.020% at 56 days. The Expansion of NP 2 and RFA 1 was 0.026% and 0.035%, respectively. RFA 1 showed the worst performance in the MCPT testing. Additionally, NP 2 and RFA 1 also failed to satisfy the expansion rate requirement of less than 0.010% per two weeks between 56 and 84 days. NP 4 had the lowest expansion at 56 days. However, at 84 days, NP 6's showed improved performance compared to NP 4. During the interval from 56 to 84 days, the rest of the mixtures, with exception of NP 6, continued to expand, and their two-week expansion rate exceeded 0.020% at 84 days.

NP 2, 3, 4, and two RFAs were selected to study the effect of SCMs replacement level on ASR mitigation. The replacement levels were increased from 20% to 30% and 40% in this test. The test results from this study are presented in Figure 5- 11. The results indicated that with an increase in SCMs replacement level, the ASR expansion was significantly mitigated. Apart from RFA 1, the 30% replacement level was adequate for all the SCMs to control ASR expansion to less than 0.020% at 56 days, and the mitigation was effective even at 84 days. RFA 1 failed even at 30% replacement level, as the average test prism expansion was 0.035% at 56 days, which is much higher than the threshold of 0.020%. However, at 40% replacement level, RFA 1 successfully controlled the expansion below the 0.020% limit; even at 84 days, the expansion was limited to only 0.018%.

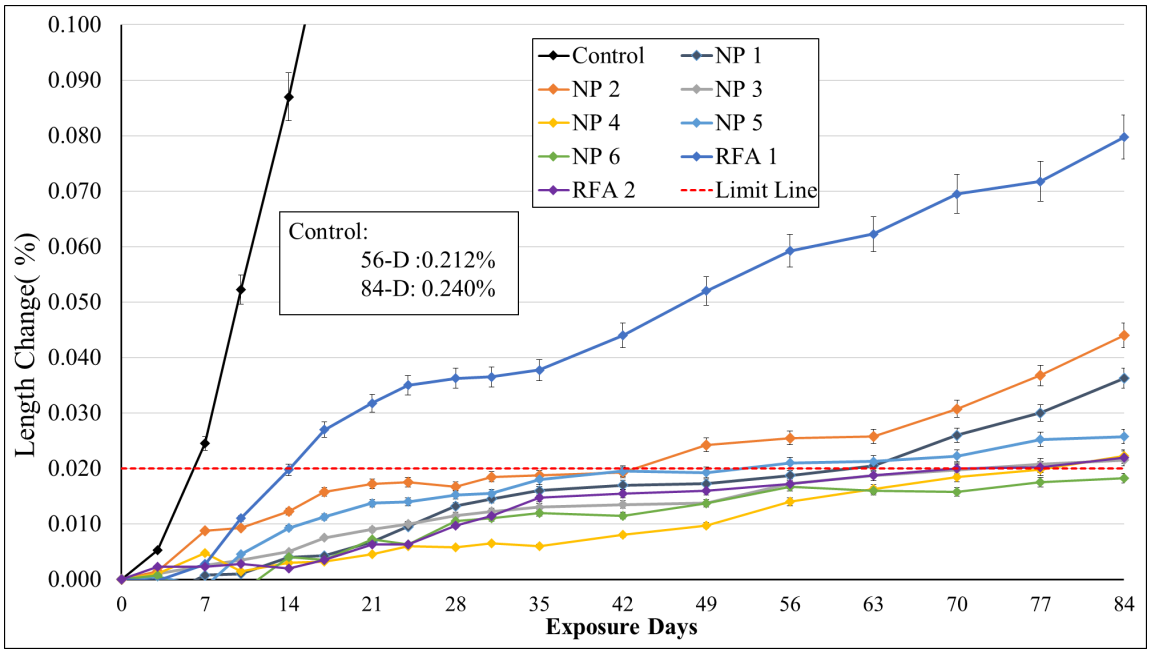

Figure 5- 9 AASHTO T380 length change of concrete prisms with 20% SCMs replacement

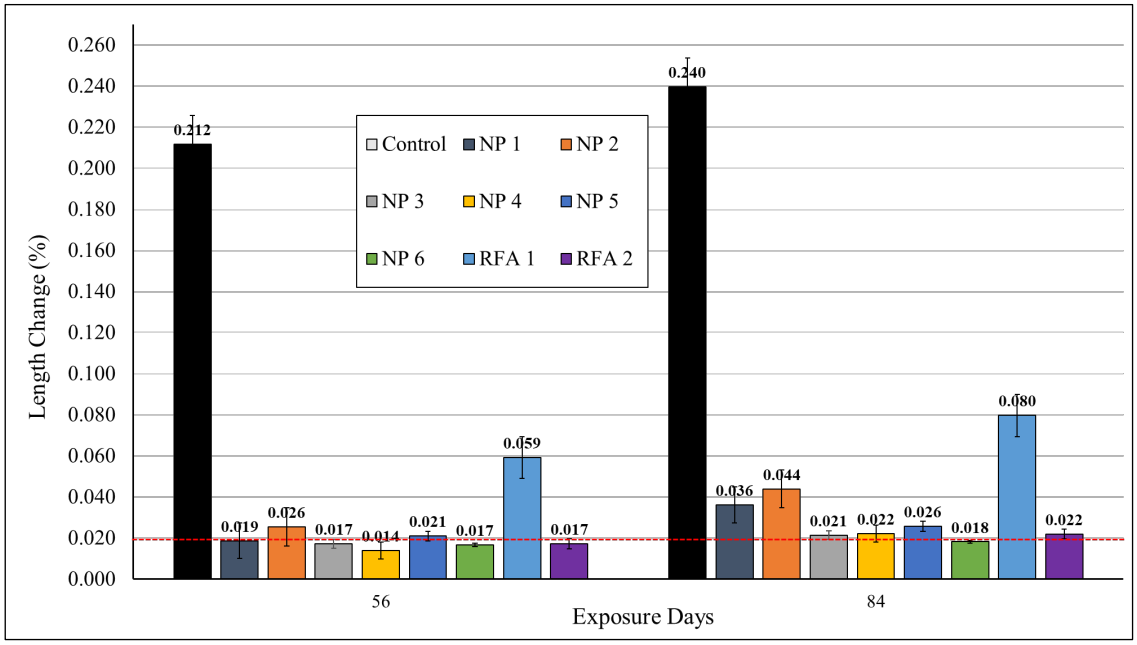

Figure 5- 10 AASHTO T380 56-D & 84-D expansion value with 20% SCMs replacement

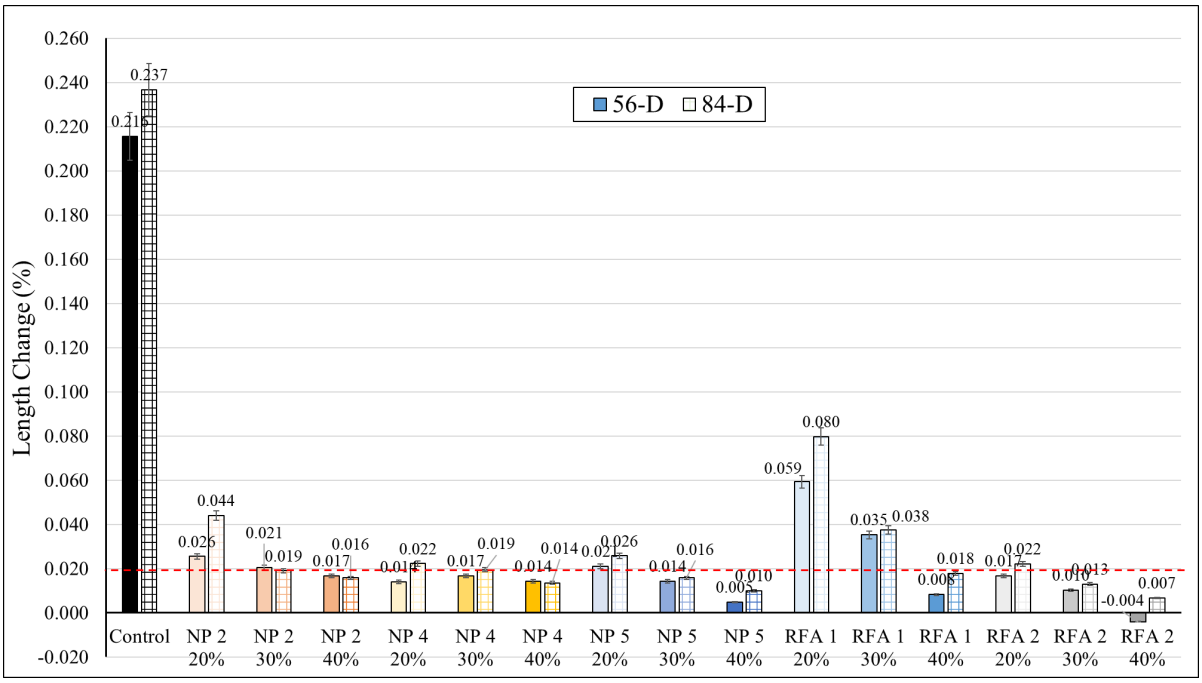

Figure 5- 11 AASHTO T380 Replacement level results comparison

5.3.6 Correlation between Various Pozzolanic Reactivity Experiments and MCPT

Table 5- 2 Correlation between MCPT Expansion with Pozzolanic Reactivity Experiments shows the simple linear regression between MCPT expansion with pozzolanic reactivity experiments displaying raw data, regression equation, P-values, and R^2. To mitigate the influence of material types on the experimental results, the data is categorized into two groups: one includes all SCMs, and the other comprises only five types of natural pozzolans. Additionally, in contrast to the other experiments, the dataset for analysis includes the values of the control group of TGA and total alkali ions, as these two tests are quantitative analyses. Furthermore, in this analysis, the median size of SCMs was selected as a parameter to investigate the correlation between SCM's particle size and MCPT expansion because, compared to the mean size, the median size was less impacted by the extreme values. Also, for this particular part, the TGA analysis used the percentage of CH consumed rather than previously relative to the control after calibration by the SCMs dilution factor.

According to the results, an excellent correlation existed between MCPT expansion and TGA weight loss and total alkali ion results, with R^2 values of 0.936 and 0.864, respectively. However, the R^2 values significantly improved to 0.9726 and 0.9674, respectively, when considering only natural pozzolans were considered. These results revealed that the ASR mitigation of SCMs was proportional to the CH consumed. A similar finding was discovered in S. Oruji et al.'s research [43]—their results showed that ASR expansion and CH content indicated a linear proportional regression with 0.993 R^2. Additionally, the impact of pore solution alkalinity on ASR expansion, as observed in this study, can also confirm the findings from previous research [44], which showed that concrete exhibited significant increase in expansion with increase in pore solution alkali ion concentration.

However, MCPT 84-D expansion did not significantly correlate with the high-alkali SCMs' amorphous level, the sum(Si+Al+Fe), and cumulative heat release in the R^3 test, and their R^2 values were lower when considering all the SCMs or only natural pozzolans. Firstly, the high alkali and temperature of R^3 reaction environment can explain its weak correlation with MCPT, which reduced the impact of relevant factors, such as particle size, on the pozzolanic reactivity [42]. Secondly, the reactivity of SCMs and their ability to mitigate ASR is generally believed to be proportional to sum of Si+Al+Fe and amorphous content of the pozzolan. However, the results of this study were not in agreement with the previous study, and this inconsistency can be attributed to the presence of high crystallinity in some SCMs [13]. The existence of crystal content in SCMs, such as NP 3, indicated that not all the available silica and alumina were amorphous and reactive, making the sum of Si+Al+Fe unsuitable for directly determining pozzolanic reactivity. Thirdly, regarding the amorphous level, the low R^2 could be attributed to the activation of the crystal phase

of SCMs during the reaction [45]. This finding suggests that some high-crystal materials were not indeed "inert," and the specific phase of the crystal also influenced their reactivity.

The correlation between SAI and ASR expansion was only 0.6781 when considering all SCMs, but decreased to 0.522 when only considering natural pozzolans. Neither value was significant, suggesting that using SAI to predict SCMs' ASR mitigation performance was ineffective. For the impact of SCMs on gaining strength, apart from the densification caused by the pozzolanic reaction, the filler effect was another factor in accelerating the strength development, which enhanced the packing density of mixtures and allowed for further binder development [41]. Furthermore, to mitigate the influence of material category differences, only natural pozzolan specimens were used for analyzing the correlation between MCPT expansion and the particle size of SCMs. In this case, the R^2 value reached 0.719, which indicates a strong relationship between particle size and the suppression of ASR expansion. This relationship has also been confirmed in previous research: smaller particles possess a higher pozzolanic reactivity [14].

Table 5- 2 Correlation between MCPT Expansion with Pozzolanic Reactivity Experiments

	MCPT-84D Expansion	Median Size	Sum of Si+Al+Fe in XRF	Amorphous	SAI	R3 Cumulative Heat Release	TGA Weight Loss (400-500oC)	Total Alkali Ions
	(%)	(µm)	%	(%)	(%)	(J/g)	%	(mmol/L)
Control	0.240						4.233	0.624
NP 1	0.036	10.82	83.67	37.67	82	299.9	3.266	0.368
NP 2	0.044	21.90	87.13	98.55	86	307.8	3.428	0.413
NP 3	0.021	15.22	78.42	3.38	107	300.6	3.038	0.407
NP 4	0.022	8.38	85.71	87.76	97	351.2	3.082	0.419
NP 5	0.026	9.58	85.10	100.00	92	354.6	3.217	0.416
NP 6	0.018	7.29	85.77	91.17	95	315	3.021	0.435
RFA 1	0.080	18.86	75.07	82.48	75	389.7	3.358	0.542
RFA 2	0.022	9.95	73.70	88.88	112	387.2	3.207	0.441
Regression Equation (All SCMs)		MCPT-84D Expansion = -0.000904 + 0.0027082*Median Size	MCPT-84D Expansion = 0.1371385 - 0.0012651*Sum (Si+Al+Fe)	MCPT-84D Expansion = 0.0278603 + 7.8179e-5*Amorphous	MCPT-84D Expansion = 0.1555723 - 0.0013077*SAI	MCPT-84D Expansion = -0.034249 + 0.0002007*R3 Cumulative Heat Release	MCPT-84D Expansion = -0.702009 + 0.2292919*TGA Weight Loss	MCPT-84D Expansion = -0.356097 + 0.8985068*Total Alkali Ions
Intercept P-Value (All SCMs)		0.9557	0.3102	0.2031	0.6117	0.6484	< 0.001	0.0034
Predictor Variable P-Value (All SCMs)		0.0554	0.4341	0.7579	0.0081	0.3760	< 0.001	0.001
R2 (All SCMs)		0.4839	0.1048	0.0171	0.0218	0.1322	0.9361	0.7959
Regression Equation (Natural Pozzolans)		MCPT-84D Expansion = 0.0116197 + 0.0013292*Median Size	MCPT-84D Expansion = -0.072121 + 0.0011857*sum(Si+Al+Fe)	MCPT-84D Expansion = 0.0253277 + 3.5921e-5*Amorphous	MCPT-84D Expansion = 0.1188651 - 0.0009713*SAI	MCPT-84D Expansion = 0.0717649 - 0.0001366*R3 Cumulative Heat Release	MCPT-84D Expansion = -0.72996 + 0.2356994*TGA Weight Loss	MCPT-84D Expansion = -0.399647 + 1.0202216*Total Alkali Ions
Intercept P-Value (Natural Pozzolans)		0.2372	0.6039	0.0618	0.5867	0.3070	0.0004	0.0024
Predictor Variable P-Value (Natural Pozzolans)		0.1043	0.4790	0.7883	0.0757	0.5125	0.0003	0.0011
R2 (Natural Pozzolans)		0.5232	0.1320	0.0202	0.5867	0.1141	0.9434	0.9000

5.4. Conclusion

From the data obtained in this study, the following conclusions can be drawn:

1. Compared to the control, the use of high-alkali SCMs can effectively reduce ASR expansion. RFA 1 did not perform as well as the rest, however, its use reduced ASR-induced expansion at the 20% replacement level compared to the control. Preliminary results indicate that at higher replacement levels (30% and 40%), high-alkali SCMs can perform much more effectively in mitigating ASR.
2. The amorphous level of high-alkali SCMs was found to be less impactful than other parameters. No apparent correlation was discovered between the amorphous level and other test results. NP 3 was a high-crystal material but still indicated good pozzolanic reactivity and ASR mitigation performance.
3. R^3 test cannot be directly used to predict high-alkali SCMs ASR mitigation performance. Also, a "weak" correlation exists between R^3 and SAI results. The primary reason for those results is that R^3 test evaluates the SCMs' pozzolanic reactivity at a high-alkali and higher-temperature environment, which can increase the reactivity of SCMs.
4. High-alkali SCMs can effectively lower the alkali ions concentration in the pore solution, supporting the MCPT results. Additionally, the use of the total alkali content of high-alkali SCMs' alkali content as criteria to evaluate their ASR mitigating ability is not appropriate. Materials with low alkalis content may also release more alkali ions into the pore solution and increase the challenge of controlling the ASR expansion. No correlation exists between the total alkali content of SCMs' and the alkali ions concentration in the pore solution.

5. Findings from TGA and pore solution analysis studies supported the expansion observed in the MCPT tests. The results of the two methods indicated "excellent" correlations with ASR expansion. Compared to other pozzolanic reactivity experiments, TGA and pore solution analysis are more persuasive in predicting high-alkali SCMs' ASR mitigation performance.
6. Not all SCMs can be treated equally. Natural pozzolans and industrial by-products such as fly ashes, must be analyzed independently for their ability to mitigate ASR.

5.5. Reference

[1] P. K. Mehta and P. J. Monteiro, *Concrete: microstructure, properties, and materials*. McGraw-Hill Education, 2014.

[2] ASTM C618-22 Specification for Coal Fly Ash and Raw or Calcined Natural Pozzolan for Use in Concrete, ASTM International

[3] T. R. Naik, "Sustainability of Concrete Construction," *Practice Periodical on Structural Design and Construction*, vol. 13, no. 2, pp. 98–103, May 2008, doi: 10.1061/(ASCE)1084-0680(2008)13:2(98).

[4] "Concrete needs to lose its colossal carbon footprint," *Nature*, vol. 597, no. 7878, pp. 593–594, Sep. 2021, doi: 10.1038/d41586-021-02612-5.

[5] "Global CO2 emissions rebounded to their highest level in history in 2021 - News," *IEA*. https://www.iea.org/news/global-co2-emissions-rebounded-to-their-highest-level-in-history-in-2021 (accessed Sep. 04, 2022).

[6] V. G. Papadakis, S. Antiohos, and S. Tsimas, "Supplementary cementing materials in concrete: Part II: A fundamental estimation of the efficiency factor," *Cement and Concrete Research*, vol. 32, no. 10, pp. 1533–1538, Oct. 2002, doi: 10.1016/S0008-8846(02)00829-3.

[7] S. A. Miller, "Supplementary cementitious materials to mitigate greenhouse gas emissions from concrete: can there be too much of a good thing?," Journal of Cleaner Production, vol. 178, pp. 587–598, Mar. 2018, doi: 10.1016/j.jclepro.2018.01.008.

[8] E. Menéndez, M. Á. Sanjuán, R. García-Roves, C. Argiz, and H. Recino, "Sustainable and Durable Performance of Pozzolanic Additions to Prevent Alkali-Silica Reaction (ASR) Promoted by Aggregates with Different Reaction Rates," *Applied Sciences*, vol. 10, no. 24, Art. no. 24, Jan. 2020, doi: 10.3390/app10249042.

[9] S. Gupta and S. Chaudhary, “State of the art review on supplementary cementitious materials in India – II: Characteristics of SCMs, effect on concrete and environmental impact,” *Journal of Cleaner Production*, vol. 357, p. 131945, Jul. 2022, doi: 10.1016/j.jclepro.2022.131945.

[10] J. D. Birchall, A. J. Howard, and J. E. Bailey, “On the hydration of Portland cement,” Proceedings of the Royal Society of London. A. Mathematical and Physical Sciences, vol. 360, no. 1702, pp. 445–453, 1978.

[11] A. A. Ramezanianpour, S. M. Motahari Karein, P. Vosoughi, A. Pilvar, S. Isapour, and F. Moodi, “Effects of calcined perlite powder as a SCM on the strength and permeability of concrete,” *Construction and Building Materials*, vol. 66, pp. 222–228, Sep. 2014, doi: 10.1016/j.conbuildmat.2014.05.086.

[12] X. Hou, L. J. Struble, and R. J. Kirkpatrick, “Formation of ASR gel and the roles of C-S-H and portlandite,” *Cement and Concrete Research*, vol. 34, no. 9, pp. 1683–1696, Sep. 2004, doi: 10.1016/j.cemconres.2004.03.026.

[13] R. Walker and S. Pavía, “Physical properties and reactivity of pozzolans, and their influence on the properties of lime–pozzolan pastes,” *Mater Struct*, vol. 44, no. 6, pp. 1139–1150, Jul. 2011, doi: 10.1617/s11527-010-9689-2.

[14] V.-T.-A. Van, C. Rößler, D.-D. Bui, and H.-M. Ludwig, “Pozzolanic reactivity of mesoporous amorphous rice husk ash in portlandite solution,” *Construction and Building Materials*, vol. 59, pp. 111–119, May 2014, doi: 10.1016/j.conbuildmat.2014.02.046.

[15] M. H. Shehata and M. D. A. Thomas, “The effect of fly ash composition on the expansion of concrete due to alkali–silica reaction,” *Cement and Concrete Research*, vol. 30, no. 7, pp. 1063–1072, Jul. 2000, doi: 10.1016/S0008-8846(00)00283-0.

[16] ASTM C311-22 Test Methods for Sampling and Testing Fly Ash or Natural Pozzolans for Use in Portland-Cement Concrete, ASTM International.

[17] ASTM C1897-20 Standard Test Methods for Measuring the Reactivity of Supplementary Cementitious Materials by Isothermal Calorimetry and Bound Water Measurements," ASTM International.

[18] F. Avet, R. Snellings, A. Alujas Diaz, M. Ben Haha, and K. Scrivener, "Development of a new rapid, relevant and reliable (R3) test method to evaluate the pozzolanic reactivity of calcined kaolinitic clays," *Cement and Concrete Research*, vol. 85, pp. 1–11, Jul. 2016, doi: 10.1016/j.cemconres.2016.02.015.

[19] G. De Schutter, "Hydration and temperature development of concrete made with blast-furnace slag cement," *Cement and Concrete Research*, vol. 29, no. 1, pp. 143–149, Jan. 1999, doi: 10.1016/S0008-8846(98)00229-4.

[20] W. Deboucha, N. Leklou, A. Khelidj, and M. N. Oudjit, "Hydration development of mineral additives blended cement using thermogravimetric analysis (TGA): Methodology of calculating the degree of hydration," *Construction and Building Materials*, vol. 146, pp. 687–701, Aug. 2017, doi: 10.1016/j.conbuildmat.2017.04.132.

[21] N. C. Collier, "Transition and decomposition temperatures of cement phases–a collection of thermal analysis data," *Ceramics-Silikaty*, vol. 60, no. 4, 2016.

[22] T. M. Research, "Fly Ash Market is Expected to be Valued at US$ 13.8 Bn by 2031, States TMR Study," *GlobeNewswire News Room*, Apr. 05, 2022. https://www.globenewswire.com/en/news-release/2022/04/05/2416875/0/en/Fly-Ash-Market-is-Expected-to-be-Valued-at-US-13-8-Bn-by-2031-States-TMR-Study.html (accessed May 05, 2022).

[23] M. C. G. Juenger, R. Snellings, and S. A. Bernal, “Supplementary cementitious materials: New sources, characterization, and performance insights,” *Cement and Concrete Research*, vol. 122, pp. 257–273, Aug. 2019, doi: 10.1016/j.cemconres.2019.05.008.

[24] M. D. A. Thomas, B. Fournier, K. J. Folliard, and Inc. Transtec Group, “Alkali-aggregate reactivity (AAR) facts book.,” FHWA-HIF-13-019, Mar. 2013.

[25] T. E. Stanton, “Studies of Use of Pozzolans for Counteracting Excessive Concrete Expansion Resulting from Reaction Between Aggregates and The Alkalies in Cement,” *Symposium on Use of Pozzolanic Materials in Mortars and Concretes*, Jan. 1950, doi: 10.1520/STP39409S.

[26] A. Vollpracht, B. Lothenbach, R. Snellings, and J. Haufe, “The pore solution of blended cements: a review,” *Mater Struct*, vol. 49, no. 8, pp. 3341–3367, Aug. 2016, doi: 10.1617/s11527-015-0724-1.

[27] J. Duchesne and M. A. Bérubé, “The effectiveness of supplementary cementing materials in suppressing expansion due to ASR: Another look at the reaction mechanisms part 2: Pore solution chemistry,” *Cement and Concrete Research*, vol. 24, no. 2, pp. 221–230, Jan. 1994, doi: 10.1016/0008-8846(94)90047-7.

[28] ASTM C1293-20a Standard Test Method for Determination of Length Change of Concrete Due to Alkali-Silica Reaction,” ASTM International

[29] ASTM C1567 Test Method for Determining the Potential Alkali-Silica Reactivity of Combinations of Cementitious Materials and Aggregate (Accelerated Mortar-Bar Method),” ASTM International.

[30] T. Kim, J. Olek, and H. Jeong, “Alkali–silica reaction: Kinetics of chemistry of pore solution and calcium hydroxide content in cementitious system,” *Cement and Concrete Research*, vol. 71, pp. 36–45, May 2015, doi: 10.1016/j.cemconres.2015.01.017.

[31] M. H. Shehata and M. D. A. Thomas, “Alkali release characteristics of blended cements,” *Cement and Concrete Research*, vol. 36, no. 6, pp. 1166–1175, Jun. 2006, doi: 10.1016/j.cemconres.2006.02.015.

[32] P. K. Mehta, “Natural pozzolans: Supplementary cementing materials,” in *Proc., Int. Symp. on Advances in Concrete Technology*, CANMET, Athens, Greece, 1987, pp. 407–430.

[33] R. E. Rodríguez-Camacho and R. Uribe-Afif, “Importance of using the natural pozzolans on concrete durability,” *Cement and Concrete Research*, vol. 32, no. 12, pp. 1851–1858, Dec. 2002, doi: 10.1016/S0008-8846(01)00714-1.

[34] “AASHTO T380 Standard Method of Test for Potential Alkali Reactivity of Aggregates and Effectiveness of ASR Mitigation Measures (Miniature Concrete Prism Test, MCPT),” American Association of State Highway and Transportation Officials.

[35] J. R. Deschamps and J. L. Flippen-Anderson, “Crystallography,” in *Encyclopedia of Physical Science and Technology (Third Edition)*, R. A. Meyers, Ed., New York: Academic Press, 2002, pp. 121–153. doi: 10.1016/B0-12-227410-5/00160-5.

[36] R. S. Barneyback and S. Diamond, “Expression and analysis of pore fluids from hardened cement pastes and mortars,” *Cement and Concrete Research*, vol. 11, no. 2, pp. 279–285, Mar. 1981, doi: 10.1016/0008-8846(81)90069-7.

[37] S. A. Saad, M. F. Nuruddin, N. Shafiq, and M. Ali, “Pozzolanic Reaction Mechanism of Rice Husk Ash in Concrete – A Review,” *Applied Mechanics and Materials*, vol. 773–774, pp. 1143–1147, 2015, doi: 10.4028/www.scientific.net/AMM.773-774.1143.

[38] A. Tironi, M. A. Trezza, A. N. Scian, and E. F. Irassar, “Assessment of pozzolanic activity of different calcined clays,” *Cement and Concrete Composites*, vol. 37, pp. 319–327, Mar. 2013, doi: 10.1016/j.cemconcomp.2013.01.002.

[39] H. Myadraboina, S. Setunge, and I. Patnaikuni, “Pozzolanic Index and lime requirement of low calcium fly ashes in high volume fly ash mortar,” *Construction and Building Materials*, vol. 131, pp. 690–695, Jan. 2017, doi: 10.1016/j.conbuildmat.2016.11.038.

[40] R. D. Kalina, S. Al-Shmaisani, R. D. Ferron, and M. C. Juenger, “False positives in ASTM C618 specifications for natural pozzolans,” *ACI Materials Journal*, vol. 116, no. 1, pp. 165–172, 2019.

[41] E. Berodier and K. Scrivener, “Understanding the Filler Effect on the Nucleation and Growth of C-S-H,” *Journal of the American Ceramic Society*, vol. 97, no. 12, pp. 3764–3773, 2014, doi: 10.1111/jace.13177.

[42] S. Al-Shmaisani, R. D. Kalina, R. D. Ferron, and M. C. G. Juenger, “Evaluation of Beneficiated and Reclaimed Fly Ashes in Concrete,” *ACI Materials Journal*, vol. 116, no. 4, Jul. 2019, doi: 10.14359/51716713.

[43] S. Oruji *et al.*, “Mitigation of ASR expansion in concrete using ultra-fine coal bottom ash,” *Construction and Building Materials*, vol. 202, pp. 814–824, Mar. 2019, doi: 10.1016/j.conbuildmat.2019.01.013.

[44] M. Bagheri, B. Lothenbach, and K. Scrivener, “The effect of paste composition, aggregate mineralogy and temperature on the pore solution composition and the extent of ASR expansion,” *Mater Struct*, vol. 55, no. 7, p. 192, Aug. 2022, doi: 10.1617/s11527-022-02015-6.

[45] C. Shi, “An overview on the activation of reactivity of natural pozzolans,” *Can. J. Civ. Eng.*, vol. 28, no. 5, pp. 778–786, Oct. 2001, doi: 10.1139/l01-041.

CHAPTER VI IMPACT OF HIGH ALKALI NATURAL POZZOLANS and RECLAIMED FLY ASH ON CONCRETE DURABILITY

Abstract

The increasing scarcity of traditional supplementary cementitious materials (SCMs) like Class F and Class C fly ashes, as well as slag, has compelled us to explore alternative SCMs that were previously considered less optimal. Specifically, high-alkali SCMs have often been avoided due to concerns that their alkali content might leach into the concrete pore solution, potentially worsening the risk of alkali-silica reaction (ASR). Nevertheless, some research conducted before indicated that not all alkalis of SCMs are able to release into concrete pore solution, and the preliminary research suggests that not all high-alkalis are deleterious, and some can effectively mitigate the expansive ASR reaction when used in appropriate dosage levels. This study evaluates the feasibility of using high-alkali SCMs, including natural pozzolans and reclaimed fly ash, to improve concrete durability performance. The ASR and sulfate attack mitigation performance of SCMs were evaluated by methods AASHTO T380 (MCPT) and ASTM C1012, respectively. ASTM C596 conducted the impact of high-alkali SCMs on drying shrinkage. Additionally, the potential effect of SCMs on concrete permeability was evaluated through a rapid chloride penetration test (RCPT) per ASTM C1202 and chloride migration test per NT Build 492. Also, concrete bulk electrical resistivity test, cementitious paste thermogravimetric analysis, and pore solution analysis of paste were performed to explain how high-alkali SCMs impact concrete durability. Ultimately, the high-alkali SCMs indicated the effectiveness of promoting concrete

durability performance, and their alkali content did not readily release into pore solution. Therefore, the materials with high alkali characteristics show the potential to be alternative SCMs in the concrete industry.

Keywords: High-Alkali Supplementary Cementitious Materials (SCMs), Concrete Durability, Pore Solution Analysis, Thermogravimetric analysis

6.1. Introduction

Concrete is the most dominant construction material worldwide and is responsible for at least 8% (36.3 billion tons) of global CO_2 emissions [1]–[3]. However, the demand for concrete persistently increases, which causes severe environmental impacts such as greenhouse emissions and significant demand for natural materials like coarse aggregate, river sand, and water. Repairing and rehabilitation of concrete also cause significant greenhouse emissions. According to the research [4], extending the infrastructure's service life by 50% can decrease 14% CO_2 emissions, which suggests the importance of concrete durability.

Concrete durability is the ability to have a long service life without deterioration caused by weathering action or chemical attack. Compared to extreme weather conditions, the primary and more pressing durability challenge in concrete structures is the occurrence of chemical reactions between the cement hydrates and various internal or external chemical compounds. Calcium hydroxide (CH) and calcium silicate hydrate (C-S-H) are the two primary cement hydration products [5]. However, in contrast to C-S-H, CH plays a limited role in enhancing compressive strength but is significantly implicated in various deteriorative chemical reactions that can harm the integrity of the concrete [6]–[8]. For example, CH in the cementitious matrix plays a significant role in alkali-silica reaction [9]. ASR is an acknowledged concrete deterioration problem that results from the reaction of reactive amorphous silica found in some natural aggregates with alkali

hydroxides (OH^-, Na^+, and K^+) present in the concrete pore solution, which forms ASR gel [10]–[13]. The gel is harmless in nature, but it exhibits hygroscopic that causes it to absorb moisture and subsequently expand. When the expanding gel is confined within tight pore structures within concrete, it generates tensile stresses, which can result in concrete cracking. The substantial presence of CH within the concrete pore solution elevates its pH level and leads to a high calcium-to-silicon (Ca/Si) ratio in the hydrates, and this, in turn, diminishes the hydrates' capacity to bind alkali ions, thereby causing an increase in the concentration of alkali ions within the concrete pore solution [9]. Also, CH is involved in the reaction with sulfate ions and calcium aluminate hydrates to form gypsum and ettringite, which results in the sulfate attack [14]. The formation of ettringite increases the solid volume and further leads to concrete cracks, loss of strength, and disintegration. Additionally, concrete sufferes softening and loss of mass and strength due to the formation of gypsum.

Using SCMs as a partial replacement for cement in concrete is a sustainable approach that reduces the overall carbon footprint of concrete by not only aiding in the sustainable disposal of industrial residues that otherwise would need to be landfilled but also using less cement clinker to reduce the overall carbon footprint of concrete [15]–[17]. Additionally, utilizing SCMs in the Portland cement-based binder matrix is considered the most effective and practical approach to improve its durability because of their pozzolanic reactivity, which can react with CH to form C-S-H or calcium alumina silicate hydrate (C-A-S-H) [5]. Consuming CH in concrete lowers not only the pH of the concrete pore solution, but also the reaction product, C-S-H and C-A-S-H, of the pozzolanic reaction can serve to sequester active alkali ions from the pore solution [7], [18]. Also, from a concrete microstructure standpoint, the pozzolanic reaction enhances the density of the interfacial transition zone (ITZ) and reduces concrete permeability by forming calcium-

silicate-hydrate (C-S-H), which is because C-S-H has a denser structure than calcium hydroxide (CH) [19]. Decreasing permeability prevents external deleterious chemical compounds like salts from ingressing into concrete and the migration of internal chemicals within the concrete matrix. The synergistic effect of reducing concrete permeability and lowering alkali ions concentration in concrete pore solution promotes concrete electrical resistivity, which further increases the resistance of concrete to chemical attack.

ASTM C618 recognizes two primary categories of SCMs: natural pozzolans and industrial by-products [20]. Natural pozzolans include volcanic ash, pumice, volcanic tuffs, and calcined clays such as metakaolin. Industrial by-products such as fly ashes are derived from activities such as coal combustion for power generation. Other SCMs, such as slag and silica fume, are derived from iron and silicon metal production. Fly ash is the primary SCM used in the concrete industry. Nevertheless, as a consequence of shifts in global environmental policies, a significant portion of coal-based power generation has shifted towards adopting clean energy sources to mitigate carbon emissions. This transformation has led to a scarcity in the supply of premium-grade fly ash, subsequently driving up the prices of the end products[21], [22]. Therefore, finding a sustainable alternative for the worldwide SCMs industry is urgent. High-alkali SCMs, whose alkali content is generally over 4%, are generally avoided in concrete due to concerns arising from the potential leaching of alkali ions into the pore solution and increasing the alkali loading in the concrete pore solution, further exacerbating the ASR. However, the impact of the alkali content of SCMs on concrete pore solutions is still controversial. Shehata et al.'s research [22] evaluated the alkali release characteristics of blended cement with high alkali SCMs, and their research indicated that some SCMs with high total alkali content released alkali ions into the pore solution, which increased alkali concentration in the pore solution. However, Mehta's research [24] indicated that

alkali content in some natural pozzolans exists as crystal phases, which did not readily release into the concrete pore solution. The same finding was discovered by Uribe-Afif et al. [25]. In their study, one of the SCMs had a total alkali content of 6.89% Na_2O_{eq}, but the available alkali content was only 1.09% Na_2O_{eq}, thus only 15% of the total alkalis were available to be released into the pore solution. These findings provide the potential feasibility of using high-alkali SCMs in concrete without concerns for ASR.

This study aims to investigate the feasibility of using high-alkali SCMs in the concrete industry as a new alternative SCMs for concrete durability. For this purpose, six natural pozzolans and two reclaimed were studied. The SCMs were characterized for their mineralogy and particle size distribution, using X-ray diffraction (XRD) and laser diffraction, respectively. X-Ray fluorescence (XRF) was conducted to study the chemical composition of the materials. The SCMs performance in promoting concrete durability was assessed in accordance with AASHTO T380 [26] and ASTM C1012 [27] for ASR and sulfate resistance, respectively. ASTM C596 was conducted to evaluate the impact of high-alkali SCMs on drying shrinkage [28]**.** ASTM C1202 rapid chloride penetration test [29] and NT Build 492 chloride migration test [30] were used to investigate the performance of high-alkali SCMs on concrete permeability. Concrete bulk electrical resistivity was conducted to evaluate the impact of high-alkali SCMs on resistivity, which is also a critical parameter for predicting concrete durability performance. Thermogravimetric analysis (TGA) was conducted on paste specimens to quantify the amount of CH consumed by high-alkali SCMs pozzolanic reactions at various ages, which helped to understand the correlation between the high-alkali SCMs' pozzolanic reactivity and their impact on concrete durability. Pore solution analysis on cementitious paste matrix was used to study alkali release and alkali-binding in mixtures with high-alkali SCMs at different sample ages. Finally, the

correlations between the various experiments were analyzed to understand and explain how the high-alkali SCMs impact the concrete durability.

6.2. Materials and Experimental Methods

6.2.1 Materials

Two types of ordinary Portland cement (OPC) meeting ASTM C150 [23] were used in this study: A low-alkali Type I/II Portland cement (Na_2O_e = 0.38%) from Argos cement company, Harleyville, SC, and a high-alkali Type I Portland cement (Na_2O_e = 1.00%) from Lehigh Hanson Inc. The chemical composition and physical properties of both Portland cements are presented in Table 6- 1.

In this study, six natural pozzolans and two reclaimed fly ashes were investigated. The natural pozzolans are identified as NP 1 through NP 6, and reclaimed fly ashes as RFA 1 and RFA 2. The material chemical compositions and particle size distributions were measured by X-Ray fluorescence and laser diffraction, respectively. These results are presented in Table 6- 1 and Figure 6- 1. XRD data of high-alkali SCMs were collected using the Rigaku X-ray diffractor. Measurements were made in flat-plate Bragg–Brentano θ–2θ geometry, and their angular range was from 10° to 80° 2θ values with a 0.02° 2θ step size. The scan rate for the test was 1° 2θ per minute. The amorphous level, i.e.the amount of non-crystallinity, was determined by the Rietveld analysis, which used the integrated surface area of the crystal compared to the total surface area [31]. Additionally, in this study, Table 6- 2 shows experiments conducted in this study.

The reactive aggregate used in this study is a known reactive aggregate from the Goldhill Quarry in North Carolina, which consists of reactive metatuff–argillite. The aggregate's specific gravity and water percent absorptions were 2.6 and 1%, respectively.

Table 6- 1 Cement and High-Alkali SCMs Chemical Composition

		SiO_2	Al_2O_3	Fe_2O_3	S+Al+Fe	CaO	MgO	Na_2O	K_2O	Na_2O_e	LOI	SG	Amorphous Level (%)
	Low-alkali Portland cement	19.93	4.77	3.13	27.83	62.27	2.70	0.06	0.48	0.37	2.6	3.15	NA
	High-alkali Portland cement	19.00	4.99	2.11	26.1	62.45	2.84	0.31	1.05	1.0	NA	3.15	NA
Volcanic rhyolitic tuff	NP 1	68.62	13.14	1.91	83.67	1.73	1.43	2.7	3.2	4.82	7.18	2.53	37.67
Pumice	NP 2	73.42	12.30	1.41	87.13	0.79	0.23	2.9	4.2	5.61	4.72	2.35	98.55
Pumice	NP 3	65.48	11.19	1.75	78.42	2.99	0.33	3.6	3.4	5.85	10.87	2.26	3.38
Volcanic rhyolitic tephra	NP 4	71.95	12.26	1.50	85.71	0.93	0.39	3.9	4.0	6.51	4.88	2.35	87.76
Volcanic glass	NP 5	71.21	12.99	0.90	85.1	0.56	0.13	3.9	4.1	6.57	5.95	2.40	100
Pumice	NP 6	71.91	11.68	2.18	85.77	0.32	0.09	5.5	4.2	8.28	3.94	2.34	91.17
Reclaimed fly ash	RFA 1	53.06	15.13	6.88	75.07	13.70	4.53	3.4	1.9	4.69	0.55	2.56	82.48
Reclaimed fly ash	RFA 2	56.81	14.20	2.69	73.7	10.13	1.41	2.8	2.7	4.56	8.42	2.42	88.88

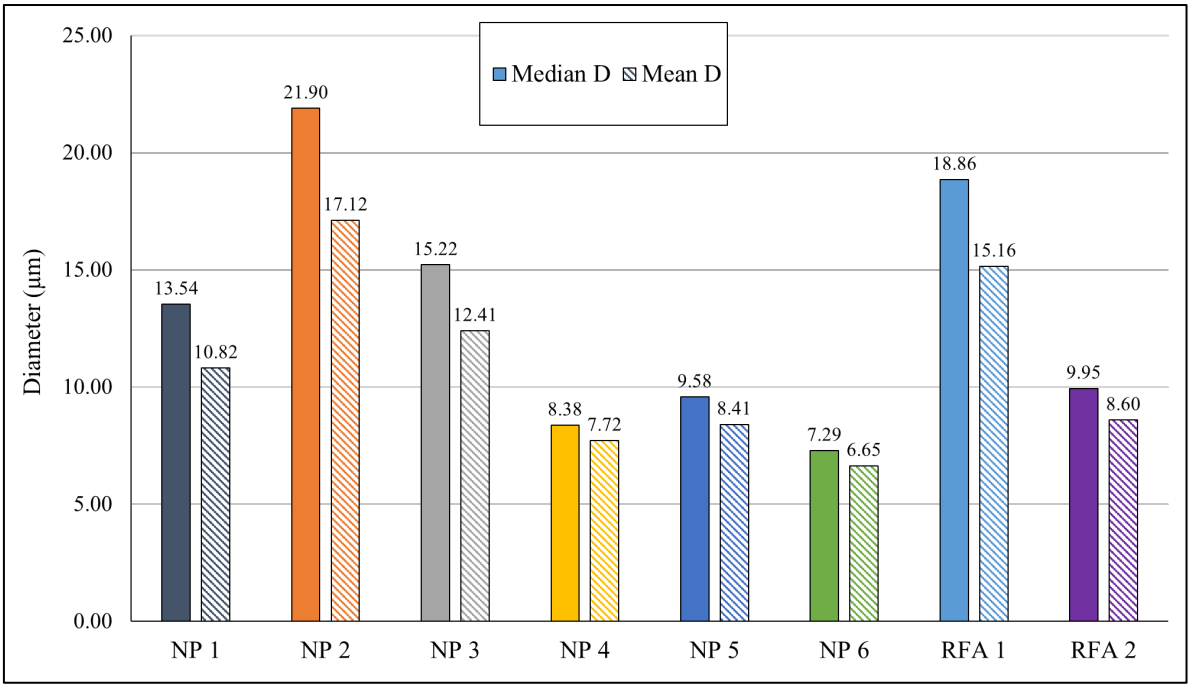

(a)

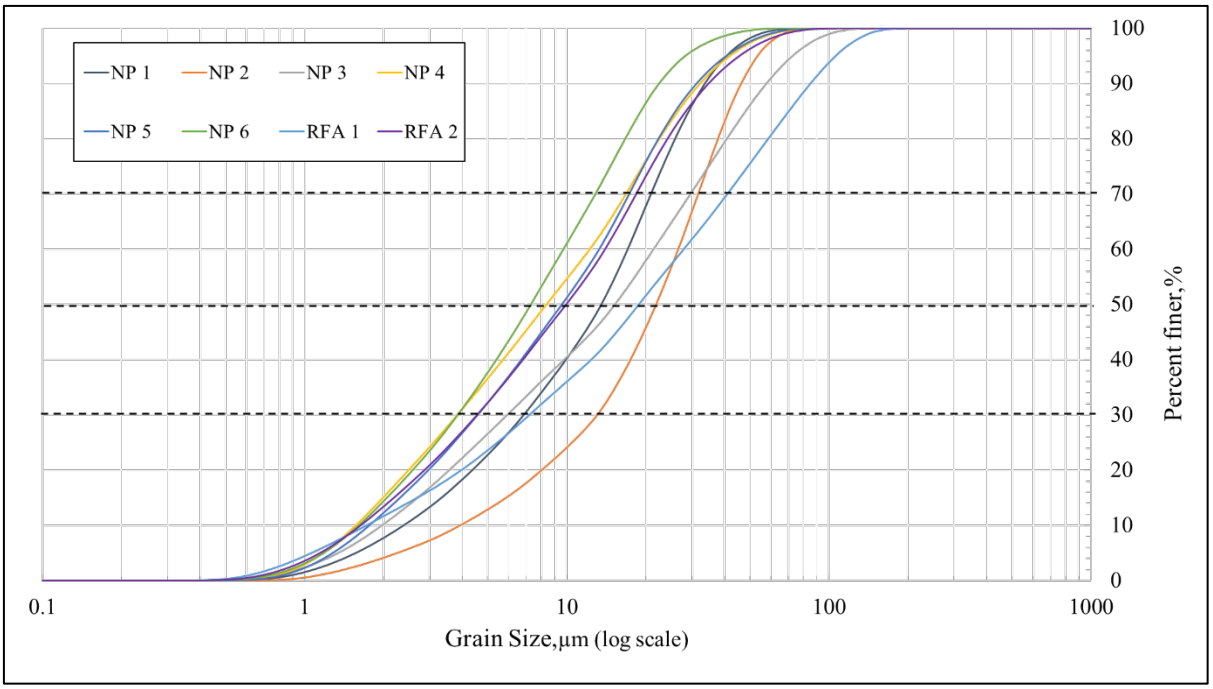

Figure 6- 1(a)SCMs' particle size; (b)Particle size distribution of natural pozzolans

Table 6- 2 Test Table

	NP 1	NP 2	NP 3	NP 4	NP 5	NP 6	RFA 1	RFA 2
AASHTO T380	✓	✓	✓	✓	✓	✓	✓	✓
AASHTO T380 Replacement Level		✓		✓	✓		✓	✓
Sulfate Resistace		✓		✓	✓		✓	✓
Drying Shrinkage		✓		✓	✓		✓	✓
Resistivity	✓	✓	✓	✓	✓	✓	✓	✓
Rapid Chloride Pernetration Test		✓		✓	✓		✓	✓
Chloride Migration Test	✓	✓	✓	✓	✓	✓	✓	✓
Thermogravimetric Analysis (TGA)	✓	✓	✓	✓	✓	✓	✓	✓
Pore Solution Analysis	✓	✓	✓	✓	✓	✓	✓	✓

6.2.2 AASHTO T380 Miniature Concrete Prism Test (MCPT) [26]

AASHTO T380 (MCPT) was used to evaluate the high-alkali SCMs to mitigate ASR in this study. In this method, the cementitious materials content of concrete mixtures was maintained at

420 kg/m3, with a w/b ratio of 0.45. The dry mass of coarse aggregate per unit volume of concrete was maintained at 0.65, and the coarse aggregates' gradation followed the recommended gradation per AASHTO T380. The fineness modulus of fine aggregates conformed to 2.60 ± 0.3. Reagent-grade NaOH pellets were dissolved in the mixing water to boost the alkali content of the concrete to 1.25% by the mass of cement. SCMs were used at dosage levels of 20%, 30%, and 40% by mass of cement.

The test specimens were cast and cured at ambient temperature and 100% RH for 24 hours. After demolding, the specimens were placed in water at 60°C for another 24 hours. The zero-day reading was taken at the end of 24 hours of water bath curing. Then, the specimens were transferred into a sealed container with 1N NaOH maintained at 60°C. The prism length changes were recorded periodically at 0, 3, 7, 10, 14, 21, 28, 42, 56, 70, and 84 days. The criteria for evaluating the efficacy of SCMs in mitigating ASR in the MCPT method at 56 days are as follows per AASHTO T380:

10. Expansion < 0.020% - Effective ASR Mitigation;
11. 0.020% < expansion < 0.025% Uncertain ASR Mitigation
12. Expansion > 0.025% Not effective ASR mitigation

If the samples exhibit expansion between 0.20 and 0.25 at 56 days, the average expansion between 56-day to 84-day (8 weeks to 12 weeks), should be less than 0.010% per 2 weeks for the mitigation measure to be considered effective.

6.2.3 ASTM C1012-18b Sulfate Resistance [27]

ASTM C1012 was used to evaluate the performance of high-alkali SCMs to suppress the external sulfate attack in this study. In this method, mortar prisms were prepared by blending low-

alkali cement with SCMs at a 20% mass replacement, at a water-to-binder ratio of 0.485 and sand-to-binder ratio of 2.75.

Six 1in. × 1in. × 11.25 in. mortar prisms and 21 cubes for each mixture were prepared in this study. After casting, the specimens were stored in an oven at 35°C with 100% RH for 24 hours, and then they were demolded and placed in saturated limewater at 23°C. The prisms were transferred to 5% sodium sulfate solution (Na_2SO_4) until the average compressive strength of the two cubes reached 2850 psi. The prisms' length change was recorded periodically at 0, 1, 2, 3, 4, 8, 13, and 15 weeks, and subsequent readings at 4,6,9,12 months. In addition, the pH of the soak solution was determined with every measurement, which was required at the range of 6.0 to 8.0

6.2.4 ASTM C596-18 Drying Shrinkage [28]

Modified ASTM C596 was used to investigate the impact of high-alkali SCMs on drying shrinkage. Four mortar prisms were cast at a water-to-binder ratio of 0.485 and a sand-to-binder ratio of 2.25. The test mixture was mixed with 20% SCMs by the cement mass.

After being cast and stored in a moist room for 24 hours, the mortar prisms were immersed in saturated limewater for 48 hours. The zero reading was recorded afterward, and the specimens were stored in the air chamber at 23 °C and 50% relative humidity before each measurement. The length change of mortar bars was continuously monitored until no further shrinkage occurred.

6.2.5 ASTM C1202-22 Rapid Chloride Penetration Test [29]

This method was applied to determine the influence of high alkali SCMs on the electrical conductance of concrete. The 4in×8in (diameter × height) concrete cylinders were cast with a 0.45 water-to-binder ratio. The cementitious materials content of concrete mixtures was maintained at 420 kg/m^3 with 20% SCMs replacement by cement mass, and the dry mass of coarse aggregate per unit volume of concrete was maintained at 0.65.

The cylinders were stored in a moist room before being cut into the size of 4in×2in by the water-cooled diamond saw. Epoxy was used to seal the side surface of the cylinders, and two-end surfaces were exposed. After the epoxy was dry, the cylinders were placed in the desiccator and pumped for 3 hours. Then, the stopcock was turned on to drain sufficient water into the desiccator. The cylinders were immersed in the water for another hour under vacuum. After that, the cylinders were kept in the water for around 18 h ± 2h before running the CHLORIDE penetration test.

The specimens were transferred into the test cell immediately after being taken out of the water, and 3.0 % sodium chloride (NaCl) solution and 0.3 N sodium hydroxide (NaOH) solution were filled into the side of the cell. The cable was connected test cell with the correct positive and negative poles, and the voltage was kept at 60 Volts. The cumulative ion penetration values were collected every half an hour till six hours. Additionally, each mixture had three samples, and the final value was the average of the three samples.

6.2.6 Thermogravimetric Analysis (TGA) for Determining Calcium Hydroxide (CH) Consumption

Thermogravimetric analysis (TGA) was conducted to determine the amount of calcium hydroxide (CH) in the cement paste. For this testing, AutoTGA Q5000 instrument was employed. The pastes were prepared by blending low-alkali cement with SCMs at a 20% mass replacement of cement, at a water-to-binder ratio of 0.42. The prepared paste samples were stored in a sealed container and were tested at the ages 12-hours, 1 day, 3-day, 7-day, 28-day, and 56-days. After casting, the specimens were sealed in air-tight test tubes to avoid potential carbonation and stored in an air chamber maintained at 23^{o}C and 50% RH. Before testing, the samples were de-molded from the tubes and ground using an agate mortar and pestle to pass the No.100 sieve (150 μm). Then, the powder samples were immersed in 50ml isopropanol for 15 minutes to remove moisture

from the powder. The suspension was filtered by using Büchner funnel to obtain the dehydrated powder, and 10 ml diethylene was added to the powder to remove extra isopropanol. After preparation, the sample was immediately stored in air-tight vials and tested. The weight loss observed in the samples between the temperatures of 400°C and 500°C was recorded and the amount of calcium hydroxide ($Ca(OH)_2$) per gram of cement in the mixture was calculated using **Equation 2:**

$$\boldsymbol{Ca(OH)_2} = \frac{(\boldsymbol{Mass_{400^oC} - Mass_{500^oC}}) \times (\boldsymbol{Ca(OH)_2\ Molor\ mass})}{\boldsymbol{H_2O\ Molar\ mass}} \quad \textbf{(2)}$$

6.2.7 Pore Solution Analysis

Pore solution extraction and analysis were performed on binder paste specimens at different ages to determine the pore solution chemistry. The samples were mixed with binders consisting of high-alkali cement and SCMs, and deionized water. The w/b ratio for this study was maintained at 0.60 for all samples in this experiment. The method used to extract pore solution in this study was using a pore solution expression die based on Barneyback and Diamond [32]. Maximum stress of about 260 MPa was applied to extract the pore solution from samples. The load rate was maintained between 1 and 1.8 kN/s. The pore solution was collected into centrifuge tubes, preventing potential contamination from carbonation, and they were stored at 4°C in a refrigerator before testing.

Inductively coupled plasma optical emission spectroscopy (ICP-OES) was used to analyze the pore solution to determine the concentration of alkalis ions (Na^+&K^+). Before running ICP, the pore solution was centrifuged for 10 mins to separate any solids and the liquid. One ml pore solution was extracted from the storage tubes and diluted with 2% Nitric acid (HNO_3) based on

mass. The pore solution's dilution factor was 100, meaning a 100 ml mixture solution contained 1 ml of pore solution. All water used in this study was deionized water.

6.3. Results and Discussion

6.3.1 AASHTO T380 Miniature Concrete Prism Test (MCPT)

Figure 6- 2 and Figure 6- 3 exhibited the length change of concrete prisms in AASHTO T380 (MCPT) with 20% SCMs. In MCPT, SCMs are considered to effectively mitigate ASR when expansion is below 0.020% at 56 days, and the expansion rate should not exceed 0.010% every two weeks from day 56 to day 84.

Except for NP 2 and RFA 1, other materials effectively limited the ASR expansion to lower than 0.020% at 56 days. The Expansion of NP 2 and RFA 1 was 0.026% and 0.035%, respectively. RFA 1 showed the worst performance in the MCPT testing. Additionally, NP 1, NP 2 and RFA 1 also failed to satisfy the expansion rate requirement of less than 0.010% per two weeks between 56 and 84 days. NP 4 had the lowest expansion at 56 days. However, at 84 days, NP 6's showed improved performance compared to NP 4. During the interval from 56 to 84 days, the rest of the mixtures, with the exception of NP 6, continued to expand, and their two-week expansion rate exceeded 0.020% at 84 days.

NP 2, 4, 5, and two RFAs were selected to study the effect of SCMs replacement level on ASR mitigation. The replacement levels were increased from 20% to 30% and 40% in this test. The test results from this study are presented in Figure 6- 4. The results indicated that with an increase in SCMs replacement level, the ASR expansion was significantly mitigated. Apart from RFA 1, the 30% replacement level was adequate for all the SCMs to control ASR expansion to less than 0.020% at 56 days, and the mitigation was effective even at 84 days. RFA 1 failed even at 30% replacement level, as the average test prism expansion was 0.035% at 56 days, which is much

higher than the threshold of 0.020%. However, at 40% replacement level, RFA 1 successfully controlled the expansion below the 0.020% limit; even at 84 days, the expansion was limited to only 0.018%.

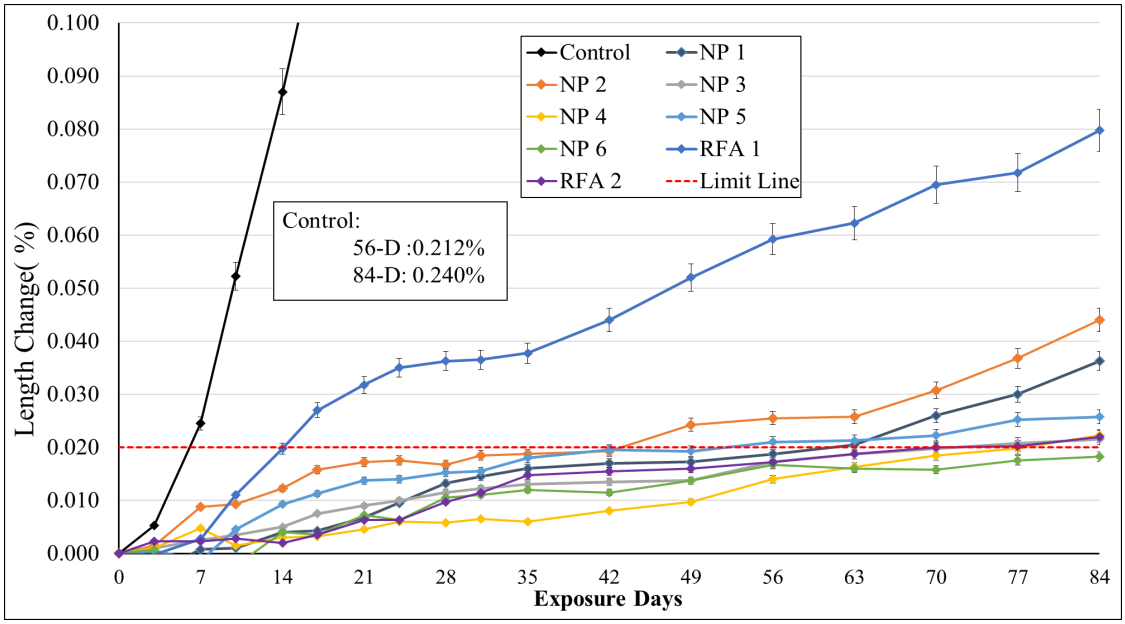

Figure 6- 2 AASHTO T380 length change of concrete prisms with 20% SCMs replacement

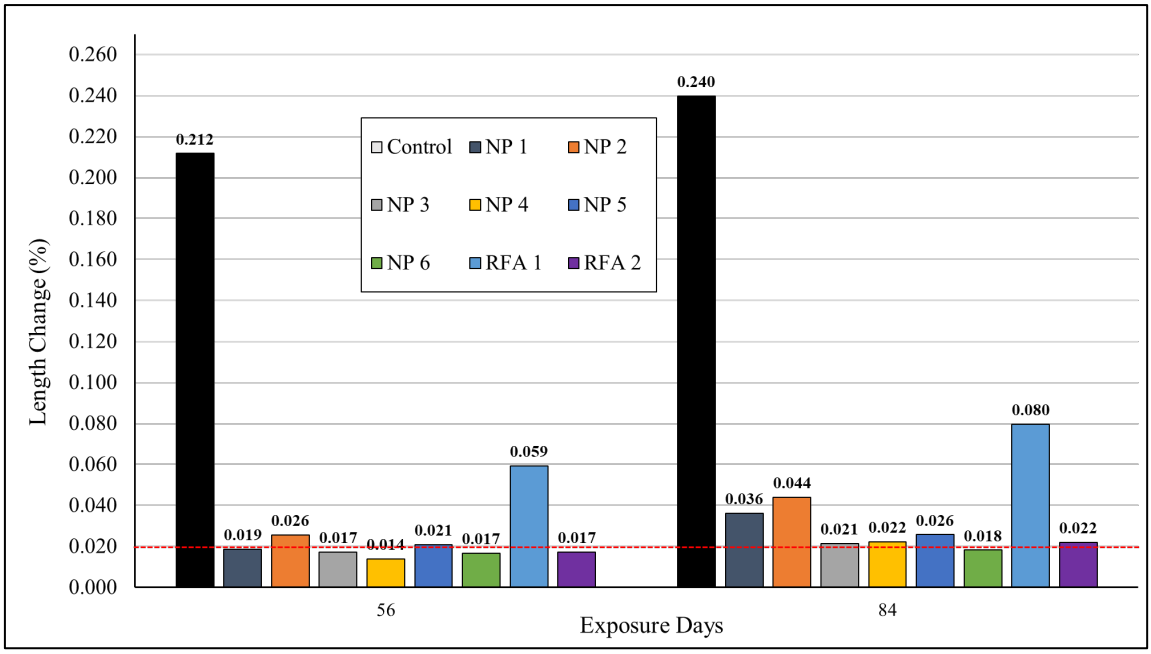

Figure 6- 3 AASHTO T380 56-D & 84-D expansion value with 20% SCMs replacement

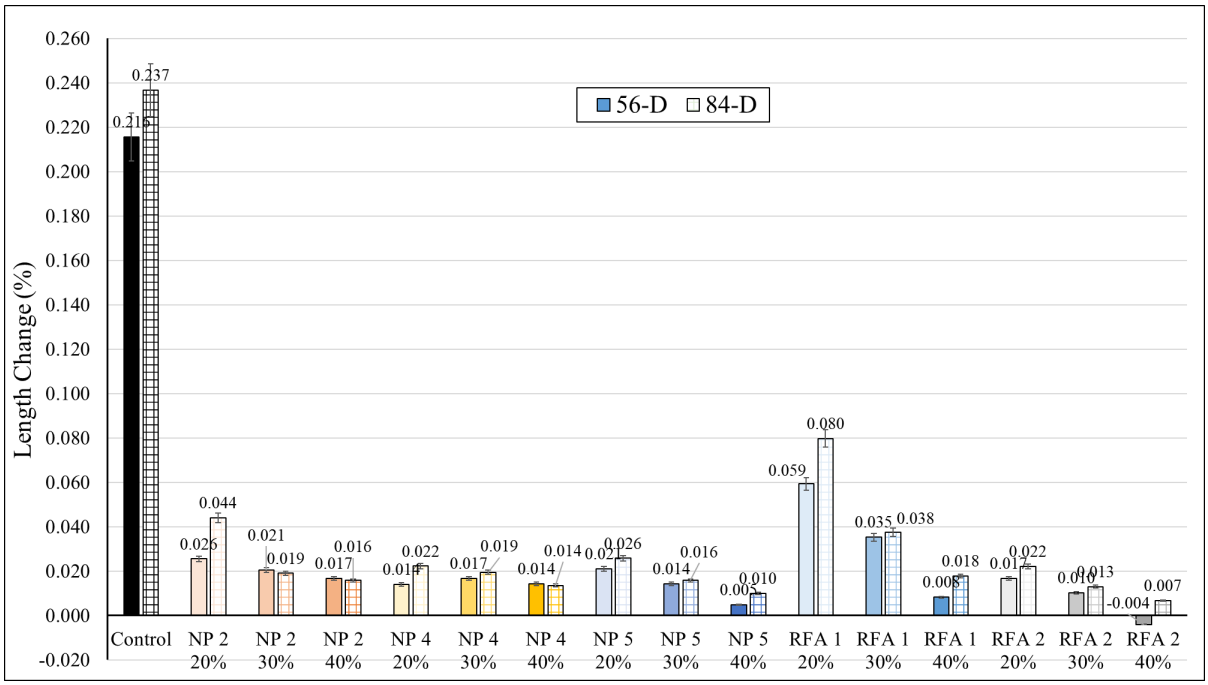

Figure 6- 4 AASHTO T380 Replacement level results comparison

6.3.2 Sulfate Attack Resistance

Five materials, NP 2, 4, 5, and two RFAs, were selected in this study, and their results are exhibited in Figure 6- 4. In contrast to the mixtures blending with SCMs, control indicated higher sulfate attack expansion, which showed that high-alkali SCMs effectively suppressed sulfate attack expansion. Before reaching week 26, while the change in length between the control groups was slightly higher, the distinction was not particularly significant. However, subsequent to that point, the control groups exhibited a rapid and pronounced expansion. Regarding the mixtures incorporating SCMs, they attained their peak expansion at approximately 26 weeks, beyond which no discernible further expansion was observed.

Among the various materials, RFA 1 demonstrated the least effective performance in controlling expansion, aligning with prior ASR mitigation outcomes. Nonetheless, compared to

the control group, RFA 1 still managed to curtail expansion by approximately 80% significantly. In this study, NP 5 indicated the most favorable performance in contrast to the other materials, while NP 4 achieved a mitigation level comparable to that of NP 5, which yielded remarkable expansion reductions of 92% and 93%, respectively.

The effectiveness of SMCs in mitigating sulfate attack expansion can be understood in two primary mechanisms: diluting clinker species and pozzolanic reaction, which was also reported in Amoudi et al. 's research [33]. The former decreases reactant C_3A to form ettringite, which is the reaction product resulting in sulfate attack, and the latter consumes CH content to form C-S-H, which results in a denser structure that prevents the deleterious chemical from ingressing into or migrating in the concrete. In this study, all the mixtures replaced 20% of the cement mass by SCMs, and the mitigation level of SCMs in sulfate attack expansion was far above the 80% control expansion. This result indicated that besides the diluting impact of SCMs, the pozzolanic reaction also played a significant role in suppressing sulfate attack expansion.

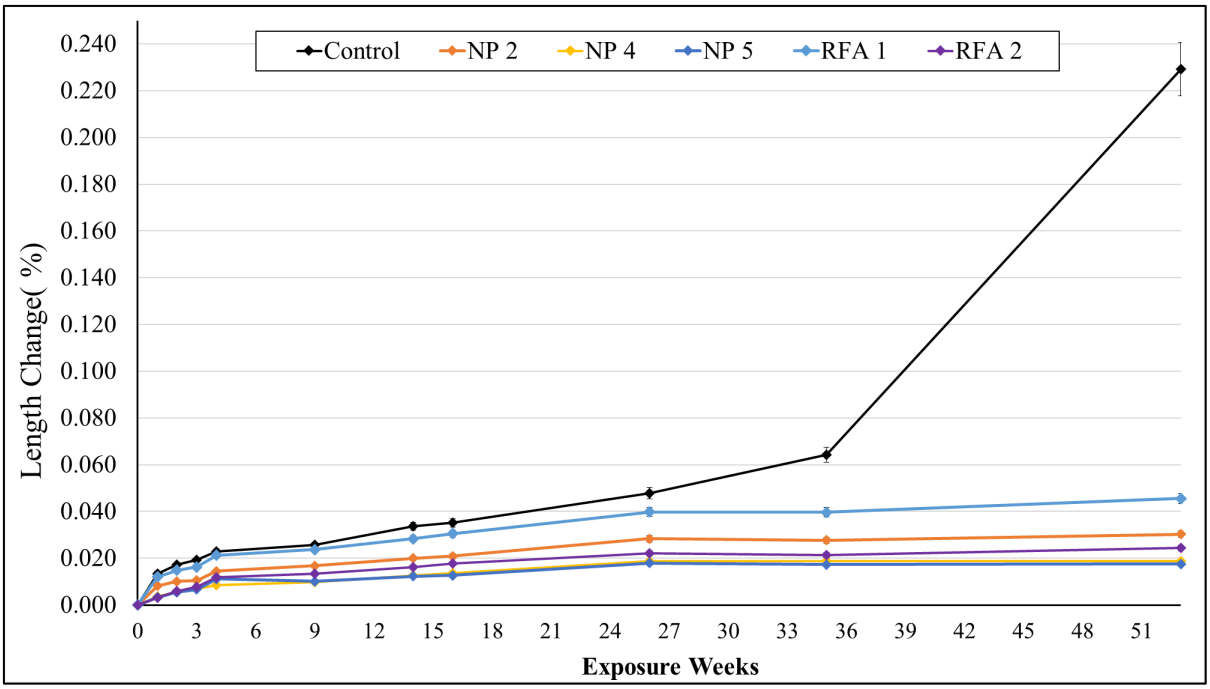

Figure 6- 4 Sulfate Attack Resistance Results

6.3.3 Drying Shrinkage

Five materials, NP 2, 4, 5, and two RFAs, were conducted in the drying shrinkage test. Figure 6- 5 exhibits the length change of drying shrinkage, and Figure 6- 6 shows the final shrinkage values at age 110 days. Including control, all the mixtures behaved very similarly. All groups' values were close, with a mere 0.013% distinction between maximum and minimum values. Additionally, a rapid shrinkage was observed across all groups during the initial four weeks, followed by a phase of sustained and stable shrinkage in their respective curves.

In this experiment, the control's value was in the middle among all groups, indicating that adding SCMs in the mortar did not impact its shrinkage change, and this result was also observed in research conducted by Radhakrishna G. et al. [34] and Pillai et al. [35]. Their study presented that blending SCMs in concrete did not influence drying shrinkage, and its shrinkage values did not differ from the OPC concrete.

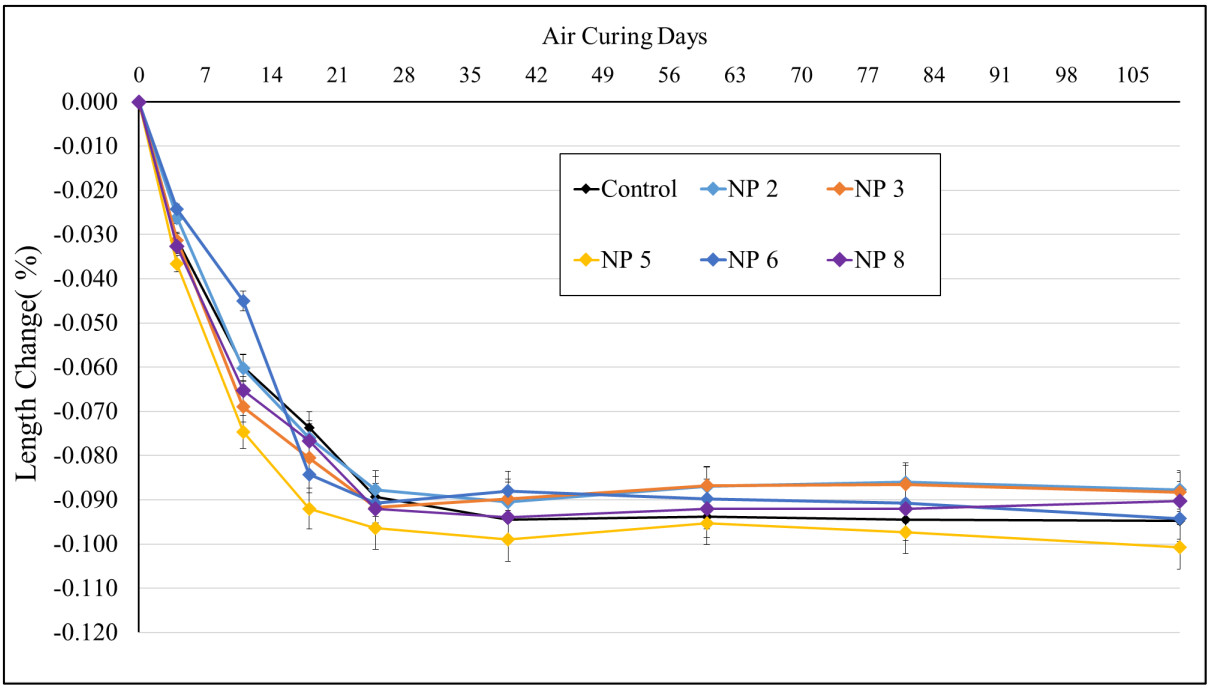

Figure 6- 5 Dry Shrinkage Results

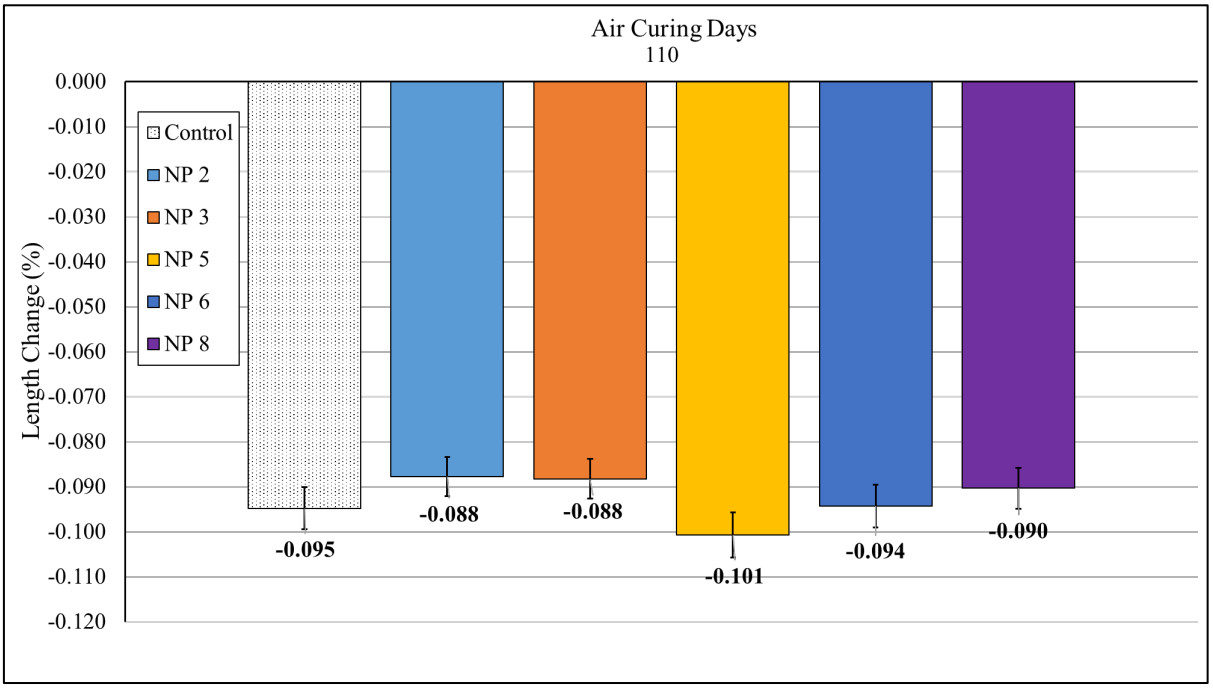

Figure 6- 6110-Day Drying Shrinkage Values

6.3.4 Rapid Chloride Penetration Test

Five selected materials, NP 2, 4, 5, and two RFAs, were tested in the rapid chloride penetration test, whose results are shown in Figure 6- 7. The criteria for evaluating concrete permeability based on the amount of chloride ions passing is also shown in Figure 6- 7. When at least 4000 coulombs pass cylinders, it is considered a high penetration, and none of these groups reached this level. As anticipated, control yielded the highest charge ions passing cylinders, measuring 3621 coulombs, which corresponded to the acknowledged moderate zone.

Regarding high-alkali SCMs mixtures, except RFA 1, the rest of groups effectively limited charges passing through cylinders less than 1000, which was considered very low. RFA 1 exhibited the worst performance compared to others, as shown in the previous experiments, and it allowed 1222 coulombs to pass through the cylinders, which was recognized as low area.

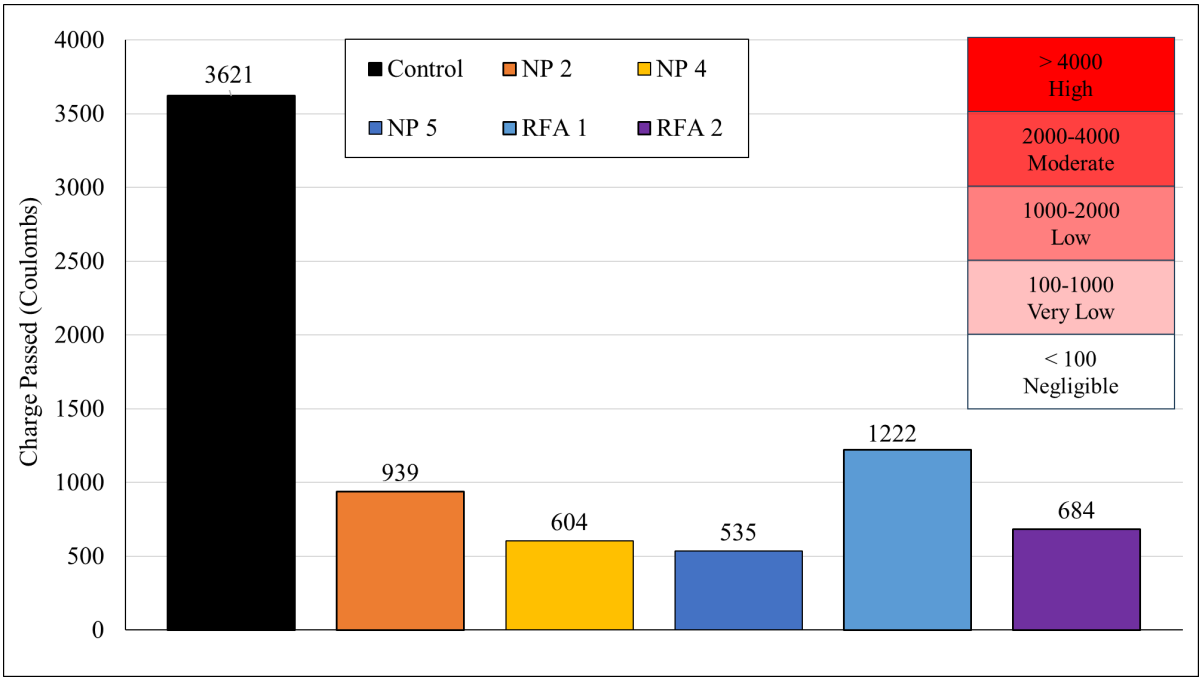

Figure 6- 7 Rapid Chloride Penetration Test (RCPT) Results

According to the report conducted by Amoudi [33], the particle packing and pozzolanic reaction of SCMs occurring in cementitious matrix lead to a dense microstructure and low

permeability of concrete that decreases the risk of external sulfate ingressing into concrete, which increases the concrete sulfate resistance. A similar correlation was discovered between ASR and permeability in Yurtdas et al.'s research [36].

6.3.5 Bulk Electrical Resistivity

In this study, Figure 6- 8 shows the impact of high-alkali SCMs on bulk electrical resistivity. Based on the data presented in Figure 6- 8, compared to the mixtures containing SCMs, the control mixture exhibited exceptionally high resistivity values during the early stages, but this performance was not persistent. At the 3-day measurement, the control reached 5.6 kΩ*cm, which was the highest among all test mixtures. However, as time progressed, its resistivity incrementally increased at a notably slower rate, and it was only 10.2 kΩ*cm at age 101 days.

For the SCMs mixtures, most groups had a slow start compared to the control. However, as the experiment progressed, they gradually exceeded the control within 28 days. Among all SCMs, NP 3 performed variously from the rest at the early stage. Its resistivity value surged rapidly and surpassed the control within the first seven days. Furthermore, the resistivity of NP 6 also raised very fast. It trailed only behind NP 3 during the initial 35 days and eventually outperformed NP 3, becoming the best performer at age 42 days. However, NP 6's resistivity entered a plateau after that, gradually relinquishing its lead to other groups. In contrast to NP 6, NP 4, NP 5, and RFA 1 continued to exhibit a pronounced inclination for resistivity growth at later stages. NP 4 showed the most notable and sustained increase, particularly so. The performance of these three groups started off in the middle tier but consistently maintained a relatively stable growth, eventually emerging as among the top-performing groups in the end.

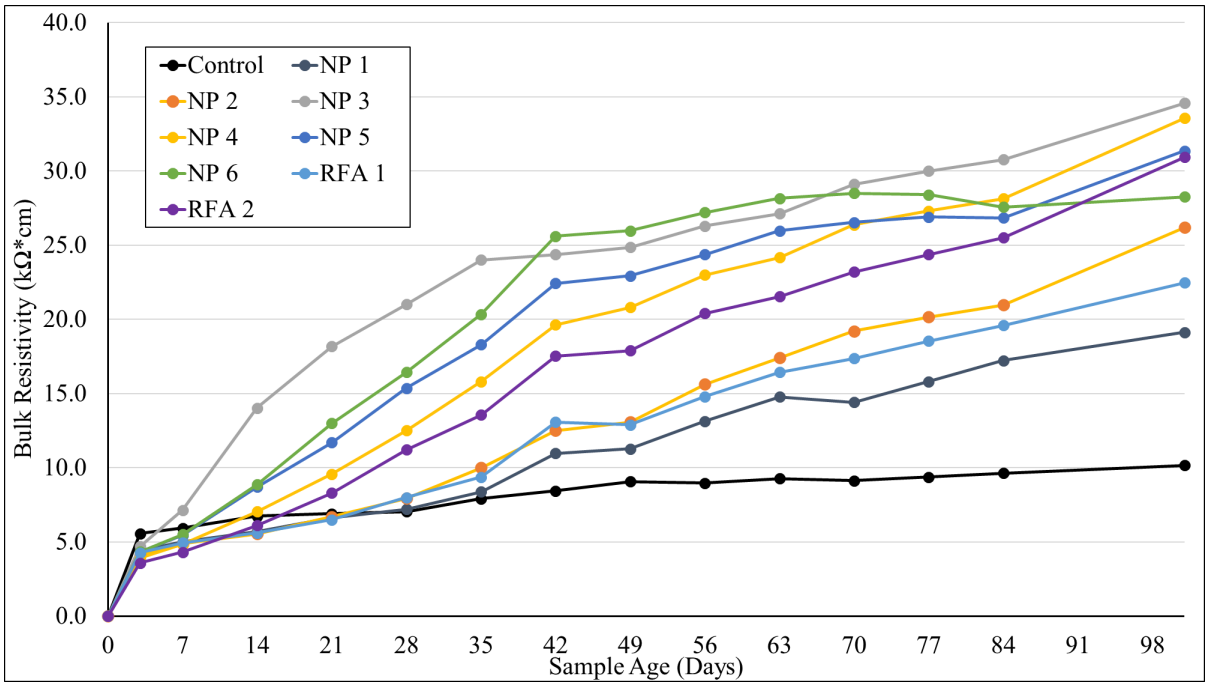

Figure 6- 8 Bulk Resistivity Results

Additionally, Figure 6- 9 indicates the correlation between bulk resistivity results and charge passing through concrete in the RCPT test. RCPT test is the most widely used approach to access concrete permeability. According to the results, the charge passed through concrete in RCPT indicated an inversely proportional relationship with bulk resistivity, and the R^2-value of the two parameters was over 0.9, which exhibited a very significant correlation. This discovery implies a direct relationship between the permeability of concrete (the amount of charge passing through it) and its resistivity, with lower permeability resulting in higher concrete resistivity, which is also discovered in research conducted by Wang et al. [37].

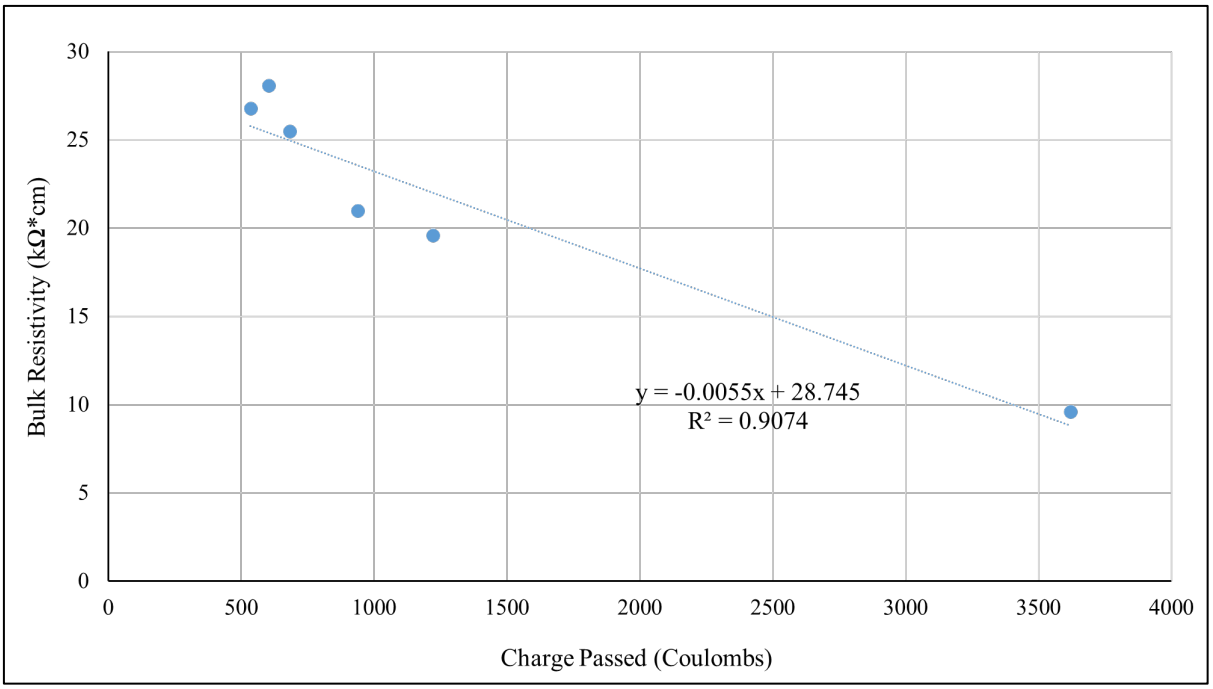

Figure 6- 9 Correlation between Bulk Resistivity and RCPT

6.3.6 Thermogravimetric Analysis

Figure 6- 10 indicates the relative CH contents in the paste. Considering the cement dilution that occurs when cement is replaced with 20% SCM, the calcium hydroxide (CH) content of the test mixtures was divided by 0.8 to correct for the dilution. The calibrated high-alkali SCMs CH consumption values were compared to the control, expressed as % control, and the results are shown in Figure 6- 10.

At early ages, at 7 days, it is clear that all the high-alkali SCMs increased the CH content in the mixtures, which resulted from the filler effect of SCMs. The filler effect increased nucleation sites, further accelerating the cement hydration process [38]. With the sample age increasing and pozzolanic reactivity, the CH content of mixtures with SCMs started to decrease, and some groups were lower than the control, indicating the occurrence of pozzolanic reactions caused by high-alkali SCMs. NP 2 and RFA 1 did not effectively lower the CH content in the mixtures compared to the control, and their CH content level was maintained at a constant level between 28 days and

56 days. It could result from the larger particle size of NP 2 and RFA 1. These two materials have larger particle sizes than the rest. For the rest of the materials, they decreased the CH content by at least 5% compared to the control.

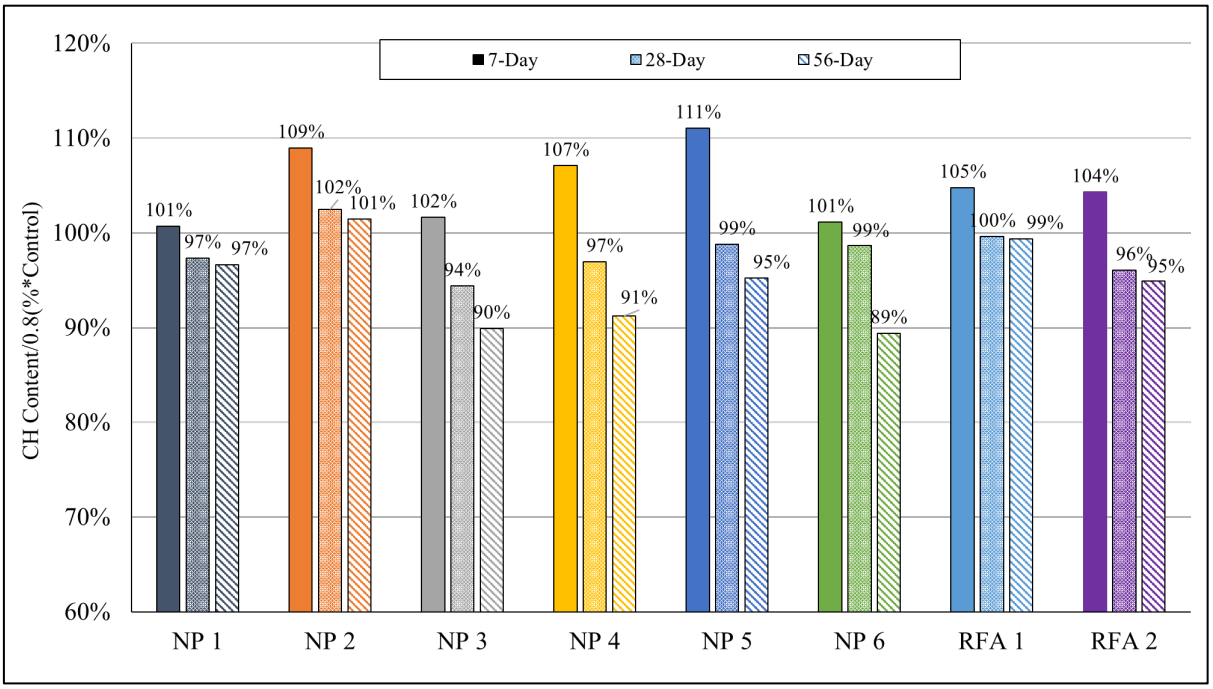

Figure 6- 10 Relative CH Contents in Pastes Containing 20% High-Alkali SCMs Replacement

Figure 6- 11 indicates the correlation between CH content with ASR and sulfate attack expansion. CH content had very strong correlations with ASR and sulfate attack expansion, and both R^2-values were over 0.9. These results revealed that the ASR and sulfate attack expansion were proportional to CH content in the cementitious matrix, which was also confirmed in S. Oruji et al.'s research [39].

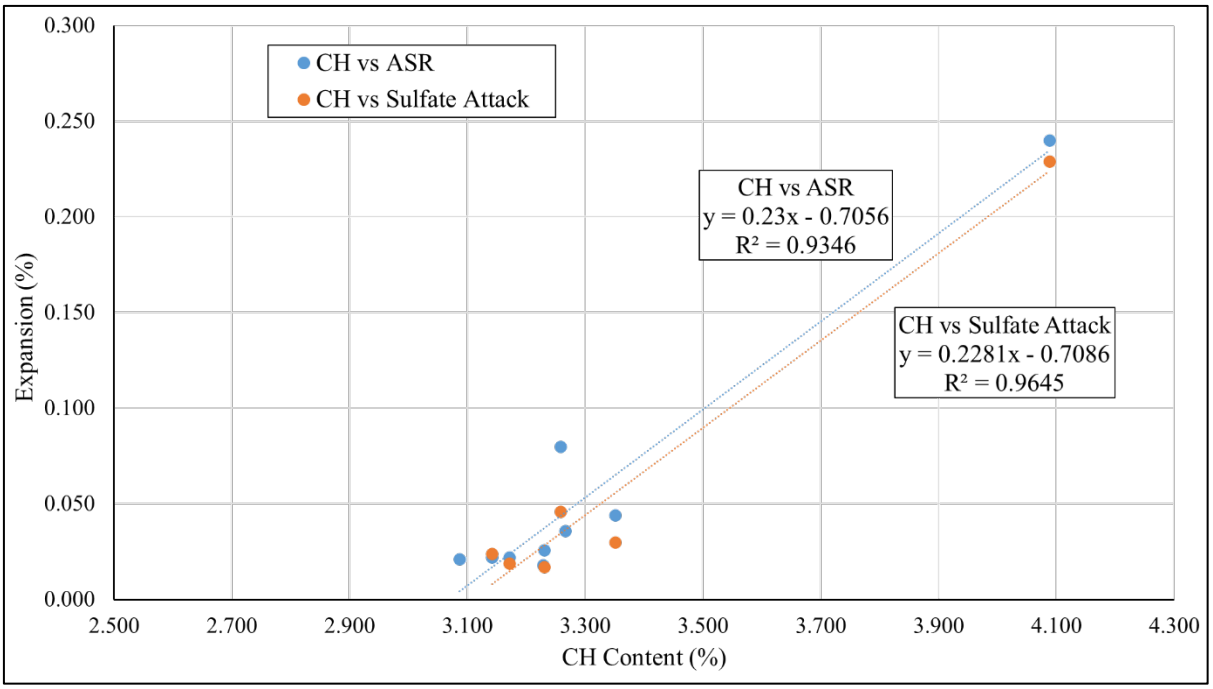

Figure 6- 11 CH Content vs ASR & Sulfate Attack Expansion

6.3.7 Pore Solution Analysis

Figure 6- 12 and Figure 6- 13 show the potassium (K^+) and sodium (Na^+) concentrations of pore solutions expressed from various paste specimens containing SCMs at 28 and 84-day test durations. Figure 6- 14 indicates the sum of alkalis ions concentration ($K^+ + Na^+$) in the same paste specimens. Since mixtures with SCMs contain only 80% cement, the red line in the figure is included to represent the 80% alkali ions concentration, resulting directly from the Portland cement. The pore solution analysis results indicate K^+ concentration was much higher than Na^+ in all the mixtures, with exception of NP 2, and this is due to the fact that K_2O is the principal alkali oxide in Portland cement. The alkali ions concentration in control mixture remained constant from 28 days to 84 days, as majority of Portland cement hydrations occurs during this period and all alkalis are essentially released during this period.

In Figure 6- 12, the K^+ concentration of all test mixtures with SCMs was below the 80% line at 28 days and 84 days. NP 2 had the lowest K^+ but increased significantly from the 28th to the 84th

day, from 0.127 to 0.172 mmol/L. For the rest of the mixtures with other SCMs, the K^+ concentration decreased with increasing sample age. RFA 1 indicated only a slight decrease from the 28th to the 84th day. Additionally, the K+ concentration of RFA 1 was much higher compared to mixtures with other SCMs. The change in K+ concentration strongly suggests the alkali binding by the pozzolanic reaction products.

Na^+ concentration behaved differently from K^+. Other mixtures, except for NP 1 and NP 2, indicated higher concentrations than the 80% control, especially NP 3. The Na^+ ion concentration of NP 3 was highest at both 28 days and 84 days, with 0.242 and 0.235 mmol/L, respectively. while that of the control was only about 0.145 mmol/L. RFA 1 still did not perform well. On the 28th day, RFA 1's Na+ concentration was about 0.188 mmol/L, the second highest, and it increased by 0.04 mmol/L to reach 0.231 on the 84th day. The increase in Na^+ concentration of all mixtures compared to the 80% of the control mixture indicated that the majority of the high-alkali SCMs released Na^+ ions into the pore solution during the pozzolanic reaction, although these values were lower than that of K^+ ion concentrations.

It was observed that the mixtures with RFA 1 had the highest total alkalis ions concentration among all the mixtures, which was also higher than the 80% of the control. NP 1 showed the lowest total alkali ions concentration, and NP 1 and NP 2 lowered the alkalis ions from 28 days to 84 days. The total alkali content of pore solution in mixtures with NP 1, NP 3, NP 4, NP 5, NP 6, and RFA 2 remained constant between the 28 and 84-day measurements. Both NP 3 and RFA 2 showed an increase in total alkali concentration in pore solution from 28 days to 84 days.

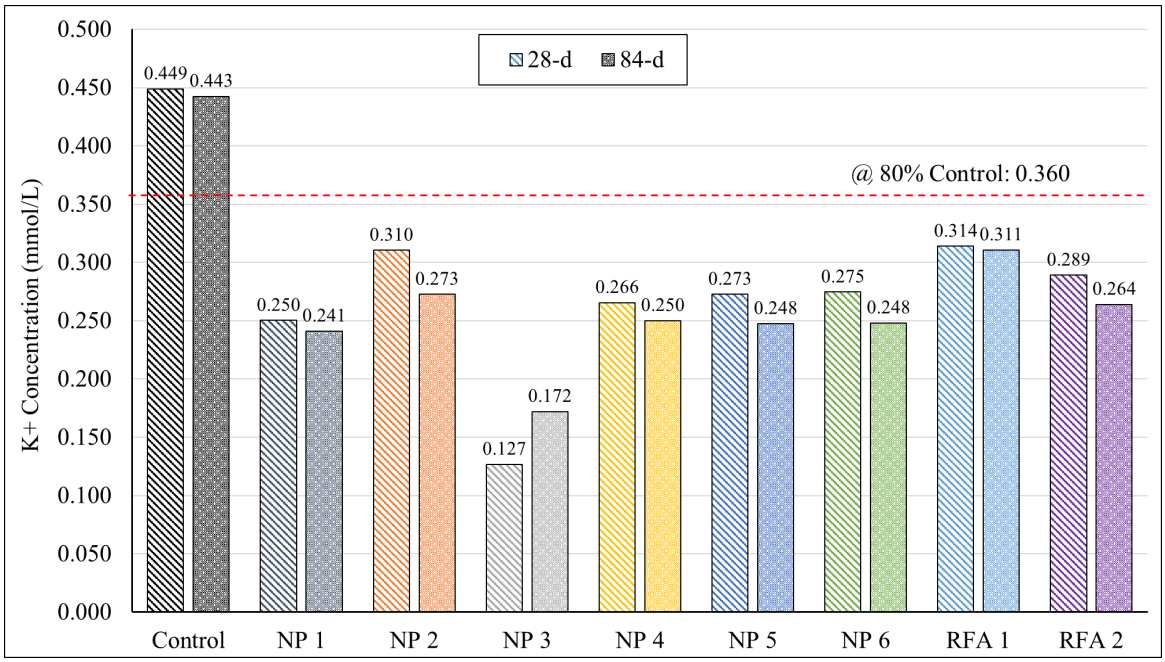

Figure 6- 12 K^+ Concentration

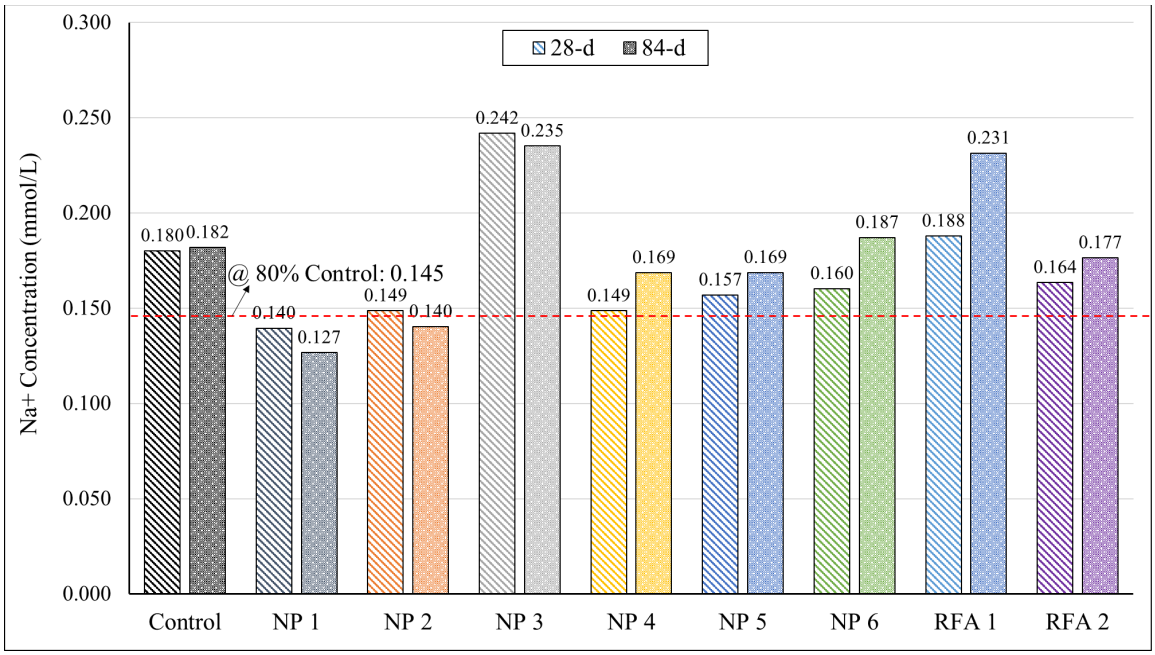

Figure 6- 13 Na^+ Concentration

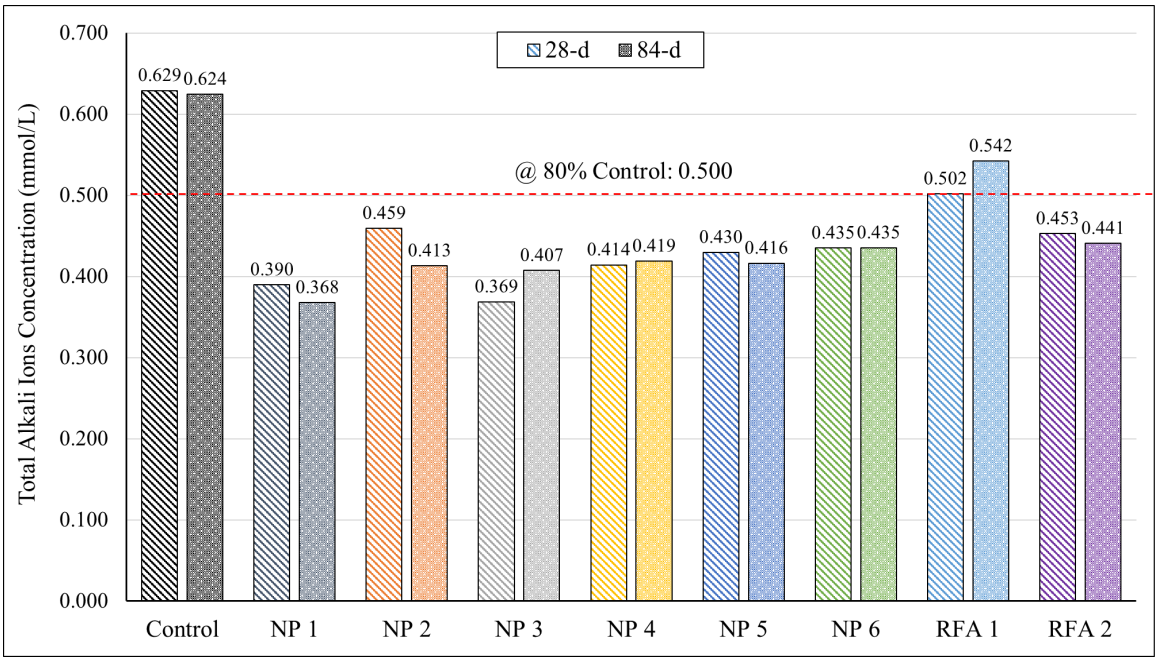

Figure 6- 14 Total Alkali Ions Concentration

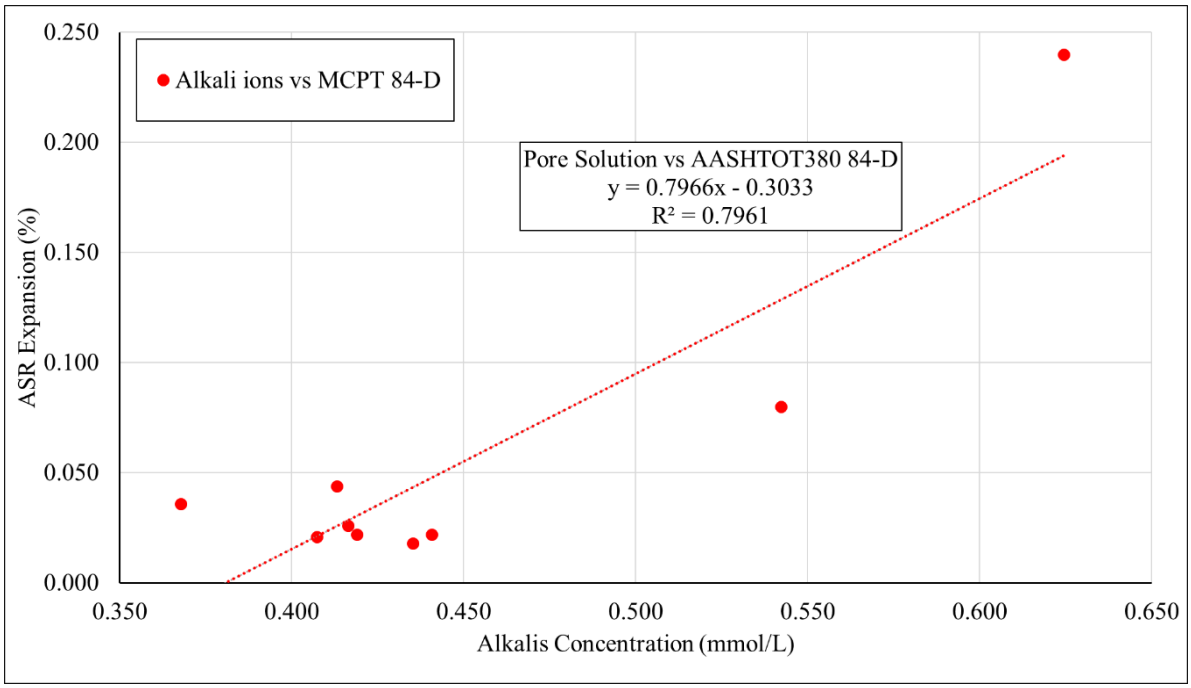

Figure 6- 15 Correlation between MCPT 84-D ASR Expansion and Total Alkali Ions in Pore Solution Analysis

ASR expansion and total alkali ions in the pore solution analysis reveal a good correlation, which is shown in Figure 6- 15. Two datasets showed a proportional relationship --- concrete had more ASR expansion with higher alkali ions in the pore solution, proving that adding SCMs in concrete increased alkali ions binding ability to mitigate ASR [9].

6.4. Conclusion

This study demonstrated the utilization of high-alkali SCMs, including natural pozzolans and reclaimed fly ash, as potential alternative new SCMs to promote concrete durability performance. For this purpose, six natural pozzolans and two reclaimed fly ashes have been investigated in various experiments.

In the concrete durability tests of AASHTO T380 and ASTM C1012, all the materials effectively promoted the concrete mitigation performance on ASR and sulfate attack. In the AASHTO T380 ASR mitigation test, RFA 1 did not perform as well as the rest of the materials, but its use reduced ASR-induced expansion at 20% replacement. Level compared to the control. Also, the mitigation performance performed much more effectively with SCMs replacement levels increasing. The CH content and alkali ions obtained in TGA and pore solution analysis supported the expansion observed in the AASHTO T380. Both two dataset values indicated significant correlations with ASR expansion. Also, pore solution analysis shows that not all alkalis in the SCMs released into the pore solution. Additionally, TGA also performed a strong correlation with sulfate resistance that the more CH content in the cementitious matrix, the higher expansion induced by sulfate attack. The mitigation mechanisms for the expansion of ASR and sulfate attack can be explained by the diluting effect of replacing cement with SCMs and pozzolanic reaction. However, different from the apparent impact on ASR and sulfate attacks, high-alkali SCMs did not affect dry shrinkage.

Blending high-alkali SCMs in the concrete also decreased the concrete permeability. RCPT test indicated that since high-alkali SCMs were added to the matrix, the amount of charge passing through concrete decreased. The dense structure of concrete also led to higher resistivity. In the bulk electrical resistivity study, adding SCMs delayed the concrete to obtain the resistivity in

contrast to the control. However, as the experiments progressed, the cementitious mixtures containing SCMs gradually caught up and eventually exceeded the control. In comparison, the control entered the resistivity plateau phase prematurely and had a very low ultimate resistivity. Also, the study evaluated the relationship between bulk electrical resistivity and the amount of charge passing through in RCPT, which indicated a strong correlation.

From the overall perspective of this study, high-alkali SCMs indicated the potential to be used as alternative SCMs for the concrete industry.

6.5. Reference

[1] T. R. Naik, "Sustainability of Concrete Construction," *Practice Periodical on Structural Design and Construction*, vol. 13, no. 2, pp. 98–103, May 2008, doi: 10.1061/(ASCE)1084-0680(2008)13:2(98).

[2] "Concrete needs to lose its colossal carbon footprint," *Nature*, vol. 597, no. 7878, pp. 593–594, Sep. 2021, doi: 10.1038/d41586-021-02612-5.

[3] "Global CO2 emissions rebounded to their highest level in history in 2021 - News," IEA. Accessed: Sep. 04, 2022. [Online]. Available: https://www.iea.org/news/global-co2-emissions-rebounded-to-their-highest-level-in-history-in-2021

[4] S. A. Miller, "The role of cement service-life on the efficient use of resources," *Environ. Res. Lett.*, vol. 15, no. 2, p. 024004, Jan. 2020, doi: 10.1088/1748-9326/ab639d.

[5] J. D. Birchall, A. J. Howard, and J. E. Bailey, "On the hydration of Portland cement," *Proceedings of the Royal Society of London. A. Mathematical and Physical Sciences*, vol. 360, no. 1702, pp. 445–453, 1978.

[6] I. G. Richardson, "The calcium silicate hydrates," *Cement and Concrete Research*, vol. 38, no. 2, pp. 137–158, Feb. 2008, doi: 10.1016/j.cemconres.2007.11.005.

[7] X. Hou, L. J. Struble, and R. J. Kirkpatrick, "Formation of ASR gel and the roles of C-S-H and portlandite," *Cement and Concrete Research*, vol. 34, no. 9, pp. 1683–1696, Sep. 2004, doi: 10.1016/j.cemconres.2004.03.026.

[8] W. Müllauer, R. E. Beddoe, and D. Heinz, "Sulfate attack expansion mechanisms," *Cement and Concrete Research*, vol. 52, pp. 208–215, 2013, doi: 10.1016/j.cemconres.2013.07.005.

[9] M. D. A. Thomas, B. Fournier, K. J. Folliard, and Inc. Transtec Group, “Alkali-aggregate reactivity (AAR) facts book.,” FHWA-HIF-13-019, Mar. 2013. Accessed: Aug. 26, 2022. [Online]. Available: https://rosap.ntl.bts.gov/view/dot/26838

[10] P. Léger, P. Côté, and R. Tinawi, “Finite element analysis of concrete swelling due to alkali-aggregate reactions in dams,” *Computers & Structures*, vol. 60, no. 4, pp. 601–611, Jun. 1996, doi: 10.1016/0045-7949(95)00440-8.

[11] L. S. Dent Glasser and N. Kataoka, “The chemistry of ‘alkali-aggregate’ reaction,” *Cement and Concrete Research*, vol. 11, no. 1, pp. 1–9, Jan. 1981, doi: 10.1016/0008-8846(81)90003-X.

[12] S. Akhtar, “A Critical Assessment to the Performance of Alkali-Silica Reaction (ASR) in Concrete”, doi: DOI:10.13179.

[13] M. Berra, T. Mangialardi, A. E. Paolini, and R. Turriziani, “Critical evaluation of accelerated test methods for detecting the alkali-reactivity of aggregates,” *Advances in Cement Research*, vol. 4, no. 13, pp. 29–37, Jan. 1991, doi: 10.1680/adcr.1991.4.1.29.

[14] J. Skalny, J. Marchand, and I. Odler, “Sulfate attack on concrete,” Taylor & Francis, 2003.

[15] V. G. Papadakis, S. Antiohos, and S. Tsimas, “Supplementary cementing materials in concrete: Part II: A fundamental estimation of the efficiency factor,” *Cement and Concrete Research*, vol. 32, no. 10, pp. 1533–1538, Oct. 2002, doi: 10.1016/S0008-8846(02)00829-3.

[16] S. A. Miller, “Supplementary cementitious materials to mitigate greenhouse gas emissions from concrete: can there be too much of a good thing?,” *Journal of Cleaner Production*, vol. 178, pp. 587–598, Mar. 2018, doi: 10.1016/j.jclepro.2018.01.008.

[17] E. Menéndez, M. Á. Sanjuán, R. García-Roves, C. Argiz, and H. Recino, “Sustainable and Durable Performance of Pozzolanic Additions to Prevent Alkali-Silica Reaction (ASR) Promoted

by Aggregates with Different Reaction Rates," *Applied Sciences*, vol. 10, no. 24, Art. no. 24, Jan. 2020, doi: 10.3390/app10249042.

[18] T. E. Stanton, "Studies of Use of Pozzolans for Counteracting Excessive Concrete Expansion Resulting from Reaction Between Aggregates and The Alkalies in Cement," *Symposium on Use of Pozzolanic Materials in Mortars and Concretes*, Jan. 1950, doi: 10.1520/STP39409S.

[19] A. A. Ramezanianpour, S. M. Motahari Karein, P. Vosoughi, A. Pilvar, S. Isapour, and F. Moodi, "Effects of calcined perlite powder as a SCM on the strength and permeability of concrete," *Construction and Building Materials*, vol. 66, pp. 222–228, Sep. 2014, doi: 10.1016/j.conbuildmat.2014.05.086.

[20] C09 Committee, "ASTM C618-22 Specification for Coal Fly Ash and Raw or Calcined Natural Pozzolan for Use in Concrete," ASTM International. doi: 10.1520/C0618-22.

[21] T. M. Research, "Fly Ash Market is Expected to be Valued at US$ 13.8 Bn by 2031, States TMR Study," GlobeNewswire News Room. Accessed: May 05, 2022. [Online]. Available: https://www.globenewswire.com/en/news-release/2022/04/05/2416875/0/en/Fly-Ash-Market-is-Expected-to-be-Valued-at-US-13-8-Bn-by-2031-States-TMR-Study.html

[22] M. C. G. Juenger, R. Snellings, and S. A. Bernal, "Supplementary cementitious materials: New sources, characterization, and performance insights," *Cement and Concrete Research*, vol. 122, pp. 257–273, Aug. 2019, doi: 10.1016/j.cemconres.2019.05.008.

[23] M. H. Shehata and M. D. A. Thomas, "Alkali release characteristics of blended cements," *Cement and Concrete Research*, vol. 36, no. 6, pp. 1166–1175, Jun. 2006, doi: 10.1016/j.cemconres.2006.02.015.

[24] P. K. Mehta, “Natural pozzolans: Supplementary cementing materials,” in *Proc., Int. Symp. on Advances in Concrete Technology*, CANMET, Athens, Greece, 1987, pp. 407–430.

[25] R. E. Rodríguez-Camacho and R. Uribe-Afif, “Importance of using the natural pozzolans on concrete durability,” *Cement and Concrete Research*, vol. 32, no. 12, pp. 1851–1858, Dec. 2002, doi: 10.1016/S0008-8846(01)00714-1.

[26] “AASHTO T380 Standard Method of Test for Potential Alkali Reactivity of Aggregates and Effectiveness of ASR Mitigation Measures (Miniature Concrete Prism Test, MCPT),” American Association of State HIghway and Transportation Officials.

[27] C01 Committee, “ASTM C1012-18b Test Method for Length Change of Hydraulic-Cement Mortars Exposed to a Sulfate Solution,” ASTM International. doi: 10.1520/C1012_C1012M-18B.

[28] “ASTM C596-18 Standard Test Method for Drying Shrinkage of Mortar Containing Hydraulic Cement,” American Society for Testing and Materials, Dec. 2018.

[29] C09 Committee, “ASTM C1202-22 Test Method for Electrical Indication of Concretes Ability to Resist Chloride Ion Penetration,” ASTM International. doi: 10.1520/C1202-22.

[30] “NT Build 492 (1999-11) (1999) Concrete, mortar and cement-based repair materials: chloride migration coefficient from non-steady-state migration experiments, Nordtest, Espoo, Finland.”

[31] J. R. Deschamps and J. L. Flippen-Anderson, “Crystallography,” in *Encyclopedia of Physical Science and Technology (Third Edition)*, R. A. Meyers, Ed., New York: Academic Press, 2002, pp. 121–153. doi: 10.1016/B0-12-227410-5/00160-5.

[32] R. S. Barneyback and S. Diamond, “Expression and analysis of pore fluids from hardened cement pastes and mortars,” *Cement and Concrete Research*, vol. 11, no. 2, pp. 279–285, Mar. 1981, doi: 10.1016/0008-8846(81)90069-7.

[33] O. S. Baghabra Al-Amoudi, “Attack on plain and blended cements exposed to aggressive sulfate environments,” *Cement and Concrete Composites*, vol. 24, no. 3, pp. 305–316, Jun. 2002, doi: 10.1016/S0958-9465(01)00082-8.

[34] R. G. Pillai, R. Gettu, and M. Santhanam, “Use of supplementary cementitious materials (SCMs) in reinforced concrete systems-Benefits and limitations,” *Revista ALCONPAT*, vol. 10, no. 2, pp. 147–164, 2020.

[35] M. Wyrzykowski, S.-I. Igarashi, P. Lura, and V. Mechtcherine, “Recommendation of RILEM TC 260-RSC: using superabsorbent polymers (SAP) to mitigate autogenous shrinkage,” *Mater Struct*, vol. 51, no. 5, p. 135, Oct. 2018, doi: 10.1617/s11527-018-1241-9.

[36] I. Yurtdas, D. Chen, D. W. Hu, and J. F. Shao, “Influence of alkali silica reaction (ASR) on mechanical properties of mortar,” *Construction and Building Materials*, vol. 47, pp. 165–174, Oct. 2013, doi: 10.1016/j.conbuildmat.2013.04.046.

[37] Y. Wang, S. Ramanathan, K. S. T. Chopperla, J. H. Ideker, and P. Suraneni, “Estimation of non-traditional supplementary cementitious materials potential to prevent alkali-silica reaction using pozzolanic reactivity and bulk resistivity,” *Cement and Concrete Composites*, vol. 133, p. 104723, Oct. 2022, doi: 10.1016/j.cemconcomp.2022.104723.

[38] E. Berodier and K. Scrivener, “Understanding the Filler Effect on the Nucleation and Growth of C-S-H,” *Journal of the American Ceramic Society*, vol. 97, no. 12, pp. 3764–3773, 2014, doi: 10.1111/jace.13177.

[39] S. Oruji *et al.*, "Mitigation of ASR expansion in concrete using ultra-fine coal bottom ash," *Construction and Building Materials*, vol. 202, pp. 814–824, Mar. 2019, doi: 10.1016/j.conbuildmat.2019.01.013.

CHAPTER VII IMPACT OF HIGH ALKALI NATURAL POZZOLANS AND RECLAIMED FLY ASH ON THE HYDRATION PERFORMANCE OF CEMENTITIOUS-BASED MATRIX

Abstract

The increasing shortage of traditional supplementary cementitious materials (SCMs) like Class F and Class C fly ashes and slag has made it necessary to investigate alternative SCMs that were previously considered less favorable. High-alkali SCMs have often been overlooked due to concerns that their alkali content might leach into the concrete's pore solution, potentially worsening the risk of alkali-silica reaction (ASR). Nevertheless, initial research suggests that not all high-alkali SCMs are harmful, and some can effectively mitigate the ASR expansion when used in adequate quantities. This study addresses how the high-alkali SCMs impact—the hydration performance of cementitious-based matrix. The research evaluated the high-alkali SCMs' ASR mitigation performance by AASHTO T380 (MCPT). The preliminary ASR results indicated that when used in a sufficient replacement dosage, high-alkali SCMs can effectively mitigate ASR, which provides a basis for the following research. ASTM C311 conducted the water demand of materials, and the impact of high-alkali SCMs on cementitious-based matrix's setting was determined by ASTM C191 automatic setting time method. Isothermal calorimetry was used to assess the hydration heat of the paste sample cooperating with high-alkali SCMs, and the ASTM C1897 R^3 test was conducted to assess the pozzolanic reactivity by quantifying the heat release.

The heat release obtained in the isothermal and R^3 test was respectively correlated with the corresponding age cube compressive strength. The change in volume and moisture within pores with early age cement hydration process was monitored by Ultrasonic pulse velocity (UPV). Thermogravimetric analysis (TGA) was used to qualify and quantify the types and amount of cement hydration phase in the paste samples with various ages; the results obtained in this experiment was used to estimate the hydration degree of the cementitious-based matrix. Based on the results of this study, all high-alkali SCMs indicated high pozzolanic reactivity, and they improved the concrete ASR mitigation performance. Additionally, these materials did not negatively impact the hydration properties. Therefore, from the impact on ASR mitigation performance and hydration perspective, high-alkali SCMs indicated the valid potential to be alternative SCMs in the concrete industry.

Keywords: High-Alkali Supplementary Cementitious Materials (SCMs), Hydration Performance, Setting Time, Degree of Cementitious-based Matrix Hydration

7.1. Introduction

Concrete is the second most widely used material behind water. Production of a ton of Portland cement releases 0.87 to 1 ton of carbon dioxide (CO_2), which is responsible for at least 8% (36.3 billion tons) of global CO_2 emissions [1]–[3]. Using supplementary cementitious materials (SCMs) as a partial replacement for cement in concrete is a sustainable approach that reduces the overall carbon footprint of concrete due to using less cement clinker [4]–[6]. Not only aiding in decreasing CO_2 emissions but incorporating SCMs in concrete makes concrete more durable, economical, and environment-friendly [7].

From a cement chemistry perspective, blending SCMs with cement complicates the cement hydration process's stoichiometry and kinetics. The mechanisms of SCMs engaged in the cement

hydration process can be categorized into filler, dilution, and chemical effects [8], [9]. SCMs generally have a smaller particle size distribution than cement, so fine SCMs can fill the voids between cement particles, which helps to densify the concrete microstructure and reduce porosity [10]. The fine SCMs also provide nucleation sites for C-S-H on their surface, and the additional nucleation sites increase the hydration rate [11]. The extent of the filler effect also depends on the microstructure and chemical nature of SCMs. Stark et al. [12] discovered different coverings of C-S-H on the different SCMs powders. The chemical effect of SCMs is the reaction between SCMs and cement hydration products. The primary reason for SCMs utilized in concrete is their pozzolanic reactivity, which chemically consumes calcium hydroxide (CH) to form calcium silicate hydrate (C-S-H) and dense concrete microstructure [13], [14]. Furthermore, the presence of SCMs in a cementitious-based matrix results in the dilution of cement. Less cement participates in the cement hydration process, further producing less C-S-H. Therefore, even though the pozzolanic reactivity of SCMs increases the strength of the cementitious-based matrix, high amounts of SCMs replacement still result in a drastic reduction in the mechanical properties of concrete, such as strength and elastic modulus [15].

Additionally, the microstructure and chemical composition of SCMs indicate the influence on hydration. Some SCMs have smooth spherical shapes, resulting in the “ball-bearing effect”, which helps reduce the friction force at the interface between cement paste and aggregate and further increases the workability [16]. However, some SCMs behave oppositely. Loss on ignition (LOI) content of SCMs is the residue mass after heating to a higher temperature, and most LOI content in SCMs is unburnt carbon content [17]. The high LOI impacts the water demand for concrete: 4% in LOI would require about 5% more water to account for the slump reduction of concrete [18]. Besides increasing the demand, other risks of utilizing high LOI SCMs in concrete

are reducing the strength, increasing the porosity and permeability, and increasing the demand for chemical admixtures, such as air-entraining agents [17], [19].

The impact of SCMs on hydration kinetics can be measured by isothermal calorimetry, which is used to quantify the heat release resulting from the hydration process, and the heat release is proportional to the rate of hydration. According to the current research, the types and particle sizes of SCMs impact the rate of hydration. Rong et al. [20] evaluated the effect of silica fume and fly ash on cement hydration, and they discovered that their silica fume accelerated the hydration, but fly ash retarded it. However, the same type but with various particle sizes of SCMs also performs differently. Ni et al. [21] assessed the impact of silica fume with different particle sizes on the hydration performance. In their study, silica fumes of particles size less than 150 μm accelerated the hydration and released more heat than the control. Whereas silica fumes greater than 150 μm hindered the hydration rate and lowered the heat release.

Thermogravimetric analysis (TGA) is another widely used approach to assessing the chemical reaction of SCMs in the cementitious matrix [22]–[24]. Also, some studies used this technique to analyze the degree of hydration. However, no model using TGA to determine the hydration degree of blended cement has gained consensus within the scientific community so far. To date, two methods developed by Bhatty [25] and Pane et al. [26] are two fundamental approaches to understanding the hydration process involved with SCMs. In recent years, according to the methods of Bhatty [25] and Pane et al. [26], Monteagudo et al. [27] provided a new method to evaluate the kinetic of SCMs blended with cement. Ultrasonic pulse velocity (UPV) is a non-destructive test (NDT) method used in the construction industry to assess the quality and integrity of concrete structures, including monitoring cement hydration. UPV testing uses the velocity of ultrasonic pulses as they travel through a concrete specimen. This velocity can provide valuable

information about the properties of the concrete, including its density, strength, elastic modulus, and degree of cement hydration [28]–[30].

This study aims to evaluate how high-alkali SCMs influence the hydration performance of cementitious-based matrix. The primary reason for analyzing the materials with high-alkali content is to seek the alternative SCMs option for the concrete industry. In recent years, with the demand for SCMs increasing and coal power transitioning to using clean energy sources to reduce carbon emissions, traditional SCMs like fly ash meet the shortage problem and price increase [31], [32]. Therefore, finding a sustainable alternative for the worldwide SCMs industry is urgent. High-alkali SCMs, whose alkali content is generally over 4%, are generally avoided in concrete due to concerns arising from the potential leaching of alkali ions into the pore solution and increasing the alkali loading in the concrete pore solution, further exacerbating the ASR. However, the current research does not reach a consensus for utilizing the high-alkali SCMs. Shehata et al.'s research [22] evaluated the alkali release characteristics of blended cement with high alkali SCMs, and their research indicated that some SCMs with high total alkali content released alkali ions into the pore solution, which increased alkali concentration in the pore solution. However, Mehta's research [34] indicated that alkali content in some natural pozzolans exists as crystal phases, which did not readily release into the concrete pore solution. The same finding was discovered by Uribe-Afif et al. [35]. In their study, one of the SCMs had a total alkali content of 6.89% Na_2O_{eq}, but the available alkali content was only 1.09% Na_2O_{eq}, thus only 15% of the total alkalis were available to be released into the pore solution. Additionally, ASTM C618 [36], as the primary evaluating basis for selecting SCMs used in concrete, does not specify the alkali content of SCMs, and the maximum equivalent alkali content ($Na_2O\%= N_2O\%+ 0.658K_2O\%$) is not clearly defined.

Therefore, these existing controversies provide feasibility for our experiments to evaluate these materials.

The study evaluated the performance of high-alkali SCMs, including six natural pozzolans and two reclaimed fly ash, in two stages. Stage I assessed the high-alkali SCMs' ASR mitigation performance, which was conducted by AASHTO T380 (MCPT) [37]. Stage II evaluated the impact of high-alkali SCMs on the hydration properties of cementitious-based matrix. The study started to exhibit water demand SCMs, per ASTM C311 [38]. The early setting performance of high-alkali was conducted by automatic setting of time following ASTM C191 [39] and UPV. Isothermal calorimetry was used to quantify the released hydration heat of the cementitious matrix involved with high-alkali SCMs. Additionally, ASTM C1897 [40] was performed to assess the pozzolanic reactivity of SCMs. All the results obtained in the isothermal calorimetry were correlated with corresponding compressive strength. Finally, TGA was executed to determine the amount of different hydration products, which helped to determine the degree of hydration at long-term age.

7.2. Materials and Methods

7.2.1 Materials

Two types of ordinary Portland cement (OPC) meeting ASTM C150 [23] were used in this study: A low-alkali Type I/II Portland cement (Na_2O_e = 0.38%) from Argos cement company, Harleyville, SC, and a high-alkali Type I Portland cement (Na_2O_e = 1.00%) from Lehigh Hanson Inc. The chemical composition and physical properties of both Portland cements are presented in Table 7- 1.

In this study, five natural pozzolans and two reclaimed fly ashes were investigated. The natural pozzolans are identified as NP 1 through NP 6, and reclaimed fly ashes as RFA 1 and RFA 2. The material chemical compositions and particle size distributions were measured by X-Ray fluorescence and laser diffraction, respectively. These results are presented in Table 7- 1 and Figure 7- 1. XRD data of high-alkali SCMs were collected using the Rigaku X-ray diffractor. Measurements were made in flat-plate Bragg–Brentano θ–2θ geometry, and their angular range was from 10° to 80° 2θ values with a 0.02° 2θ step size. The scan rate for the test was 1° 2θ per minute. The amorphous level, i.e.the amount of non-crystallinity, was determined by the Rietveld analysis, which used the integrated surface area of the crystal compared to the total surface area [41]. In this study, XRD results, shown in Figure 7- 2 and Cement and High-Alkali SCMs Chemical Composition, indicate that all the materials have a high amorphous content except NP 2. NP 2 did not exhibit a significant amorphous hump, rather it had many crystal peaks that often overlapped.

The reactive aggregate used in this study is a known reactive aggregate from the Goldhill Quarry in North Carolina, which consists of reactive metatuff–argillite. The aggregate's specific gravity and water percent absorptions were 2.6 and 1%, respectively.

Table 7- 1 Cement and High-Alkali SCMs Chemical Composition

		SiO_2	Al_2O_3	Fe_2O_3	S+Al+Fe	CaO	MgO	Na_2O	K_2O	Na_2O_e	LOI	SG	Amorphous Level (%)
	Low-alkali Portland cement	19.93	4.77	3.13	27.83	62.27	2.70	0.06	0.48	0.37	2.6	3.15	NA
	High-alkali Portland cement	19.00	4.99	2.11	26.1	62.45	2.84	0.31	1.05	1.0	NA	3.15	NA
Volcanic rhyolitic tuff	NP 1	68.62	13.14	1.91	83.67	1.73	1.43	2.7	3.2	4.82	7.18	2.53	37.67
Pumice	NP 2	73.42	12.30	1.41	87.13	0.79	0.23	2.9	4.2	5.61	4.72	2.35	98.55
Pumice	NP 3	65.48	11.19	1.75	78.42	2.99	0.33	3.6	3.4	5.85	10.87	2.26	3.38
Volcanic rhyolitic tephra	NP 4	71.95	12.26	1.50	85.71	0.93	0.39	3.9	4.0	6.51	4.88	2.35	87.76
Volcanic glass	NP 5	71.21	12.99	0.90	85.1	0.56	0.13	3.9	4.1	6.57	5.95	2.40	100
Pumice	NP 6	71.91	11.68	2.18	85.77	0.32	0.09	5.5	4.2	8.28	3.94	2.34	91.17
Reclaimed fly ash	RFA 1	53.06	15.13	6.88	75.07	13.70	4.53	3.4	1.9	4.69	0.55	2.56	82.48
Reclaimed fly ash	RFA 2	56.81	14.20	2.69	73.7	10.13	1.41	2.8	2.7	4.56	8.42	2.42	88.88

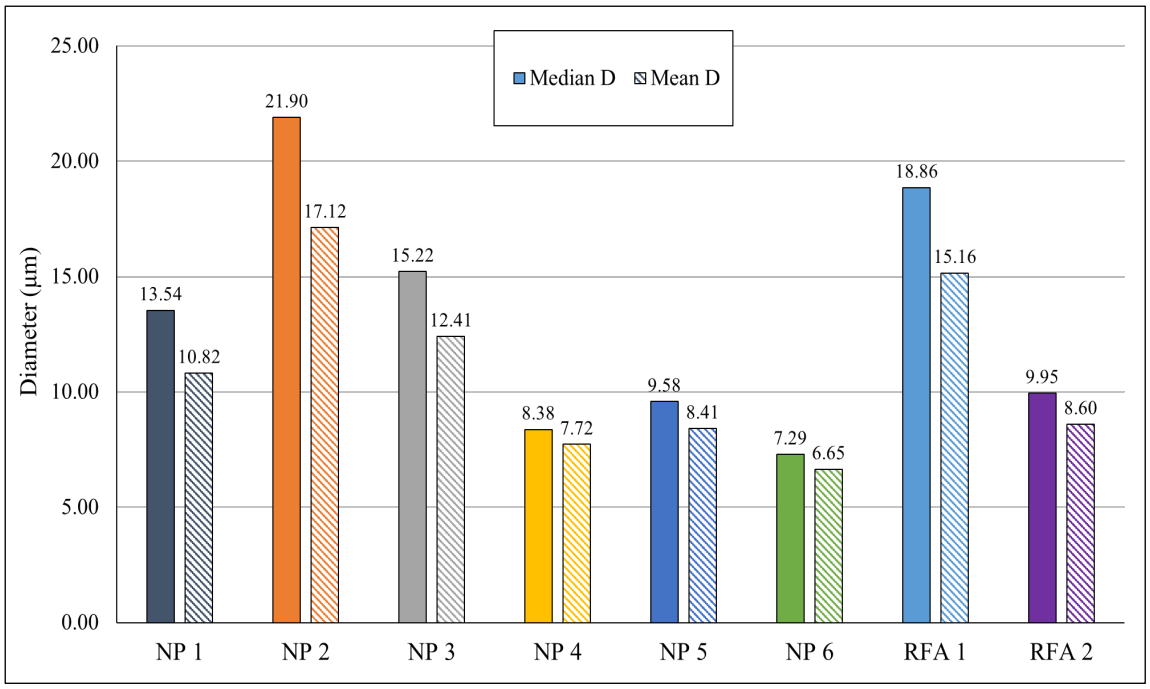
Median D
Mean D
Diameter (µm)
25.00
20.00
15.00
10.00
5.00
0.00
13.54
10.82
21.90
17.12
15.22
12.41
8.38
7.72
9.58
8.41
7.29
6.65
18.86
15.16
9.95
8.60
NP 1
NP 2
NP 3
NP 4
NP 5
NP 6
RFA 1
RFA 2

(a)

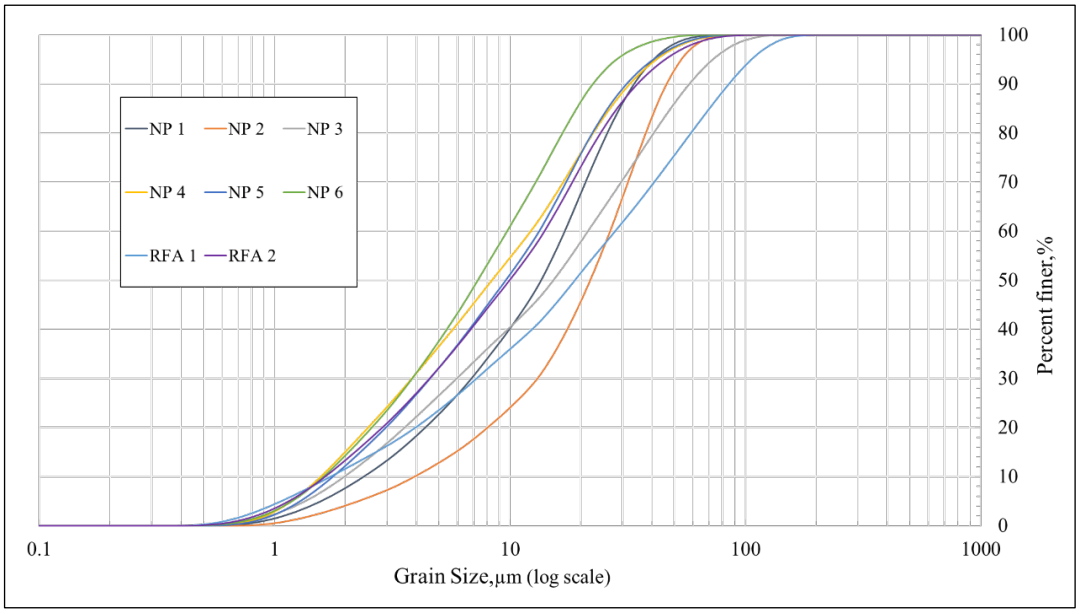

Figure 7- 1(a)SCMs' particle size; (b)Particle size distribution of natural pozzolans

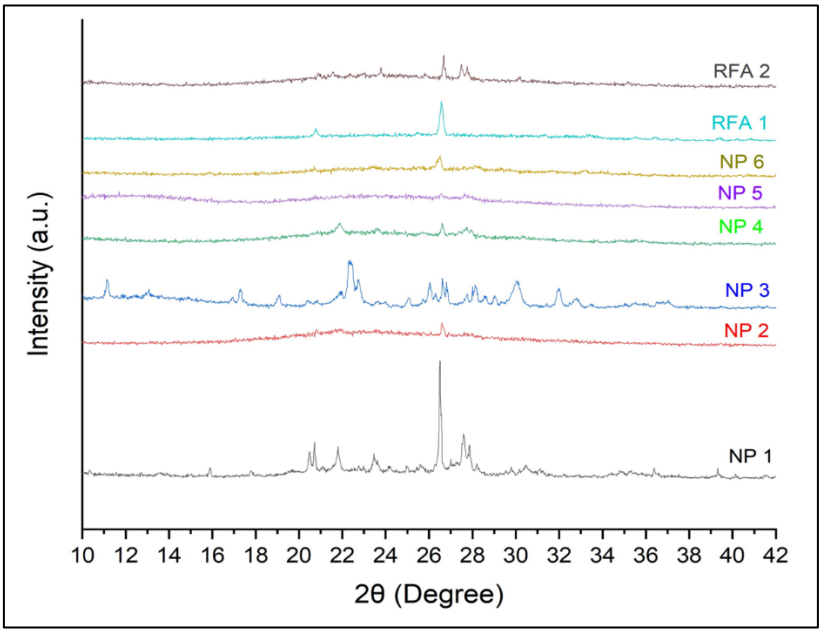

Figure 7- 2 XRD Pattern

7.2.2 AASHTO T380 Miniature Concrete Prism Test (MCPT) [37]

AASHTO T380 (MCPT) was used to evaluate the high-alkali SCMs to mitigate ASR in this study. In this method, the cementitious materials content of concrete mixtures was maintained at 420 kg/m3, with a w/b ratio of 0.45. The dry mass of coarse aggregate per unit volume of concrete

was maintained at 0.65, and the coarse aggregates' gradation followed the recommended gradation per AASHTO T380. The fineness modulus of fine aggregates conformed to 2.60 ± 0.3. Reagent-grade NaOH pellets were dissolved in the mixing water to boost the alkali content of the concrete to 1.25% by the mass of cement. SCMs were used at dosage levels of 20%, 30%, and 40% by mass of cement.

The test specimens were cast and cured at ambient temperature and 100% RH for 24 hours. After demolding, the specimens were placed in water at 60°C for another 24 hours. The zero-day reading was taken at the end of 24 hours of water bath curing. Then, the specimens were transferred into a sealed container with 1N NaOH maintained at 60°C. The prism length changes were recorded periodically at 0, 3, 7, 10, 14, 21, 28, 42, 56, 70, and 84 days. The criteria for evaluating the efficacy of SCMs in mitigating ASR in the MCPT method at 56 days are as follows per AASHTO T380:

13. Expansion < 0.020% - Effective ASR Mitigation;
14. 0.020% < expansion < 0.025% Uncertain ASR Mitigation
15. Expansion > 0.025% Not effective ASR mitigation

If the samples exhibit expansion between 0.20 and 0.25 at 56 days, the average expansion between 56-day to 84-day (8 weeks to 12 weeks), should be less than 0.010% per 2 weeks for the mitigation measure to be considered effective.

7.2.3 Water Demand

Following ASTM C311, the flow table test was used to quantify the water demand for fixed workability of mortars containing the SCMs. The control was mixed at 0.485 water-cement-ratio, and test specimens contained 20% SCMs with the same sand-cement ratio. Water demand was recorded until the flow of test specimens reached ± 5% of the control mixture.

7.2.4 Automatic Vicat Setting of Time

The setting time of the paste was determined based on the ASTM C191 method B with modifications using the automatic Vicat apparatus. The paste's water-binder ratio was 0.42, and high-alkali SCMs replacement levels were 20% and 40% by cement mass, and the test samples were under a water bath during the process to prevent evaporation. This study determined the initial and final setting when the needle penetration achieved 35mm and 0.1mm, respectively.

7.2.5 Isothermal Calorimetry Study

The heat flow of the investigated paste mixtures, with 0.42 water-binder- ratio, containing 20% SCMs, was determined at 23^{o}C with a four-channel Isothermal Calorimeter. After casting, 100 g of mixtures was placed in the measuring bottle, and the heat flow of each specimen was recorded for 7 days.

Pozzolanic reactivity of SCMs was evaluated using the R^3 test per ASTM C1897-20 method A by using Isothermal calorimetry The mixtures consisted of SCMs, calcium hydroxide (CH), calcium carbonate (CaCO3), potassium sulfate (K_2SO_4), and potassium hydroxide (KOH). The mass ratio of SCMs to CH and $CaCO_3$ was 1 to 3 and 2 to 1, respectively. The potassium solution was prepared by dissolving 4.00 g of KOH and 20.0 g of K_2SO_4 in 1.00 L of reagent water. The mass ratio of potassium to the solids, i.e., blend of SCMs, CH, and CaCO3, was 1.2. The cumulative heat was measured at 40°C for 7 days. All the materials were mixed at 1600 ± 50 r/min for 2 min using the high-shear blender to achieve a homogeneous paste.

7.2.6 Ultrasonic pulse velocity test (UPV)

The ultrasonic pulse velocity test (UPV) was conducted to monitor changes in volume pores and moisture content within pores with the cement hydration process. For the test, Ultrasonic Tester BP-700 series was employed. The pastes were prepared by blending low-alkali cement with

20% SCMs by mass of cement at a water-to-binder ratio of 0.42. To ensure precise results, the paste mixture underwent vacuum mixing to eliminate the influence of air bubbles. The test configuration involved positioning the sensors 40mm apart, with data collection occurring at one-minute intervals. After casting, the specimens were stored in the air chamber at 23°C and 50% RH for 24 hours.

7.2.7 Compressive Strength

The strength activity index test (SAI) was used to evaluate the pozzolanic activity of SCMs in mixtures blended with low-alkali cement, and the mixture proportions were followed in accordance with ASTM C311. In this test, nine mixtures with six samples were prepared for 7-day and 28-day strength measurements. After casting, the specimens were placed in the standard curing room for 24 h. After demolding, the samples were cured at ambient temperature in lime-saturated water. Compressive strength was measured using TEST MARK CM-3000 SD compression testing machine at a loading rate of 50 psi/s. The SAI was calculated using Equation (10):

$$\mathbf{S} \quad \boldsymbol{AI} = \frac{\text{Average compressive strength of test mixtures}}{\text{Average compressive strength of control}} \times \qquad (1)$$

100%

The compressive strength of paste was also studied in this research to evaluate the early-age performance of SCMs and the correlation between strength and other paste studies. The paste was mixed at a 0.42 water-binder ratio. Nine mixtures with nine samples were prepared for 1-day, 3-day, and 7-day strength measurements. After casting and demolding, the specimens were stored in the standard curing until measurement.

7.2.8 Thermogravimetric Analysis (TGA) for Degree of Hydration

Thermogravimetric analysis (TGA) was conducted to assess the cement paste's degree of hydration (α) by determining the chemically bound water. Auto TGA Q5000 instrument was

employed for this testing, and test samples were heated from ambient temperature to 1000 degrees Celsius at 10 degrees Celsius per minute.

The pastes were prepared by blending low-alkali cement with SCMs at a 20% mass replacement of cement at a water-to-binder ratio of 0.42. The prepared paste samples were stored in a sealed container and were tested at the ages 1 day, 3-day, 7-day, 28-day, and 56 days. After casting, the specimens were sealed in air-tight test tubes to avoid potential carbonation and stored in an air chamber maintained at 23^{o}C and 50% RH. Before testing, the samples were de-molded from the tubes and ground using an agate mortar and pestle to pass the No.100 sieve (150 μm). Then, the powder samples were immersed in 50ml isopropanol for 15 minutes to remove moisture from the powder. The suspension was filtered by using Büchner funnel to obtain the dehydrated powder, and 10 ml diethylene was added to the powder to remove extra isopropanol. After preparation, the sample was immediately stored in air-tight vials and tested.

The samples' chemically bound water was determined using methods of Bhatty, Pane, and Monteagudo, respectively. For the method of Bhatty, the hydration degree of cement paste was obtained by the following equations [25]:

$$w_B = Ldh + Ldx + 0.41(Ldc) \quad (2)$$

$$\alpha = \frac{W_B}{0.24} \quad (3)$$

where Ldh, Ldx, and Ldc are the relative mass loss on TGA curves during dehydration of C-S-H, dehydroxylation of Ca $(OH)_2$, and decarbonation of $CaCO_3$, respectively. 0.41 was the conversion factor, which allowed to assume the bound water derived from carbonated portlandite. W_B is the

chemically bound water at time t. Additionally, α was the degree of hydration, and 0.24 was the chemically bound water at infinite time ($W_{B\infty}$) estimated from the theoretical stoichiometry of cement (Bogue's formulae)

The method of Pan et al. assessed the chemically bound water by the following euqations [26]:

$$w_B = Ldh + Ldx + 0.41(Ldc - Ldc_a) \quad (4)$$

$$W_B = W_{B\infty} \times e^{[-\frac{\tau^a}{t}]} \quad (5)$$

$$\alpha = \frac{W_B}{W_{B\infty}} \quad (6)$$

where Ldc_a is the relative mass loss within the temperature range of 600–780 °C, this mass loss is due to the decomposition of $CaCO_3$ during TGA tests on anhydrous materials (cement and SCMs used). In this paper, Ldc_a was assumed to be 0. Additionally, $W_{B\infty}$ was calculated with three parameters based on the data, where τ, a, and t were the intercept, curvature of the plot in a logarithmic scale, and sample curing age, respectively, and the values of $W_{B\infty}$, τ, and a were determined by using the Matlab fitting model.

The third method, Monteagudo et al., determined the chemically bound water according to the following equations [27]:

$$w_B = Ldh + Ldx + 0.41(Ldc - Ldc_a) \quad (7)$$

$$W_B = \frac{W_{B\infty} \times t}{t + k} \tag{8}$$

$$\alpha = \frac{W_B}{W_{B\infty}} \tag{9}$$

where k was a constant. The $W_{B\infty}$ and k were determined by using the Matlab fitting model.

Additionally, even though all methods conducted chemically bound water by using Ldh, Ldx, and Ldc, the exact temperature intervals in the three methods were different. In order to keep the results consistent, the temperature ranges of Ldh, Ldx, and Ldc are shown in Table 7- 2

Table 7- 2 Temperature Ranges

Region	Temperature range (°C)
Dehydration (Ldh)	105 -400
Dehydroxylation (Ldx)	400 -600
Decarbonation (Ldc)	600-1000

7.3. Results and Discussion

7.3.1 MCPT

Figure 7- 3 and Figure 7- 4 exhibited the length change of concrete prisms in AASHTO T380 (MCPT) with 20% SCMs. In MCPT, SCMs are considered to effectively mitigate ASR when expansion is below 0.020% at 56 days, and the expansion rate should not exceed 0.010% every two weeks from day 56 to day 84.

Except for NP 2 and RFA 1, the rest of the materials were able to limit the ASR expansion to approximately or lower than 0.020% at 56 days. The expansion of NP 2 and RFA 1 was 0.026% and 0.035%, respectively. RFA 1 performed the worst in this MCPT, which kept consistent with the previous ASR experiments. Additionally, NP 2 and RFA 1 also failed to satisfy the requirement of expansion rate, and both expansion rates exceeded 0.010% per two weeks. Even though NP 1's 56^{th}-day expansion was 0.019%, less than 0.020%, meeting the requirement, its expansion rate was over 0.010%; therefore, NP 1 was not considered successful in mitigating ASR expansion. NP 4 had the lowest expansion on the 56^{th} day, but on the 84^{th} day, NP 7 performance exceeded NP 4 because NP 4 expanded a lot during the 56^{th} to 84^{th} day. During the interval, from the 56^{th} to the 84^{th} day, the rest mixtures, except NP 7, continued to expand, and their expansion values exceeded 0.020% at 84 days.

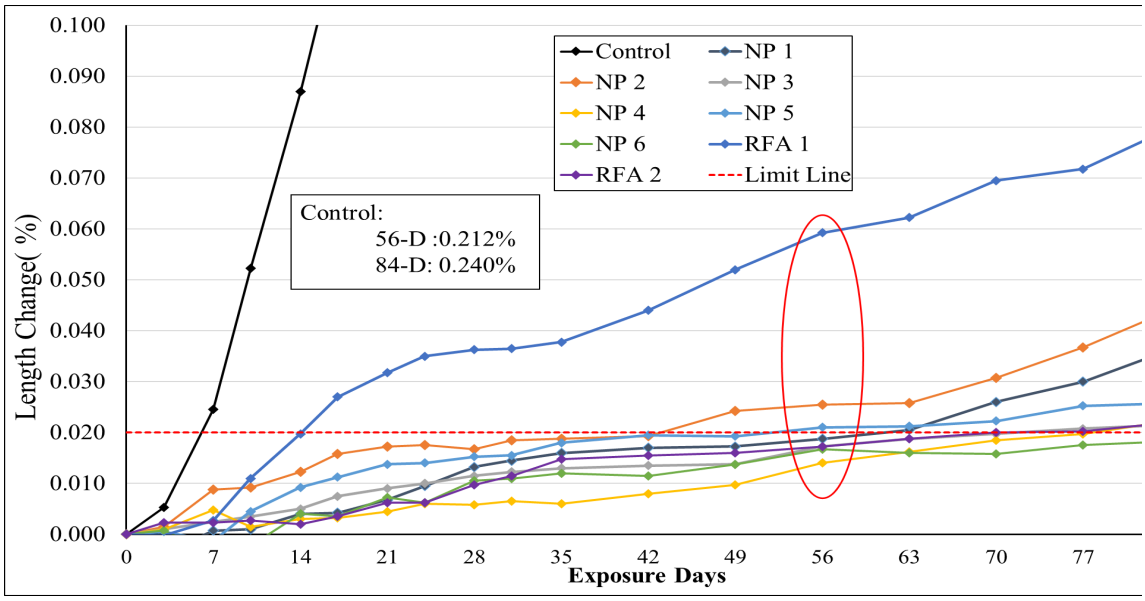

Figure 7- 3 AASHTO T380 length change of concrete prisms with 20% SCMs replacement

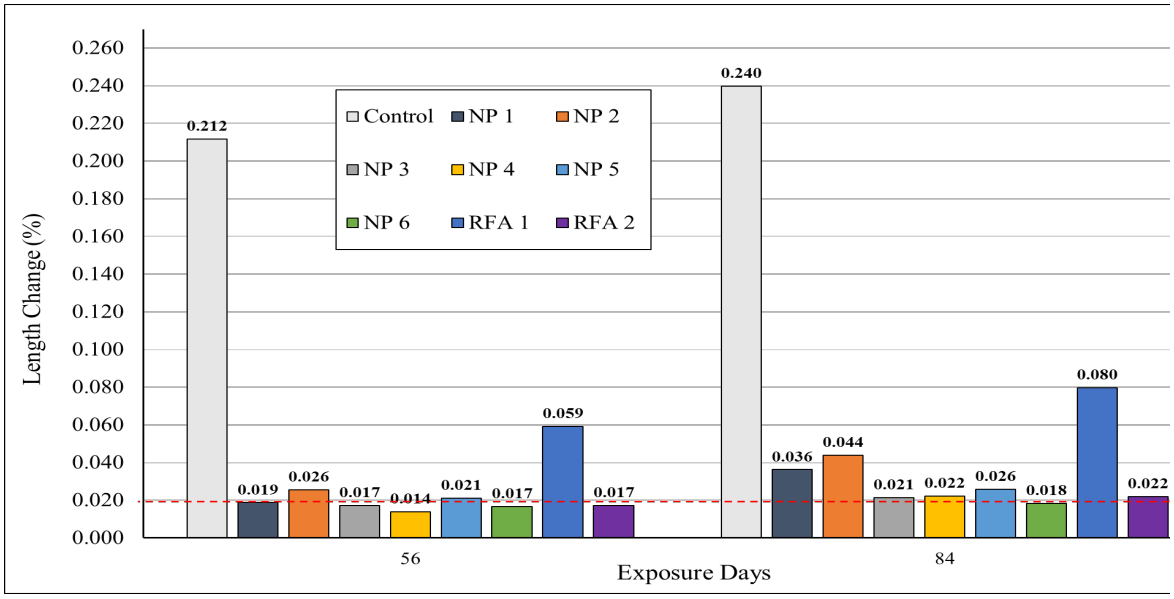

Figure 7- 4 AASHTO T380 56-D & 84-D expansion value with 20% SCMs replacement

7.3.2 Water Demand

The flow behavior of mortars mixed with SCMs is shown in Figure 7- 5. NP 1 required a higher water demand the reaching the same flow as the control, which needed around 20% more

water to reach the flow range. However, NP 2 yielded less water demand, requiring only 93% of water to get the flow. The water demand for the rest of the materials was around 100%.

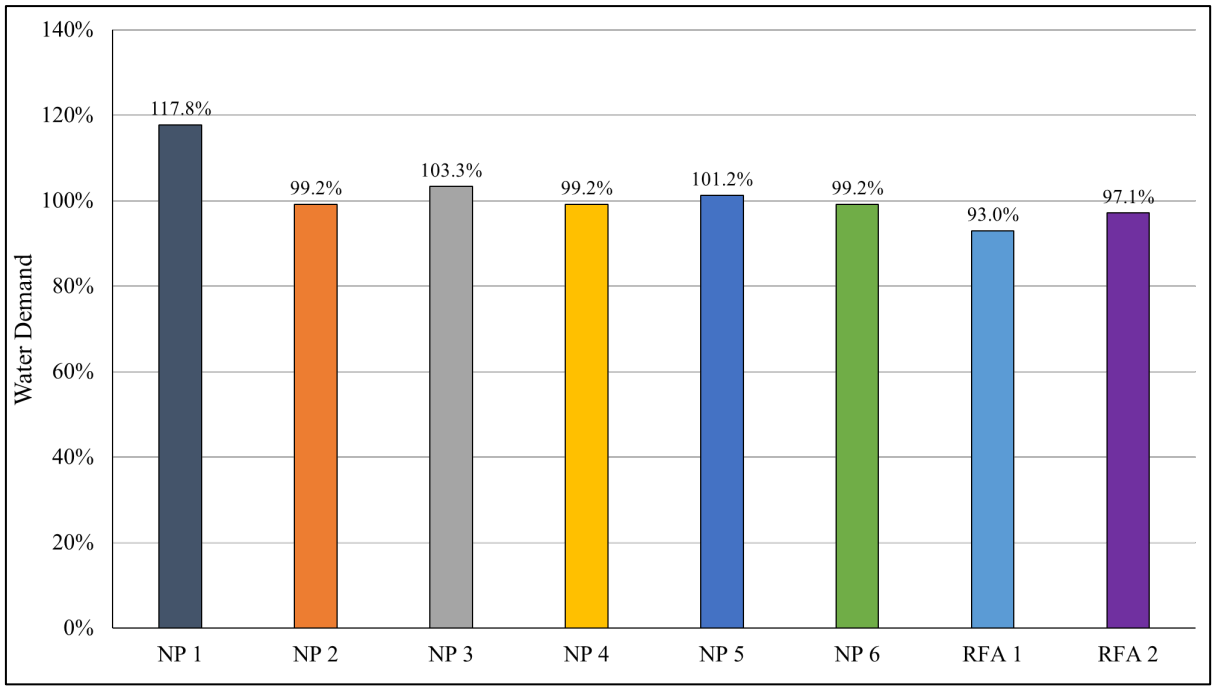

Figure 7- 5 High-Alkali SCMs Water Demand

7.3.3 Automatic Setting of Time

Figure 7- 6 shows the setting time of high-alkali SCMs, which indicates RFAs behaved differently with natural pozzolans. According to the results, the inclusion of RFAs resulted in the delay of both initial and final setting time in comparison to the control. Moreover, the degree of this time delay exhibited an upward trend corresponding to higher replacement levels. However, natural pozzolans behaved oppositely. With the exception of NP 4, which demonstrated a minor delay in setting time, the remaining materials exhibited either a comparable level of setting time or a tendency towards acceleration, which was also discovered in a previous study [42]. This acceleration can be attributed to the ample specific surface area of the natural pozzolans. This surface area facilitates a continuous uptake of free water, resulting in a self-desiccation process within the hydrating system.[43].

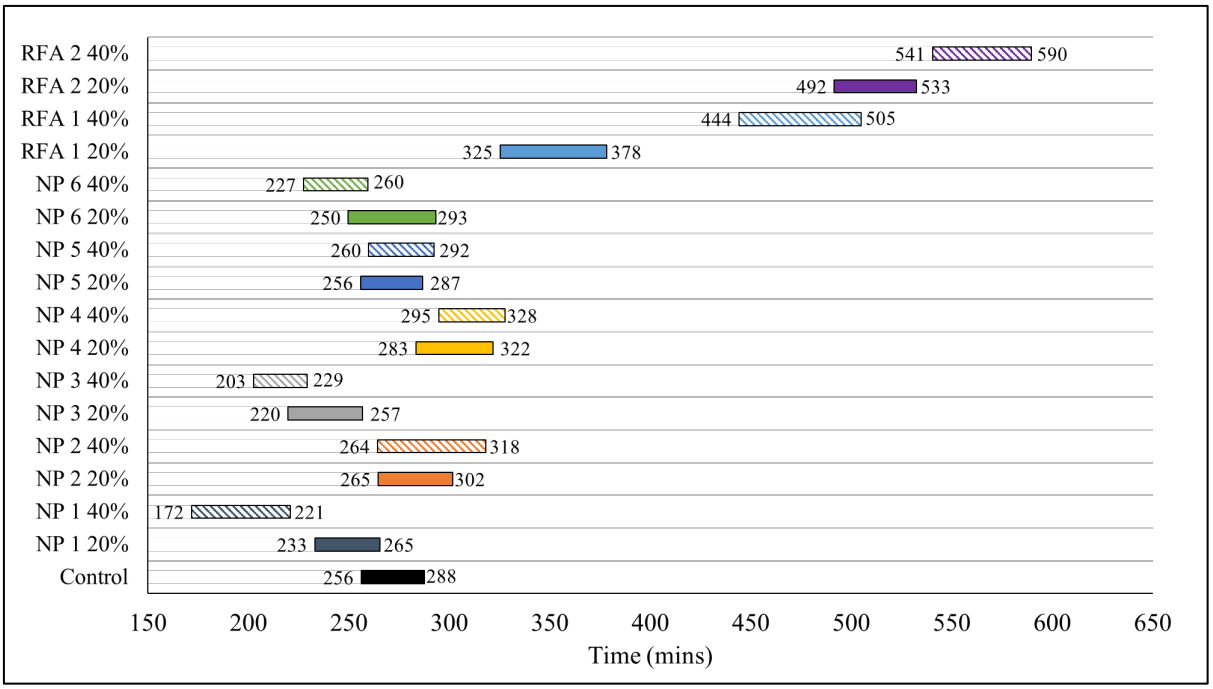

Figure 7- 6 High-Alkali SCMs Automatic Setting Time

7.3.4 Isothermal Calorimetry Study

Figure 7- 7, Figure 7- 8, Figure 7- 9, and Figure 7- 10 show the isothermal calorimetry results. Figure 7- 7 indicates the 7-D exothermic process of the specimens, and Figure 7- 8 represents the cumulative heat of the exact sample age. Based on the cumulative heat analysis, RFA 2 exhibited the lowest heat release during the initial 30 hours compared to the other groups, which was only 149.28 J/g. However, as the samples aged, the cumulative heat generated by RFA 2 gradually increased, ultimately reaching the highest level among all the samples, 295.75 J/g. Additionally, for the rest groups, the heat release was very close.

Figure 7- 9 reveals the heat rate results, and Figure 7- 10 exhibits the zoom results of the heat rate at the initial four hours. During the heat rate analysis, RFA 2 distinctly displayed a retardation effect on cement hydration in the early stages. Upon closer examination of the Zoom results, it was observed that most materials exhibited endothermic reactions, except for NP 1 and NP 3, which displayed exothermic processes.

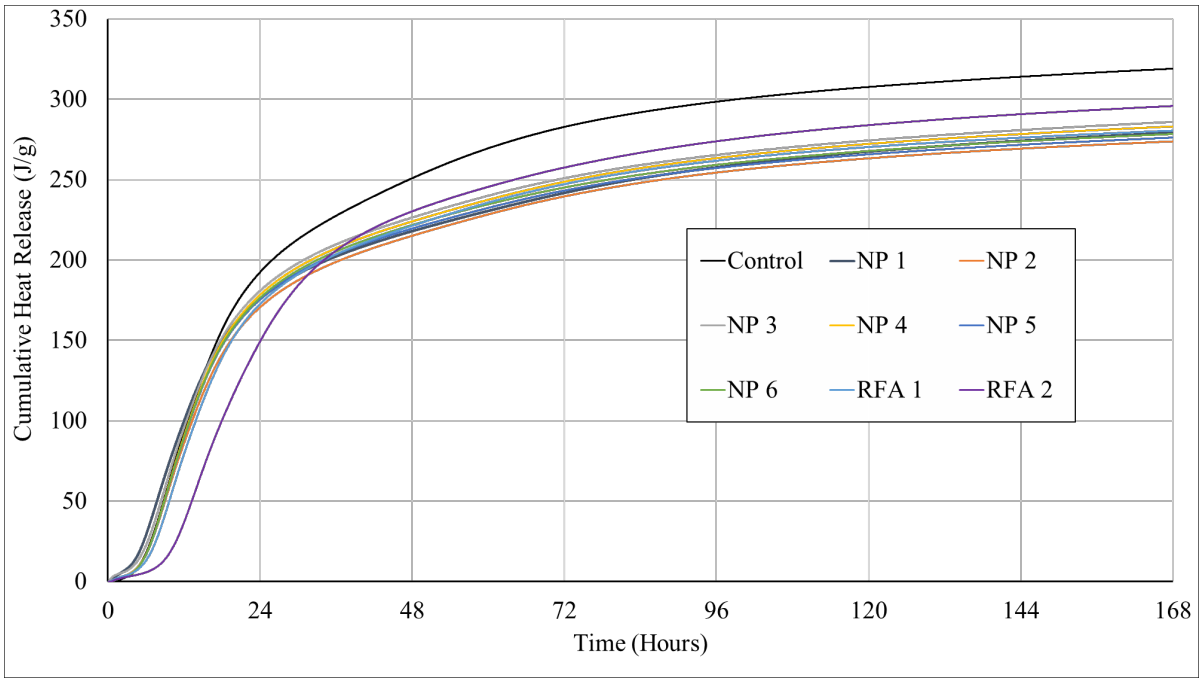

Figure 7- 7 Cumulative Heat

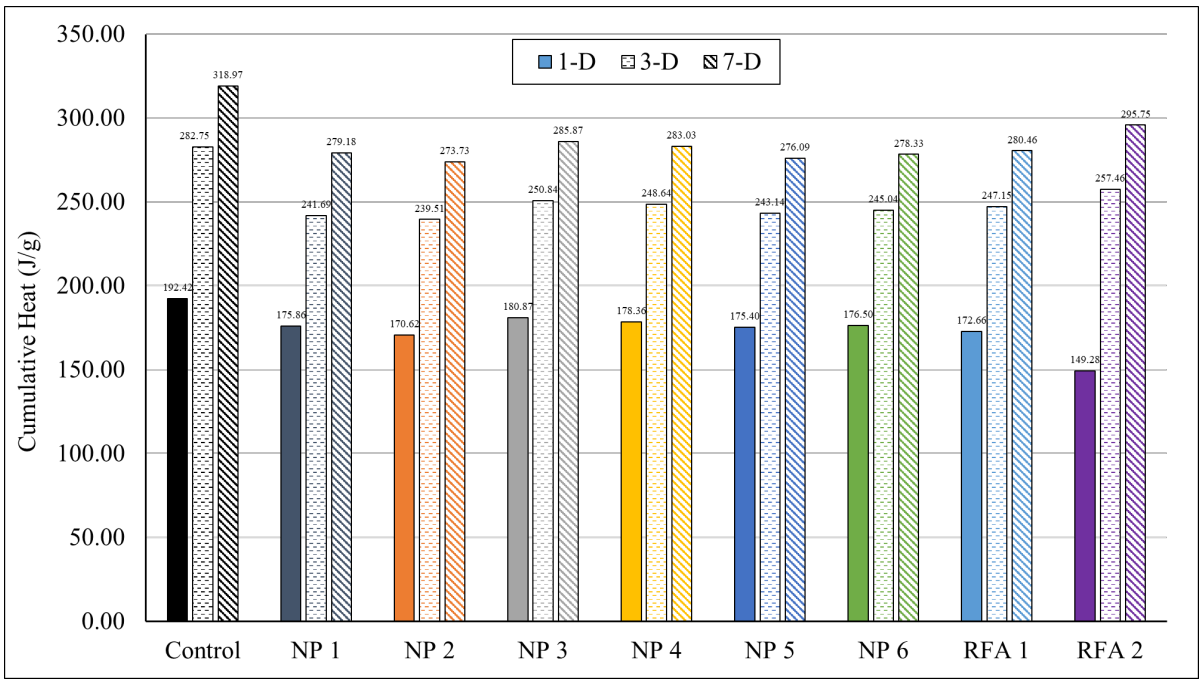

Figure 7- 81D, 3D and 7D Cumulative Heat

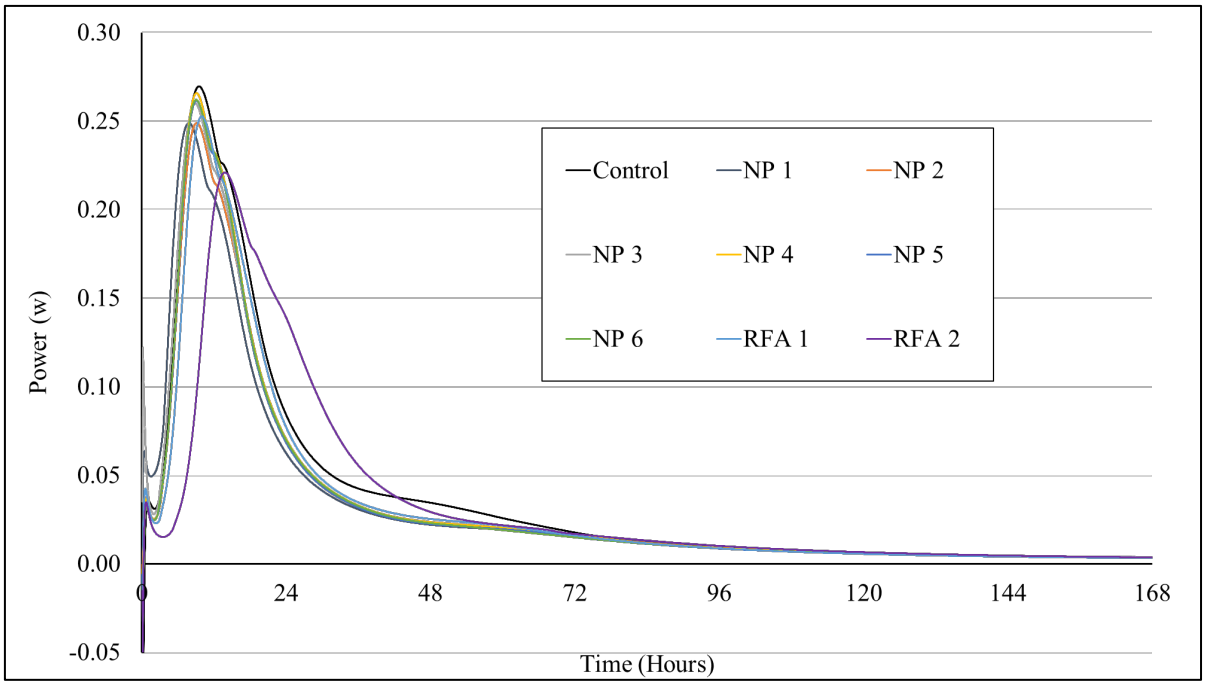

Figure 7- 9 Heat Rate

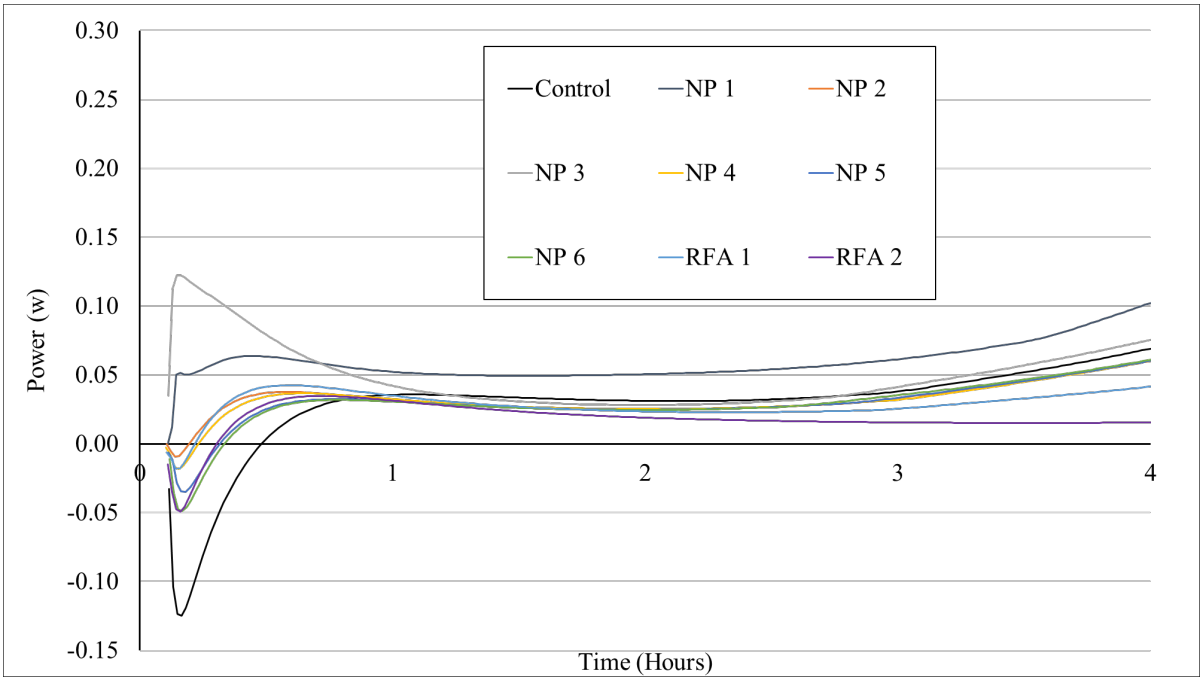

Figure 7- 10 Heat Rate of the First 4-Hour

Figure 7- 11 indicates the 7-day cumulative heat release for the R^3 results. All the paste specimens with SCMs investigated in this study showed a 7-day cumulative heat above 300 J/g. A

previous study concluded that the if the material's 7-day cumulative heat exceeded 200 J/g, it was a highly pozzolanic material; on the contrary, if the cumulative heat was below 100 J/g, it indicated an inert material [44]. Therefore, all the high-alkali SCMs in this test are highly pozzolanic materials. Two reclaimed fly ash had the highest cumulative heat in this test, with RFA 1 and RFA 2 leading other natural pozzolans. The cumulative heat of NP 3 and NP 4 was around 350 J/g, and NP1 and NP2 were about 300 J/g.

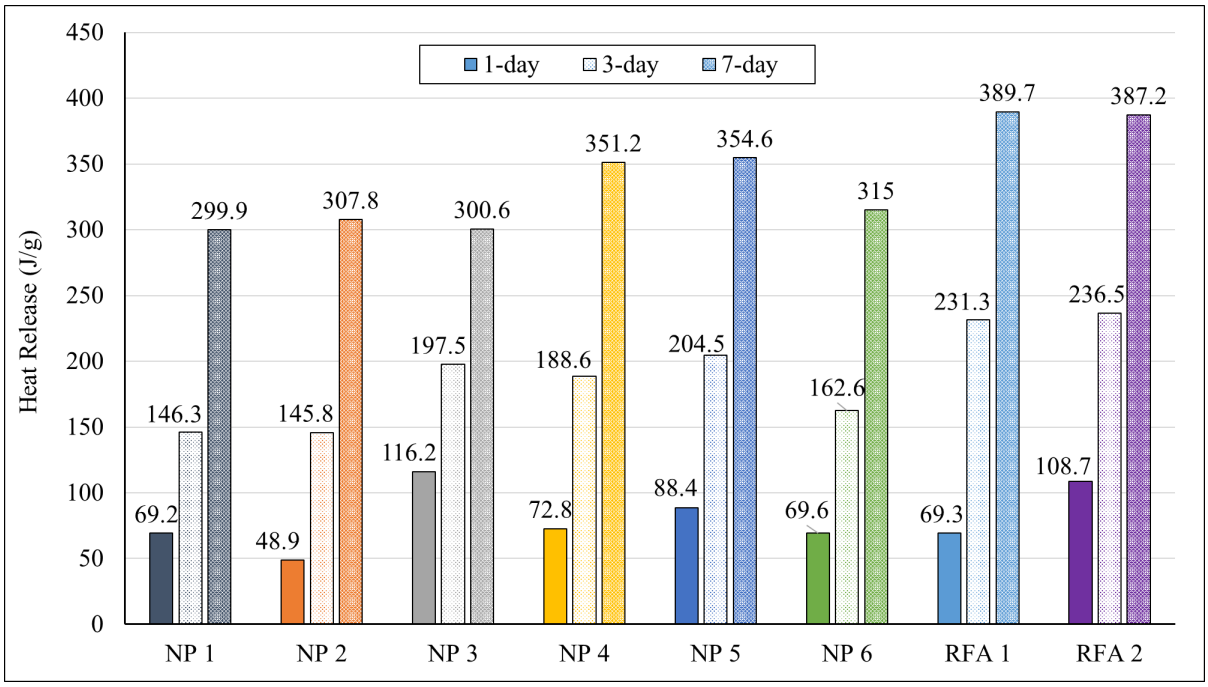

Figure 7- 11 Heat Release of High-Alkali SCMs in R^3 test

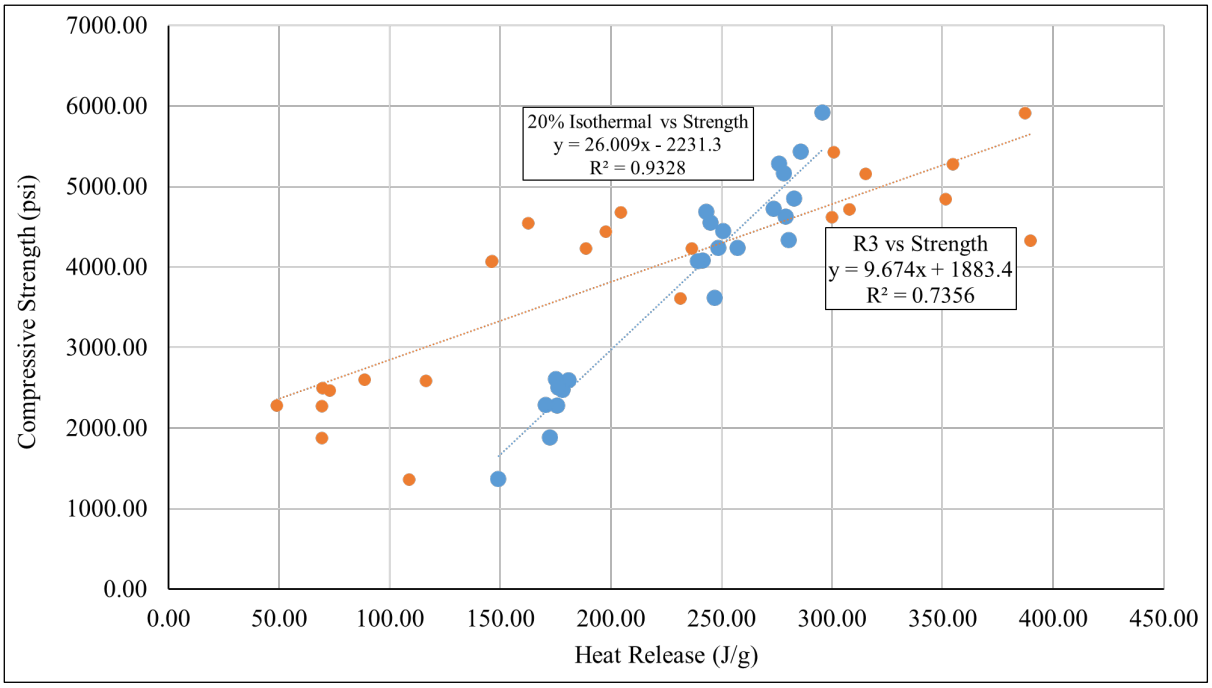

Figure 7- 12 Correlation between Compressive Strength and Heat Release

Furthermore, Figure 7- 12 illustrates the correlation between the compressive strength of cubes and two different tests: the isothermal study and the R3 test, both conducted at corresponding sample ages. The results reveal a highly significant correlation between the isothermal study and compressive strength, with an impressive R^2 value of 0.9329. In contrast, the correlation between strength and the R3 test did not exhibit the same level of performance, yielding a lower R^2 value of 0.7356. However, if only compared to natural pozzolans without fly ash, the R^2 increased to 0.9573, which indicated the limitations of R^3 in evaluating fly ash.

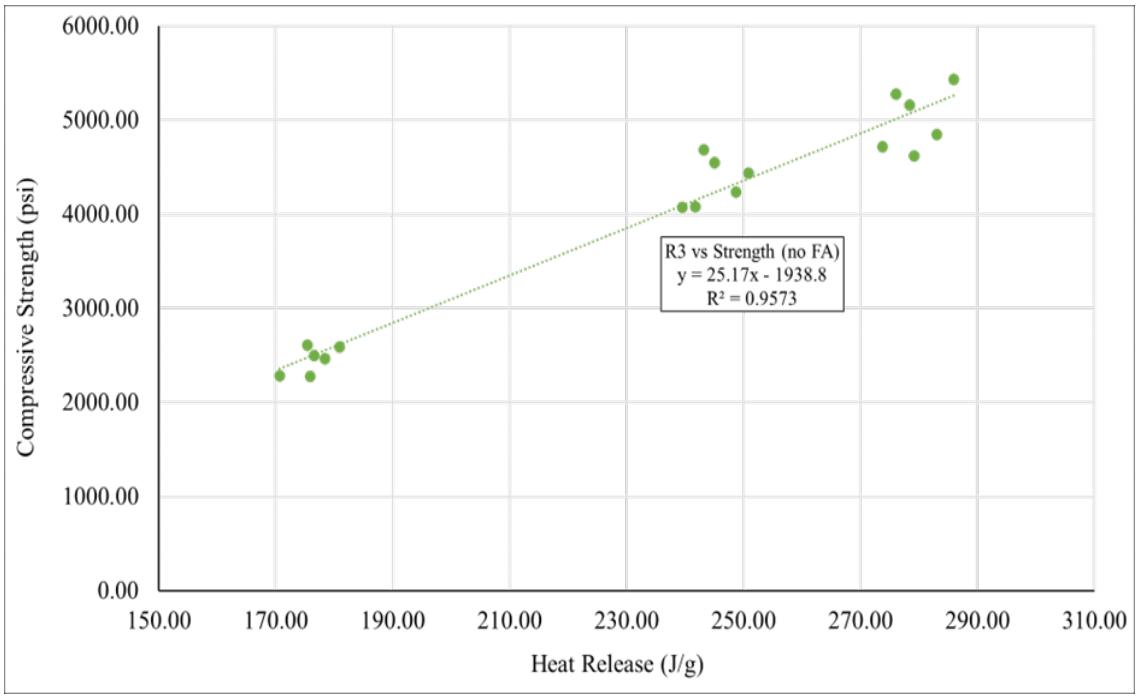

Figure 7- 13 Correlation between Compressive Strength and R^3 without FA

7.3.5 Strength Activity Index

Figure 7- 14 shows the strength activity index (SAI) results, expressed as a percent of the Portland cement control. At 7 days, except NP 2 and RFA 1, the rest of the test materials had a strength activity index of approximately 85%. NP 2 indicated a greater value than other materials and was very close to that of control mixture at 99%. However, the strength activity index of RFA 1 was only 70%, lower than the requirement of ASTM C618 of 75%. At 28 days, apart from NP 1, the other SCMs showed a significant increase in SAI compared to the corresponding value at 7 days, especially RFA 2, which increased from 85% to 112%. The pozzolanic reaction is the predominant reason for the relative increase in the strength activity index at this age [45]–[47]. The 28-day SAI of NP 3, 4, and 5 increased by around 10% from 7-day, reaching around 95%. However, NP 1's 28-day SAI stayed constant at 86%.

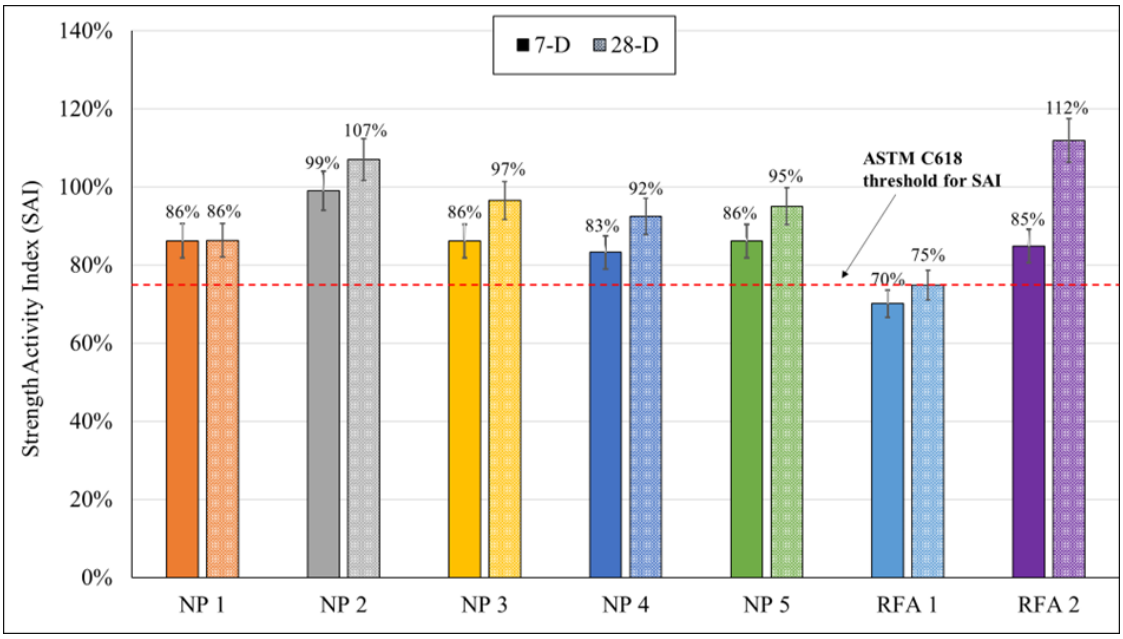

Figure 7- 14 High-Alkali SCMs Strength Activity Index Results (SAI)

7.3.6 Ultrasonic pulse velocity test (UPV)

Figure 7- 15 and Figure 7- 16 illustrate UPV speed curves and final speed at 24 hours. According to the results, the control speed was 2623 m/s, and it was only higher than RFA 2, which was 2414.4 m/s. This can be explained by the filler effect of fine SCMs, which can increase the number of nucleation sites in the matrix and further accelerate the hydration rate [11]. RFA 2 still indicated a slow hydration rate at an early age, consistent with previous results in automatic setting time and isothermal calorimetry. For the rest of the materials, NP 2, NP 3, NP5, and NP 6 were above 2750 m/s, and NP 5 had the highest value of 2787.5 m/s. Additionally, NP 1 and NP 4 were at the same level, and RFA 1 had the same speed as the control.

From the results, two RFAs did not perform consistently with NPs, and both two RFAs had relatively low values compared to NPs. The same findings were found in the automatic setting time. Furthermore, the filler effect was not proportional to the size distribution of SCMs. For example, NP 2 was coarser than the other materials shown in Figure 7- 1, but it still indicated a

high speed. Also, NP 4 was one of the finest SCMs, but its speed was the lowest among NPs and only higher than two RFAs. Therefore, based on the results, the filler effect of materials evaluated in this study was more impacted by the chemical nature than their particle size distribution.

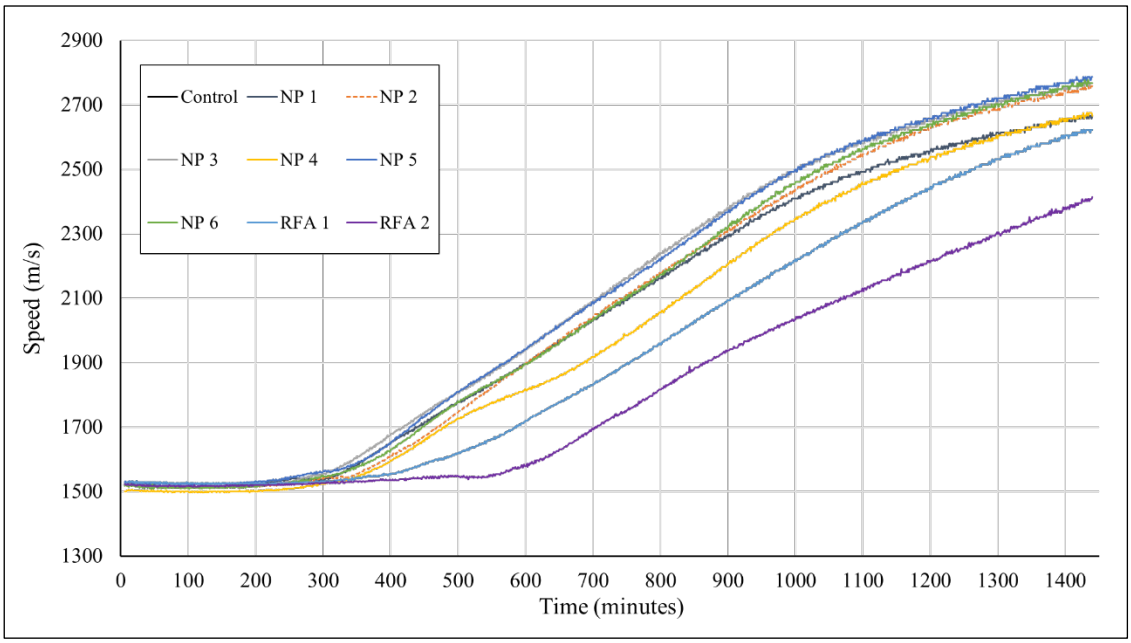

Figure 7- 15 UPV Results

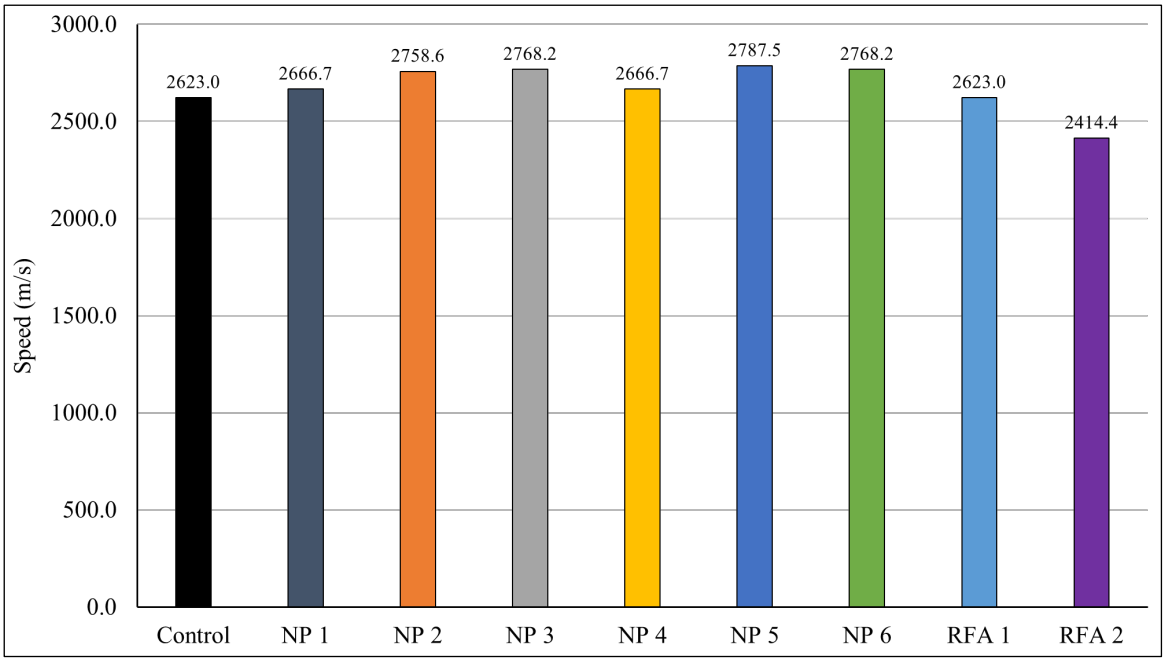

Figure 7- 16 1-D UPV Speed

7.3.7 Thermogravimetric Analysis (TGA) for Degree of Hydration

Table 7- 3 illustrates the relative weight loss of the samples as determined in the TGA study. According to the raw data, the mass loss associated with the dehydration temperature range (Ldh) increased with the aging of the samples, indicating a higher production of calcium silicate hydrate (C-S-H) within the matrix. However, it's worth noting that different materials exhibited varying behaviors. For instance, materials like NP 4 and NP 5 entered a plateau phase in mass loss within the Ldh range between 28 days and 56 days. In contrast, some materials, such as RFA 1 and RFA 2, continued to exhibit an increasing trend in mass loss during this period.

At an early age, especially at one day age, most test materials had higher amounts of C-S-H contrasted to the control, which indicated that the filler effect of SCMs accelerated the cement hydration process. Furthermore, the control's mass loss in Ldh was 11.200% at 56 days, and all materials were very close compared to the control. However, if considering the dilution effect by SCMs, C-S-H of control was lower than the matrix blended with SCMs. All groups' value was

above 8.960%, which was 80% of control. These results indicated that the pozzolanic reaction occurred in the matrix caused by high-alkali SCMs, which produced more C-S-H.

The mass loss in dehydroxylation (Ldx) represents the cementitious-based matrix's calcium hydroxide (CH) amount. Control had the highest value at 4.844% because it was 100% pure cement. After calibrating the value by cement dilution factor, the value was 3.875%, lower than most SCMs mixes. Considering the occurrence of pozzolanic reaction, this finding was not reasonable and probably caused by the temperature ranges selected. In all methods using TGA to assess degree hydration, the selected temperature ranges of the hydration phase with chemical change were very wide. The broad temperature ranges encompassed not only the intended phase for evaluation but also included other hydration phases. For instance, in the paper summarized by Collier[48], cement hydration phases like $Mg(OH)_2$ and $Ca_3Al_2O_6$ $CaSO_4 12H_2O$ also potentially undergo chemical phase change within the temperature range of 400°C and 600°C. The paper also indicated that CH decomposed only at the temperature range of 450°C to 500°C, which was much narrower than the temperature range selected in this study. As for the temperature range of decarbonation (Ldc), the values of all samples fluctuated within a certain range.

Table 7- 4 exhibits the degree of hydration (α) calculated by three different methods. In the Bhatty method, all groups' degrees of hydration increased with time, representing that hydration was still going on at 56 days. Additionally, except for RFA 2, the control's α was higher than the rest of the materials at 56 days, whose value was 71.7%. In contrast, excluding RFA 2, other SCMs' α was centered around 66%. Compared to other SCMs, RFA 2 had a slow start, consistent with the previous experiments' results. After that, RFA 2 showed a significantly high rate of hydration, and its 3-day hydration rate was 0.582 and only second to the control.

First of all, α calculated by Pane and Monteagudo kept the same increase tendency, but the difference between the control and SCMs groups was much closer than the distinction in the Bhatty. In addition, compared to the Bhatty method, the results conducted by the methods of Pane and Monteagudo exhibit higher values. For example, the control's α in the Pane and Mounteaudo was around 50% on day one, but the corresponding value in Pane was only 37.1%. Furthermore, some groups' values on day 56 were over 100%, which was unreasonable. Deboucha et al. [23] explained this finding. Firstly, the lack of a sufficient number of samples could lead to errors in the model. Secondly, the sample's maximum measuring age was not old enough to fit the model. The paper conducted by Pane et al. [49] discovered that the ultimate chemically bound water with a 0.45 water-to-binder ratio was very close to 0.23 after 200 days of water curing. Nevertheless, the oldest sample age in this study was only 56 days, resulting in a chemically bound value relatively lower than its anticipated maximum.

According to α values in the three methods, high-alkali SCMs did not have a negative impact on the cement hydration performance. In comparison to the approaches of Pane and Monteagudo, Bhatty's α value was found to be more fitting in this study. The sample age was not old enough to simulate an accurate ultimate chemically bound water value, which caused errors in the fitting model.

Additionally, other correlations between TGA data and other experiment results were also conducted in this study. Figure 7- 17 indicates the correlation between compressive strength in SAI test and their corresponding Ldx weight loss, representing the amount of C-S-H gel in the samples. The two results indicated a proportional correlation, and their R^2 was 0.695. Also, the study evaluated the potential relationship between equivalent alkali content (Na_2O_{eq}) and degree of α, shown in Figure 7- 18. In this analysis, the α was selected from the 56-day Bhatty method,

and the results showed that the alkali content of SCMs was not the factor that impact the α, because their R^2 was less than 0.5, which was very low.

Table 7- 3 Mass Loss Value in TGA

		Mass Loss Percentage (%)		
Group	**Age**	**Ldh (105-400°C)**	**Ldx (400-600°C)**	**Ldc (600-1000°C)**
Control	1-D	4.934	2.880	2.680
	3-D	8.677	4.163	3.390
	7-D	9.734	4.301	2.375
	28-D	11.420	4.748	3.893
	56-D	11.200	4.844	2.834
NP 1	1-D	4.321	2.588	2.438
	3-D	7.811	3.396	2.927
	7-D	8.900	3.602	3.258
	28-D	9.828	3.784	2.819
	56-D	10.610	3.890	2.770
NP 2	1-D	5.421	2.876	2.207
	3-D	7.896	3.714	2.318
	7-D	8.591	3.843	2.355
	28-D	10.120	3.940	2.458
	56-D	10.910	4.087	2.913
NP 3	1-D	6.243	2.748	2.710
	3-D	8.748	3.498	2.457
	7-D	9.569	3.611	2.321
	28-D	12.660	3.681	2.206
	56-D	12.220	3.649	2.307
NP 4	1-D	5.751	2.887	2.500
	3-D	7.611	3.685	2.968
	7-D	8.963	3.795	2.635
	28-D	11.110	3.779	2.529
	56-D	11.100	3.711	2.843

	1-D	5.458	2.919	2.248
	3-D	7.694	3.688	2.728
NP 5	7-D	9.588	3.921	2.496
	28-D	11.210	3.838	2.406
	56-D	11.080	3.899	3.461
	1-D	5.352	2.928	2.563
	3-D	7.232	3.695	2.574
NP 6	7-D	9.263	3.542	2.946
	28-D	10.390	3.839	2.841
	56-D	11.180	3.640	2.532
	1-D	4.110	2.411	2.025
	3-D	7.592	3.479	2.418
RFA 1	7-D	8.694	3.635	2.251
	28-D	10.260	3.808	2.454
	56-D	11.120	3.925	2.424
	1-D	4.481	2.106	2.309
	3-D	9.474	3.528	2.367
RFA 2	7-D	10.780	3.674	2.473
	28-D	11.470	3.739	2.434
	56-D	12.350	3.903	3.359

Table 7- 4 Degree of hydration Based on TGA

		Bhatty		Pane					Monteagudo			
Group	**Age**	WB	α	WB	WB∞	τ	a	α	WB	WB∞	K	α
	1-D	0.089	0.371	0.089				0.501	0.089			0.500
	3-D	0.142	0.593	0.142				0.799	0.142			0.799
Control	7-D	0.150	0.625	0.150	0.178	15.530	0.881	0.843	0.150	0.178	22.610	0.843
	28-D	0.178	0.740	0.178				0.998	0.178			0.997
	56-D	0.172	0.717	0.172				0.967	0.172			0.966
	1-D	0.079	0.330	0.079				0.509	0.079			0.505
	3-D	0.124	0.517	0.124				0.798	0.124			0.792
NP 1	7-D	0.138	0.577	0.138	0.156	15.680	0.939	0.890	0.138	0.157	22.050	0.883
	28-D	0.148	0.615	0.148				0.950	0.148			0.942
	56-D	0.156	0.651	0.156				1.006	0.156			0.998
	1-D	0.092	0.383	0.092				0.534	0.092			0.587
	3-D	0.126	0.523	0.126				0.729	0.126			0.802
NP 2	7-D	0.134	0.558	0.134	0.172	9.063	0.504	0.778	0.134	0.157	17.950	0.855
	28-D	0.151	0.628	0.151				0.875	0.151			0.962
	56-D	0.162	0.675	0.162				0.940	0.162			1.033
	1-D	0.101	0.421	0.101				0.531	0.101			0.598
	3-D	0.133	0.552	0.133				0.697	0.133			0.785
NP 3	7-D	0.141	0.589	0.141	0.190	8.694	0.455	0.743	0.141	0.169	18.050	0.837
	28-D	0.172	0.719	0.172				0.907	0.172			1.022
	56-D	0.168	0.701	0.168				0.884	0.168			0.996
	1-D	0.097	0.403	0.097				0.555	0.097			0.606
	3-D	0.125	0.521	0.125				0.719	0.125			0.785
NP 4	7-D	0.138	0.577	0.138	0.174	8.531	0.513	0.795	0.138	0.159	17.220	0.868
	28-D	0.159	0.664	0.159				0.915	0.159			0.999
	56-D	0.160	0.666	0.160				0.918	0.160			1.002
	1-D	0.093	0.387	0.093				0.538	0.093			0.566
	3-D	0.125	0.521	0.125				0.723	0.125			0.761
NP 5	7-D	0.145	0.606	0.145	0.173	11.360	0.630	0.841	0.145	0.164	19.820	0.885
	28-D	0.160	0.668	0.160				0.927	0.160			0.976
	56-D	0.164	0.683	0.164				0.948	0.164			0.998
NP 6	1-D	0.093	0.389	0.093	0.170	9.611	0.549	0.549	0.093	0.158	18.380	0.592

	3-D	0.120	0.499	0.120				0.705	0.120			0.761
	7-D	0.140	0.584	0.140				0.825	0.140			0.890
	28-D	0.154	0.641	0.154				0.906	0.154			0.977
	56-D	0.159	0.661	0.159				0.933	0.159			1.007
	1-D	0.074	0.306	0.074				0.451	0.074			0.461
	3-D	0.121	0.503	0.121				0.740	0.121			0.756
RFA 1	7-D	0.133	0.552	0.133	0.163	17.290	0.757	0.813	0.133	0.160	27.140	0.830
	28-D	0.151	0.628	0.151				0.924	0.151			0.944
	56-D	0.160	0.668	0.160				0.983	0.160			1.005
	1-D	0.075	0.314	0.075				0.441	0.075			0.425
	3-D	0.140	0.582	0.140				0.818	0.140			0.789
RFA 2	7-D	0.155	0.644	0.155	0.171	20.080	1.182	0.906	0.155	0.177	26.820	0.873
	28-D	0.162	0.675	0.162				0.949	0.162			0.915
	56-D	0.176	0.735	0.176				1.032	0.176			0.995

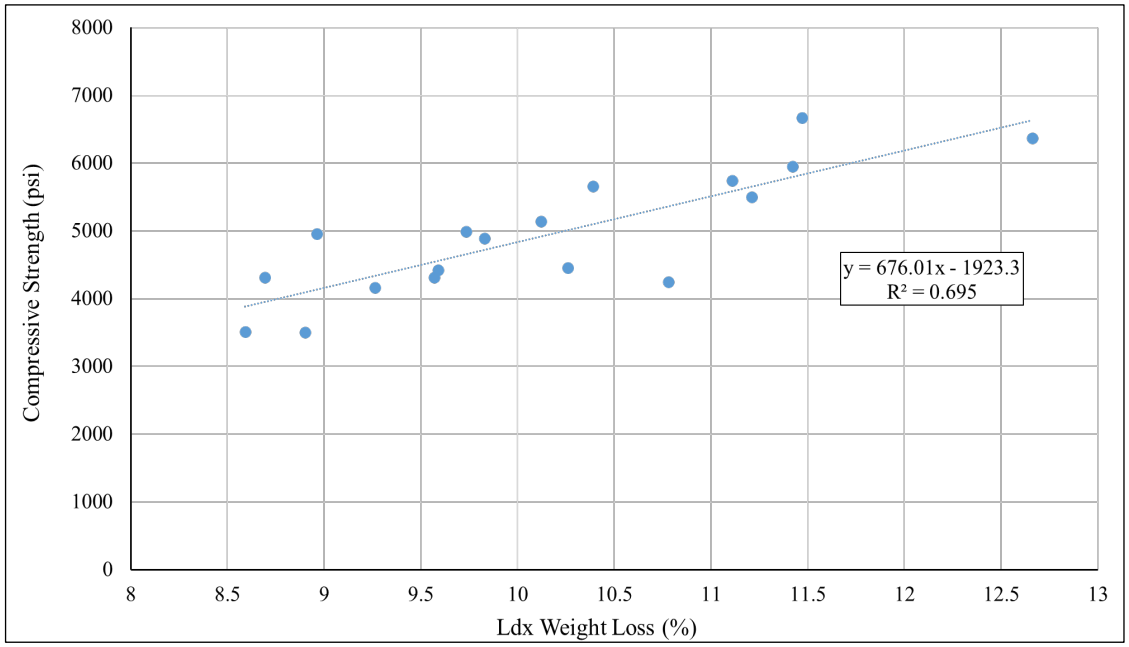

Figure 7- 17 Correlation between Compressive Strength vs Ldx Weight Loss

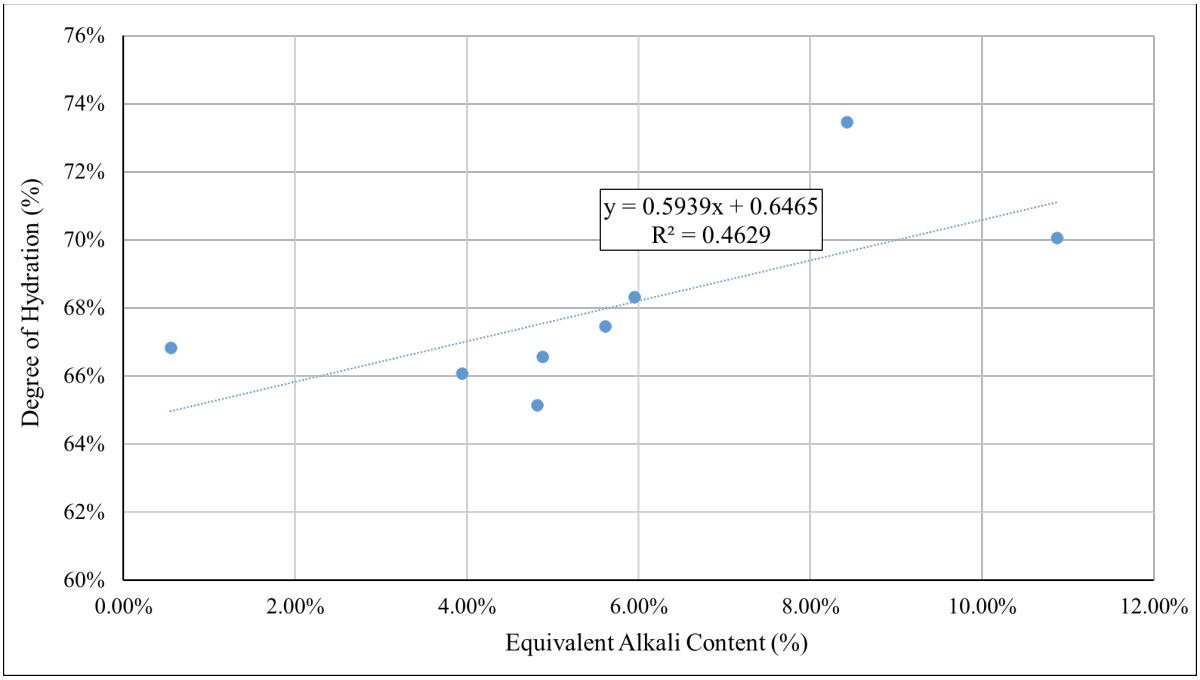

Figure 7- 18 Correlation between Equivalent Alkali Content (Na_2O_{eq}) vs Degree of Hydration (α)

7.4. Conclusion

This study commenced by assessing the viability of employing high-alkali SCMs, such as natural pozzolans and reclaimed fly ash, as potential alternatives to alleviate ASR expansion. Subsequently, various experiments were conducted to evaluate these high-alkali SCMs' influence on the cement-based matrix's hydration performance, which evaluated these materials comprehensively.

In the ASR mitigation test, all the materials effectively promoted the concrete mitigation performance on ASR, which indicated the potential of these materials as alternative SCMs used in the concrete industry. The water demand was influenced by factors beyond just the LOI content and particle size of the SCMs; other parameters also played a significant role. Even though NP 1 did not have the highest LOI content or the smallest particle size, it still required a minimum of 10% additional water to achieve the desired flow characteristics. In the automatic vicat setting time test, NPs behaved differently compared to the RFAs. The addition of NPs in the matrix accelerated or maintained a similar level of setting time as the control, but RFAs significantly retarded the setting time, especially RFA2. All tested SCMs indicated a pronounced filler effect in the various experiments, reflected in the accelerated hydration reaction rate. According to the UPV results, except RFA 2, the other regimes with SCMs possessed a higher speed than the control, which indicated a high degree of hydration of the matrix. This tendency can be explained by the heat release measured by isothermal calorimetry. The released heat and UPV indicated a good correlation.

Based on the TGA data, this study used three well-established methods to estimate the degree of hydration, which investigated the potential impact of high-alkali SCMs on the cementitious-based matrix's hydration process. All high-alkali SCMs possessed no adverse impact on the

hydration process. While there were slight variations in the results due to differences in calculation methods, the overarching trend remained consistent across all methods: all SCMs actively participated in the pozzolanic reaction within the matrix, leading to a continuous increase in the degree of hydration. Compared to the methods of Pane and Monteagudo, the result conducted by the method of Bhatty was more reasonable because the sample age in this study was not old enough to simulate very accurate model.

From the overall perspective of this study, high-alkali SCMs indicated the potential to be used as alternative SCMs for the concrete industry.

7.5. Reference

[1] T. R. Naik, “Sustainability of Concrete Construction,” *Practice Periodical on Structural Design and Construction*, vol. 13, no. 2, pp. 98–103, May 2008, doi: 10.1061/(ASCE)1084-0680(2008)13:2(98).

[2] “Concrete needs to lose its colossal carbon footprint,” *Nature*, vol. 597, no. 7878, pp. 593–594, Sep. 2021, doi: 10.1038/d41586-021-02612-5.

[3] “Global CO2 emissions rebounded to their highest level in history in 2021 - News,” IEA. Accessed: Sep. 04, 2022. [Online]. Available: https://www.iea.org/news/global-co2-emissions-rebounded-to-their-highest-level-in-history-in-2021

[4] V. G. Papadakis, S. Antiohos, and S. Tsimas, “Supplementary cementing materials in concrete: Part II: A fundamental estimation of the efficiency factor,” *Cement and Concrete Research*, vol. 32, no. 10, pp. 1533–1538, Oct. 2002, doi: 10.1016/S0008-8846(02)00829-3.

[5] S. A. Miller, “Supplementary cementitious materials to mitigate greenhouse gas emissions from concrete: can there be too much of a good thing?,” *Journal of Cleaner Production*, vol. 178, pp. 587–598, Mar. 2018, doi: 10.1016/j.jclepro.2018.01.008.

[6] E. Menéndez, M. Á. Sanjuán, R. García-Roves, C. Argiz, and H. Recino, “Sustainable and Durable Performance of Pozzolanic Additions to Prevent Alkali-Silica Reaction (ASR) Promoted by Aggregates with Different Reaction Rates,” *Applied Sciences*, vol. 10, no. 24, Art. no. 24, Jan. 2020, doi: 10.3390/app10249042.

[7] P. Mehta, “Concrete technology for sustainable development–an overview of essential elements,” *Concrete technology for a sustainable development in the 21st century*, vol. 86, 2000.

[8] D. Wang, C. Shi, N. Farzadnia, Z. Shi, H. Jia, and Z. Ou, "A review on use of limestone powder in cement-based materials: Mechanism, hydration and microstructures," *Construction and Building Materials*, vol. 181, pp. 659–672, Aug. 2018, doi: 10.1016/j.conbuildmat.2018.06.075.

[9] G. Medjigbodo, E. Rozière, K. Charrier, L. Izoret, and A. Loukili, "Hydration, shrinkage, and durability of ternary binders containing Portland cement, limestone filler and metakaolin," *Construction and Building Materials*, vol. 183, pp. 114–126, Sep. 2018, doi: 10.1016/j.conbuildmat.2018.06.138.

[10] G. D. Moon, S. Oh, S. H. Jung, and Y. C. Choi, "Effects of the fineness of limestone powder and cement on the hydration and strength development of PLC concrete," *Construction and Building Materials*, vol. 135, pp. 129–136, Mar. 2017, doi: 10.1016/j.conbuildmat.2016.12.189.

[11] J. J. Thomas, H. M. Jennings, and J. J. Chen, "Influence of Nucleation Seeding on the Hydration Mechanisms of Tricalcium Silicate and Cement," *J. Phys. Chem. C*, vol. 113, no. 11, pp. 4327–4334, Mar. 2009, doi: 10.1021/jp809811w.

[12] J. Stark, B. Möser, and F. Bellmann, "Nucleation and growth of C-S-H phases on mineral admixtures," in *Advances in Construction Materials 2007*, C. U. Grosse, Ed., Berlin, Heidelberg: Springer, 2007, pp. 531–538. doi: 10.1007/978-3-540-72448-3_54.

[13] P. K. Mehta and P. J. Monteiro, *Concrete: microstructure, properties, and materials*. McGraw-Hill Education, 2014.

[14] A. A. Ramezanianpour, S. M. Motahari Karein, P. Vosoughi, A. Pilvar, S. Isapour, and F. Moodi, "Effects of calcined perlite powder as a SCM on the strength and permeability of concrete," *Construction and Building Materials*, vol. 66, pp. 222–228, Sep. 2014, doi: 10.1016/j.conbuildmat.2014.05.086.

[15] O. Kayali and M. Sharfuddin Ahmed, “Assessment of high volume replacement fly ash concrete – Concept of performance index,” *Construction and Building Materials*, vol. 39, pp. 71–76, Feb. 2013, doi: 10.1016/j.conbuildmat.2012.05.009.

[16] W. Sun, H. Yan, and B. Zhan, “Analysis of mechanism on water-reducing effect of fine ground slag, high-calcium fly ash, and low-calcium fly ash,” *Cement and Concrete Research*, vol. 33, no. 8, pp. 1119–1125, Aug. 2003, doi: 10.1016/S0008-8846(03)00022-X.

[17] L. L. Sutter, “Supplementary Cementitious Materials-Best Practices for Concrete Pavements:[techbrief],” *Supplementary Cementitious Materials-Best Practices for Concrete Pavements:[techbrief]*, no. Journal Article, 2016.

[18] M. Thomas, *Optimizing the use of fly ash in concrete*, vol. 5420. Portland Cement Association Skokie, IL, 2007.

[19] J. C. Hower *et al.*, “Coal-derived unburned carbons in fly ash: A review,” *International Journal of Coal Geology*, vol. 179, pp. 11–27, Jun. 2017, doi: 10.1016/j.coal.2017.05.007.

[20] Z. D. Rong, W. Sun, H. J. Xiao, and W. Wang, “Effect of silica fume and fly ash on hydration and microstructure evolution of cement based composites at low water–binder ratios,” *Construction and Building Materials*, vol. 51, pp. 446–450, Jan. 2014, doi: 10.1016/j.conbuildmat.2013.11.023.

[21] C. Ni, Q. Wu, Z. Yu, and X. Shen, “Hydration of Portland cement paste mixed with densified silica fume: From the point of view of fineness,” *Construction and Building Materials*, vol. 272, p. 121906, Feb. 2021, doi: 10.1016/j.conbuildmat.2020.121906.

[22] G. De Schutter, “Hydration and temperature development of concrete made with blast-furnace slag cement,” *Cement and Concrete Research*, vol. 29, no. 1, pp. 143–149, Jan. 1999, doi: 10.1016/S0008-8846(98)00229-4.

[23] W. Deboucha, N. Leklou, A. Khelidj, and M. N. Oudjit, “Hydration development of mineral additives blended cement using thermogravimetric analysis (TGA): Methodology of calculating the degree of hydration,” *Construction and Building Materials*, vol. 146, pp. 687–701, Aug. 2017, doi: 10.1016/j.conbuildmat.2017.04.132.

[24] J. I. Bhatty, “Hydration versus strength in a portland cement developed from domestic mineral wastes — a comparative study,” *Thermochimica Acta*, vol. 106, pp. 93–103, Sep. 1986, doi: 10.1016/0040-6031(86)85120-6.

[25] J. I. Bhatty, “Hydration versus strength in a portland cement developed from domestic mineral wastes — a comparative study,” *Thermochimica Acta*, vol. 106, pp. 93–103, Sep. 1986, doi: 10.1016/0040-6031(86)85120-6.

[26] I. Pane and W. Hansen, “Investigation of blended cement hydration by isothermal calorimetry and thermal analysis,” *Cement and Concrete Research*, vol. 35, no. 6, pp. 1155–1164, Jun. 2005, doi: 10.1016/j.cemconres.2004.10.027.

[27] S. M. Monteagudo, A. Moragues, J. C. Gálvez, M. J. Casati, and E. Reyes, “The degree of hydration assessment of blended cement pastes by differential thermal and thermogravimetric analysis. Morphological evolution of the solid phases,” *Thermochimica Acta*, vol. 592, pp. 37–51, Sep. 2014, doi: 10.1016/j.tca.2014.08.008.

[28] G. Hong, S. Oh, S. Choi, W.-J. Chin, Y.-J. Kim, and C. Song, “Correlation between the Compressive Strength and Ultrasonic Pulse Velocity of Cement Mortars Blended with Silica Fume: An Analysis of Microstructure and Hydration Kinetics,” *Materials*, vol. 14, no. 10, Art. no. 10, Jan. 2021, doi: 10.3390/ma14102476.

[29] S. A. Abo-Qudais, “Effect of concrete mixing parameters on propagation of ultrasonic waves,” *Construction and Building Materials*, vol. 19, no. 4, pp. 257–263, May 2005, doi: 10.1016/j.conbuildmat.2004.07.022.

[30] A. Ashrafian, M. J. Taheri Amiri, M. Rezaie-Balf, T. Ozbakkaloglu, and O. Lotfi-Omran, “Prediction of compressive strength and ultrasonic pulse velocity of fiber reinforced concrete incorporating nano silica using heuristic regression methods,” *Construction and Building Materials*, vol. 190, pp. 479–494, Nov. 2018, doi: 10.1016/j.conbuildmat.2018.09.047.

[31] T. M. Research, “Fly Ash Market is Expected to be Valued at US$ 13.8 Bn by 2031, States TMR Study,” GlobeNewswire News Room. Accessed: May 05, 2022. [Online]. Available: https://www.globenewswire.com/en/news-release/2022/04/05/2416875/0/en/Fly-Ash-Market-is-Expected-to-be-Valued-at-US-13-8-Bn-by-2031-States-TMR-Study.html

[32] M. C. G. Juenger, R. Snellings, and S. A. Bernal, “Supplementary cementitious materials: New sources, characterization, and performance insights,” *Cement and Concrete Research*, vol. 122, pp. 257–273, Aug. 2019, doi: 10.1016/j.cemconres.2019.05.008.

[33] M. H. Shehata and M. D. A. Thomas, “Alkali release characteristics of blended cements,” *Cement and Concrete Research*, vol. 36, no. 6, pp. 1166–1175, Jun. 2006, doi: 10.1016/j.cemconres.2006.02.015.

[34] P. K. Mehta, “Natural pozzolans: Supplementary cementing materials,” in *Proc., Int. Symp. on Advances in Concrete Technology*, CANMET, Athens, Greece, 1987, pp. 407–430.

[35] R. E. Rodríguez-Camacho and R. Uribe-Afif, “Importance of using the natural pozzolans on concrete durability,” *Cement and Concrete Research*, vol. 32, no. 12, pp. 1851–1858, Dec. 2002, doi: 10.1016/S0008-8846(01)00714-1.

[36] C09 Committee, “ASTM C618-22 Specification for Coal Fly Ash and Raw or Calcined Natural Pozzolan for Use in Concrete,” ASTM International. doi: 10.1520/C0618-22.

[37] “AASHTO T380 Standard Method of Test for Potential Alkali Reactivity of Aggregates and Effectiveness of ASR Mitigation Measures (Miniature Concrete Prism Test, MCPT),” American Association of State HIghway and Transportation Officials.

[38] C09 Committee, “ASTM C311-22 Test Methods for Sampling and Testing Fly Ash or Natural Pozzolans for Use in Portland-Cement Concrete,” ASTM International. doi: 10.1520/C0311_C0311M-22.

[39] C01 Committee, “ASTM C191-21 Test Methods for Time of Setting of Hydraulic Cement by Vicat Needle,” ASTM International. doi: 10.1520/C0191-21.

[40] C09 Committee, “ASTM C1897-20 Standard Test Methods for Measuring the Reactivity of Supplementary Cementitious Materials by Isothermal Calorimetry and Bound Water Measurements,” ASTM International. [Online]. Available: https://www.astm.org/c1897-20.html

[41] J. R. Deschamps and J. L. Flippen-Anderson, “Crystallography,” in *Encyclopedia of Physical Science and Technology (Third Edition)*, R. A. Meyers, Ed., New York: Academic Press, 2002, pp. 121–153. doi: 10.1016/B0-12-227410-5/00160-5.

[42] L. Turanli, B. Uzal, and F. Bektas, “Effect of large amounts of natural pozzolan addition on properties of blended cements,” *Cement and Concrete Research*, vol. 35, no. 6, pp. 1106–1111, Jun. 2005, doi: 10.1016/j.cemconres.2004.07.022.

[43] B. Uzal, “7 - Properties of concrete with high-volume pozzolans,” in *Eco-Efficient Concrete*, F. Pacheco-Torgal, S. Jalali, J. Labrincha, and V. M. John, Eds., in Woodhead Publishing Series in Civil and Structural Engineering. , Woodhead Publishing, 2013, pp. 138–152. doi: 10.1533/9780857098993.2.138.

[44] R. D. Kalina, S. Al-Shmaisani, R. D. Ferron, and M. C. Juenger, “False positives in ASTM C618 specifications for natural pozzolans,” *ACI Materials Journal*, vol. 116, no. 1, pp. 165–172, 2019.

[45] S. A. Saad, M. F. Nuruddin, N. Shafiq, and M. Ali, “Pozzolanic Reaction Mechanism of Rice Husk Ash in Concrete – A Review,” *Applied Mechanics and Materials*, vol. 773–774, pp. 1143–1147, 2015, doi: 10.4028/www.scientific.net/AMM.773-774.1143.

[46] A. Tironi, M. A. Trezza, A. N. Scian, and E. F. Irassar, “Assessment of pozzolanic activity of different calcined clays,” *Cement and Concrete Composites*, vol. 37, pp. 319–327, Mar. 2013, doi: 10.1016/j.cemconcomp.2013.01.002.

[47] H. Myadraboina, S. Setunge, and I. Patnaikuni, “Pozzolanic Index and lime requirement of low calcium fly ashes in high volume fly ash mortar,” *Construction and Building Materials*, vol. 131, pp. 690–695, Jan. 2017, doi: 10.1016/j.conbuildmat.2016.11.038.

[48] N. C. Collier, “Transition and decomposition temperatures of cement phases–a collection of thermal analysis data,” *Ceramics-Silikaty*, vol. 60, no. 4, 2016.

[49] I. Pane and W. Hansen, “Investigation of blended cement hydration by isothermal calorimetry and thermal analysis,” *Cement and Concrete Research*, vol. 35, no. 6, pp. 1155–1164, Jun. 2005, doi: 10.1016/j.cemconres.2004.10.027.

CHAPTER VIII – USE OF AASHTO T380 (MCPT) AS AN EVALUATION TOOL FOR CONCRETE JOB MIXTURES

8.1. Introduction

The objective of this study is to explore more industrial possibilities for using AASHTO T380 (MCPT). In the field of concrete job mix, constrained by the limitations of experimental resources, the availability of local construction materials, the timeline of the construction project, and other potential reasons, the contractor cannot comprehensively evaluate their mix proportion on mitigating alkali-silica reaction (ASR). Within the existing classic methods for evaluating ASR mitigation, ASTM C1567 is a time-efficient method (14 days), but its accuracy is questionable. Another typical method, ASTM C1293, is more accurate, but its experimental duration is too long, lasting two years. Therefore, contrasted to the previous two methods, MCPT holds better prospects because it is more precise than ASTM C1567 and more efficient than ASTM C1293.

This section focuses on using MCPT to predict job mix concrete's performance on ASR mitigation. The concrete mixing parameters evaluated in this study included alkali loading in concrete, concrete's water-to-binder ratio, and the amount of supplementary cementitious materials (SCMs) in the concrete. The study initially indicated the single variable's impact on ASR expansion, then compared with other parameters and shown as expansion reduction%.

8.2. Materials and Method

8.2.1 Materials

A high-alkali Type I Portland cement (Na_2O_e = 1.00%) from Lehigh Hanson Inc was used in this study. The reactive aggregate used in this study is a known reactive aggregate from the Goldhill Quarry in North Carolina, which consists of reactive metatuff–argillite. The aggregate's specific gravity and percent absorptions were 2.6 and 1%, respectively.

Table 8- 1 Materials Chemical Composition

		SiO_2	Al_2O_3	Fe_2O_3	S+Al+Fe	CaO	MgO	Na_2O	K_2O	Na_2O_e	LOI	SG	Amorphous Level (%)
	High-alkali cement	19.00	4.99	2.11	26.1	62.45	2.84	0.31	1.05	1.0	NA	3.15	NA
Volcanic rhyolitic tephra	NP	71.95	12.26	1.50	85.71	0.93	0.39	3.9	4.0	6.51	4.88	2.35	87.76

8.2.2 AASHTO T380 Miniature Concrete Prism Test (MCPT) [2]

In this method, the cementitious materials content of concrete mixtures was maintained at 420 kg/m^3, with a w/b ratio of 0.45. The dry mass of coarse aggregate per unit volume of concrete was maintained at 0.65, and the coarse aggregates' gradation followed the recommended gradation per AASHTO T380. The fineness modulus of fine aggregates conformed to 2.60 ± 0.3. In this study, only for boosted groups, reagent-grade NaOH pellets were dissolved in the mixing water to boost the alkali content of concrete to 1.25% by the mass of cement. Additionally, NP 4 was selected in this research as an SCMs additive, and its replacement levels were 20% and 30% by cement mass, respectively.

The test specimens were cast and cured at ambient temperature and 100% RH for 24 hours. After demolding, the specimens were placed in water at 60°C for another 24 hours. The zero-day

reading was taken at the end of 24 hours of water bath curing. Then, the specimens were transferred into a sealed container with different concentrations of NaOH solution to let the soak solution have the same alkali ions concentration and pH in the concrete pore solution, which helped prevent ions leakage from the concrete and simulate all groups under equivalent conditions. The concentration was calculated by the equation (1) and (2)

$$Na_2O_{eq} = Na_2O + 0.658 \times K_2O \quad (1)$$

$$(OH^-) = \frac{0.339 \times Na_2O_{eq}\%}{(\frac{w}{c})} + 0.022 \pm 0.06\, mol/L \quad (2)$$

Where Na_2O_{eq} is the equivalent alkali content in the cement, and w/c is the water-to-cement ratio. In this equation, for the w/c, only the mass of the cement was considered, and the mass of other cementitious materials was not accounted. For example, the water-to-cementitious ratio of concrete with 20% SCMs replacement levels was 0.45. However, its water-to-cement ratio was 0.56, which was used for calculating the concentration of the soak solution. The concentration of soak solution used in this study is shown in Table 8- 2.

The prism length changes were recorded periodically at 0, 3, 7, 10, 14, 21, 28, 42, 56, 70, and 84 days. The criteria for evaluating the efficacy of SCMs in mitigating ASR in the MCPT method at 56-days are as follows per AASHTO T380:

16. Expansion < 0.020% - Effective ASR Mitigation;
17. 0.020% < expansion < 0.025% Uncertain ASR Mitigation
18. Expansion > 0.025% Not effective ASR mitigation

If the samples exhibit expansion between 0.20 and 0.25 at 56 days, the average expansion between 56-day to 84-day (8 weeks to 12 weeks), should be less than 0.010% per 2 weeks for the

mitigation measure to be considered effective. Additionally, the test groups' ASR expansion reduction level compared to the control was calculated by following equation (3):

$$Reduction\% = \frac{\left(Sample_{Corresponding\ age} - Control_{Corresponding\ age}\right)}{Control_{Corresponding\ age}} \times 100\% \quad (3)$$

Table 8- 2 Soak Solution Concentration

N0.	Label	Set (OH-) (mol/L)	Calculated (OH-) (mol/L)	Cement Na_2O_{eq}%	w/c	Alkali Loading (lb/yd^3)
1	Control boosted	1	0.96	1.25	0.45	8.85
2	Control unboosted 0.45 w/c	0.85	0.78	1	0.45	7.08
3	0.35 w/c boosted	1.05	0.99	1	0.35	7.08
4	0.55 w/c boosted	0.7	0.64	1	0.55	7.08
5	20% NP boosted	0.7	0.63	1.25	0.56	7.08
6	20% NP No unboosted	1	0.63	1	0.56	5.66
7	30% NP boosted	0.6	0.55	1.25	0.64	6.19
8	30% NP unboosted	1	0.55	1	0.64	4.96

w/c = water/cement, not cementitious

8.3. Results and Discussion

All groups' length change curve is shown in Figure 8- 1. There were eight groups conducted in this study. Control boosted was the group following the mix proportions in the MCPT, and control no boosted 0.45 w/c was the group following MCPT mix proportions but without adding boosted alkali content. 0.35 and 0.55 w/c were two groups with different w/c against MCPT standard mix proportion and without adding boosted alkali content. 20% NP boosted and 20% NP

no boosted are two groups mixed with 20% NP 4 with and without adding boosted alkali content, which was the same meaning as 30% NP boosted and 30% NP no boosted.

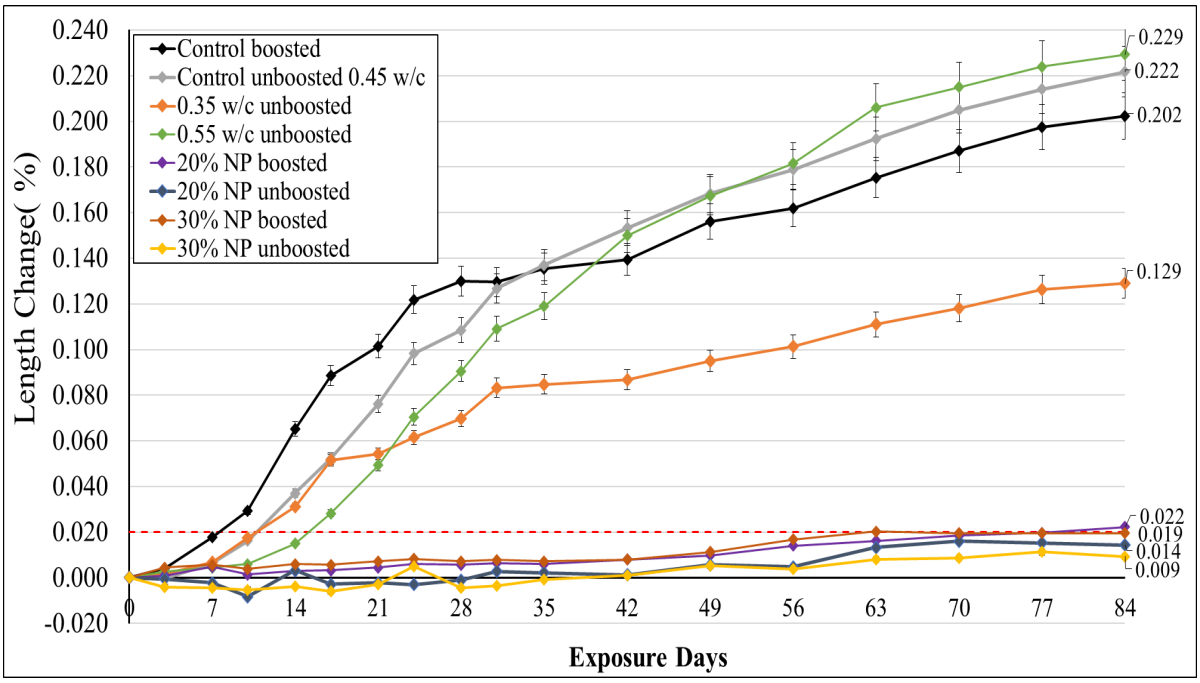

Figure 8- 1 Jod Design Results

8.3.1 Impact of Water-to-Binder Ratio

In order to assess the influence of ratio on the test specimen in MCPT, three different w/c ratios, 0.35, 0.45, and 0.55, were prepared in this study, and their results are shown in Figure 8- 2. Additionally, the control boosted was also shown in the section. The soak solution's concentrations were 1, 0.85, 1.05, and 0.7 N, which followed Figure 8- 2's legend order.

Firstly, all the groups failed in this analysis, and the 0.55 w/c group had the highest ASR expansion at the final measurement, 0.229% at 84 days. However, 0.55 w/c did not have the highest expansion all the time. In the initial two weeks, 0.35 w/c had higher expansion values and expansion rates than 0.55 w/c. Starting from week two, 0.35 w/c's expansion rate became slow and maintained a slower growth rate than 0.45 and 0.55 w/c consistently until the experiment's

conclusion. The 84-day expansion value of 0.35 w/c was 0.129%, 56.3% of 0.55 w/c. As for the 0.45 w/c group, its final value was 0.222% and very close to 0.55 w/c.

According to the results, it was clear that the lowering w/c ratio in the design helped lower the concrete ASR expansion. However, it was insufficient to control ASR expansion below the 0.020% threshold limit in MCPT. Additionally, the relationship between w/c and ASR expansion was not linearly proportional. Even though in this study, the ASR expansion increased with the w/c ratio increased, the difference between the two w/c ranges of 0.35 to 0.45 and 0.45 to 0.55 was not equal, which were 0.093% and 0.007%, respectively. These results indicated that after reaching a certain threshold, increasing the concrete's w/c ratio would not significantly impact the ASR expansion. Furthermore, the soak solution's concentration did not play a dominant role in the experiment. For example, the soak solution concentration of 0.35 w/c was 1.05 N, and 0.55 w/c was 0.7 N, but 0.35 w/c's ASR expansion was still much lower than 0.55 w/c.

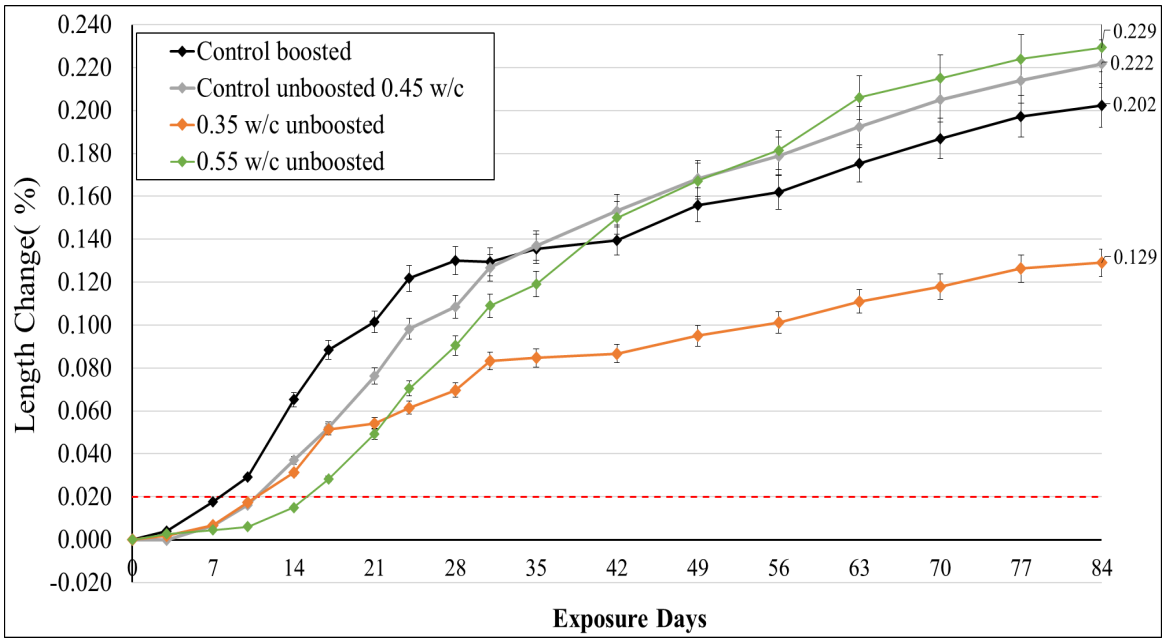

Figure 8- 2 Impact of Water-to-Binder Ratio

8.3.2 Impact of Adding Natural Pozzolans

In order to assess the influence of adding various amounts of natural pozzolans on test specimens in MCPT, two replacement levels of natural pozzolans were conducted in this study: 20% and 30%, respectively. The results for this section are shown in Figure 8- 3.

Compared to the decreasing w/c ratio shown in Figure 8- 2, blending with natural pozzolans was much more effective in mitigating ASR expansion. During the experimental duration, two groups containing natural pozzolans successfully controlled ASR expansion below the 0.020% threshold limit, and their values were 0.014% and 0.009%, respectively. Unlike control groups expanding immediately from the test beginning, two natural pozzolans did not appear in apparent expansion until 42 days. Additionally, even though 30% NP no boosted had a smaller value than 20%, the improvement was not noticeable, only a 0.005% difference. The potential reason for this was that 20% was sufficient for this reactive aggregate in MCPT. Therefore, adding more natural pozzolans to the concrete was not helpful to have further improvements.

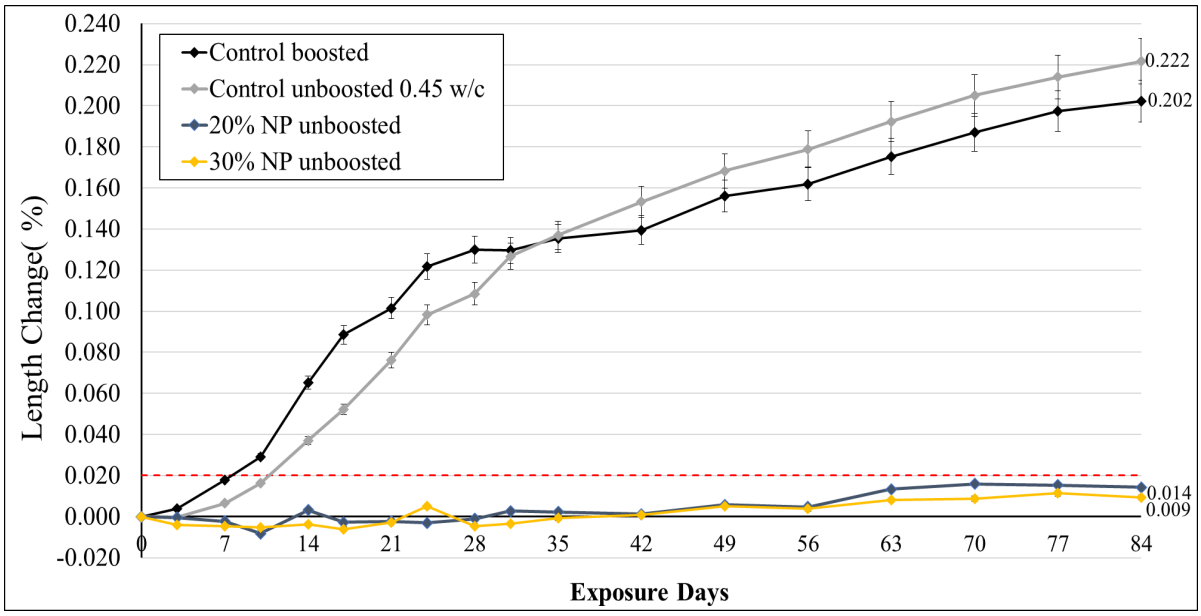

Figure 8- 3 Impact of Adding Natural Pozzolans (Unboosted)

Figure 8- 4 indicates the correlation between SCMs replacement level and ASR expansion reduction level. The data shown in this figure was obtained from previous MCPT SCMs replacement level studies. One NP and one reclaimed fly ash (RFA) were selected for this figure. The results showed that increasing the amount of SCMs in the concrete significantly improved concrete's ASR mitigation performance, especially RFA.

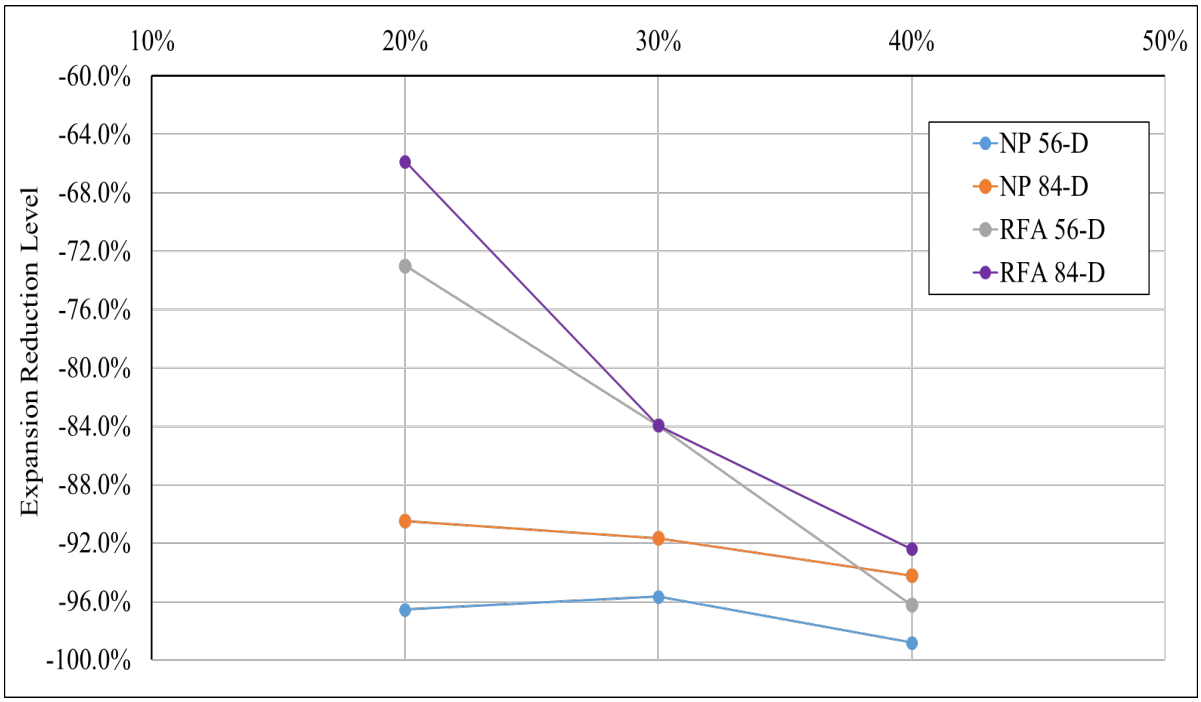

Figure 8- 4 Replacement Level vs Expansion Reduction

8.3.3 Impact of Boosting Alkali Level of Mixture on ASR Expansion

This section investigates the impact of alkali boosted on concrete ASR expansion, and results are shown in Figure 8- 5. This section shows three comparison groups: control, 20% NP, and 30% NP. 20% and 30% NP boosted were higher than their non-boosted groups. However, the control exhibited a different behavior. Even though the control boosted indicated a higher rate than non-boosted at the initial four weeks, its ultimate was lower than the non-boosted. The difference value of the control comparison was 0.02, 10% of control boosted, which was insignificant. Therefore, the two groups were considered to have the same ASR expansion level. Additionally, boosted alkali content in the concrete played the role of accelerating the ASR process at the initial time but not the determined factor for the final value.

As for the NP compassions, boosted alkali accelerated the ASR process and increased their ultimate ASR expansion values. NP 20% boosted was 0.022% at 84 days, and it was higher than its non-boosted by 0.008. Even though this difference was smaller than control, if it is converted

proportionally, its value reached 36.4%, which was much higher than control's 10%. Additionally, for NP 30%, this reduction percentage was 35.7%.

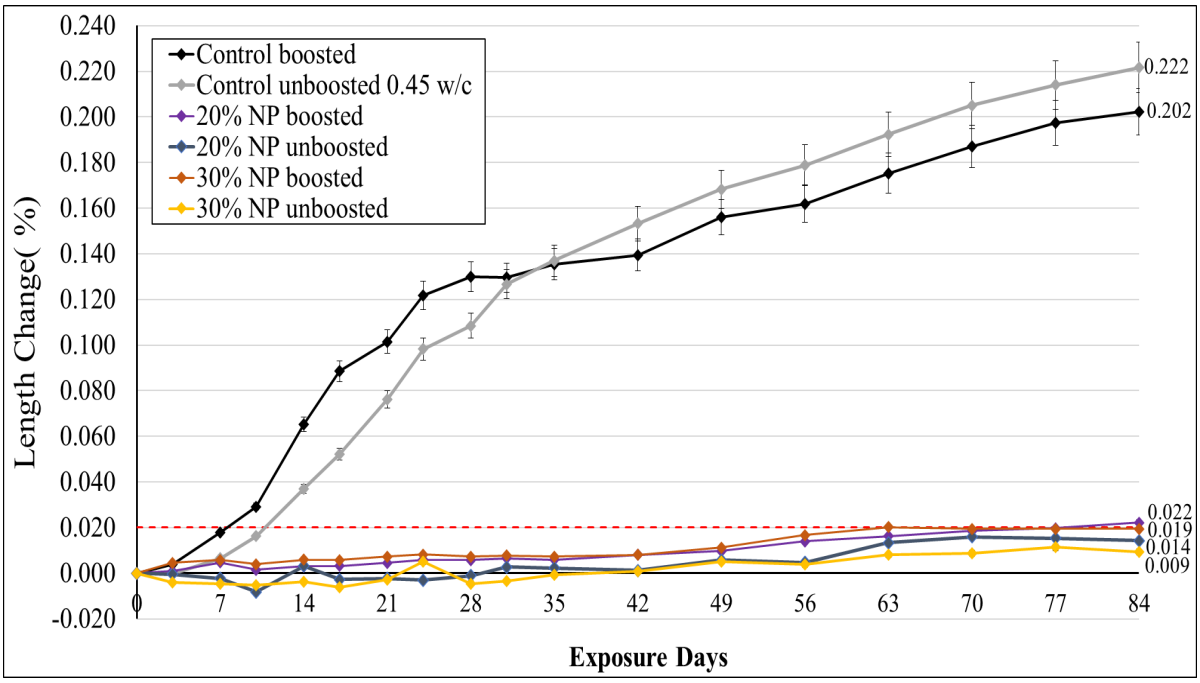

Figure 8- 5 Impact of Whether Boosted

8.3.4 Job Design Reduction Level

Figure 8- 6 indicates all test groups' ASR expansion reduction levels compared to the control boosted. In this figure, four time points' reduction levels were selected for comparison, which were 7-day, 28-day, 56-day, and 84-day, respectively. The reduction level is characterized by both positive and negative values. Positive values signify the percentage of test specimens with ASR expansion lower than that of the control boosted, while negative values indicate the percentage of specimens with ASR expansion higher than that of the control boosted.

At the 7-day mark, all specimens except for the two NP non-boosted groups exhibited a concentration of expansion levels between 60% and 75% compared to the control boosted. However, differences gradually became evident between the 7-day and 28-day periods. During this time, the percentage of groups without SCM blending declined, whereas the groups incorporating

SCMs began to increase. For example, the control no boosted's reduction level was 63.4% at 7 days but dropped to 16.5% at 28 days. Also, 20% and 30% NP non-boosted groups were around 70% at 7 days, and the percentage raised to 90% at 28 days.

For the period between 28 and 56 days, SCM groups did not appear to change during the interval, but non-SCM groups continued to decrease. Control no boosted w/c and 0.55 w.c no boosted dropped from 16.5% and 30.4% to -10.3% and -12.0%, respectively. As for 0.35 w/c, it also decreased, but the extent was not as significant as the other two groups. Additionally, none of the groups' reduction levels exhibited evident change for the time interval from 56 days to 84 days. The values at 84 days remained relatively consistent with those at 56 days.

According to the results, a relative ASR expansion of SCMs groups compared to those without SCMs entered a stable phase earlier. SCMs boosted groups showed slightly larger results compared to the non-boosted groups. Due to NP used in this study was effective in mitigating ASR at a 20% dosage level, there was no apparent difference between 20% and 30% SCMs replacement levels. For non-SCM groups, their ASR reaction process was relatively slower because of no boosted alkali in concrete compared to the control boosted. However, sufficient alkali ions were in the soak solution, and they were ingressed into concrete and involved in the reaction. Therefore, adding the boosted alkali pellets did not impact these groups' ultimate ASR expansion values, and it only relatively delayed the ASR process.

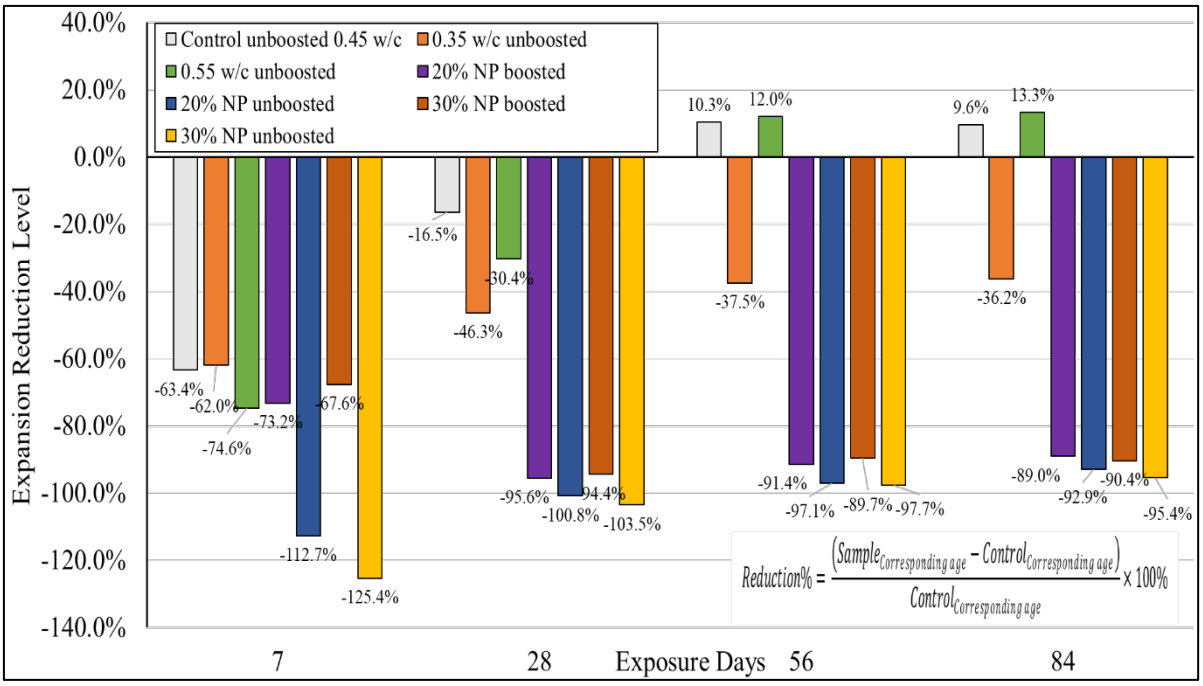

Figure 8- 6. Job Design Reduction Level

8.4. CONCLUSION

Based on the studies conducted on the job concrete mixtures, the following conclusions are drawn:

1. The results indicated that decreasing the w/c ratio helped to decrease ASR expansion. In this study, 0.35 w/c concrete apparently had a lower ASR expansion than the 0.45 w/c and 0.55 w/c. Even though ASR expansion increased with the rise in the w/c ratio, the two parameters did not have a proportional relationship. Additionally, compared to utilizing SCMs to mitigate ASR, lowering w/c was not sufficient to suppress the ASR expansion. In this study, the 84-day expansion of 0.35 w/c, the lowest w/c evaluated, was 0.129%, which far surpassed the threshold of 0.020%.
2. Blending SCMs in concrete was the most effective approach to mitigating ASR expansion. Two NP replacement levels lower the ASR expansion compared to the control by 90%. Additionally, in this study, 30% of NP did not have evident improvement compared to the

20%, which indicated that when materials were sufficient to suppress the ASR, increasing the replacement level would not improve further.

3. Adding boosted alkali did not impact the control's ultimate expansion value compared to non-boosted but accelerated the ASR process. In this study, control boosted had a lower final expansion than non-boosted, but it had a very early age expansion. A similar phenomenon was observed in the NP boosted comparison.
4. For the group blending with NP, boosted alkali accelerated ASR reaction at an early age. In the reduction level results, at 7 days, the NP boosted groups had lower reduction levels than their non-boosted, and then their reduction level entered a stable phase. From 28 days to 84 days, their reduction level did not indicate a significant change. However, groups without NP and boosted alkali had a relatively extended change period. They have apparent change until 56 days.
5. Based on the results shown in this study, MCPT had the potential to predict concrete job design because their results effectively indicated how different strategies impact ASR mitigation. For example, lowering the w/c ratio is a knowledge-based approach to decrease ASR expansion, but this study indicates that lowering the w/c partially mitigates the expansion to some extent, but achieving highly effective control of expansion remains challenging to experiment thoroughly, especially when compared to utilizing SCMs.

8.5 Reference

[1] “ASTM C1260-21 Standard Test Method for Potential Alkali Reactivity of Aggregates (Mortar-Bar Method).pdf.”

[2] “AASHTO T380 Standard Method of Test for Potential Alkali Reactivity of Aggregates and Effectiveness of ASR Mitigation Measures (Miniature Concrete Prism Test, MCPT),” American Association of State HIghway and Transportation Officials.

CHAPTER IX CONCLUSIONS

Based on the extensive studies in this investigation, the following summary comments and conclusions are drawn:

High-alkali SCMs improve concrete's ASR mitigation performance. In various ASR evaluation experiments, ASTM C1567 (AMBT), ASTM C1293 (CPT), and AASHTO T380 (MCPT), high-alkali SCMs effectively lower ASR expansion, but different test methods yielded different mitigation efficiencies. In AMBT, 20% replacement of high-alkali SCMs effectively controlled the length change of mortar bars below the threshold limit of 0.10% at 14 days. However, all mixtures failed to pass the CPT test. Even though the duration of CPT was two years, the majority of the test specimens exceeded the 0.040% limit within less than a year. Also, in the MCPT method, the majority of the mixtures failed to suppress the ASR expansion below 0.025% at 56 days, which was the threshold limit for this test method. In the replacement level test of ASR evaluation, the results indicated that when the SCMs replacement level was increased to a sufficient level, i.e., 30% by mass replacement of cement and above, they could effectively control the ASR expansion in all the test methods, and their performance significantly improved compared to the 20% dosage level.

The pore solution analysis from cementitious paste specimens showed that high-alkali SCMs lowered the alkali concentration in the pore solution compared to that of the control mixture. However, there was no correlation between the amount of alkali content of the SCMs and the alkali ions in the pore solution. It was observed that some of the SCMs with lower alkali content contributed more alkali ions in the pore solution compared to some of the SCMs with higher alkali content. These results indicated that not all the alkalis present in SCMs were released into the solution. For example, RFA 1's alkali content was not the highest, but its ASR mitigation

performance was the most inferior in all three ASR evaluation test methods, and its alkali concentration in the pore solution was the highest among all SCMs.

In order to evaluate the pozzolanic reactivity of high-alkali SCMs and to elucidate the variations in their effectiveness in mitigating ASR, a series of experiments were conducted. Firstly, the study evaluated the correlation between the amorphous content of SCMs and their ASR mitigation performance, and the results indicated that the amorphous level of high-alkali SCMs did not directly correlate with their pozzolanic reactivity. For example, NP3 was a highly crystalline material but still showed good pozzolanic reactivity and ASR mitigation performance. ASTM C 311 strength activity index (SAI) did not show a good correlation with high-alkali SCMs ASR mitigation performance. Similarly, the pozzolanic reactivity of high-alkali SCMs, as measured using the heat of hydration in ASTM C1897 R^3 test, did not correlate well with the ASR mitigation performance of high-alkali SCMs. The potential reason for this inconsistency was likely due to the fact that the R^3 test was conducted at a high-alkali and higher-temperature environment, which increased the reactivity of SCMs. In the R^3 test, RFA 1 released the highest heat, which meant it was supposed to be the most reactive SCM, while its performance was the most inferior in the ASR mitigation and SAI tests. Findings from the TGA and pore solution analysis studies supported the expansion observed in the MCPT tests. The results of the two methods indicated "excellent" correlations with the ASR mitigation performance of high-alkali SCMs. Compared to other pozzolanic reactivity experiments, data from the TGA and pore solution analysis experiments were more persuasive in predicting high-alkali SCMs' ASR mitigation performance.

According to the results obtained from these pozzolanic reactivity experiments, not all SCMs can be treated equally. Natural pozzolans and industrial by-products, such as fly ashes, must be analyzed independently for their ability to mitigate ASR. When considering all high-alkali SCMs

(i.e., natural pozzolans and reclaimed fly ashes), the coefficient of correlation (R^2 values) values between the MCPT expansion and the TGA weight loss, and the total alkali ion content results were 0.936 and 0.864, respectively. However, the R^2 values significantly improved to 0.9726 and 0.9674, respectively, when considering only natural pozzolans were considered.

Not only did high-alkali SCMs improve concrete's ASR mitigation performance, but they also promoted other durability properties. ASTM C1012 was conducted to evaluate the sulfate attack resistance of mortar bars cooperating with high-alkali SCMs. Compared to the control, the high-alkali SCMs effectively decreased the sulfate expansion by over 90% in the one-year test. The order of performance of SCMs in the sulfate resistance tests was consistent with the order of their performance in ASR evaluation. For instance, RFA 1 indicated the weakest ability to control both ASR and sulfate attack expansion. Additionally, results from the TGA results supported the performance in the sulfate resistance study, i.e., the more CH content in the cementitious matrix, the higher expansion induced by sulfate attack. Additionally, the influence of high-alkali SCMs on mortar bar drying shrinkage, evaluated by ASTM C596, was found to be negligible. Including the control, the difference between maximum and minimum drying shrinkage values was only 0.013%.

In addition, the use of high-alkali SCMs in the concrete also decreased the concrete permeability to chloride ion ingress. In ASTM C1202 chloride permeability test (RCPT), the amount of charge passing through decreased with the addition of high-alkali SCMs in concrete. Also, the performance of SCMs in the RCPT correlated well with the performance of SCMs in the ASR mitigation and sulfate resistance studies. The correlation coefficient and R^2 values between RCPT and MCPT ASR expansion and RCPT and sulfate resistance were over 0.99 in both cases. These correlations exhibited that decreasing the concrete permeability was another reason for improving concrete resistance to ASR and sulfate attack. The use of high-alkali SCMs delayed

the gain in bulk electrical resistivity compared to the control samples. However, with time, the bulk resistivity of the matrix containing SCMs exceeded the control. In comparison, the control entered a resistivity plateau at an early age and finally reached a low ultimate value. For the groups cooperating with SCMs, their resistivity values were at least 200% of the control and still indicated the tendency to rise at the final measurement. Also, bulk electrical resistivity was very consistent with RCPT results.

The impact of high-alkali SCMs on the hydration performance of cementitious-based matrix was also analyzed in this study. In the ASTM C311 water demand test, the water demand was influenced by factors beyond just the LOI content and particle size of the SCMs. Even though NP 1 did not have a high LOI content or the smallest particle size, it required a minimum of 10% additional water to achieve the desired flow characteristics. NPs and RFAs behaved significantly differently in setting time tests. The addition of NPs in the matrix accelerated or maintained a similar level of setting time as the control, but RFAs retarded the setting time significantly, especially RFA 2.

Some SCMs indicated a filler effect and accelerated hydration reaction rate at an early age, which was supported by TGA and UPV tests. According to the UPV results, except RFA 2, the other SCMs resulted in a higher pulse velocity than the control, which indicated a high degree of hydration and denser microstructure within the matrix. Also, in the TGA study, mixtures with SCMs had higher relative CH content than control. However, this result was inconsistent with data obtained from isothermal calorimetry. With the same mixing proportion, the control released much more heat than the test groups within 7 days. This inconsistency showed that the higher ultrasonic pulse velocity in mixtures with SCMs may be caused by the physical effect of SCMs rather than their chemical influence. Additionally, heat release in isothermal calorimetry studies also indicated

a significant correlation with corresponding compressive strength. Among these SCMs, RFA 2 had a slow start in pozzolanic reaction compared to other materials, as shown in various tests, including Vicat setting time, UPV, and TGA.

Based on the analysis of the data from this study, it is concluded that high-alkali SCMs could be effective alternative SCMs for use in the concrete industry. The reasons are the following:

1. The primary concern previously was that alkalies from the high-alkali SCMs could be released into concrete pore solution and thus excebrating the ASR. However, in this study, these SCMs effectively lowered the ASR expansion and improved ASR mitigation. Additionally, pore solution analysis indicated that not all alkali content is released into the pore solution, and the extent of alkali ions in the pore solution depends on the materials themselves. Low-alkali content SCMs could release more alkali ions into pore solutions than materials with high-alkali content.
2. High-alkali SCMs also improved other concrete durability, such as sulfate resistance, permeability, and bulk electrical resistivity. Therefore, from the durability perspective, these materials satisfied the requirements.

In addition, some misconceptions were discovered in this study:

1. High pozzolanic reactivity based on the ASTM C1897 test did not correlate well with excellent performance in consuming CH in the concrete or promotion of the durability performance of concrete.
2. Not all SCMs behave similarly, and therefore, they should be evaluated depending on the nature of the material. In this study, even though natural pozzolans and reclaimed fly ash were both SCMs, their reactivity and performance in durability studies were not similar.

In the end, there are some suggestions for using high-alkali SCMs in concrete: using appropriate methods to evaluate high-alkali SCMs is very significant. In this study, simply utilizing the alkali content of SCMs to assess their alkali content readily available in concrete pore solution and ASR mitigation performance was proved to be insufficient. TGA and pore solution tests are more representative compared to the other material characterization test methods in evaluating the performance of SCMs in ASR mitigation. Based on the test results, the available alkali content and physical properties of SCMs really depend on each individual material. Different materials have different formation processes; therefore, they have different phase content and reactivity. Therefore, the physical properties and chemical composition of SCMs can be the reference but not the primary basis for evaluating SCMs' pozzolanic reactivity. Compared to these natural properties, TGA and pore solution methods directly quantify the parameters that impact deleterious chemical reactions; therefore, their results reflect these materials' characteristics more directly and accurately.

APPENDIX

Table A- 1 Laser Diffraction Results

Size	NP 1	RFA 1	NP 2	NP 3	NP 4	NP 5	NP 6	RFA 2
2500	100	100	100	100	100	100	100	100
2219.551	100	100	100	100	100	100	100	100
1970.562	100	100	100	100	100	100	100	100
1749.505	100	100	100	100	100	100	100	100
1553.246	100	100	100	100	100	100	100	100
1379.004	100	100	100	100	100	100	100	100
1224.308	100	100	100	100	100	100	100	100
1086.965	100	100	100	100	100	100	100	100
965.0298	100	100	100	100	100	100	100	100
856.7731	100	100	100	100	100	100	100	100
760.6606	100	100	100	100	100	100	100	100
675.3299	100	100	100	100	100	100	100	100
599.5716	100	100	100	100	100	100	100	100

0.603526	0.064791	0.864086	0.002288	0.260877	0.141403	0.100854	0.308849	0.474391
0.535823	0.011598	0.451009	0	0.11197	0.033174	0.020692	0.127002	0.22109
0.475715	0.002554	0.186862	0	0.040567	0.008912	0.005298	0.042867	0.084391
0.422349	0	0.0592	0	0.007984	0	0	0.005698	0.020975
0.37497	0	0.01442	0	0.002617	0	0	0.00158	0.005619
0.332906	0	0	0	0	0	0	0	0
0.295561	0	0	0	0	0	0	0	0

Table A- 2 ASTM C1260

					Specimen 1	Specimen 2	Specimen 3	Specimen 4
description	cast date	reading date	Age of specimen, days	reference bar reading	Reading	Reading	Reading	Reading
100% Reactive Sand+ Regular Cement	Wednesday, October 28, 2020	Thursday, October 29, 2020	1	Demold, label, and place in a 23 water container, then place in 60C oven for 24 hrs				
		Friday, October 30, 2020	0	0.0196	0.2464	0.2886	0.2307	0.2974
		Monday, November 2, 2020	3	0.0197	0.2509	0.2914	0.2333	0.3005
		Wednesday, November 4, 2020	5	0.0199	0.2639	0.3035	0.2455	0.3139
		Thursday, November 5, 2020	6	0.0197	0.2712	0.3110	0.2533	0.3205
		Sunday, November 8, 2020	9	0.0198	0.2851	0.3253	0.2684	0.3356
		Monday, November 9, 2020	10	0.0188	0.2873	0.3279	0.2710	0.3381
		Tuesday, November 10, 2020	11	0.0188	0.2898	0.3305	0.2736	0.3407
		Friday, November 13, 2020	14	0.0186	0.2924	0.3332	0.2762	0.3435
		Friday, November 20, 2020	21	0.0189	0.3162	0.3567	0.3006	0.3669
		Monday, November 23, 2020	24	0.0187	0.3225	0.3630	0.3074	0.3734
		Friday, November 27, 2020	28	0.0183	0.3297	0.3707	0.3156	0.3734
		Friday, December 4, 2020	35	0.0191	0.3408	0.3822	0.3276	0.3922
		Friday, December 11, 2020	42	0.0184	0.3466	0.3893	0.3351	0.3989
		Friday, December 18, 2020	49	0.0207	0.3535	0.3970	0.3426	0.4066
		Friday, December 25, 2020	56	0.0191	0.3540	0.3980	0.3432	0.4075

Table A- 3 ASTM C1567---Control

					Specimen 1	Specimen 2	Specimen 3	Specimen 4
specimen label	cast date	reading date	Age of specimen, days	reference bar reading	Reading	Reading	Reading	Reading
Control	Wednesday, November 11, 2020	Thursday, November 12, 2020	1	Demold, label, and place in a 23 water container, then place in 80C oven for 24 hrs				
		Friday, November 13, 2020	0	0.0187	0.2783	0.2730	0.2969	0.2737
		Monday, November 16, 2020	3	0.0189	0.2821	0.2770	0.3004	0.2776
		Friday, November 20, 2020	7	0.0187	0.3131	0.3060	0.3247	0.3012
		Monday, November 23, 2020	10	0.0185	0.3239	0.3147	0.3344	0.3098
		Friday, November 27, 2020	14	0.0183	0.3325	0.3229	0.3427	0.3179
		Tuesday, December 1, 2020	18	0.0188	0.3418	0.3303	0.3517	0.3262
		Friday, December 4, 2020	21	0.0187	0.3482	0.3382	0.3575	0.3312
		Monday, December 7, 2020	24	0.0185	0.3540	0.3439	0.3637	0.3363
		Friday, December 11, 2020	28	0.0183	0.3601	0.3490	0.3691	0.3416
		Monday, December 14, 2020	31	0.0188	0.3634	0.3522	0.3723	0.3447
		Friday, December 18, 2020	35	0.0206	0.3716	0.3591	0.3798	0.3517
		Monday, December 21, 2020	38	0.0202	0.3732	0.3614	0.3821	0.3534
		Friday, December 25, 2020	42	0.0209	0.3767	0.3655	0.3862	0.3575
		Wednesday, December 30, 2020	47	0.0211	0.3785	0.3674	0.3868	0.3584
		Monday, January 4, 2021	52	0.0209	0.3821	0.3709	0.3906	0.3618
		Friday, January 8, 2021	56	0.0215	0.3842	0.3729	0.3926	0.3838

Table A- 4 ASTM C1567---20% NP 1 + 80% Cement

NP1	Wednesday, November 11, 2020	Thursday, November 12, 2020	1	Demold, label, and place in a 23 water container, then place in 60C oven for 24 hrs				
		Friday, November 13, 2020	0	0.0187	0.2808	0.2679	0.2855	0.2896
		Monday, November 16, 2020	3	0.0190	0.2815	0.2688	0.2856	0.2897
		Friday, November 20, 2020	7	0.0188	0.2829	0.2704	0.2870	0.2918
		Monday, November 23, 2020	10	0.0187	0.2833	0.2713	0.2884	0.2926
		Friday, November 27, 2020	14	0.0185	0.2839	0.2715	0.2882	0.2926
		Tuesday, December 1, 2020	18	0.0190	0.2860	0.2736	0.2901	0.2943
		Friday, December 4, 2020	21	0.0189	0.2876	0.2748	0.2910	0.2950
		Monday, December 7, 2020	24	0.0190	0.2881	0.2763	0.2925	0.2960
		Friday, December 11, 2020	28	0.0184	0.2890	0.2771	0.2932	0.2966
		Monday, December 14, 2020	31	0.0187	0.2899	0.2782	0.2937	0.2978
		Friday, December 18, 2020	35	0.0208	0.2936	0.2828	0.2970	0.3017
		Monday, December 21, 2020	38	0.0203	0.2939	0.2831	0.2991	0.3020
		Friday, December 25, 2020	42	0.0209	0.2950	0.2850	0.2993	0.3035
		Wednesday, December 30, 2020	47	0.0212	0.2970	0.2863	0.3012	0.3039
		Monday, January 4, 2021	52	0.0210	0.2990	0.2883	0.3027	0.3056
		Friday, January 8, 2021	56	0.0216	0.3001	0.2896	0.3043	0.3069

Table A- 5 ASTM C1567---20% NP 2 + 80% Cement

NP 2	Wednesday, November 11, 2020	Thursday, November 12, 2020	1	Demold, label, and place in a 23 water container, then place in 60C oven for 24 hrs				
		Friday, November 13, 2020	0	0.0187	0.2945	0.3078	0.2922	0.3127
		Monday, November 16, 2020	3	0.0191	0.2953	0.3092	0.2930	0.3129
		Friday, November 20, 2020	7	0.0188	0.2965	0.3113	0.2947	0.3137
		Monday, November 23, 2020	10	0.0187	0.2972	0.3121	0.2957	0.3145
		Friday, November 27, 2020	14	0.0189	0.2976	0.3118	0.2955	0.3141
		Tuesday, December 1, 2020	18	0.0189	0.2993	0.3156	0.2972	0.3156
		Friday, December 4, 2020	21	0.0189	0.3007	0.3165	0.2984	0.3165
		Monday, December 7, 2020	24	0.0191	0.3015	0.3174	0.2988	0.3169
		Friday, December 11, 2020	28	0.0183	0.3020	0.3178	0.2991	0.3169
		Monday, December 14, 2020	31	0.0187	0.3031	0.3191	0.2999	0.3183
		Friday, December 18, 2020	35	0.0206	0.3063	0.3227	0.3032	0.3210
		Monday, December 21, 2020	38	0.0204	0.3068	0.3221	0.3033	0.3214
		Friday, December 25, 2020	42	0.0209	0.3078	0.3232	0.3042	0.3218
		Wednesday, December 30, 2020	47	0.0212	0.3089	0.3240	0.3050	0.3224
		Monday, January 4, 2021	52	0.0211	0.3101	0.3256	0.3061	0.3235
		Friday, January 8, 2021	56	0.0216	0.3118	0.3272	0.3076	0.3249

Table A- 6 ASTM C1567---20% NP 3 + 80% Cement

NP 3	Wednesday, November 11, 2020	Thursday, November 12, 2020	1	water container, then place in 60C oven for 24 hrs			
		Friday, November 13, 2020	0	0.0185	0.3269	0.3116	0.2857	0.2686
		Monday, November 16, 2020	3	0.0188	0.3277	0.3122	0.2865	0.2692
		Friday, November 20, 2020	7	0.0188	0.3292	0.3135	0.2870	0.2701
		Monday, November 23, 2020	10	0.0188	0.3300	0.3144	0.2872	0.2711
		Friday, November 27, 2020	14	0.0184	0.3299	0.3140	0.2869	0.2705
		Tuesday, December 1, 2020	18	0.0190	0.3317	0.3158	0.2884	0.2720
		Friday, December 4, 2020	21	0.0188	0.3316	0.3157	0.2885	0.2721
		Monday, December 7, 2020	24	0.0188	0.3320	0.3166	0.2888	0.2725
		Friday, December 11, 2020	28	0.0183	0.3334	0.3180	0.2903	0.2728
		Monday, December 14, 2020	31	0.0186	0.3346	0.3192	0.2901	0.2735
		Friday, December 18, 2020	35	0.0205	0.3385	0.3233	0.2936	0.2770
		Monday, December 21, 2020	38	0.0203	0.3392	0.3238	0.2939	0.2783
		Friday, December 25, 2020	42	0.0209	0.3418	0.3256	0.2959	0.2795
		Wednesday, December 30, 2020	47	0.0212	0.3419	0.3260	0.2960	0.2799
		Monday, January 4, 2021	52	0.0209	0.3441	0.3282	0.2982	0.2820
		Friday, January 8, 2021	56	0.0207	0.3451	0.3288	0.2984	0.2824

Table A- 7 ASTM C1567---20% NP 4 + 80% Cement

NP 4	Wednesday, November 11, 2020	Thursday, November 12, 2020	1	water container, then place in 60C oven for 24 hrs				
		Friday, November 13, 2020	0	0.0188	0.1993	0.2377	0.2527	0.2730
		Monday, November 16, 2020	3	0.0189	0.2000	0.2378	0.2536	0.2742
		Friday, November 20, 2020	7	0.0188	0.2005	0.2384	0.2542	0.2742
		Monday, November 23, 2020	10	0.0186	0.2010	0.2390	0.2546	0.2746
		Friday, November 27, 2020	14	0.0183	0.2007	0.2393	0.2554	0.2753
		Tuesday, December 1, 2020	18	0.0189	0.2022	0.2404	0.2565	0.2765
		Friday, December 4, 2020	21	0.0188	0.2023	0.2402	0.2564	0.2764
		Monday, December 7, 2020	24	0.0186	0.2030	0.2406	0.2571	0.2768
		Friday, December 11, 2020	28	0.0184	0.2036	0.2412	0.2574	0.2769
		Monday, December 14, 2020	31	0.0188	0.2045	0.2420	0.2583	0.2776
		Friday, December 18, 2020	35	0.0206	0.2074	0.2443	0.2611	0.2809
		Monday, December 21, 2020	38	0.0202	0.2081	0.2453	0.2625	0.2825
		Friday, December 25, 2020	42	0.0211	0.2099	0.2478	0.2652	0.2836
		Wednesday, December 30, 2020	47	0.0213	0.2105	0.2485	0.2666	0.2845
		Monday, January 4, 2021	52	0.0209	0.2126	0.2509	0.2690	0.2869
		Friday, January 8, 2021	56	0.0208	0.2134	0.2511	0.2692	0.2873

Table A- 8 ASTM C1567---20% NP 5 + 80% Cement

NP 5	Monday, November 16, 2020	Tuesday, November 17, 2020	1	water container, then place in 60C oven for 24 hrs				
		Wednesday, November 18, 2020	0	0.0190	0.2527	0.2401	0.3008	0.2913
		Saturday, November 21, 2020	3	0.0193	0.2530	0.2413	0.3016	0.2916
		Wednesday, November 25, 2020	7	0.0189	0.2523	0.2401	0.3003	0.2901
		Sunday, November 29, 2020	11	0.0189	0.2543	0.2423	0.3028	0.2924
		Wednesday, December 2, 2020	14	0.0190	0.2547	0.2426	0.3032	0.2926
		Sunday, December 6, 2020	18	0.0191	0.2548	0.2430	0.3036	0.2930
		Wednesday, December 9, 2020	21	0.0194	0.2567	0.2448	0.3055	0.2948
		Monday, December 14, 2020	26	0.0186	0.2560	0.2435	0.3041	0.2936
		Wednesday, December 16, 2020	28	0.0199	0.2593	0.2464	0.3075	0.2907
		Friday, December 18, 2020	30	0.0207	0.2595	0.2469	0.3083	0.2974
		Monday, December 21, 2020	33	0.0201	0.2605	0.2470	0.3086	0.2979
		Wednesday, December 23, 2020	35	0.0203	0.2618	0.2484	0.3104	0.2996
		Friday, December 25, 2020	37	0.0208	0.2630	0.2493	0.3110	0.3000
		Wednesday, December 30, 2020	42	0.0214	0.2643	0.2506	0.3112	0.3006
		Monday, January 4, 2021	47	0.0207	0.2648	0.2511	0.3121	0.3016
		Friday, January 8, 2021	51	0.0216	0.2671	0.2545	0.3157	0.3051
		Wednesday, January 13, 2021	56	0.0200	0.2646	0.2513	0.3127	0.3022

Table A- 9 ASTM C1567---20% NP 6 + 80% Cement

NP 6	Monday, November 16, 2020	Tuesday, November 17, 2020	1	water container, then place in 60C oven for 24 hrs			
		Wednesday, November 18, 2020	0	0.0189	0.2900	0.2633	0.3133	0.2907
		Saturday, November 21, 2020	3	0.0192	0.2917	0.2651	0.3147	0.2909
		Wednesday, November 25, 2020	7	0.0188	0.2923	0.2654	0.3140	0.2906
		Sunday, November 29, 2020	11	0.0188	0.2915	0.2648	0.3139	0.2896
		Wednesday, December 2, 2020	14	0.0190	0.2933	0.2662	0.3154	0.2908
		Sunday, December 6, 2020	18	0.0192	0.2936	0.2662	0.3152	0.2904
		Wednesday, December 9, 2020	21	0.0193	0.2942	0.2666	0.3158	0.2910
		Monday, December 14, 2020	26	0.0184	0.2952	0.2682	0.3177	0.2926
		Wednesday, December 16, 2020	28	0.0202	0.2955	0.2687	0.3185	0.2934
		Friday, December 18, 2020	30	0.0206	0.2963	0.2695	0.3185	0.2943
		Monday, December 21, 2020	33	0.0202	0.2970	0.2703	0.3197	0.2948
		Wednesday, December 23, 2020	35	0.0201	0.2968	0.2705	0.3198	0.2959
		Friday, December 25, 2020	37	0.0210	0.2974	0.2711	0.3209	0.2959
		Wednesday, December 30, 2020	42	0.0214	0.2988	0.2722	0.3219	0.2976
		Monday, January 4, 2021	47	0.0207	0.2975	0.2710	0.3203	0.2960
		Friday, January 8, 2021	51	0.0214	0.3002	0.2736	0.3234	0.2985
		Wednesday, January 13, 2021	56	0.0200	0.2982	0.2714	0.3210	0.2961

Table A- 10 ASTM C1567---20% RFA 1 + 80% Cement

RFA 1	Wednesday, November 11, 2020	Thursday, November 12, 2020	1	Demold, label, and place in a 23 water container, then place in 60C oven for 24 hrs			
		Friday, November 13, 2020	0	0.0184	0.2085	0.2611	0.2420	0.2795
		Monday, November 16, 2020	3	0.0189	0.2106	0.2629	0.2434	0.2806
		Friday, November 20, 2020	7	0.0187	0.2129	0.2657	0.2458	0.2839
		Monday, November 23, 2020	10	0.0187	0.2143	0.2675	0.2473	0.2861
		Friday, November 27, 2020	14	0.0184	0.2156	0.2692	0.2483	0.2876
		Tuesday, December 1, 2020	18	0.0188	0.2191	0.2728	0.2511	0.2910
		Friday, December 4, 2020	21	0.0186	0.2212	0.2745	0.2524	0.2929
		Monday, December 7, 2020	24	0.0186	0.2238	0.2775	0.2549	0.2958
		Friday, December 11, 2020	28	0.0182	0.2260	0.2796	0.2565	0.2980
		Monday, December 14, 2020	31	0.0187	0.2276	0.2813	0.2582	0.3004
		Friday, December 18, 2020	35	0.0207	0.2326	0.2855	0.2629	0.3055
		Monday, December 21, 2020	38	0.0202	0.2346	0.2878	0.2645	0.3075
		Friday, December 25, 2020	42	0.0210	0.2374	0.2912	0.2670	0.3112
		Wednesday, December 30, 2020	47	0.0212	0.2395	0.2935	0.2693	0.3145
		Monday, January 4, 2021	52	0.0209	0.2424	0.2960	0.2715	0.3167
		Friday, January 8, 2021	56	0.0216	0.2462	0.2995	0.2745	0.3206

Table A- 11 ASTM C1567---20% RFA 2 + 80% Cement

RFA 2	Monday, November 16, 2020	Tuesday, November 17, 2020	1	water container, then place in 60C oven for 24 hrs			
		Wednesday, November 18, 2020	0	0.0191	0.4023	0.2666	0.2568	0.3179
		Saturday, November 21, 2020	3	0.0194	0.4034	0.2673	0.2575	0.3179
		Wednesday, November 25, 2020	7	0.0188	0.4051	0.2680	0.2587	0.3190
		Sunday, November 29, 2020	11	0.0187	0.4065	0.2699	0.2602	0.3193
		Wednesday, December 2, 2020	14	0.0190	0.4073	0.2706	0.2609	0.3201
		Sunday, December 6, 2020	18	0.0191	0.4082	0.2716	0.2616	0.3211
		Wednesday, December 9, 2020	21	0.0193	0.4094	0.2728	0.2628	0.3224
		Monday, December 14, 2020	26	0.0186	0.4103	0.2731	0.2634	0.3227
		Wednesday, December 16, 2020	28	0.0199	0.4134	0.2754	0.2664	0.3256
		Friday, December 18, 2020	30	0.0205	0.4138	0.2756	0.2669	0.3264
		Monday, December 21, 2020	33	0.0201	0.4142	0.2762	0.2672	0.3263
		Wednesday, December 23, 2020	35	0.0202	0.4165	0.2786	0.2695	0.3291
		Friday, December 25, 2020	37	0.0210	0.4165	0.2785	0.2698	0.3288
		Wednesday, December 30, 2020	42	0.0215	0.4196	0.2817	0.2727	0.3317
		Monday, January 4, 2021	47	0.0208	0.4201	0.2825	0.2730	0.3316
		Friday, January 8, 2021	51	0.0214	0.4234	0.2856	0.2755	0.3347
		Wednesday, January 13, 2021	56	0.0201	0.4231	0.2852	0.2751	0.3334

Table A- 12 ASTM C1293 Control

						Specimen 1	Specimen 2	Specimen 3
specimen label	cast date	reading date	Week	Age of specimen, days	reference bar reading	Reading	Reading	Reading
Control	Wednesday, February 10, 2021	Thursday, February 11, 2021		1	ld, label, and place in a 23 water container, then place in 80C oven for 2			
		Wednesday, February 10, 2021	0	0	0.0232	0.2073	0.3196	0.2420
		Wednesday, February 17, 2021	1	7	0.0238	0.2068	0.3190	0.2415
		Wednesday, March 10, 2021	4	28	0.0250	0.2109	0.3215	0.2451
		Wednesday, April 7, 2021	8	56	0.0194	0.2116	0.3195	0.2437
		Tuesday, May 11, 2021	13	90	0.0192	0.2150	0.3223	0.2472
		Thursday, June 24, 2021	19	134	0.0186	0.2165	0.3246	0.2503
		Thursday, August 19, 2021	27	190	0.0168	0.2169	0.3249	0.2501
		Thursday, November 18, 2021	40	281	0.0160	0.2171	0.3250	0.2505
		Thursday, February 10, 2022	52	365	0.0176	0.2195	0.3264	0.2530
		Wednesday, May 11, 2022	65	455	0.0148	0.2172	0.3249	0.2512
		Friday, August 12, 2022	78	548	0.0146	0.2176	0.3248	0.2509
		Thursday, November 17, 2022	92	645	0.0159	0.2196	0.3263	0.2518
		Friday, February 10, 2023	104	730	0.0140	0.2178	0.3246	0.2496

Table A- 13 ASTM C1293 20% NP 1 + 80% Cement

NP1	Wednesday, February 10, 2021	Thursday, February 11, 2021	1	ld, label, and place in a 23 water container, then place in 60C oven for 2			
		Wednesday, February 10, 2021	0	0.0232	0.2425	0.2314	0.2295
		Wednesday, February 17, 2021	7	0.0239	0.2409	0.2305	0.2290
		Wednesday, March 10, 2021	28	0.0250	0.2421	0.2313	0.2304
		Wednesday, April 7, 2021	56	0.0192	0.2391	0.2275	0.2270
		Tuesday, May 11, 2021	90	0.0193	0.2398	0.2281	0.2272
		Thursday, June 24, 2021	134	0.0188	0.2407	0.2290	0.2285
		Thursday, August 19, 2021	190	0.0167	0.2412	0.2297	0.2284
		Thursday, November 18, 2021	281	0.0159	0.2430	0.2313	0.2294
		Thursday, February 10, 2022	365	0.0176	0.2461	0.2334	0.2317
		Wednesday, May 11, 2022	455	0.0146	0.2453	0.2327	0.2304
		Friday, August 12, 2022	548	0.0146	0.2461	0.2333	0.2310
		Thursday, November 17, 2022	645	0.0160	0.2475	0.2348	0.2325
		Friday, February 10, 2023	730	0.0145	0.2465	0.2343	0.2320

Table A- 14 ASTM C1293 20% NP 2 + 80% Cement

NP 2	Wednesday, February 17, 2021	Thursday, February 18, 2021	1				
		Wednesday, February 17, 2021	0	0.0238	0.2797	0.3177	0.2871
		Wednesday, February 24, 2021	7	0.0242	0.2792	0.3171	0.2869
		Wednesday, March 17, 2021	28	0.0190	0.2750	0.3135	0.2831
		Wednesday, April 14, 2021	56	0.0194	0.2758	0.3142	0.2836
		Tuesday, May 18, 2021	90	0.0184	0.2751	0.3148	0.2835
		Thursday, July 1, 2021	134	0.0175	0.2751	0.3149	0.2830
		Thursday, August 26, 2021	190	0.0168	0.2765	0.3158	0.2838
		Thursday, November 25, 2021	281	0.0181	0.2792	0.3181	0.2866
		Thursday, February 17, 2022	365	0.0175	0.2801	0.3191	0.2875
		Wednesday, May 18, 2022	455	0.0147	0.2786	0.3177	0.2863
		Friday, August 19, 2022	548	0.0146	0.2794	0.3192	0.2872
		Thursday, November 24, 2022	645	0.0160	0.2806	0.3209	0.2890
		Friday, February 17, 2023	730	0.0143	0.2802	0.3205	0.2884

Table A- 15 ASTM C1293 20% NP 3 + 80% Cement

NP 3	Wednesday, February 10, 2021	Thursday, February 11, 2021	1	ld, label, and place in a 23 water container, then place in 60C oven for 2			
		Wednesday, February 10, 2021	0	0.0230	0.3705	0.2356	0.1860
		Wednesday, February 17, 2021	7	0.0238	0.3699	0.2347	0.1855
		Wednesday, March 10, 2021	28	0.0248	0.3704	0.2363	0.1865
		Wednesday, April 7, 2021	56	0.0196	0.3675	0.2323	0.1838
		Tuesday, May 11, 2021	90	0.0193	0.3675	0.2335	0.1841
		Thursday, June 24, 2021	134	0.0188	0.3679	0.2333	0.1853
		Thursday, August 19, 2021	190	0.0168	0.3670	0.2329	0.1858
		Thursday, November 18, 2021	281	0.0159	0.3678	0.2336	0.1866
		Thursday, February 10, 2022	365	0.0176	0.3702	0.2357	0.1889
		Wednesday, May 11, 2022	455	0.0147	0.3688	0.2338	0.1875
		Friday, August 12, 2022	548	0.0146	0.3694	0.2343	0.1884
		Thursday, November 17, 2022	645	0.0160	0.3710	0.2358	0.1901
		Friday, February 10, 2023	730	0.0143	0.3702	0.2350	0.1895

Table A- 16 ASTM C1293 20% NP 4 + 80% Cement

NP 4	Thursday, February 18, 2021	Friday, February 19, 2021	1				
		Thursday, February 18, 2021	0	0.0237	0.2916	0.2816	0.2964
		Thursday, February 25, 2021	7	0.0244	0.2902	0.2797	0.2952
		Thursday, March 18, 2021	28	0.0191	0.2850	0.2744	0.2915
		Thursday, April 15, 2021	56	0.0194	0.2853	0.2755	0.2926
		Wednesday, May 19, 2021	90	0.0191	0.2855	0.2761	0.2923
		Friday, July 2, 2021	134	0.0174	0.2843	0.2755	0.2907
		Friday, August 27, 2021	190	0.0168	0.2849	0.2764	0.2913
		Friday, November 26, 2021	281	0.0181	0.2867	0.2781	0.2931
		Friday, February 18, 2022	365	0.0176	0.2867	0.2784	0.2936
		Thursday, May 19, 2022	455	0.0147	0.2858	0.2778	0.2923
		Saturday, August 20, 2022	548	0.0147	0.2860	0.2781	0.2929
		Friday, November 25, 2022	645	0.0159	0.2875	0.2800	0.2944
		Saturday, February 18, 2023	730	0.0143	0.2862	0.2793	0.2936

Table A- 17 ASTM C1293 20% NP 5 + 80% Cement

NP 5	Wednesday, February 17, 2021	Thursday, February 18, 2021	1				
		Wednesday, February 17, 2021	0	0.0237	0.3335	0.2601	0.3089
		Wednesday, February 24, 2021	7	0.0238	0.3317	0.2564	0.3092
		Wednesday, March 17, 2021	28	0.0190	0.3270	0.2404	0.3040
		Wednesday, April 14, 2021	56	0.0194	0.3282	0.2423	0.3043
		Tuesday, May 18, 2021	90	0.0184	0.3273	0.2424	0.3031
		Thursday, July 1, 2021	134	0.0175	0.3269	0.2422	0.3034
		Thursday, August 26, 2021	190	0.0168	0.3276	0.2429	0.3047
		Thursday, November 25, 2021	281	0.0181	0.3292	0.2437	0.3066
		Thursday, February 17, 2022	365	0.0177	0.3294	0.2451	0.3076
		Wednesday, May 18, 2022	455	0.0147	0.3286	0.2440	0.3058
		Friday, August 19, 2022	548	0.0146	0.3292	0.2450	0.3066
		Thursday, November 24, 2022	645	0.0160	0.3310	0.2468	0.3084
		Friday, February 17, 2023	730	0.0144	0.3300	0.2448	0.3068

Table A- 18 ASTM C1293 20% NP 6 + 80% Cement

NP 6	Wednesday, February 17, 2021	Thursday, February 18, 2021	1				
		Wednesday, February 17, 2021	0	0.0237	0.1482	0.3353	0.2847
		Wednesday, February 24, 2021	7	0.0238	0.1484	0.3350	0.2845
		Wednesday, March 17, 2021	28	0.0192	0.1438	0.3304	0.2794
		Wednesday, April 14, 2021	56	0.0194	0.1456	0.3317	0.2805
		Tuesday, May 18, 2021	90	0.0183	0.1454	0.3310	0.2799
		Thursday, July 1, 2021	134	0.0176	0.1455	0.3310	0.2800
		Thursday, August 26, 2021	190	0.0168	0.1457	0.3312	0.2804
		Thursday, November 25, 2021	281	0.0181	0.1481	0.3338	0.2838
		Thursday, February 17, 2022	365	0.0176	0.1492	0.3345	0.2846
		Wednesday, May 18, 2022	455	0.0147	0.1486	0.3342	0.2838
		Friday, August 19, 2022	548	0.0146	0.1492	0.3349	0.2840
		Thursday, November 24, 2022	645	0.0160	0.1511	0.3368	0.2856
		Friday, February 17, 2023	730	0.0144	0.1508	0.3361	0.2848

Table A- 19 ASTM C1293 20% RFA 1 + 80% Cement

RFA 1	Wednesday, February 10, 2021	Thursday, February 11, 2021	1	ld, label, and place in a 23 water container, then place in 60C oven for 2			
		Wednesday, February 10, 2021	0	0.0232	0.3436	0.2139	0.1399
		Wednesday, February 17, 2021	7	0.0238	0.3440	0.2143	0.1403
		Wednesday, March 10, 2021	28	0.0247	0.3453	0.2157	0.1423
		Wednesday, April 7, 2021	56	0.0196	0.3434	0.2116	0.1388
		Tuesday, May 11, 2021	90	0.0192	0.3446	0.2129	0.1396
		Thursday, June 24, 2021	134	0.0187	0.3452	0.2149	0.1412
		Thursday, August 19, 2021	190	0.0168	0.3456	0.2151	0.1413
		Thursday, November 18, 2021	281	0.0161	0.3469	0.2166	0.1426
		Thursday, February 10, 2022	365	0.0176	0.3493	0.2186	0.1449
		Wednesday, May 11, 2022	455	0.0147	0.3478	0.2174	0.1434
		Friday, August 12, 2022	548	0.0146	0.3486	0.2184	0.1440
		Thursday, November 17, 2022	645	0.0158	0.3500	0.2198	0.1455
		Friday, February 10, 2023	730	0.0145	0.3497	0.2192	0.1445

Table A- 20 ASTM C1293 20% RFA 2 + 80% Cement

RFA 2	Thursday, February 18, 2021	Friday, February 19, 2021	1				
		Thursday, February 18, 2021	0	0.0238	0.2448	0.2466	0.2150
		Thursday, February 25, 2021	7	0.0243	0.2442	0.2457	0.2138
		Thursday, March 18, 2021	28	0.0192	0.2397	0.2420	0.2086
		Thursday, April 15, 2021	56	0.0194	0.2412	0.2427	0.2107
		Wednesday, May 19, 2021	90	0.0191	0.2415	0.2428	0.2111
		Friday, July 2, 2021	134	0.0173	0.2410	0.2429	0.2121
		Friday, August 27, 2021	190	0.0168	0.2418	0.2436	0.2140
		Friday, November 26, 2021	281	0.0181	0.2442	0.2459	0.2169
		Friday, February 18, 2022	365	0.0175	0.2445	0.2468	0.2174
		Thursday, May 19, 2022	455	0.0147	0.2437	0.2454	0.2169
		Saturday, August 20, 2022	548	0.0147	0.2440	0.2461	0.2176
		Friday, November 25, 2022	645	0.0160	0.2457	0.2475	0.2193
		Saturday, February 18, 2023	730	0.0143	0.2449	0.2465	0.2185

Table A- 21 ASTM C1293 30% NP 2 + 70% Cement

NP 2	Tuesday, March 22, 2022	Wednesday, March 23, 2022	1	ld, label, and place in a 23 water container, then place in 60C oven for 2			
		Tuesday, March 22, 2022	0	0.0159	0.2748	0.2688	0.2921
		Friday, April 1, 2022	10	0.0151	0.2745	0.2686	0.2914
		Friday, April 15, 2022	24	0.0154	0.2742	0.2683	0.2909
		Tuesday, May 17, 2022	56	0.0149	0.2745	0.2683	0.2910
		Monday, June 20, 2022	90	0.0145	0.2747	0.2679	0.2906
		Wednesday, August 3, 2022	134	0.0139	0.2758	0.2694	0.2917
		Wednesday, September 28, 2022	190	0.0153	0.2777	0.2700	0.2929
		Thursday, January 5, 2023	289	0.0159	0.2791	0.2712	0.2939
		Wednesday, March 22, 2023	365	0.0140	0.2777	0.2704	0.2930
		Tuesday, June 20, 2023	455	0.0112	0.2759	0.2678	0.2912
		Tuesday, September 26, 2023	553	0.0081	0.2734	0.2652	0.2893

Table A- 22 ASTM C1293 30% NP 5 + 70% Cement

NP 5	Tuesday, March 22, 2022	Wednesday, March 23, 2022	1	ld, label, and place in a 23 water container, then place in 60C oven for 2			
		Tuesday, March 22, 2022	0	0.0157	0.3433	0.3473	0.3415
		Friday, April 1, 2022	10	0.0157	0.3601	0.3455	0.3400
		Friday, April 15, 2022	24	0.0153	0.3596	0.3459	0.3402
		Tuesday, May 17, 2022	56	0.0149	0.3593	0.3462	0.3401
		Monday, June 20, 2022	90	0.0145	0.3438	0.3457	0.3398
		Wednesday, August 3, 2022	134	0.0139	0.3233	0.3458	0.3417
		Wednesday, September 28, 2022	190	0.0152	0.3315	0.3468	0.3429
		Thursday, January 5, 2023	289	0.0159	0.3250	0.3474	0.3437
		Wednesday, March 22, 2023	365	0.0141	0.3242	0.3466	0.3427
		Tuesday, June 20, 2023	455	0.0112	0.3220	0.3445	0.3400
		Tuesday, September 26, 2023	553	0.0081	0.3199	0.3417	0.3385

Table A- 23 ASTM C1293 30% NP 4 + 70% Cement

NP 4	Wednesday, March 23, 2022	Thursday, March 24, 2022	1				
		Wednesday, March 23, 2022	0	0.0152	0.3313	0.2728	0.3234
		Friday, April 1, 2022	9	0.0150	0.3305	0.2683	0.3227
		Friday, April 15, 2022	23	0.0153	0.3309	0.2683	0.3227
		Wednesday, May 18, 2022	56	0.0149	0.3304	0.2681	0.3223
		Tuesday, June 21, 2022	90	0.0145	0.3304	0.2682	0.3225
		Thursday, August 4, 2022	134	0.0140	0.3305	0.2682	0.3224
		Thursday, September 29, 2022	190	0.0152	0.3315	0.2695	0.3228
		Friday, January 6, 2023	289	0.0159	0.3321	0.2703	0.3243
		Thursday, March 23, 2023	365	0.0141	0.3313	0.2692	0.3234
		Wednesday, June 21, 2023	455	0.0113	0.3287	0.2669	0.3211
		Wednesday, September 27, 2023	553	0.0081	0.3270	0.2648	0.3192

Table A- 24 ASTM C1293 30% RFA 1 + 70% Cement

specimen label	cast date	reading date	Age of specimen, days	reference bar reading	Reading	Reading	Reading
RFA 1	Tuesday, March 22, 2022	Wednesday, March 23, 2022	1	ld, label, and place in a 23 water container, then place in 80C oven for 2			
		Tuesday, March 22, 2022	0	0.0158	0.2450	0.3603	0.3412
		Tuesday, March 29, 2022	7	0.0152	0.2460	0.3611	0.3419
		Friday, April 15, 2022	24	0.0154	0.2448	0.3608	0.3414
		Tuesday, May 17, 2022	56	0.0149	0.2448	0.3609	0.3415
		Monday, June 20, 2022	90	0.0145	0.2448	0.3606	0.3416
		Wednesday, August 3, 2022	134	0.0139	0.2453	0.3612	0.3421
		Wednesday, September 28, 2022	190	0.0152	0.2495	0.3641	0.3449
		Thursday, January 5, 2023	289	0.0158	0.2506	0.3662	0.3463
		Wednesday, March 22, 2023	365	0.0141	0.2507	0.3655	0.3460
		Tuesday, June 20, 2023	455	0.0111	0.2491	0.3635	0.3440
		Tuesday, September 26, 2023	553	0.0081	0.2472	0.3614	0.3416

Table A- 25 ASTM C1293 30% RFA 2 + 70% Cement

RFA 2	Tuesday, March 22, 2022	Wednesday, March 23, 2022	1	ld, label, and place in a 23 water container, then place in 60C oven for 2			
		Tuesday, March 22, 2022	0	0.0157	0.3126	0.2346	0.3517
		Tuesday, March 29, 2022	7	0.0151	0.3109	0.2325	0.3494
		Friday, April 15, 2022	24	0.0153	0.3109	0.2325	0.3496
		Tuesday, May 17, 2022	56	0.0152	0.3116	0.2328	0.3503
		Monday, June 20, 2022	90	0.0145	0.3118	0.2325	0.3496
		Wednesday, August 3, 2022	134	0.0139	0.3121	0.2328	0.3499
		Wednesday, September 28, 2022	190	0.0152	0.3129	0.2345	0.3510
		Thursday, January 5, 2023	289	0.0159	0.3144	0.2351	0.3521
		Wednesday, March 22, 2023	365	0.0141	0.3134	0.2343	0.3511
		Tuesday, June 20, 2023	455	0.0112	0.3114	0.2314	0.3490
		Tuesday, September 26, 2023	553	0.0081	0.3090	0.2286	0.3475

Table A- 26 AASHTO T380 Control (Coarse Reactive Aggregate)

Control	Wednesday, May 5, 2021	Thursday, May 6, 2021	1	Demold, label, and place in a 23 water container, then place in 80C oven for 24 hrs			
		Friday, May 7, 2021	0	0.0195	0.2184	0.2306	0.2797	0.2885
		Monday, May 10, 2021	3	0.0194	0.2186	0.2308	0.2802	0.2893
		Friday, May 14, 2021	7	0.0192	0.2199	0.2332	0.2821	0.2906
		Monday, May 17, 2021	10	0.0190	0.2223	0.2349	0.2848	0.2941
		Friday, May 21, 2021	14	0.0193	0.2260	0.2380	0.2892	0.2980
		Monday, May 24, 2021	17	0.0186	0.2280	0.2398	0.2918	0.3005
		Friday, May 28, 2021	21	0.0188	0.2303	0.2423	0.2941	0.3030
		Monday, May 31, 2021	24	0.0188	0.2320	0.2437	0.2958	0.3051
		Friday, June 4, 2021	28	0.0188	0.2327	0.2444	0.2965	0.3058
		Monday, June 7, 2021	31	0.0185	0.2333	0.2451	0.2977	0.3067
		Friday, June 11, 2021	35	0.0186	0.2340	0.2460	0.2980	0.3073
		Friday, June 18, 2021	42	0.0184	0.2343	0.2469	0.2991	0.3086
		Friday, June 25, 2021	49	0.0181	0.2350	0.2477	0.2994	0.3094
		Friday, July 2, 2021	56	0.0177	0.2355	0.2483	0.3003	0.3106
		Friday, July 9, 2021	63	0.0173	0.2355	0.2479	0.3005	0.3122
		Friday, July 16, 2021	70	0.0168	0.2357	0.2488	0.3014	0.3113
		Friday, July 23, 2021	77	0.0173	0.2370	0.2499	0.3022	0.3121
		Friday, July 30, 2021	84	0.0172	0.2374	0.2504	0.3027	0.3134

Table A- 27 AASHTO T380 20% NP 1 + 80% Cement (Coarse Reactive Aggregate)

NP 1	Wednesday, May 5, 2021	Thursday, May 6, 2021	1	Demold, label, and place in a 23 water container, then place in 60C oven for 24 hrs			
		Friday, May 7, 2021	0	0.0196	0.1983	0.2599	0.2489	0.2661
		Monday, May 10, 2021	3	0.0193	0.1982	0.2595	0.2478	0.2651
		Friday, May 14, 2021	7	0.0191	0.1984	0.2597	0.2479	0.2655
		Monday, May 17, 2021	10	0.0188	0.1980	0.2592	0.2478	0.2654
		Friday, May 21, 2021	14	0.0186	0.1982	0.2593	0.2478	0.2655
		Monday, May 24, 2021	17	0.0187	0.1982	0.2595	0.2479	0.2657
		Friday, May 28, 2021	21	0.0184	0.1982	0.2595	0.2480	0.2654
		Monday, May 31, 2021	24	0.0187	0.1987	0.2600	0.2486	0.2661
		Friday, June 4, 2021	28	0.0186	0.1989	0.2603	0.2489	0.2664
		Monday, June 7, 2021	31	0.0185	0.1988	0.2603	0.2491	0.2664
		Friday, June 11, 2021	35	0.0183	0.1988	0.2603	0.2489	0.2664
		Friday, June 18, 2021	42	0.0181	0.1988	0.2603	0.2488	0.2661
		Friday, June 25, 2021	49	0.0179	0.1985	0.2601	0.2487	0.2660
		Friday, July 2, 2021	56	0.0179	0.1987	0.2603	0.2487	0.2662
		Friday, July 9, 2021	63	0.0169	0.1976	0.2593	0.2481	0.2656
		Friday, July 16, 2021	70	0.0167	0.1983	0.2599	0.2483	0.2655
		Friday, July 23, 2021	77	0.0173	0.1991	0.2609	0.2493	0.2667
		Friday, July 30, 2021	84	0.0171	0.1994	0.2613	0.2497	0.2673

Table A- 28 AASHTO T380 20% NP 2 + 80% Cement (Coarse Reactive Aggregate)

NP 2	Wednesday, May 5, 2021	Thursday, May 6, 2021	1	Demold, label, and place in a 23 water container, then place in 60C oven for 24 hrs				
		Friday, May 7, 2021	0	0.0196	0.2112	0.2580	0.2472	0.2275
		Monday, May 10, 2021	3	0.0192	0.2113	0.2576	0.2463	0.2277
		Friday, May 14, 2021	7	0.0192	0.2118	0.2584	0.2472	0.2284
		Monday, May 17, 2021	10	0.0191	0.2121	0.2585	0.2468	0.2282
		Friday, May 21, 2021	14	0.0186	0.2119	0.2584	0.2466	0.2279
		Monday, May 24, 2021	17	0.0186	0.2121	0.2591	0.2468	0.2282
		Friday, May 28, 2021	21	0.0185	0.2122	0.2593	0.2468	0.2281
		Monday, May 31, 2021	24	0.0188	0.2125	0.2597	0.2471	0.2284
		Friday, June 4, 2021	28	0.0187	0.2122	0.2595	0.2470	0.2283
		Monday, June 7, 2021	31	0.0183	0.2120	0.2593	0.2468	0.2280
		Friday, June 11, 2021	35	0.0184	0.2120	0.2592	0.2472	0.2282
		Friday, June 18, 2021	42	0.0182	0.2119	0.2590	0.2471	0.2280
		Friday, June 25, 2021	49	0.0179	0.2123	0.2593	0.2472	0.2280
		Friday, July 2, 2021	56	0.0176	0.2120	0.2591	0.2470	0.2280
		Friday, July 9, 2021	63	0.0168	0.2116	0.2585	0.2459	0.2270
		Friday, July 16, 2021	70	0.0168	0.2119	0.2589	0.2467	0.2275
		Friday, July 23, 2021	77	0.0171	0.2130	0.2600	0.2474	0.2282
		Friday, July 30, 2021	84	0.0171	0.2142	0.2604	0.2479	0.2290

Table A- 29 AASHTO T380 20% NP 3 + 80% Cement (Coarse Reactive Aggregate)

NP 3	Wednesday, May 5, 2021	Thursday, May 6, 2021	1	Demold, label, and place in a 23 water container, then place in 60C oven for 24 hrs				
		Friday, May 7, 2021	0	0.0197	0.2681	0.2690	0.2732	0.2870
		Monday, May 10, 2021	3	0.0193	0.2676	0.2688	0.2730	0.2867
		Friday, May 14, 2021	7	0.0191	0.2672	0.2686	0.2731	0.2870
		Monday, May 17, 2021	10	0.0190	0.2673	0.2688	0.2729	0.2869
		Friday, May 21, 2021	14	0.0186	0.2667	0.2686	0.2729	0.2867
		Monday, May 24, 2021	17	0.0187	0.2673	0.2689	0.2730	0.2871
		Friday, May 28, 2021	21	0.0185	0.2671	0.2687	0.2732	0.2871
		Monday, May 31, 2021	24	0.0189	0.2677	0.2692	0.2736	0.2876
		Friday, June 4, 2021	28	0.0187	0.2675	0.2692	0.2736	0.2876
		Monday, June 7, 2021	31	0.0187	0.2679	0.2693	0.2735	0.2875
		Friday, June 11, 2021	35	0.0185	0.2676	0.2691	0.2735	0.2875
		Friday, June 18, 2021	42	0.0183	0.2674	0.2690	0.2735	0.2872
		Friday, June 25, 2021	49	0.0179	0.2668	0.2685	0.2732	0.2871
		Friday, July 2, 2021	56	0.0179	0.2675	0.2690	0.2733	0.2872
		Friday, July 9, 2021	63	0.0170	0.2669	0.2684	0.2724	0.2863
		Friday, July 16, 2021	70	0.0168	0.2664	0.2679	0.2727	0.2866
		Friday, July 23, 2021	77	0.0173	0.2673	0.2688	0.2731	0.2868
		Friday, July 30, 2021	84	0.0170	0.2670	0.2683	0.2730	0.2868

Table A- 30 AASHTO T380 20% NP 4 + 80% Cement (Coarse Reactive Aggregate)

NP 4	Monday, May 3, 2021	Thursday, May 6, 2021	1	Demold, label, and place in a 23 water container, then place in 60C oven for 24 hrs				
		Friday, May 7, 2021	0	0.0192	0.2280	0.2454	0.2714	0.2502
		Monday, May 10, 2021	3	0.0190	0.2277	0.2452	0.2716	0.2501
		Friday, May 14, 2021	7	0.0192	0.2284	0.2459	0.2721	0.2505
		Monday, May 17, 2021	10	0.0187	0.2277	0.2450	0.2711	0.2498
		Friday, May 21, 2021	14	0.0186	0.2276	0.2451	0.2712	0.2499
		Monday, May 24, 2021	17	0.0187	0.2277	0.2454	0.2712	0.2500
		Friday, May 28, 2021	21	0.0184	0.2275	0.2452	0.2711	0.2498
		Monday, May 31, 2021	24	0.0188	0.2280	0.2458	0.2717	0.2503
		Friday, June 4, 2021	28	0.0186	0.2278	0.2456	0.2714	0.2501
		Monday, June 7, 2021	31	0.0184	0.2277	0.2455	0.2713	0.2499
		Friday, June 11, 2021	35	0.0184	0.2277	0.2454	0.2712	0.2499
		Friday, June 18, 2021	42	0.0183	0.2279	0.2456	0.2713	0.2498
		Friday, June 25, 2021	49	0.0179	0.2276	0.2454	0.2710	0.2497
		Friday, July 2, 2021	56	0.0176	0.2278	0.2457	0.2710	0.2497
		Friday, July 9, 2021	63	0.0167	0.2269	0.2449	0.2704	0.2493
		Friday, July 16, 2021	70	0.0167	0.2273	0.2454	0.2704	0.2493
		Friday, July 23, 2021	77	0.0171	0.2278	0.2457	0.2710	0.2500
		Friday, July 30, 2021	84	0.0171	0.2282	0.2462	0.2709	0.2502

Table A- 31 AASHTO T380 20% NP 5+ 80% Cement (Coarse Reactive Aggregate)

NP 5	Friday, May 7, 2021	Saturday, May 8, 2021	1	Demold, label, and place in a 23 water container, then place in 60C oven for 24 hrs				
		Sunday, May 9, 2021	0	0.0196	0.2892	0.2491	0.2363	0.2742
		Wednesday, May 12, 2021	3	0.0191	0.2885	0.2490	0.2358	0.2737
		Sunday, May 16, 2021	7	0.0193	0.2884	0.2492	0.2359	0.2736
		Wednesday, May 19, 2021	10	0.0183	0.2880	0.2493	0.2354	0.2727
		Sunday, May 23, 2021	14	0.0184	0.2885	0.2497	0.2358	0.2737
		Wednesday, May 26, 2021	17	0.0185	0.2889	0.2499	0.2366	0.2735
		Sunday, May 30, 2021	21	0.0188	0.2891	0.2503	0.2376	0.2741
		Wednesday, June 2, 2021	24	0.0185	0.2889	0.2503	0.2373	0.2735
		Sunday, June 6, 2021	28	0.0187	0.2892	0.2504	0.2378	0.2739
		Wednesday, June 9, 2021	31	0.0187	0.2893	0.2504	0.2378	0.2739
		Sunday, June 13, 2021	35	0.0185	0.2895	0.2504	0.2378	0.2739
		Sunday, June 20, 2021	42	0.0181	0.2891	0.2502	0.2377	0.2736
		Sunday, June 27, 2021	49	0.0174	0.2883	0.2500	0.2370	0.2724
		Sunday, July 4, 2021	56	0.0174	0.2884	0.2498	0.2372	0.2730
		Sunday, July 11, 2021	63	0.0165	0.2876	0.2490	0.2363	0.2720
		Sunday, July 18, 2021	70	0.0169	0.2879	0.2494	0.2370	0.2726
		Sunday, July 25, 2021	77	0.0170	0.2884	0.2501	0.2372	0.2728
		Sunday, August 1, 2021	84	0.0167	0.2881	0.2498	0.2370	0.2726

Table A- 32 AASHTO T380 20% NP 6 + 80% Cement (Coarse Reactive Aggregate)

NP 6	Wednesday, May 12, 2021	Thursday, May 13, 2021	1	Demold, label, and place in a 23 water container, then place in 60C oven for 24 hrs				
		Friday, May 14, 2021	0	0.0196	0.2601	0.2544	0.2968	0.2882
		Monday, May 17, 2021	3	0.0189	0.2599	0.2540	0.2959	0.2872
		Friday, May 21, 2021	7	0.0193	0.2600	0.2539	0.2958	0.2871
		Monday, May 24, 2021	10	0.0183	0.2594	0.2532	0.2948	0.2860
		Friday, May 28, 2021	14	0.0186	0.2602	0.2540	0.2960	0.2869
		Monday, May 31, 2021	17	0.0186	0.2604	0.2540	0.2958	0.2867
		Friday, June 4, 2021	21	0.0188	0.2608	0.2544	0.2963	0.2877
		Monday, June 7, 2021	24	0.0185	0.2605	0.2541	0.2960	0.2870
		Friday, June 11, 2021	28	0.0187	0.2610	0.2546	0.2965	0.2880
		Monday, June 14, 2021	31	0.0187	0.2610	0.2548	0.2966	0.2879
		Friday, June 18, 2021	35	0.0187	0.2616	0.2554	0.2962	0.2875
		Friday, June 25, 2021	42	0.0182	0.2607	0.2545	0.2959	0.2874
		Friday, July 2, 2021	49	0.0176	0.2603	0.2542	0.2955	0.2870
		Friday, July 9, 2021	56	0.0174	0.2604	0.2542	0.2957	0.2871
		Friday, July 16, 2021	63	0.0167	0.2596	0.2533	0.2949	0.2865
		Friday, July 23, 2021	70	0.0170	0.2601	0.2538	0.2951	0.2864
		Friday, July 30, 2021	77	0.0170	0.2601	0.2537	0.2954	0.2869
		Friday, August 6, 2021	84	0.0168	0.2601	0.2537	0.2952	0.2866

Table A- 33 AASHTO T380 20% RFA 1 + 80% Cement (Coarse Reactive Aggregate)

RFA 1	Wednesday, May 5, 2021	Thursday, May 6, 2021	1	Demold, label, and place in a 23 water container, then place in 60C oven for 24 hrs				
		Friday, May 7, 2021	0	0.0194	0.2448	0.2618	0.2923	0.2723
		Monday, May 10, 2021	3	0.0190	0.2433	0.2615	0.2924	0.2723
		Friday, May 14, 2021	7	0.0191	0.2440	0.2626	0.2922	0.2723
		Monday, May 17, 2021	10	0.0190	0.2446	0.2627	0.2933	0.2734
		Friday, May 21, 2021	14	0.0186	0.2452	0.2634	0.2936	0.2737
		Monday, May 24, 2021	17	0.0186	0.2457	0.2640	0.2945	0.2746
		Friday, May 28, 2021	21	0.0187	0.2463	0.2645	0.2948	0.2755
		Monday, May 31, 2021	24	0.0189	0.2465	0.2652	0.2953	0.2762
		Friday, June 4, 2021	28	0.0186	0.2466	0.2648	0.2949	0.2762
		Monday, June 7, 2021	31	0.0185	0.2468	0.2646	0.2946	0.2762
		Friday, June 11, 2021	35	0.0186	0.2469	0.2648	0.2949	0.2765
		Friday, June 18, 2021	42	0.0183	0.2472	0.2650	0.2953	0.2769
		Friday, June 25, 2021	49	0.0180	0.2480	0.2657	0.2953	0.2774
		Friday, July 2, 2021	56	0.0176	0.2481	0.2657	0.2954	0.2785
		Friday, July 9, 2021	63	0.0173	0.2482	0.2661	0.2954	0.2780
		Friday, July 16, 2021	70	0.0168	0.2487	0.2665	0.2953	0.2781
		Friday, July 23, 2021	77	0.0172	0.2492	0.2669	0.2961	0.2789
		Friday, July 30, 2021	84	0.0171	0.2500	0.2675	0.2969	0.2795

Table A- 34 AASHTO T380 20% RFA 2 + 80% Cement (Coarse Reactive Aggregate)

RFA 2	Wednesday, May 12, 2021	Thursday, May 13, 2021	1	Demold, label, and place in a 23 water container, then place in 60C oven for 24 hrs			
		Friday, May 14, 2021	0	0.0195	0.2759	0.2685	0.2740	0.2721
		Monday, May 17, 2021	3	0.0190	0.2760	0.2682	0.2733	0.2719
		Friday, May 21, 2021	7	0.0193	0.2757	0.2685	0.2739	0.2725
		Monday, May 24, 2021	10	0.0183	0.2751	0.2674	0.2725	0.2718
		Friday, May 28, 2021	14	0.0181	0.2750	0.2675	0.2719	0.2713
		Monday, May 31, 2021	17	0.0183	0.2752	0.2676	0.2725	0.2718
		Friday, June 4, 2021	21	0.0188	0.2763	0.2683	0.2730	0.2726
		Monday, June 7, 2021	24	0.0185	0.2758	0.2681	0.2729	0.2722
		Friday, June 11, 2021	28	0.0185	0.2763	0.2688	0.2731	0.2722
		Monday, June 14, 2021	31	0.0187	0.2766	0.2689	0.2731	0.2733
		Friday, June 18, 2021	35	0.0184	0.2768	0.2687	0.2731	0.2734
		Friday, June 25, 2021	42	0.0182	0.2767	0.2685	0.2736	0.2727
		Friday, July 2, 2021	49	0.0176	0.2765	0.2682	0.2728	0.2718
		Friday, July 9, 2021	56	0.0173	0.2760	0.2681	0.2729	0.2716
		Friday, July 16, 2021	63	0.0167	0.2757	0.2677	0.2721	0.2713
		Friday, July 23, 2021	70	0.0170	0.2762	0.2681	0.2727	0.2715
		Friday, July 30, 2021	77	0.0170	0.2764	0.2680	0.2727	0.2715
		Friday, August 6, 2021	84	0.0168	0.2761	0.2680	0.2728	0.2716

Table A- 35 AASHTO T380 Control (Fine Reactive Aggregate)

Control	Wednesday, June 2, 2021	Thursday, June 3, 2021	1	Demold, label, and place in a 23 water container, then place in 80C oven for 24 hrs			
		Friday, June 4, 2021	0	0.0183	0.2941	0.2582	0.2845	0.2271
		Monday, June 7, 2021	3	0.0188	0.2949	0.2591	0.2843	0.2280
		Friday, June 11, 2021	7	0.0184	0.2990	0.2634	0.2887	0.2319
		Monday, June 14, 2021	10	0.0182	0.3050	0.2694	0.2948	0.2380
		Friday, June 18, 2021	14	0.0181	0.3148	0.2794	0.3047	0.2478
		Tuesday, June 22, 2021	18	0.0181	0.3211	0.2857	0.3116	0.2542
		Friday, June 25, 2021	21	0.0178	0.3287	0.2935	0.3188	0.2617
		Monday, June 28, 2021	24	0.0178	0.3329	0.2979	0.3231	0.2664
		Friday, July 2, 2021	28	0.0178	0.3379	0.3028	0.3280	0.2719
		Monday, July 5, 2021	31	0.0172	0.3415	0.3067	0.3317	0.2758
		Friday, July 9, 2021	35	0.0169	0.3432	0.3087	0.3336	0.2778
		Friday, July 16, 2021	42	0.0172	0.3477	0.3131	0.3381	0.2827
		Friday, July 23, 2021	49	0.0169	0.3516	0.3169	0.3419	0.2866
		Friday, July 30, 2021	56	0.0168	0.3536	0.3202	0.3455	0.2899
		Friday, August 6, 2021	63	0.0173	0.3598	0.3256	0.3499	0.2954
		Friday, August 13, 2021	70	0.0171	0.3632	0.3289	0.3531	0.2988
		Friday, August 20, 2021	77	0.0170	0.3671	0.3323	0.3564	0.3024
		Friday, August 27, 2021	84	0.0168	0.3704	0.3359	0.3593	0.3056

Table A- 36 AASHTO T380 20% NP 1 + 80% Cement (Fine Reactive Aggregate)

NP1	Wednesday, June 2, 2021	Thursday, June 3, 2021	1	Demold, label, and place in a 23 water container, then place in 60C oven for 24 hrs			
		Friday, June 4, 2021	0	0.0185	0.2233	0.2795	0.2561	0.2568
		Monday, June 7, 2021	3	0.0187	0.2230	0.2790	0.2563	0.2569
		Friday, June 11, 2021	7	0.0185	0.2229	0.2802	0.2568	0.2573
		Monday, June 14, 2021	10	0.0183	0.2240	0.2808	0.2574	0.2579
		Friday, June 18, 2021	14	0.0183	0.2251	0.2823	0.2589	0.2594
		Tuesday, June 22, 2021	18	0.0181	0.2270	0.2836	0.2603	0.2606
		Friday, June 25, 2021	21	0.0178	0.2288	0.2853	0.2619	0.2623
		Monday, June 28, 2021	24	0.0178	0.2298	0.2861	0.2628	0.2632
		Friday, July 2, 2021	28	0.0179	0.2319	0.2880	0.2646	0.2652
		Monday, July 5, 2021	31	0.0172	0.2331	0.2895	0.2660	0.2665
		Friday, July 9, 2021	35	0.0169	0.2336	0.2897	0.2661	0.2668
		Friday, July 16, 2021	42	0.0174	0.2365	0.2925	0.2689	0.2695
		Friday, July 23, 2021	49	0.0169	0.2383	0.2942	0.2704	0.2710
		Friday, July 30, 2021	56	0.0169	0.2401	0.2959	0.2723	0.2729
		Friday, August 6, 2021	63	0.0171	0.2434	0.2992	0.2754	0.2760
		Friday, August 13, 2021	70	0.0169	0.2454	0.3012	0.2772	0.2776
		Friday, August 20, 2021	77	0.0168	0.2471	0.3025	0.2785	0.2788
		Friday, August 27, 2021	84	0.0165	0.2484	0.3035	0.2794	0.2802

Table A- 37 AASHTO T380 20% NP 2 + 80% Cement (Fine Reactive Aggregate)

NP2	Wednesday, June 2, 2021	Thursday, June 3, 2021	1	Demold, label, and place in a 23 water container, then place in 60C oven for 24 hrs				
		Friday, June 4, 2021	0	0.0184	0.2966	0.2958	0.2668	0.2511
		Monday, June 7, 2021	3	0.0187	0.2965	0.2957	0.2670	0.2513
		Friday, June 11, 2021	7	0.0184	0.2964	0.2956	0.2668	0.2511
		Monday, June 14, 2021	10	0.0181	0.2968	0.2958	0.2671	0.2513
		Friday, June 18, 2021	14	0.0181	0.2979	0.2962	0.2681	0.2523
		Tuesday, June 22, 2021	18	0.0181	0.2990	0.2971	0.2689	0.2532
		Friday, June 25, 2021	21	0.0179	0.2999	0.2983	0.2698	0.2541
		Monday, June 28, 2021	24	0.0178	0.3002	0.2987	0.2702	0.2544
		Friday, July 2, 2021	28	0.0178	0.3018	0.3004	0.2717	0.2559
		Monday, July 5, 2021	31	0.0172	0.3024	0.3010	0.2720	0.2564
		Friday, July 9, 2021	35	0.0169	0.3030	0.3016	0.2727	0.2569
		Friday, July 16, 2021	42	0.0172	0.3047	0.3034	0.2743	0.2585
		Friday, July 23, 2021	49	0.0169	0.3055	0.3043	0.2753	0.2592
		Friday, July 30, 2021	56	0.0168	0.3074	0.3063	0.2769	0.2611
		Friday, August 6, 2021	63	0.0173	0.3102	0.3088	0.2794	0.2634
		Friday, August 13, 2021	70	0.0170	0.3114	0.3100	0.2803	0.2647
		Friday, August 20, 2021	77	0.0170	0.3138	0.3121	0.2818	0.2668
		Friday, August 27, 2021	84	0.0168	0.3138	0.3126	0.2825	0.2676

Table A- 38 AASHTO T380 20% NP 3 + 80% Cement (Fine Reactive Aggregate)

NP3	Wednesday, June 2, 2021	Thursday, June 3, 2021	1	Demold, label, and place in a 23 water container, then place in 60C oven for 24 hrs				
		Friday, June 4, 2021	0	0.0185	0.2375	0.2576	0.2224	0.1156
		Monday, June 7, 2021	3	0.0187	0.2378	0.2576	0.2224	0.1152
		Friday, June 11, 2021	7	0.0184	0.2382	0.2581	0.2228	0.1158
		Monday, June 14, 2021	10	0.0183	0.2383	0.2579	0.2230	0.1161
		Friday, June 18, 2021	14	0.0183	0.2395	0.2592	0.2242	0.1173
		Tuesday, June 22, 2021	18	0.0183	0.2398	0.2595	0.2245	0.1178
		Friday, June 25, 2021	21	0.0178	0.2408	0.2604	0.2252	0.1180
		Monday, June 28, 2021	24	0.0178	0.2420	0.2618	0.2264	0.1192
		Friday, July 2, 2021	28	0.0179	0.2437	0.2636	0.2280	0.1209
		Monday, July 5, 2021	31	0.0172	0.2436	0.2637	0.2280	0.1208
		Friday, July 9, 2021	35	0.0169	0.2443	0.2644	0.2287	0.1212
		Friday, July 16, 2021	42	0.0175	0.2465	0.2668	0.2308	0.1232
		Friday, July 23, 2021	49	0.0170	0.2482	0.2685	0.2325	0.1245
		Friday, July 30, 2021	56	0.0173	0.2499	0.2704	0.2341	0.1263
		Friday, August 6, 2021	63	0.0171	0.2528	0.2734	0.2373	0.1287
		Friday, August 13, 2021	70	0.0169	0.2545	0.2745	0.2383	0.1296
		Friday, August 20, 2021	77	0.0166	0.2558	0.2759	0.2391	0.1304
		Friday, August 27, 2021	84	0.0165	0.2567	0.2773	0.2403	0.1308

Table A- 39 AASHTO T380 20% NP 4 + 80% Cement (Fine Reactive Aggregate)

NP4	Wednesday, June 2, 2021	Thursday, June 3, 2021	1	Demold, label, and place in a 23 water container, then place in 60C oven for 24 hrs				
		Friday, June 4, 2021	0	0.0184	0.2652	0.2589	0.2682	0.2103
		Monday, June 7, 2021	3	0.0188	0.2650	0.2590	0.2681	0.2106
		Friday, June 11, 2021	7	0.0180	0.2649	0.2591	0.2685	0.2106
		Monday, June 14, 2021	10	0.0183	0.2649	0.2590	0.2686	0.2106
		Friday, June 18, 2021	14	0.0181	0.2663	0.2602	0.2698	0.2114
		Tuesday, June 22, 2021	18	0.0182	0.2673	0.2611	0.2707	0.2126
		Friday, June 25, 2021	21	0.0178	0.2678	0.2614	0.2711	0.2126
		Monday, June 28, 2021	24	0.0177	0.2680	0.2618	0.2714	0.2130
		Friday, July 2, 2021	28	0.0179	0.2696	0.2626	0.2723	0.2137
		Monday, July 5, 2021	31	0.0172	0.2701	0.2631	0.2728	0.2146
		Friday, July 9, 2021	35	0.0169	0.2701	0.2634	0.2733	0.2149
		Friday, July 16, 2021	42	0.0175	0.2721	0.2650	0.2749	0.2162
		Friday, July 23, 2021	49	0.0170	0.2722	0.2654	0.2752	0.2167
		Friday, July 30, 2021	56	0.0173	0.2729	0.2662	0.2759	0.2176
		Friday, August 6, 2021	63	0.0172	0.2752	0.2682	0.2783	0.2199
		Friday, August 13, 2021	70	0.0170	0.2766	0.2692	0.2793	0.2208
		Friday, August 20, 2021	77	0.0168	0.2785	0.2711	0.2800	0.2224
		Friday, August 27, 2021	84	0.0165	0.2791	0.2717	0.2805	0.2228

Table A- 40 AASHTO T380 20% NP 5 + 80% Cement (Fine Reactive Aggregate)

NP5	Wednesday, June 9, 2021	Thursday, June 10, 2021	1	Demold, label, and place in a 23 water container, then place in 60C oven for 24 hrs				
		Friday, June 11, 2021	0	0.0184	0.2888	0.2750	0.2847	0.2736
		Monday, June 14, 2021	3	0.0184	0.2885	0.2744	0.2844	0.2727
		Friday, June 18, 2021	7	0.0180	0.2886	0.2747	0.2849	0.2730
		Monday, June 21, 2021	10	0.0179	0.2890	0.2749	0.2852	0.2734
		Friday, June 25, 2021	14	0.0178	0.2897	0.2756	0.2857	0.2741
		Tuesday, June 29, 2021	18	0.0176	0.2903	0.2758	0.2860	0.2744
		Friday, July 2, 2021	21	0.0177	0.2909	0.2765	0.2864	0.2749
		Monday, July 5, 2021	24	0.0172	0.2917	0.2773	0.2874	0.2758
		Friday, July 9, 2021	28	0.0169	0.2917	0.2772	0.2873	0.2757
		Monday, July 12, 2021	31	0.0176	0.2932	0.2787	0.2888	0.2771
		Friday, July 16, 2021	35	0.0170	0.2933	0.2787	0.2888	0.2772
		Friday, July 23, 2021	42	0.0168	0.2941	0.2796	0.2896	0.2779
		Friday, July 30, 2021	49	0.0168	0.2949	0.2805	0.2904	0.2788
		Friday, August 6, 2021	56	0.0170	0.2968	0.2824	0.2925	0.2804
		Friday, August 13, 2021	63	0.0169	0.2983	0.2839	0.2936	0.2817
		Friday, August 20, 2021	70	0.0166	0.2995	0.2858	0.2950	0.2830
		Friday, August 27, 2021	77	0.0166	0.3006	0.2867	0.2958	0.2837
		Friday, September 3, 2021	84	0.0166	0.3006	0.2867	0.2965	0.2837

Table A- 41 AASHTO T380 20% NP 6 + 80% Cement (Fine Reactive Aggregate)

NP6	Wednesday, June 9, 2021	Thursday, June 10, 2021	1	Demold, label, and place in a 23 water container, then place in 60C oven for 24 hrs				
		Friday, June 11, 2021	0	0.0184	0.2655	0.2516	0.2528	0.2775
		Monday, June 14, 2021	3	0.0182	0.2649	0.2510	0.2521	0.2770
		Friday, June 18, 2021	7	0.0180	0.2650	0.2514	0.2525	0.2771
		Monday, June 21, 2021	10	0.0178	0.2649	0.2512	0.2523	0.2769
		Friday, June 25, 2021	14	0.0178	0.2651	0.2510	0.2523	0.2770
		Tuesday, June 29, 2021	18	0.0176	0.2653	0.2515	0.2526	0.2774
		Friday, July 2, 2021	21	0.0177	0.2662	0.2524	0.2534	0.2781
		Monday, July 5, 2021	24	0.0172	0.2662	0.2527	0.2536	0.2782
		Friday, July 9, 2021	28	0.0169	0.2658	0.2521	0.2531	0.2778
		Monday, July 12, 2021	31	0.0176	0.2671	0.2535	0.2545	0.2791
		Friday, July 16, 2021	35	0.0170	0.2674	0.2539	0.2549	0.2794
		Friday, July 23, 2021	42	0.0168	0.2677	0.2541	0.2552	0.2797
		Friday, July 30, 2021	49	0.0168	0.2688	0.2553	0.2562	0.2808
		Friday, August 6, 2021	56	0.0169	0.2704	0.2567	0.2577	0.2822
		Friday, August 13, 2021	63	0.0168	0.2710	0.2572	0.2582	0.2827
		Friday, August 20, 2021	70	0.0166	0.2719	0.2583	0.2593	0.2834
		Friday, August 27, 2021	77	0.0166	0.2728	0.2595	0.2603	0.2844
		Friday, September 3, 2021	84	0.0166	0.2733	0.2604	0.2612	0.2860

Table A- 42 AASHTO T380 20% RFA 1 + 80% Cement (Fine Reactive Aggregate)

RFA1	Wednesday, June 2, 2021	Thursday, June 3, 2021	1	Demold, label, and place in a 23 water container, then place in 60C oven for 24 hrs				
		Friday, June 4, 2021	0	0.0183	0.2888	0.2350	0.2805	0.2655
		Monday, June 7, 2021	3	0.0185	0.2888	0.2357	0.2804	0.2656
		Friday, June 11, 2021	7	0.0184	0.2894	0.2350	0.2812	0.2662
		Monday, June 14, 2021	10	0.0183	0.2904	0.2364	0.2823	0.2673
		Friday, June 18, 2021	14	0.0182	0.2928	0.2386	0.2845	0.2699
		Tuesday, June 22, 2021	18	0.0183	0.2944	0.2403	0.2862	0.2718
		Friday, June 25, 2021	21	0.0178	0.2961	0.2418	0.2877	0.2736
		Monday, June 28, 2021	24	0.0178	0.2975	0.2431	0.2893	0.2749
		Friday, July 2, 2021	28	0.0178	0.2997	0.2454	0.2916	0.2774
		Monday, July 5, 2021	31	0.0172	0.3007	0.2461	0.2925	0.2783
		Friday, July 9, 2021	35	0.0169	0.3016	0.2470	0.2936	0.2791
		Friday, July 16, 2021	42	0.0178	0.3036	0.2489	0.2954	0.2812
		Friday, July 23, 2021	49	0.0169	0.3057	0.2512	0.2978	0.2833
		Friday, July 30, 2021	56	0.0170	0.3072	0.2527	0.2994	0.2848
		Friday, August 6, 2021	63	0.0173	0.3102	0.2555	0.3024	0.2875
		Friday, August 13, 2021	70	0.0170	0.3124	0.2575	0.3046	0.2896
		Friday, August 20, 2021	77	0.0168	0.3145	0.2595	0.3068	0.2913
		Friday, August 27, 2021	84	0.0165	0.3152	0.2610	0.3082	0.2921

Table A- 43 AASHTO T380 20% RFA 2 + 80% Cement (Fine Reactive Aggregate)

RFA2	Wednesday, June 9, 2021	Thursday, June 10, 2021	1	Demold, label, and place in a 23 water container, then place in 60C oven for 24 hrs			
		Friday, June 11, 2021	0	0.0184	0.2720	0.2435	0.2823	0.2552
		Monday, June 14, 2021	3	0.0182	0.2718	0.2432	0.2821	0.2546
		Friday, June 18, 2021	7	0.0179	0.2718	0.2431	0.2817	0.2547
		Monday, June 21, 2021	10	0.0179	0.2727	0.2437	0.2826	0.2556
		Friday, June 25, 2021	14	0.0178	0.2736	0.2447	0.2840	0.2570
		Tuesday, June 29, 2021	18	0.0176	0.2740	0.2450	0.2842	0.2576
		Friday, July 2, 2021	21	0.0177	0.2760	0.2471	0.2862	0.2595
		Monday, July 5, 2021	24	0.0171	0.2769	0.2481	0.2870	0.2602
		Friday, July 9, 2021	28	0.0169	0.2777	0.2491	0.2879	0.2614
		Monday, July 12, 2021	31	0.0176	0.2796	0.2511	0.2899	0.2633
		Friday, July 16, 2021	35	0.0170	0.2797	0.2512	0.2899	0.2633
		Friday, July 23, 2021	42	0.0169	0.2816	0.2532	0.2918	0.2652
		Friday, July 30, 2021	49	0.0167	0.2828	0.2543	0.2928	0.2664
		Friday, August 6, 2021	56	0.0170	0.2856	0.2573	0.2958	0.2694
		Friday, August 13, 2021	63	0.0169	0.2871	0.2588	0.2971	0.2708
		Friday, August 20, 2021	70	0.0166	0.2892	0.2609	0.2990	0.2737
		Friday, August 27, 2021	77	0.0166	0.2900	0.2624	0.3005	0.2752
		Friday, September 3, 2021	84	0.0167	0.2910	0.2636	0.3014	0.2761

Table A- 44 AASHTO T380 30% NP 2 + 70% Cement (Coarse Reactive Aggregate)

NP 2	Wednesday, November 17, 2021	Thursday, November 11, 2021	1	Demold, label, and place in a 23 water container, then place in 60C oven for 24 hrs			
		Friday, November 19, 2021	0	0.0174	0.2929	0.2746	0.2818	0.2937
		Thursday, January 5, 1900	3	0.0173	0.2933	0.2749	0.2822	0.2939
		Monday, January 9, 1900	7	0.0169	0.2934	0.2749	0.2822	0.2939
		Thursday, January 12, 1900	10	0.0171	0.2936	0.2751	0.2824	0.2941
		Monday, January 16, 1900	14	0.0161	0.2928	0.2743	0.2815	0.2931
		Thursday, January 19, 1900	17	0.0169	0.2936	0.2753	0.2827	0.2940
		Monday, January 23, 1900	21	0.0169	0.2936	0.2753	0.2832	0.2940
		Thursday, January 26, 1900	24	0.0167	0.2934	0.2751	0.2830	0.2938
		Monday, January 30, 1900	28	0.0168	0.2936	0.2753	0.2833	0.2939
		Thursday, February 2, 1900	31	0.0169	0.2937	0.2756	0.2836	0.2942
		Monday, February 6, 1900	35	0.0167	0.2937	0.2755	0.2835	0.2938
		Monday, February 13, 1900	42	0.0169	0.2942	0.2760	0.2838	0.2942
		Monday, February 20, 1900	49	0.0172	0.2947	0.2763	0.2845	0.2949
		Monday, February 27, 1900	56	0.0175	0.2949	0.2766	0.2848	0.2953
		Monday, March 5, 1900	63	0.0178	0.2953	0.2766	0.2853	0.2953
		Monday, March 12, 1900	70	0.0177	0.2953	0.2766	0.2852	0.2952
		Monday, March 19, 1900	77	0.0172	0.2948	0.2762	0.2845	0.2947
		Monday, March 26, 1900	84	0.0174	0.2949	0.2763	0.2847	0.2947

Table A- 45 AASHTO T380 40% NP 2 + 60% Cement (Coarse Reactive Aggregate)

NP 2	Wednesday, November 17, 2021	Thursday, November 18, 2021	1	Demold, label, and place in a 23 water container, then place in 60C oven for 24 hrs			
		Friday, November 19, 2021	0	0.0173	0.2580	0.2417	0.2905	0.2879
		Monday, November 22, 2021	3	0.0173	0.2583	0.2416	0.2910	0.2881
		Friday, November 26, 2021	7	0.0169	0.2579	0.2414	0.2908	0.2879
		Monday, November 29, 2021	10	0.0172	0.2582	0.2417	0.2905	0.2882
		Friday, December 3, 2021	14	0.0161	0.2572	0.2408	0.2896	0.2874
		Monday, December 6, 2021	17	0.0169	0.2579	0.2417	0.2906	0.2886
		Friday, December 10, 2021	21	0.0169	0.2582	0.2417	0.2908	0.2888
		Monday, December 13, 2021	24	0.0168	0.2583	0.2418	0.2908	0.2888
		Friday, December 17, 2021	28	0.0168	0.2584	0.2419	0.2908	0.2890
		Monday, December 20, 2021	31	0.0168	0.2585	0.2418	0.2908	0.2889
		Friday, December 24, 2021	35	0.0167	0.2585	0.2417	0.2908	0.2889
		Friday, December 31, 2021	42	0.0168	0.2586	0.2427	0.2909	0.2890
		Friday, January 7, 2022	49	0.0171	0.2592	0.2429	0.2915	0.2897
		Friday, January 14, 2022	56	0.0174	0.2599	0.2432	0.2918	0.2903
		Friday, January 21, 2022	63	0.0179	0.2604	0.2438	0.2922	0.2909
		Friday, January 28, 2022	70	0.0177	0.2602	0.2436	0.2921	0.2907
		Friday, February 4, 2022	77	0.0173	0.2598	0.2431	0.2917	0.2903
		Friday, February 11, 2022	84	0.0175	0.2600	0.2434	0.2915	0.2903

Table A- 46 AASHTO T380 30% NP 4 + 70% Cement (Coarse Reactive Aggregate)

NP 4	Wednesday, November 17, 2021	Thursday, November 18, 2021	1	Demold, label, and place in a 23 water container, then place in 60C oven for 24 hrs				
		Friday, November 19, 2021	0	0.0174	0.3214	0.2700	0.3204	0.2947
		Monday, November 22, 2021	3	0.0173	0.3222	0.2705	0.3207	0.2945
		Friday, November 26, 2021	7	0.0169	0.3219	0.2701	0.3206	0.2942
		Monday, November 29, 2021	10	0.0171	0.3219	0.2701	0.3206	0.2943
		Friday, December 3, 2021	14	0.0161	0.3211	0.2691	0.3199	0.2936
		Monday, December 6, 2021	17	0.0168	0.3217	0.2701	0.3204	0.2942
		Friday, December 10, 2021	21	0.0168	0.3219	0.2702	0.3206	0.2943
		Monday, December 13, 2021	24	0.0167	0.3217	0.2702	0.3208	0.2943
		Friday, December 17, 2021	28	0.0165	0.3216	0.2700	0.3203	0.2939
		Monday, December 20, 2021	31	0.0168	0.3220	0.2703	0.3207	0.2942
		Friday, December 24, 2021	35	0.0168	0.3219	0.2702	0.3207	0.2942
		Friday, December 31, 2021	42	0.0167	0.3220	0.2702	0.3206	0.2941
		Friday, January 7, 2022	49	0.0170	0.3225	0.2708	0.3212	0.2949
		Friday, January 14, 2022	56	0.0172	0.3233	0.2716	0.3222	0.2961
		Friday, January 21, 2022	63	0.0176	0.3238	0.2722	0.3230	0.2964
		Friday, January 28, 2022	70	0.0175	0.3240	0.2721	0.3222	0.2964
		Friday, February 4, 2022	77	0.0170	0.3236	0.2717	0.3215	0.2959
		Friday, February 11, 2022	84	0.0173	0.3238	0.2720	0.3215	0.2962

Table A- 47 AASHTO T380 40% NP 4 + 60% Cement (Coarse Reactive Aggregate)

NP 4	Wednesday, November 17, 2021	Thursday, November 18, 2021	1	Demold, label, and place in a 23 water container, then place in 60C oven for 24 hrs				
		Friday, November 19, 2021	0	0.0173	0.2773	0.2763	0.2403	0.2293
		Monday, November 22, 2021	3	0.0176	0.2776	0.2765	0.2400	0.2292
		Friday, November 26, 2021	7	0.0169	0.2771	0.2762	0.2398	0.2289
		Monday, November 29, 2021	10	0.0171	0.2773	0.2764	0.2400	0.2290
		Friday, December 3, 2021	14	0.0161	0.2763	0.2754	0.2389	0.2279
		Monday, December 6, 2021	17	0.0167	0.2771	0.2761	0.2397	0.2286
		Friday, December 10, 2021	21	0.0168	0.2772	0.2760	0.2399	0.2286
		Monday, December 13, 2021	24	0.0167	0.2771	0.2760	0.2399	0.2284
		Friday, December 17, 2021	28	0.0167	0.2773	0.2760	0.2398	0.2285
		Monday, December 20, 2021	31	0.0168	0.2775	0.2762	0.2400	0.2287
		Friday, December 24, 2021	35	0.0166	0.2776	0.2762	0.2397	0.2286
		Friday, December 31, 2021	42	0.0167	0.2778	0.2764	0.2401	0.2290
		Friday, January 7, 2022	49	0.0169	0.2783	0.2767	0.2406	0.2295
		Friday, January 14, 2022	56	0.0172	0.2788	0.2778	0.2415	0.2304
		Friday, January 21, 2022	63	0.0176	0.2793	0.2784	0.2420	0.2304
		Friday, January 28, 2022	70	0.0173	0.2789	0.2779	0.2417	0.2304
		Friday, February 4, 2022	77	0.0170	0.2786	0.2773	0.2413	0.2302
		Friday, February 11, 2022	84	0.0173	0.2788	0.2775	0.2414	0.2305

Table A- 48 AASHTO T380 30% NP 5 + 70% Cement (Coarse Reactive Aggregate)

NP 5	Wednesday, November 17, 2021	Thursday, November 18, 2021	1	Demold, label, and place in a 23 water container, then place in 60C oven for 24 hrs				
		Friday, November 19, 2021	0	0.0173	0.2990	0.2976	0.2679	0.2795
		Monday, November 22, 2021	3	0.0173	0.2993	0.2977	0.2676	0.2793
		Friday, November 26, 2021	7	0.0169	0.2992	0.2978	0.2668	0.2787
		Monday, November 29, 2021	10	0.0171	0.2992	0.2979	0.2668	0.2787
		Friday, December 3, 2021	14	0.0161	0.2983	0.2970	0.2658	0.2778
		Monday, December 6, 2021	17	0.0168	0.2992	0.2977	0.2665	0.2785
		Friday, December 10, 2021	21	0.0169	0.2993	0.2980	0.2668	0.2788
		Monday, December 13, 2021	24	0.0167	0.2992	0.2979	0.2667	0.2789
		Friday, December 17, 2021	28	0.0166	0.2991	0.2978	0.2665	0.2787
		Monday, December 20, 2021	31	0.0168	0.2993	0.2982	0.2667	0.2789
		Friday, December 24, 2021	35	0.0168	0.2993	0.2980	0.2665	0.2788
		Friday, December 31, 2021	42	0.0168	0.2995	0.2983	0.2669	0.2790
		Friday, January 7, 2022	49	0.0170	0.3000	0.2990	0.2672	0.2797
		Friday, January 14, 2022	56	0.0172	0.3006	0.2995	0.2689	0.2803
		Friday, January 21, 2022	63	0.0177	0.3011	0.3005	0.2691	0.2815
		Friday, January 28, 2022	70	0.0176	0.3010	0.3003	0.2690	0.2814
		Friday, February 4, 2022	77	0.0170	0.3005	0.2997	0.2687	0.2808
		Friday, February 11, 2022	84	0.0170	0.3004	0.2995	0.2687	0.2805

Table A- 49 AASHTO T380 40% NP 5 + 60% Cement (Coarse Reactive Aggregate)

NP 5	Wednesday, November 17, 2021	Thursday, November 18, 2021	1	Demold, label, and place in a 23 water container, then place in 60C oven for 24 hrs				
		Friday, November 19, 2021	0	0.0174	0.2606	0.2723	0.2695	0.2773
		Monday, November 22, 2021	3	0.0173	0.2610	0.2731	0.2705	0.2778
		Friday, November 26, 2021	7	0.0169	0.2607	0.2730	0.2700	0.2776
		Monday, November 29, 2021	10	0.0172	0.2610	0.2733	0.2703	0.2778
		Friday, December 3, 2021	14	0.0161	0.2600	0.2723	0.2692	0.2766
		Monday, December 6, 2021	17	0.0168	0.2608	0.2729	0.2699	0.2772
		Friday, December 10, 2021	21	0.0169	0.2607	0.2731	0.2697	0.2774
		Monday, December 13, 2021	24	0.0168	0.2604	0.2731	0.2696	0.2773
		Friday, December 17, 2021	28	0.0166	0.2604	0.2727	0.2698	0.2769
		Monday, December 20, 2021	31	0.0168	0.2607	0.2730	0.2699	0.2771
		Friday, December 24, 2021	35	0.0168	0.2607	0.2729	0.2698	0.2771
		Friday, December 31, 2021	42	0.0167	0.2607	0.2730	0.2698	0.2773
		Friday, January 7, 2022	49	0.0170	0.2610	0.2734	0.2702	0.2776
		Friday, January 14, 2022	56	0.0172	0.2614	0.2738	0.2706	0.2780
		Friday, January 21, 2022	63	0.0177	0.2623	0.2748	0.2715	0.2791
		Friday, January 28, 2022	70	0.0178	0.2628	0.2750	0.2715	0.2792
		Friday, February 4, 2022	77	0.0171	0.2620	0.2741	0.2709	0.2787
		Friday, February 11, 2022	84	0.0170	0.2618	0.2740	0.2707	0.2786

Table A- 50 AASHTO T380 30% RFA 1 + 70% Cement (Coarse Reactive Aggregate)

RFA 1	Wednesday, November 10, 2021	Thursday, November 11, 2021	1	Demold, label, and place in a 23 water container, then place in 60C oven for 24 hrs				
		Friday, November 12, 2021	0	0.0162	0.2379	0.2719	0.2830	0.2841
		Monday, November 15, 2021	3	0.0166	0.2380	0.2721	0.2834	0.2846
		Friday, November 19, 2021	7	0.0175	0.2390	0.2728	0.2845	0.2856
		Monday, November 22, 2021	10	0.0174	0.2392	0.2732	0.2848	0.2858
		Friday, November 26, 2021	14	0.0170	0.2390	0.2730	0.2848	0.2858
		Monday, November 29, 2021	17	0.0174	0.2397	0.2741	0.2854	0.2865
		Friday, December 3, 2021	21	0.0163	0.2388	0.2734	0.2848	0.2856
		Monday, December 6, 2021	24	0.0171	0.2400	0.2744	0.2860	0.2866
		Friday, December 10, 2021	28	0.0172	0.2402	0.2745	0.2864	0.2868
		Monday, December 13, 2021	31	0.0172	0.2404	0.2747	0.2864	0.2869
		Friday, December 17, 2021	35	0.0170	0.2402	0.2746	0.2864	0.2868
		Friday, December 24, 2021	42	0.0170	0.2407	0.2748	0.2870	0.2872
		Friday, December 31, 2021	49	0.0169	0.2414	0.2758	0.2878	0.2881
		Friday, January 7, 2022	56	0.0174	0.2419	0.2769	0.2885	0.2885
		Friday, January 14, 2022	63	0.0175	0.2425	0.2766	0.2894	0.2883
		Friday, January 21, 2022	70	0.0184	0.2434	0.2771	0.2901	0.2888
		Friday, January 28, 2022	77	0.0181	0.2432	0.2769	0.2900	0.2889
		Friday, February 4, 2022	84	0.0173	0.2427	0.2761	0.2893	0.2882

Table A- 51 AASHTO T380 40% RFA 1 + 60% Cement (Coarse Reactive Aggregate)

RFA 1	Wednesday, November 10, 2021	Thursday, November 11, 2021	1	Demold, label, and place in a 23 water container, then place in 60C oven for 24 hrs				
		Friday, November 12, 2021	0	0.0160	0.2728	0.2650	0.2855	0.2335
		Monday, November 15, 2021	3	0.0165	0.2731	0.2652	0.2860	0.2337
		Friday, November 19, 2021	7	0.0174	0.2740	0.2658	0.2863	0.2348
		Monday, November 22, 2021	10	0.0173	0.2743	0.2665	0.2860	0.2346
		Friday, November 26, 2021	14	0.0171	0.2740	0.2658	0.2856	0.2344
		Monday, November 29, 2021	17	0.0174	0.2745	0.2665	0.2861	0.2348
		Friday, December 3, 2021	21	0.0162	0.2734	0.2654	0.2853	0.2338
		Monday, December 6, 2021	24	0.0171	0.2746	0.2661	0.2863	0.2348
		Friday, December 10, 2021	28	0.0171	0.2748	0.2662	0.2862	0.2349
		Monday, December 13, 2021	31	0.0171	0.2748	0.2662	0.2862	0.2349
		Friday, December 17, 2021	35	0.0168	0.2748	0.2661	0.2860	0.2347
		Friday, December 24, 2021	42	0.0169	0.2751	0.2664	0.2862	0.2348
		Friday, December 31, 2021	49	0.0169	0.2754	0.2667	0.2864	0.2350
		Friday, January 7, 2022	56	0.0175	0.2761	0.2673	0.2869	0.2358
		Friday, January 14, 2022	63	0.0175	0.2764	0.2676	0.2873	0.2362
		Friday, January 21, 2022	70	0.0183	0.2779	0.2690	0.2881	0.2370
		Friday, January 28, 2022	77	0.0181	0.2778	0.2689	0.2880	0.2368
		Friday, February 4, 2022	84	0.0170	0.2765	0.2679	0.2874	0.2361

Table A- 52 30% RFA 2 + 70% Cement (Coarse Reactive Aggregate)

RFA 2	Wednesday, November 10, 2021	Thursday, November 11, 2021	1	Demold, label, and place in a 23 water container, then place in 60C oven for 24 hrs				
		Friday, November 12, 2021	0	0.0160	0.2922	0.2813	0.2713	0.2702
		Monday, November 15, 2021	3	0.0166	0.2923	0.2816	0.2716	0.2706
		Friday, November 19, 2021	7	0.0173	0.2930	0.2826	0.2724	0.2714
		Monday, November 22, 2021	10	0.0173	0.2932	0.2827	0.2723	0.2716
		Friday, November 26, 2021	14	0.0170	0.2928	0.2825	0.2720	0.2712
		Monday, November 29, 2021	17	0.0173	0.2933	0.2831	0.2724	0.2716
		Friday, December 3, 2021	21	0.0162	0.2922	0.2823	0.2713	0.2705
		Monday, December 6, 2021	24	0.0170	0.2933	0.2831	0.2726	0.2714
		Friday, December 10, 2021	28	0.0170	0.2933	0.2830	0.2727	0.2717
		Monday, December 13, 2021	31	0.0169	0.2935	0.2827	0.2724	0.2716
		Friday, December 17, 2021	35	0.0168	0.2932	0.2828	0.2725	0.2717
		Friday, December 24, 2021	42	0.0168	0.2934	0.2829	0.2724	0.2715
		Friday, December 31, 2021	49	0.0169	0.2936	0.2833	0.2727	0.2718
		Friday, January 7, 2022	56	0.0173	0.2944	0.2839	0.2735	0.2725
		Friday, January 14, 2022	63	0.0175	0.2949	0.2844	0.2738	0.2728
		Friday, January 21, 2022	70	0.0182	0.2955	0.2854	0.2742	0.2736
		Friday, January 28, 2022	77	0.0177	0.2950	0.2849	0.2738	0.2732
		Friday, February 4, 2022	84	0.0171	0.2944	0.2844	0.2733	0.2725

Table A- 53 AASHTO T380 40% RFA 2 + 60% Cement (Coarse Reactive Aggregate)

RFA 2	Wednesday, November 10, 2021	Thursday, November 11, 2021	1	Demold, label, and place in a 23 water container, then place in 60C oven for 24 hrs				
		Friday, November 12, 2021	0	0.0159	0.2606	0.2635	0.3190	0.2877
		Monday, November 15, 2021	3	0.0164	0.2607	0.2637	0.3192	0.2883
		Friday, November 19, 2021	7	0.0173	0.2611	0.2646	0.3200	0.2889
		Monday, November 22, 2021	10	0.0173	0.2609	0.2645	0.3200	0.2889
		Friday, November 26, 2021	14	0.0169	0.2605	0.2641	0.3197	0.2885
		Monday, November 29, 2021	17	0.0173	0.2608	0.2644	0.3200	0.2887
		Friday, December 3, 2021	21	0.0161	0.2597	0.2633	0.3188	0.2875
		Monday, December 6, 2021	24	0.0170	0.2608	0.2642	0.3198	0.2885
		Friday, December 10, 2021	28	0.0170	0.2608	0.2643	0.3198	0.2885
		Monday, December 13, 2021	31	0.0168	0.2604	0.2640	0.3195	0.2882
		Friday, December 17, 2021	35	0.0168	0.2606	0.2642	0.3198	0.2884
		Friday, December 24, 2021	42	0.0168	0.2604	0.2641	0.3194	0.2881
		Friday, December 31, 2021	49	0.0169	0.2605	0.2644	0.3199	0.2884
		Friday, January 7, 2022	56	0.0172	0.2608	0.2648	0.3201	0.2887
		Friday, January 14, 2022	63	0.0174	0.2619	0.2653	0.3205	0.2893
		Friday, January 21, 2022	70	0.0180	0.2625	0.2664	0.3213	0.2899
		Friday, January 28, 2022	77	0.0177	0.2630	0.2664	0.3211	0.2900
		Friday, February 4, 2022	84	0.0170	0.2622	0.2657	0.3206	0.2894

Table A- 54 AASHTO T380 Control (Job Mix)

0.45 w/c Control boosted	Wednesday, July 19, 2023	Thursday, July 20, 2023	1	Demold, label, and place in a 23 water container, then place in 80C oven for 24 hrs				
		Friday, July 21, 2023	0	0.0110	0.2883	0.2746	0.2822	0.2755
		Monday, July 24, 2023	3	0.0089	0.2865	0.2727	0.2806	0.2740
		Friday, July 28, 2023	7	0.0086	0.2874	0.2736	0.2819	0.2752
		Monday, July 31, 2023	10	0.0089	0.2894	0.2750	0.2832	0.2763
		Friday, August 4, 2023	14	0.0088	0.2929	0.2785	0.2867	0.2798
		Monday, August 7, 2023	17	0.0083	0.2951	0.2801	0.2885	0.2815
		Friday, August 11, 2023	21	0.0091	0.2974	0.2822	0.2903	0.2837
		Tuesday, August 15, 2023	25	0.0079	0.2987	0.2831	0.2908	0.2843
		Friday, August 18, 2023	28	0.0078	0.2998	0.2837	0.2912	0.2851
		Tuesday, August 22, 2023	32	0.0079	0.3000	0.2837	0.2912	0.2851
		Friday, August 25, 2023	35	0.0080	0.3009	0.2846	0.2916	0.2857
		Friday, September 1, 2023	42	0.0081	0.3017	0.2849	0.2920	0.2862
		Friday, September 8, 2023	49	0.0082	0.3039	0.2866	0.2936	0.2877
		Friday, September 15, 2023	56	0.0086	0.3050	0.2875	0.2945	0.2888
		Friday, September 22, 2023	63	0.0079	0.3056	0.2883	0.2945	
		Friday, September 29, 2023	70	0.0080	0.3071	0.2890	0.2961	
		Friday, October 6, 2023	77	0.0081	0.3074	0.2909	0.2973	
		Friday, October 13, 2023	84	0.0087	0.3090	0.2917	0.2982	

Table A- 55 AASHTO T380 Control Unboosted (Job Mix)

0.45 w/c Control unboosted	Wednesday, July 19, 2023	Thursday, July 20, 2023	1	Demold, label, and place in a 23 water container, then place in 60C oven for 24 hrs				
		Friday, July 21, 2023	0	0.0110	0.2858	0.2767	0.2799	0.2578
		Monday, July 24, 2023	3	0.0091	0.2840	0.2752	0.2776	0.2557
		Friday, July 28, 2023	7	0.0086	0.2842	0.2754	0.2777	0.2559
		Monday, July 31, 2023	10	0.0088	0.2854	0.2769	0.2787	0.2569
		Friday, August 4, 2023	14	0.0088	0.2868	0.2794	0.2808	0.2592
		Monday, August 7, 2023	17	0.0080	0.2882	0.2801	0.2811	0.2597
		Friday, August 11, 2023	21	0.0091	0.2919	0.2835	0.2845	0.2632
		Tuesday, August 15, 2023	25	0.0077	0.2930	0.2841	0.2852	0.2640
		Friday, August 18, 2023	28	0.0080	0.2948	0.2851	0.2864	0.2653
		Tuesday, August 22, 2023	32	0.0079	0.2962	0.2867	0.2881	0.2675
		Friday, August 25, 2023	35	0.0080	0.2972	0.2875	0.2897	0.2686
		Friday, September 1, 2023	42	0.0080	0.2990	0.2894	0.2913	0.2698
		Friday, September 8, 2023	49	0.0084	0.3006	0.2913	0.2934	0.2718
		Friday, September 15, 2023	56	0.0085	0.3020	0.2920	0.2946	0.2731
		Friday, September 22, 2023	63	0.0080	0.3030	0.2927		0.2733
		Friday, September 29, 2023	70	0.0081	0.3040	0.2948		0.2743
		Friday, October 6, 2023	77	0.0082	0.3047	0.2960		0.2754
		Friday, October 13, 2023	84	0.0087	0.3060	0.2974		0.2765

Table A- 56 AASHTO T380 0.35 w/c Unboosted (Job Mix)

0.35 w/c unboosted	Wednesday, July 19, 2023	Thursday, July 20, 2023	1	Demold, label, and place in a 23 water container, then place in 60C oven for 24 hrs				
		Friday, July 21, 2023	0	0.0105	0.2894	0.2989	0.2603	0.2686
		Monday, July 24, 2023	3	0.0088	0.2873	0.2977	0.2592	0.2669
		Friday, July 28, 2023	7	0.0086	0.2877	0.2982	0.2592	0.2672
		Monday, July 31, 2023	10	0.0089	0.2889	0.2995	0.2607	0.2687
		Friday, August 4, 2023	14	0.0086	0.2900	0.3006	0.2616	0.2699
		Monday, August 7, 2023	17	0.0081	0.2915	0.3020	0.2631	0.2716
		Friday, August 11, 2023	21	0.0090	0.2927	0.3030	0.2642	0.2730
		Tuesday, August 15, 2023	25	0.0078	0.2922	0.3026	0.2634	0.2728
		Friday, August 18, 2023	28	0.0078	0.2929	0.3033	0.2643	0.2738
		Tuesday, August 22, 2023	32	0.0080	0.2938	0.3042	0.2680	0.2745
		Friday, August 25, 2023	35	0.0080	0.2947	0.3051	0.2658	0.2755
		Friday, September 1, 2023	42	0.0081	0.2952	0.3055	0.2659	0.2757
		Friday, September 8, 2023	49	0.0084	0.2964	0.3064	0.2672	0.2768
		Friday, September 15, 2023	56	0.0083	0.2969	0.3070	0.2677	0.2773
		Friday, September 22, 2023	63	0.0080	0.2976		0.2683	0.2782
		Friday, September 29, 2023	70	0.0081	0.2985		0.2691	0.2789
		Friday, October 6, 2023	77	0.0081	0.2992		0.2701	0.2797
		Friday, October 13, 2023	84	0.0089	0.3004		0.2713	0.2806

Table A- 57 AASHTO T380 0.55 w/c Unboosted (Job Mix)

0.55 w/c unboosted	Wednesday, July 19, 2023	Thursday, July 20, 2023	1	Demold, label, and place in a 23 water container, then place in 60C oven for 24 hrs				
		Friday, July 21, 2023	0	0.0108	0.2952	0.3053	0.2824	0.2654
		Monday, July 24, 2023	3	0.0088	0.2936	0.3038	0.2806	0.2634
		Friday, July 28, 2023	7	0.0087	0.2939	0.3041	0.2804	0.2633
		Monday, July 31, 2023	10	0.0088	0.2940	0.3041	0.2807	0.2639
		Friday, August 4, 2023	14	0.0086	0.2945	0.3051	0.2811	0.2648
		Monday, August 7, 2023	17	0.0081	0.2955	0.3061	0.2817	0.2655
		Friday, August 11, 2023	21	0.0090	0.2989	0.3093	0.2843	0.2683
		Tuesday, August 15, 2023	25	0.0078	0.2999	0.3105	0.2850	0.2691
		Friday, August 18, 2023	28	0.0080	0.3021	0.3129	0.2871	0.2712
		Tuesday, August 22, 2023	32	0.0080	0.3038	0.3151	0.2889	0.2729
		Friday, August 25, 2023	35	0.0080	0.3054	0.3159	0.2897	0.2737
		Friday, September 1, 2023	42	0.0080	0.3084	0.3190	0.2928	0.2769
		Friday, September 8, 2023	49	0.0082	0.3105	0.3209	0.2947	0.2787
		Friday, September 15, 2023	56	0.0083	0.3120	0.3223	0.2960	0.2806
		Friday, September 22, 2023	63	0.0079	0.3132	0.3237		0.2821
		Friday, September 29, 2023	70	0.0081	0.3144	0.3250		0.2829
		Friday, October 6, 2023	77	0.0082	0.3153	0.3260		0.2840
		Friday, October 13, 2023	84	0.0089	0.3164	0.3272		0.2854

Table A- 58 AASHTO T380 20% SCMs Replacement Level Unboosted (Job Mix)

20% NP unboosted	Wednesday, July 19, 2023	Thursday, July 20, 2023	1	Demold, label, and place in a 23 water container, then place in 60C oven for 24 hrs			
		Friday, July 21, 2023	0	0.0110	0.2878	0.2825	0.2608	0.2692
		Monday, July 24, 2023	3	0.0088	0.2850	0.2807	0.2583	0.2673
		Friday, July 28, 2023	7	0.0083	0.2848	0.2799	0.2575	0.2664
		Monday, July 31, 2023	10	0.0087	0.2844	0.2800	0.2571	0.2663
		Friday, August 4, 2023	14	0.0086	0.2852	0.2808	0.2585	0.2675
		Monday, August 7, 2023	17	0.0082	0.2843	0.2800	0.2575	0.2662
		Friday, August 11, 2023	21	0.0090	0.2843	0.2808	0.2587	0.2676
		Tuesday, August 15, 2023	25	0.0080	0.2841	0.2796	0.2572	0.2662
		Friday, August 18, 2023	28	0.0078	0.2842	0.2797	0.2572	0.2660
		Tuesday, August 22, 2023	32	0.0080	0.2845	0.2801	0.2579	0.2669
		Friday, August 25, 2023	35	0.0079	0.2842	0.2801	0.2580	0.2665
		Friday, September 1, 2023	42	0.0080	0.2845	0.2802	0.2576	0.2665
		Friday, September 8, 2023	49	0.0081	0.2849	0.2806	0.2583	0.2672
		Friday, September 15, 2023	56	0.0080	0.2848	0.2805	0.2580	0.2669
		Friday, September 22, 2023	63	0.0079		0.2809	0.2587	0.2676
		Friday, September 29, 2023	70	0.0081		0.2813	0.2593	0.2680
		Friday, October 6, 2023	77	0.0082		0.2813	0.2593	0.2681
		Friday, October 13, 2023	84	0.0089		0.2819	0.2600	0.2686

Table A- 59 AASHTO T380 30% SCMs Replacement Level Unboosted (Job Mix)

30% NP unboosted	Wednesday, July 19, 2023	Thursday, July 20, 2023	1	Demold, label, and place in a 23 water container, then place in 60C oven for 24 hrs			
		Friday, July 21, 2023	0	0.0088	0.2604	0.2604	0.2788	0.2677
		Monday, July 24, 2023	3	0.0089	0.2602	0.2598	0.2781	0.2680
		Friday, July 28, 2023	7	0.0086	0.2600	0.2592	0.2777	0.2678
		Monday, July 31, 2023	10	0.0088	0.2603	0.2593	0.2778	0.2678
		Friday, August 4, 2023	14	0.0088	0.2604	0.2592	0.2783	0.2679
		Monday, August 7, 2023	17	0.0080	0.2587	0.2585	0.2773	0.2672
		Friday, August 11, 2023	21	0.0090	0.2605	0.2595	0.2790	0.2680
		Tuesday, August 15, 2023	25	0.0080	0.2604	0.2592	0.2785	0.2680
		Friday, August 18, 2023	28	0.0080	0.2594	0.2583	0.2775	0.2671
		Tuesday, August 22, 2023	32	0.0080	0.2596	0.2584	0.2776	0.2671
		Friday, August 25, 2023	35	0.0078	0.2598	0.2584	0.2776	0.2672
		Friday, September 1, 2023	42	0.0078	0.2597	0.2586	0.2777	0.2677
		Friday, September 8, 2023	49	0.0080	0.2603	0.2591	0.2786	0.2682
		Friday, September 15, 2023	56	0.0080	0.2602	0.2592	0.2783	0.2679
		Friday, September 22, 2023	63	0.0078		0.2595	0.2786	0.2682
		Friday, September 29, 2023	70	0.0081		0.2598	0.2790	0.2686
		Friday, October 6, 2023	77	0.0080		0.2600	0.2791	0.2688
		Friday, October 13, 2023	84	0.0089		0.2607	0.2798	0.2695

Table A- 60 ASTM C311 7-D Strength Activity Index

7-day Compressive Strength						
		1	2	3	Average	Ratio
Control	Load (lb)	19960	19540	20520	20006.67	100.00%
	Strength (psi)	4991	4855	5130	4992	
NP1	Load (lb)	14180	13590	14250	14006.67	70.01%
	Strength (psi)	3544	3399	3563	3502	
NP2	Load (lb)	15260	13300	13540	14033.33	70.14%
	Strength (psi)	3816	3325	3385	3508.667	
NP3	Load (lb)	16720	17600	17430	17250	86.22%
	Strength (psi)	4181	4399	4358	4312.667	
NP4	Load (lb)	21410	18240	19790	19813.33	99.03%
	Strength (psi)	5352	4559	4948	4953	
NP5	Load (lb)	16700	19210	15790	17233.33	86.14%
	Strength (psi)	4412	4904	3948	4421.333	
NP6	Load (lb)	15040	18150	16770	16653.33	83.24%
	Strength (psi)	3760	4537	4193	4163.333	
NP7	Load (lb)	17650	17600	16470	17240	86.17%
	Strength (psi)	4412	4399	4118	4309.667	
NP8	Load (lb)	17700	17530	15730	16986.67	84.91%
	Strength (psi)	4424	4383	3933	4246.667	

Table A- 61 ASTM C311 28-D Strength Activity Index

28-day Compressive Strength						
		1	2	3	Average	Ratio
Control	Load (lb)	24290	24720	22380	23796.67	100.00%
	Strength (psi)	6072	6181	5596	5949.667	
NP1	Load (lb)	20840	19920	17930	19563.33	82.21%
	Strength (psi)	5211	4981	4483	4891.667	
NP2	Load (lb)	17010	18070	18370	17816.67	74.87%
	Strength (psi)	4253	4518	4593	4454.667	
NP3	Load (lb)	25780	18060	17800	20546.67	86.34%
	Strength (psi)	6446	4514	4451	5137	
NP4	Load (lb)	24840	24860	26750	25483.33	107.09%
	Strength (psi)	6211	6214	6689	6371.333	
NP5	Load (lb)	21880	21880	25180	22980	96.57%
	Strength (psi)	5469	5471	6295	5745	
NP6	Load (lb)	24560	21370	20090	22006.67	92.48%
	Strength (psi)	6139	5343	5021	5501	
NP7	Load (lb)	23770	21880	22230	22626.67	95.08%
	Strength (psi)	5942	5469	5558	5656.333	
NP8	Load (lb)	28200	26390	25340	26643.33	111.96%
	Strength (psi)	7051	6598	6360	6669.667	

Table A- 62 ASTM C311 Water Demand

	Water (g)	w/c	Flow (cm)	% Flow	Flow Ratio	Water Ratio
Control	242	0.484	15.7	0.57	1	100.0%
NP 1	285	0.55	15	0.5	87.7%	117.8%
NP 2	240	0.48	15.5	0.55	96.5%	99.2%
NP 3	250	0.49	15.2	0.52	91.2%	103.3%
NP 4	240	0.47	15.1	0.51	89.5%	99.2%
NP 5	245	0.48	15.1	0.51	89.5%	101.2%
NP 6	240	0.48	15.6	0.56	98.2%	99.2%
RFA 1	225	0.48	16.2	0.62	108.8%	93.0%
RFA 2	235	0.47	15.2	0.52	91.2%	97.1%

Table A- 63 Mortar Cubes Compressive Strength (20%,30%,40% SCMs Replacement)

7-day Compressive Strength				
	1	2	3	Average
Control (SAI)	4991	4855	5130	4992.00
Control	5166	4542	4706	4804.67
NP 2 20%	4181	4399	4358	4312.67
NP 2 30%	3827	3564	3539	3643.33
NP 2 40%	3213	3461	3394	3356.00
NP 4 20%	4412	4904	3948	4421.33
NP 4 30%	3233	3362	3231	3275.33
NP 4 40%	2940	2836	2760	2845.33
NP 5 20%	3760	4537	4193	4163.33
NP 5 30%	4407	4344	4342	4364.33
NP 5 40%	3648	3187	3784	3539.67
RFA 1 20%	3816	3325	3385	3508.67
RFA 1 30%	3322	3731	3916	3656.33
RFA 1 40%	2792	3024	2953	2923.00
RFA 2 20%	4412	4399	4118	4309.67
RFA 2 30%	4670	4630	4669	4656.33
RFA 2 40%	4512	4552	4321	4461.67

Table A- 64 Mortar Cubes Compressive Strength (20%,30%,40% SCMs Replacement)

28-day Compressive Strength				
	1	2	3	Average
Control (SAI)	6072	6181	5596	5949.67
Control	5627	6068	5685	5793.33
NP 2 20%	6446	4514	4451	5137.00
NP 2 30%	4814	4446	4173	4477.67
NP 2 40%	3933	4539	4563	4345.00
NP 4 20%	5469	5471	6295	5745.00
NP 4 30%	5223	5125	5136	5161.33
NP 4 40%	4158	4683	4279	4373.33
NP 5 20%	6139	5343	5021	5501.00
NP 5 30%	5581	4948	5374	5301.00
NP 5 40%	5673	3531	3669	4291.00
RFA 1 20%	4253	4518	4593	4454.67
RFA 1 30%	5449	4586	5327	5120.67
RFA 1 40%	3868	4922	5327	4705.67
RFA 2 20%	7051	6598	6360	6669.67
RFA 2 30%	6987	6856	6160	6667.67
RFA 2 40%	5859	6561	4399	5606.33

Table A- 65 Concrete Cylinders Compressive Strength

		28-Day	Average	Ratio	56-Day	Average	Ratio	IncreaseRatio
Control	Control	4809	4816	100.00%	5503	5526.5	100.00%	14.75%
		4823			5550			
BFA	RFA 1	4431	4691.5	97.41%	5608	5606.5	101.45%	19.50%
		4952			5605			
Hess	NP 2	5134	4873.5	101.19%	4505	4986	90.22%	2.31%
		4613			5467			
Sunrise	NP 4	5620	5163	107.21%	5902	5824.5	105.39%	12.81%
		4706			5747			
NP	NP 5	5069	5506.5	114.34%	6112	6472	117.11%	17.53%
		5944			6832			
RFA	RFA 2	5651	5948	123.50%	6501	6489.5	117.43%	9.10%
		6245			6478			

Table A- 66 Mortar Flow Results (20%,30%,40% SCMs Replacement)

	w/c= 0.485			s/c= 2.25	
	Flow 1	Flow 2	Flow 3	Flow 4	Average
Control	21.9	22.2	22.2	21.7	22.00
RFA 1 20%	22.7	23.1	23	22.9	22.93
RFA 1 30%	23.4	23.6	23.8	23.4	23.55
RFA 1 40%	25	25	25	25	25.00
RFA 2 20%	20.8	20.6	20.2	20.6	20.55
RFA 2 30%	19.4	19.8	20.1	19.6	19.73
RFA 2 40%	16.7	16.6	16.7	16.6	16.65
NP 2 20%	20.3	20.7	20.8	20.3	20.53
NP 2 30%	20.2	20.8	20.2	20.4	20.40
NP 2 40%	19.6	19.7	19.8	19.4	19.63
NP 5 20%	19.8	19.6	19.8	19.6	19.70
NP 5 30%	19.1	19.3	19.6	19.2	19.30
NP 5 40%	18.3	18.3	17.9	18.3	18.20
NP 4 20%	20.9	21.2	20.9	20.9	20.98
NP 4 30%	25.4	24.6	24.4	24.6	24.75
NP 4 40%	25.4	25.4	25.4	25.4	25.40

Table A- 67 ASTM C596 Drying Shrinkage Control

Control	Thursday, January 20, 2022	Friday, January 21, 2022	1	Demold, label, and place in a 23 water container, then place in 80C oven for 24 hrs			
		Sunday, January 23, 2022	0	0.0184	0.2801	0.2641	0.2850	0.2658
		Thursday, January 27, 2022	4	0.0183	0.2770	0.2608	0.2819	0.2625
		Thursday, February 3, 2022	11	0.0178	0.2735	0.2572	0.2789	0.2590
		Thursday, February 10, 2022	18	0.0179	0.2723	0.2559	0.2776	0.2577
		Thursday, February 17, 2022	25	0.0176	0.2705	0.2542	0.2754	0.2560
		Thursday, March 3, 2022	39	0.0147	0.2671	0.2505	0.2721	0.2527
		Thursday, March 24, 2022	60	0.0153	0.2679	0.2512	0.2727	0.2533
		Thursday, April 14, 2022	81	0.0153	0.2677	0.2512	0.2728	0.2531
		Friday, May 13, 2022	110	0.0151	0.2675	0.2509	0.2726	0.2529

Table A- 68 ASTM C596 Drying Shrinkage --- 20% NP 2

NP 2	Thursday, January 20, 2022	Friday, January 21, 2022	1	Demold, label, and place in a 23 water container, then place in 60C oven for 24 hrs			
		Sunday, January 23, 2022	0	0.0183	0.2971	0.2744	0.2560	0.2854
		Thursday, January 27, 2022	4	0.0181	0.2936	0.2710	0.2533	0.2817
		Thursday, February 3, 2022	11	0.0179	0.2898	0.2672	0.2490	0.2777
		Thursday, February 10, 2022	18	0.0176	0.2888	0.2659	0.2474	0.2758
		Thursday, February 17, 2022	25	0.0176	0.2875	0.2644	0.2464	0.2751
		Thursday, March 3, 2022	39	0.0147	0.2848	0.2619	0.2436	0.2723
		Thursday, March 24, 2022	60	0.0153	0.2857	0.2629	0.2445	0.2731
		Thursday, April 14, 2022	81	0.0153	0.2856	0.2629	0.2446	0.2732
		Friday, May 13, 2022	110	0.0152	0.2853	0.2625	0.2444	0.2730

Table A- 69 ASTM C596 Drying Shrinkage --- 20% NP 4

NP 4	Thursday, January 20, 2022	Friday, January 21, 2022	1	Demold, label, and place in a 23 water container, then place in 60C oven for 24 hrs				
		Sunday, January 23, 2022	0	0.0181	0.3150	0.2308	0.2651	0.3096
		Thursday, January 27, 2022	4	0.0179	0.3109	0.2271	0.2615	0.3058
		Thursday, February 3, 2022	11	0.0179	0.3072	0.2231	0.2570	0.3021
		Thursday, February 10, 2022	18	0.0176	0.3052	0.2210	0.2552	0.3001
		Thursday, February 17, 2022	25	0.0174	0.3045	0.2206	0.2545	0.2993
		Thursday, March 3, 2022	39	0.0148	0.3017	0.2175	0.2515	0.2966
		Thursday, March 24, 2022	60	0.0152	0.3025	0.2181	0.2526	0.2975
		Thursday, April 14, 2022	81	0.0153	0.3024	0.2181	0.2524	0.2973
		Friday, May 13, 2022	110	0.0153	0.3021	0.2176	0.2521	0.2971

Table A- 70 ASTM C596 Drying Shrinkage --- 20% NP 5

NP 5	Thursday, January 20, 2022	Friday, January 21, 2022	1	Demold, label, and place in a 23 water container, then place in 60C oven for 24 hrs				
		Sunday, January 23, 2022	0	0.0182	0.3250	0.3280	0.3557	0.3363
		Thursday, January 27, 2022	4	0.0180	0.3234	0.3257	0.3523	0.3331
		Thursday, February 3, 2022	11	0.0179	0.3184	0.3212	0.3484	0.3378
		Thursday, February 10, 2022	18	0.0176	0.3163	0.3192	0.3464	0.3270
		Thursday, February 17, 2022	25	0.0174	0.3155	0.3181	0.3455	0.3264
		Thursday, March 3, 2022	39	0.0146	0.3127	0.3156	0.3433	0.3238
		Thursday, March 24, 2022	60	0.0153	0.3131	0.3163	0.3436	0.3245
		Thursday, April 14, 2022	81	0.0153	0.3131	0.3163	0.3434	0.3243
		Friday, May 13, 2022	110	0.0154	0.3127	0.3161	0.3434	0.3239

Table A- 71 ASTM C596 Drying Shrinkage --- 20% RFA 1

RFA 1	Thursday, January 20, 2022	Friday, January 21, 2022	1	Demold, label, and place in a 23 water container, then place in 60C oven for 24 hrs				
		Sunday, January 23, 2022	0	0.0183	0.2434	0.2839	0.2707	0.3307
		Thursday, January 27, 2022	4	0.0182	0.2407	0.2815	0.2682	0.3274
		Thursday, February 3, 2022	11	0.0178	0.2369	0.2771	0.2647	0.3239
		Thursday, February 10, 2022	18	0.0177	0.2354	0.2759	0.2627	0.3219
		Thursday, February 17, 2022	25	0.0176	0.2341	0.2742	0.2615	0.3210
		Thursday, March 3, 2022	39	0.0148	0.2309	0.2712	0.2585	0.3179
		Thursday, March 24, 2022	60	0.0153	0.2318	0.2720	0.2593	0.3188
		Thursday, April 14, 2022	81	0.0151	0.2316	0.2720	0.2592	0.3187
		Friday, May 13, 2022	110	0.0151	0.2316	0.2717	0.2590	0.3185

Table A- 72 ASTM C596 Drying Shrinkage --- 20% RFA 2

RFA 2	Thursday, January 20, 2022	Friday, January 21, 2022	1	Demold, label, and place in a 23 water container, then place in 60C oven for 24 hrs				
		Sunday, January 23, 2022	0	0.0182	0.2958	0.2785	0.2575	
		Thursday, January 27, 2022	4	0.0182	0.2925	0.2756	0.2539	
		Thursday, February 3, 2022	11	0.0178	0.2884	0.2720	0.2506	
		Thursday, February 10, 2022	18	0.0176	0.2870	0.2707	0.2493	
		Thursday, February 17, 2022	25	0.0176	0.2857	0.2687	0.2480	
		Thursday, March 3, 2022	39	0.0147	0.2828	0.2653	0.2450	
		Thursday, March 24, 2022	60	0.0153	0.2837	0.2660	0.2458	
		Thursday, April 14, 2022	81	0.0153	0.2835	0.2662	0.2458	
		Friday, May 13, 2022	110	0.0150	0.2833	0.2662	0.2456	

Table A- 73 ASTM C1012 Sulfate Resistance Control

Control	Thursday, April 21, 2022	Friday, April 22, 2022	1						
		Thursday, April 21, 2022	0	0.0167	0.2593	0.2743	0.2809	0.2862	0.2692	0.3167
		Thursday, April 28, 2022	1	0.0152	0.2593	0.2739	0.2809	0.2861	0.2692	0.3163
		Thursday, May 5, 2022	2	0.0150	0.2595	0.2740	0.2810	0.2864	0.2696	0.3162
		Thursday, May 12, 2022	3	0.0150	0.2596	0.2741	0.2812	0.2865	0.2699	0.3166
		Thursday, May 19, 2022	4	0.0145	0.2597	0.2739	0.2810	0.2864	0.2695	0.3166
		Thursday, June 23, 2022	9	0.0143	0.2596	0.2740	0.2811	0.2866	0.2698	0.3165
		Thursday, July 28, 2022	14	0.0138	0.2598	0.2743	0.2816	0.2864	0.2704	0.3169
		Thursday, August 11, 2022	16	0.0145	0.2608	0.2751	0.2824	0.2873	0.2712	0.3177
		Thursday, October 20, 2022	26	0.0155	0.2627	0.2771	0.2847	0.2896	0.2740	0.3200
		Thursday, December 22, 2022	35	0.0162	0.2649	0.2795	0.2874	0.2911	0.2768	0.3224
		Thursday, April 27, 2023	53	0.0119	0.2722	0.2870	0.3046	0.3031	0.2960	0.3324

Table A- 74 ASTM C1012 Sulfate Resistance --- 20% NP 2

NP 2	Thursday, January 20, 2022	Friday, January 21, 2022	1	Demold, label, and place in a 23 water container, then place in 60C oven for 24 hrs					
		Sunday, January 23, 2022	0	0.0158	0.2933	0.2472	0.2925	0.2213	0.2626	0.2473
		Monday, January 24, 2022	1	0.0152	0.2935	0.2478	0.2925	0.2215	0.2628	0.2474
		Tuesday, January 25, 2022	2	0.0150	0.2936	0.2475	0.2926	0.2215	0.2628	0.2475
		Wednesday, January 26, 2022	3	0.0151	0.2936	0.2476	0.2927	0.2216	0.2630	0.2478
		Thursday, January 27, 2022	4	0.0145	0.2935	0.2474	0.2925	0.2215	0.2628	0.2474
		Tuesday, February 1, 2022	9	0.0144	0.2937	0.2477	0.2925	0.2216	0.2629	0.2475
		Sunday, February 6, 2022	14	0.0138	0.2933	0.2473	0.2922	0.2213	0.2627	0.2474
		Tuesday, February 8, 2022	16	0.0145	0.2942	0.2481	0.2930	0.2221	0.2634	0.2481
		Friday, February 18, 2022	26	0.0153	0.2957	0.2497	0.2946	0.2236	0.2650	0.2496
		Sunday, February 27, 2022	35	0.0160	0.2963	0.2504	0.2953	0.2241	0.2657	0.2502
		Thursday, March 17, 2022	53	0.0118	0.2923	0.2464	0.2913	0.2203	0.2617	0.2464

Table A- 75 ASTM C1012 Sulfate Resistance --- 20% NP 4

NP 4	Thursday, January 20, 2022	Friday, January 21, 2022	1	Demold, label, and place in a 23 water container, then place in 60C oven for 24 hrs					
		Sunday, January 23, 2022	0	0.0152	0.2749	0.2686	0.2439	0.3089	0.2155	0.2230
		Wednesday, January 4, 1900	1	0.0152	0.2752	0.2691	0.2439	0.3094	0.2159	0.2234
		Thursday, January 5, 1900	2	0.0150	0.2752	0.2692	0.2439	0.3094	0.2159	0.2234
		Friday, January 6, 1900	3	0.0151	0.2753	0.2694	0.2442	0.3096	0.2161	0.2237
		Saturday, January 7, 1900	4	0.0145	0.2748	0.2689	0.2437	0.3092	0.2158	0.2233
		Thursday, January 12, 1900	9	0.0144	0.2748	0.2688	0.2438	0.3094	0.2158	0.2233
		Tuesday, January 17, 1900	14	0.0138	0.2745	0.2687	0.2434	0.3089	0.2154	0.2230
		Thursday, January 19, 1900	16	0.0145	0.2753	0.2696	0.2442	0.3097	0.2162	0.2238
		Sunday, January 29, 1900	26	0.0154	0.2768	0.2708	0.2455	0.3112	0.2177	0.2252
		Tuesday, February 7, 1900	35	0.0161	0.2774	0.2713	0.2466	0.3119	0.2183	0.2259
		Saturday, February 25, 1900	53	0.0118	0.2733	0.2672	0.2420	0.3076	0.2140	0.2216

Table A- 76 ASTM C1012 Sulfate Resistance --- 20% NP 5

NP 5	Thursday, January 20, 2022	Friday, January 21, 2022	1	Demold, label, and place in a 23 water container, then place in 60C oven for 24 hrs					
		Sunday, January 23, 2022	0	0.0152	0.2635	0.3368	0.2556	0.2663	0.2697	0.2753
		Monday, January 24, 2022	1	0.0152	0.2638	0.3373	0.2559	0.2666	0.2699	0.2757
		Tuesday, January 25, 2022	2	0.0150	0.2640	0.3372	0.2559	0.2666	0.2698	0.2758
		Wednesday, January 26, 2022	3	0.0151	0.2641	0.3375	0.2561	0.2669	0.2700	0.2760
		Thursday, January 27, 2022	4	0.0145	0.2639	0.3373	0.2565	0.2665	0.2697	0.2758
		Tuesday, February 1, 2022	9	0.0143	0.2636	0.3370	0.2557	0.2664	0.2696	0.2756
		Sunday, February 6, 2022	14	0.0138	0.2633	0.3369	0.2553	0.2661	0.2693	0.2753
		Tuesday, February 8, 2022	16	0.0145	0.2641	0.3376	0.2560	0.2668	0.2700	0.2761
		Friday, February 18, 2022	26	0.0154	0.2656	0.3390	0.2575	0.2682	0.2714	0.2775
		Sunday, February 27, 2022	35	0.0161	0.2661	0.3396	0.2580	0.2690	0.2721	0.2782
		Thursday, March 17, 2022	53	0.0119	0.2622	0.3354	0.2539	0.2648	0.2676	0.2740

Table A- 77 ASTM C1012 Sulfate Resistance --- 20% RFA 1

RFA 1	Thursday, April 21, 2022	Friday, April 22, 2022	1	Demold, label, and place in a 23 water container, then place in 60C oven for 24 hrs					
		Sunday, April 24, 2022	0	0.0166	0.3067	0.2998	0.3448	0.3203	0.2778	0.2643
		Monday, April 25, 2022	1	0.0152	0.3063	0.2998	0.3449	0.3201	0.2774	0.2640
		Tuesday, April 26, 2022	2	0.0151	0.3063	0.3001	0.3454	0.3203	0.2774	0.2641
		Wednesday, April 27, 2022	3	0.0151	0.3067	0.3002	0.3453	0.3205	0.2776	0.2642
		Thursday, April 28, 2022	4	0.0145	0.3064	0.3003	0.3450	0.3204	0.2777	0.2641
		Tuesday, May 3, 2022	9	0.0144	0.3068	0.3003	0.3452	0.3206	0.2776	0.2642
		Sunday, May 8, 2022	14	0.0138	0.3064	0.3002	0.3452	0.3207	0.2774	0.2640
		Tuesday, May 10, 2022	16	0.0145	0.3074	0.3012	0.3459	0.3216	0.2783	0.2650
		Friday, May 20, 2022	26	0.0153	0.3091	0.3031	0.3474	0.3236	0.2799	0.2667
		Sunday, May 29, 2022	35	0.0162	0.3101	0.3039	0.3484	0.3244	0.2808	0.2675
		Thursday, June 16, 2022	53	0.0118	0.3057	0.3009	0.3444	0.3206	0.2766	0.2640

Table A- 78 ASTM C1012 Sulfate Resistance --- 20% RFA 2

RFA 2	Thursday, January 20, 2022	Friday, January 21, 2022	1	Demold, label, and place in a 23 water container, then place in 60C oven for 24 hrs					
		Sunday, January 23, 2022	0	0.0152	0.3800	0.2715	0.2537	0.3020	0.2725	0.2540
		Monday, January 24, 2022	1	0.0152	0.3801	0.2719	0.2540	0.3024	0.2729	0.2543
		Tuesday, January 25, 2022	2	0.0150	0.3802	0.2720	0.2541	0.3024	0.2730	0.2544
		Wednesday, January 26, 2022	3	0.0151	0.3807	0.2721	0.2546	0.3026	0.2732	0.2545
		Thursday, January 27, 2022	4	0.0145	0.3803	0.2722	0.2542	0.3026	0.2729	0.2544
		Tuesday, February 1, 2022	9	0.0143	0.3802	0.2721	0.2542	0.3025	0.2730	0.2543
		Sunday, February 6, 2022	14	0.0138	0.3800	0.2719	0.2538	0.3024	0.2728	0.2541
		Tuesday, February 8, 2022	16	0.0145	0.3809	0.2728	0.2547	0.3032	0.2736	0.2549
		Friday, February 18, 2022	26	0.0155	0.3824	0.2742	0.2561	0.3048	0.2750	0.2563
		Sunday, February 27, 2022	35	0.0162	0.3830	0.2748	0.2568	0.3054	0.2757	0.2568
		Thursday, March 17, 2022	53	0.0119	0.3791	0.2705	0.2530	0.3013	0.2715	0.2531

Table A- 79 Isothermal Calorimetry Cumulative Heat Release (20% SCMs)

	Control	NP 1	NP 2	NP 3	NP 4	NP 5	NP 6	RFA 1	RFA 2
1-D	192.42	175.86	170.62	180.87	178.36	175.40	176.50	172.66	149.28
3-D	282.75	241.69	239.51	250.84	248.64	243.14	245.04	247.15	257.46
7-D	318.97	279.18	273.73	285.87	283.03	276.09	278.33	280.46	295.75

Table A- 80 ASTM C1897 Isothermal Calorimetry R^3 Cumulative Heat Release (20% SCMs)

	NP 1	NP 2	NP 3	NP 4	NP 5	NP 6	RFA 1	RFA 2
1-day	69.2	48.9	116.2	72.8	88.4	69.6	69.3	108.7
3-day	146.3	145.8	197.5	188.6	204.5	162.6	231.3	236.5
7-day	299.9	307.8	300.6	351.2	354.6	315	389.7	387.2

Table A- 81 UPV Results

Minute	Control	NP 1	NP 2	NP 3	NP 4	NP 5	NP 6	RFA 1	RFA 2
0.0									
1.0									
2.0									
3.0									
4.0									
5.0				1520.9					1518.0
6.0	1,523.8	1523.8	1520.9	1520.9	1520.9	1506.6	1,518.0	1,523.8	1518.0
7.0	1,526.7	1523.8	1520.9	1520.9	1520.9	1506.6	1,520.9	1,526.7	1518.0
8.0	1,526.7	1523.8	1520.9	1520.9	1520.9	1509.4	1,520.9	1,526.7	1515.2
9.0	1,526.7	1520.9	1520.9	1520.9	1520.9	1509.4	1,518.0	1,526.7	1518.0
10.0	1,529.6	1526.7	1518.0	1520.9	1520.9	1506.6	1,520.9	1,529.6	1515.2
11.0	1,529.6	1520.9	1520.9	1520.9	1520.9	1512.3	1,518.0	1,529.6	1515.2
12.0	1,529.6	1520.9	1518.0	1520.9	1520.9	1509.4	1,515.2	1,529.6	1518.0
13.0	1,532.6	1526.7	1520.9	1523.8	1520.9	1506.6	1,520.9	1,532.6	1518.0
14.0	1,529.6	1523.8	1520.9	1523.8	1520.9	1506.6	1,520.9	1,529.6	1518.0
15.0	1,529.6	1526.7	1520.9	1520.9	1520.9	1509.4	1,518.0	1,529.6	1515.2
16.0	1,532.6	1518.0	1520.9	1520.9	1523.8	1500.9	1,518.0	1,532.6	1518.0
17.0	1,529.6	1526.7	1520.9	1520.9	1520.9	1509.4	1,518.0	1,529.6	1518.0
1431.0	2623.0	2666.7	2749.1	2768.2	2484.5	2439.0	2768.2	2623.0	2191.8
1432.0	2623.0	2657.8	2758.6	2777.8	2492.2	2461.5	2758.6	2623.0	2191.8
1433.0	2623.0	2666.7	2758.6	2768.2	2484.5	2431.6	2768.2	2623.0	2191.8
1434.0	2623.0	2666.7	2758.6	2768.2	2484.5	2446.5	2777.8	2623.0	2191.8
1435.0	2623.0	2657.8	2749.1	2768.2	2492.2	2461.5	2768.2	2623.0	2197.8
1436.0	2623.0	2666.7	2749.1	2758.6	2492.2	2461.5	2768.2	2623.0	2191.8
1437.0	2614.4	2666.7	2749.1	2768.2	2492.2	2476.8	2768.2	2614.4	2191.8
1438.0	2623.0	2666.7	2758.6	2768.2	2492.2	2476.8	2768.2	2623.0	2191.8
1439.0	2623.0	2657.8	2758.6	2768.2	2500.0	2446.5	2768.2	2623.0	2197.8
1440.0	2623.0	2666.7	2758.6	2768.2	2500.0	2461.5	2768.2	2623.0	2197.8

Table A- 82 TGA Control

	Control					
	50 - 100	100 - 150	150 - 200	200 - 250	400 - 500	550 -800
12-Hour	4.600%	1.678%	0.652%	0.370%	1.200%	2.720%
1-Day	5.399%	2.662%	0.988%	0.577%	2.446%	2.576%
3-Day	6.936%	4.917%	1.674%	0.919%	3.620%	2.521%
7-Day	8.805%	5.561%	1.867%	1.002%	3.784%	2.004%
28-Day	6.102%	5.813%	2.433%	1.242%	4.088%	2.425%
56-Day	6.290%	5.444%	2.388%	1.278%	4.223%	2.067%

Table A- 83 TGA NP 2

	NP 2					
	50 - 100	100 - 150	150 - 200	200 - 250	400 - 500	550 -800
12-Hour	5.083%	1.660%	0.642%	0.421%	1.222%	2.256%
1-Day	6.514%	3.065%	0.957%	0.606%	2.409%	2.143%
3-Day	6.329%	4.301%	1.487%	0.860%	3.198%	2.071%
7-Day	6.988%	4.487%	1.678%	0.986%	3.299%	2.005%
28-Day	7.317%	4.982%	2.133%	1.149%	3.351%	1.927%
56-Day	6.071%	5.205%	2.379%	1.246%	3.428%	2.065%

Table A- 84 TGA NP 3

	NP 3					
	50 - 100	100 - 150	150 - 200	200 - 250	400 - 500	550 -800
12-Hour	4.612%	2.105%	0.921%	0.546%	1.264%	2.103%
1-Day	5.259%	3.431%	1.278%	0.758%	2.316%	2.301%
3-Day	6.950%	4.699%	1.817%	1.107%	3.018%	2.052%
7-Day	7.824%	4.909%	2.054%	1.127%	3.077%	1.848%
28-Day	7.909%	6.621%	2.833%	1.359%	3.087%	1.802%
56-Day	7.305%	6.175%	2.755%	1.378%	3.038%	1.864%

Table A- 85 TGA NP 4

`	NP 4					
	50 - 100	100 - 150	150 - 200	200 - 250	400 - 500	550 -800
12-Hour	3.384%	1.321%	0.594%	0.391%	1.175%	2.162%
1-Day	6.302%	3.238%	1.024%	0.650%	2.390%	2.409%
3-Day	6.139%	3.933%	1.501%	0.882%	3.159%	2.231%
7-Day	5.550%	4.502%	1.846%	1.028%	3.242%	2.206%
28-Day	7.487%	5.578%	2.410%	1.211%	3.171%	2.035%
56-Day	6.045%	5.307%	2.473%	1.281%	3.082%	2.190%

Table A- 86 TGA NP 5

	NP 5					
	50 - 100	100 - 150	150 - 200	200 - 250	400 - 500	550 -800
12-Hour	3.487%	1.246%	0.622%	0.440%	1.149%	2.306%
1-Day	7.388%	2.893%	1.024%	0.679%	2.440%	2.182%
3-Day	6.160%	3.934%	1.513%	0.929%	3.115%	2.352%
7-Day	5.225%	4.728%	2.026%	1.117%	3.362%	2.065%
28-Day	7.826%	5.719%	2.394%	1.234%	3.231%	1.918%
56-Day	6.689%	5.369%	2.451%	1.279%	3.217%	2.277%

Table A- 87 TGA NP 6

	NP 6					
	50 - 100	100 - 150	150 - 200	200 - 250	400 - 500	550 -800
12-Hour	4.827%	1.381%	0.636%	0.418%	1.137%	2.269%
1-Day	4.534%	2.802%	1.025%	0.643%	2.458%	2.308%
3-Day	6.358%	3.625%	1.430%	0.889%	3.166%	2.203%
7-Day	7.114%	4.947%	1.916%	0.993%	3.062%	2.574%
28-Day	8.331%	5.251%	2.212%	1.173%	3.228%	1.966%
56-Day	7.039%	5.576%	2.436%	1.254%	3.021%	2.057%

Table A- 88 TGA RFA 1

	RFA 1					
	50 - 100	100 - 150	150 - 200	200 - 250	400 - 500	550 -800
12-Hour	2.803%	1.228%	0.484%	0.275%	0.737%	2.404%
1-Day	4.782%	2.296%	0.820%	0.471%	2.025%	1.954%
3-Day	6.584%	4.396%	1.449%	0.799%	3.015%	2.147%
7-Day	6.663%	4.752%	1.749%	0.937%	3.172%	1.849%
28-Day	6.214%	5.172%	2.221%	1.124%	3.258%	1.869%
56-Day	5.686%	5.377%	2.501%	1.239%	3.358%	1.774%

Table A- 89 TGA RFA 2

	RFA 2					
	50 - 100	100 - 150	150 - 200	200 - 250	400 - 500	550 -800
12-Hour	2.626%	1.353%	0.525%	0.342%	0.403%	2.704%
1-Day	4.963%	2.386%	0.868%	0.529%	1.677%	2.218%
3-Day	6.641%	5.328%	1.814%	0.967%	3.033%	2.039%
7-Day	6.966%	5.732%	2.205%	1.137%	3.158%	1.991%
28-Day	6.895%	5.679%	2.463%	1.286%	3.142%	1.875%
56-Day	5.972%	5.984%	2.743%	1.382%	3.207%	2.285%

Table A- 90 ASTM C1202 Rapid Chloride Penetration Results

The Amount of Charge Passed (Couloumbs)							
Measuring Time	Time Period	Control	NP 2	NP 4	NP 5	RFA 1	RFA 2
11:30	0	0	0	0	0	0	0
12:00	0.5	258	80	47	45	80.5	52.5
12:30	1	540	162	94	90	175.5	104.5
1:00	1.5	838	244	141	135	268	157.5
1:30	2	1143	327	189	181	371	206.5
2:00	2.5	1463	410	238	227	472.5	267.5
2:30	3	1802	493.5	288	272	575.5	322
3:00	3.5	2146	568.5	339	317	681	378.5
3:30	4	2494	640.5	390	363	788	436
4:00	4.5	2846	714	443	409	896	497
4:30	5	3141	787	496	453	1004	559
5:00	5.5	3357	862.5	550	494	1113	621.5
5:30	6	3621	938.5	604	535	1222	683.5

Table A- 91 Pore Solution --- 20% SCMs Replacement

	K mmol/L				Na mmol/L			
	7-d	28-d	56-d	84-d	7-d	28-d	56-d	84-d
Control	0.459	0.449	0.445	0.443	0.186	0.180	0.189	0.182
NP 1	0.225	0.250	0.272	0.241	0.126	0.140	0.146	0.127
NP 2	0.307	0.310	0.311	0.273	0.130	0.149	0.159	0.140
NP 3	0.088	0.127	0.190	0.172	0.311	0.242	0.284	0.235
NP 4	0.346	0.266	0.258	0.250	0.164	0.149	0.168	0.169
NP 5	0.310	0.273	0.279	0.248	0.161	0.157	0.187	0.169
NP 6	0.300	0.275	0.269	0.248	0.147	0.160	0.193	0.187
RFA 1	0.345	0.314	0.334	0.311	0.163	0.188	0.243	0.231
RFA 2	0.283	0.289	0.284	0.264	0.141	0.164	0.186	0.177

Table A- 92 Pore Solution --- 20% SCMs Replacement

	K mmol/L				Na mmol/L			
	7-d	28-d	56-d	84-d	7-d	28-d	56-d	84-d
Control	0.459	0.443	0.439	0.443	0.186	0.182	0.185	0.182
NP 1	0.161	0.186	0.271	0.243	0.122	0.117	0.114	0.114
NP 2	0.286	0.266	0.269	0.261	0.132	0.131	0.136	0.144
NP 3	0.192	0.081	0.104	0.116	0.063	0.264	0.251	0.240
NP 4	0.276	0.231	0.110	0.121	0.147	0.147	0.176	0.176
NP 5	0.277	0.227	0.230	0.216	0.164	0.152	0.179	0.178
NP 6	0.290	0.222	0.214	0.214	0.153	0.153	0.183	0.191
RFA 1	0.309	0.313	0.184	0.187	0.167	0.217	0.237	0.259
RFA 2	0.314	0.249	0.231	0.204	0.175	0.165	0.188	0.188

Table A- 93 Bulk Resistivity Control

Control	Monday, May 15, 2023	Monday, May 15, 2023	0	0.0	0.0	0.0	0.0
		Thursday, May 18, 2023	3	5.4	5.9	5.4	5.6
		Monday, May 22, 2023	7	5.5	6.1	6.2	5.9
		Monday, May 29, 2023	14	6.1	7.0	7.1	6.7
		Monday, June 5, 2023	21	6.3	7.1	7.3	6.9
		Monday, June 12, 2023	28	6.4	7.3	7.4	7.0
		Monday, June 19, 2023	35	7.9	8.0	7.8	7.9
		Monday, June 26, 2023	42	8.1	8.8	8.4	8.4
		Monday, July 3, 2023	49	9.1	9.1	9.0	9.1
		Monday, July 10, 2023	56	8.3	9.2	9.4	9.0
		Monday, July 17, 2023	63	8.1	9.1	10.6	9.3
		Monday, July 24, 2023	70	8.9	9.2	9.3	9.1
		Monday, July 31, 2023	77	9.1	9.5	9.5	9.4
		Monday, August 7, 2023	84	9.3	9.9	9.7	9.6
		Thursday, August 24, 2023	101	9.5	10.4	10.6	10.2
		Friday, September 15, 2023	123	12.0	12.7	12.3	12.3

Table A- 94 Bulk Resistivity --- 20% NP 1

NP 1	Monday, May 15, 2023	Monday, May 15, 2023	0	0.0	0.0	0.0
		Thursday, May 18, 2023	3	4.7	4.0	4.5
		Monday, May 22, 2023	7	5.3	4.5	5.2
		Monday, May 29, 2023	14	5.6	5.4	6.1
		Monday, June 5, 2023	21	6.7	6.1	7.1
		Monday, June 12, 2023	28	6.9	6.9	7.8
		Monday, June 19, 2023	35	8.3	7.6	9.2
		Monday, June 26, 2023	42	11.7	10.1	11.1
		Monday, July 3, 2023	49	11.1	10.4	12.3
		Monday, July 10, 2023	56	12.4	13.2	13.8
		Monday, July 17, 2023	63	14.0	15.1	15.2
		Monday, July 24, 2023	70	14.2	14.0	15.0
		Monday, July 31, 2023	77	15.7	15.4	16.3
		Monday, August 7, 2023	84	17.8	16.5	17.4
		Thursday, August 24, 2023	101	19.8	18.2	19.4
		Friday, September 15, 2023	123	23.2	21.5	24.2

Table A- 95 Bulk Resistivity --- 20% NP 2

NP 2	Monday, May 15, 2023	Monday, May 15, 2023	0	0.0	0.0	0.0
		Thursday, May 18, 2023	3	3.8	4.1	4.4
		Monday, May 22, 2023	7	4.6	4.7	5.3
		Monday, May 29, 2023	14	5.7	5.2	5.7
		Monday, June 5, 2023	21	6.6	6.1	7.4
		Monday, June 12, 2023	28	7.4	8.1	8.3
		Monday, June 19, 2023	35	9.5	9.6	10.9
		Monday, June 26, 2023	42	13.0	12.5	12.0
		Monday, July 3, 2023	49	13.3	12.9	13.0
		Monday, July 10, 2023	56	16.0	14.8	16.1
		Monday, July 17, 2023	63	18.0	16.6	17.6
		Monday, July 24, 2023	70	20.0	17.8	19.8
		Monday, July 31, 2023	77	21.5	19.0	20.0
		Monday, August 7, 2023	84	22.8	20.7	19.4
		Thursday, August 24, 2023	101	28.1	25.2	25.3
		Friday, September 15, 2023	123	33.6	29.5	28.9

Table A- 96 Bulk Resistivity --- 20% NP 3

NP 3	Monday, May 15, 2023	Monday, May 15, 2023	0	0.0	0.0	0.0
		Thursday, May 18, 2023	3	4.2	4.8	5.1
		Monday, May 22, 2023	7	6.2	7.3	7.9
		Monday, May 29, 2023	14	12.6	14.7	14.8
		Monday, June 5, 2023	21	16.7	19.0	18.8
		Monday, June 12, 2023	28	19.9	21.4	21.7
		Monday, June 19, 2023	35	23.0	25.0	24.0
		Monday, June 26, 2023	42	23.8	24.8	24.5
		Monday, July 3, 2023	49	24.2	25.0	25.4
		Monday, July 10, 2023	56	25.6	26.7	26.6
		Monday, July 17, 2023	63	27.4	26.8	27.2
		Monday, July 24, 2023	70	29.8	28.4	29.1
		Monday, July 31, 2023	77	30.6	29.6	29.8
		Monday, August 7, 2023	84	31.9	30.3	30.1
		Thursday, August 24, 2023	101	35.6	34.7	33.4
		Friday, September 15, 2023	123	38.6	36.5	34.5

Table A- 97 Bulk Resistivity --- 20% NP 4

NP 4	Monday, May 15, 2023	Monday, May 15, 2023	0	0.0	0.0	0.0
		Thursday, May 18, 2023	3	3.7	3.8	4.2
		Monday, May 22, 2023	7	4.5	4.9	5.1
		Monday, May 29, 2023	14	6.7	7.1	7.3
		Monday, June 5, 2023	21	9.3	9.8	9.6
		Monday, June 12, 2023	28	12.5	12.6	12.4
		Monday, June 19, 2023	35	15.3	15.4	16.7
		Monday, June 26, 2023	42	20.0	19.2	19.7
		Monday, July 3, 2023	49	21.0	20.3	21.1
		Monday, July 10, 2023	56	23.0	22.4	23.6
		Monday, July 17, 2023	63	24.4	23.0	25.1
		Monday, July 24, 2023	70	26.1	25.3	27.7
		Monday, July 31, 2023	77	27.5	25.9	28.5
		Monday, August 7, 2023	84	29.5	26.2	28.7
		Thursday, August 24, 2023	101	33.2	32.2	35.3
		Friday, September 15, 2023	123	43.9	43.7	35.0

Table A- 98 Bulk Resistivity --- 20% NP 5

NP 5	Monday, May 15, 2023	Monday, May 15, 2023	0	0.0	0.0	0.0
		Thursday, May 18, 2023	3	4.3	4.3	4.3
		Monday, May 22, 2023	7	5.1	5.7	5.5
		Monday, May 29, 2023	14	8.4	8.9	8.8
		Monday, June 5, 2023	21	11.2	12.0	11.9
		Monday, June 12, 2023	28	15.2	15.2	15.7
		Monday, June 19, 2023	35	17.3	19.2	18.4
		Monday, June 26, 2023	42	22.1	22.1	23.1
		Monday, July 3, 2023	49	22.8	22.8	23.2
		Monday, July 10, 2023	56	24.8	23.8	24.5
		Monday, July 17, 2023	63	27.0	24.8	26.1
		Monday, July 24, 2023	70	27.7	24.6	27.3
		Monday, July 31, 2023	77	28.4	25.0	27.3
		Monday, August 7, 2023	84	28.8	25.6	26.1
		Thursday, August 24, 2023	101	34.9	29.9	29.3
		Friday, September 15, 2023	123	39.9	31.0	31.2

Table A- 99 Bulk Resistivity --- 20% NP 6

NP 6	Monday, May 15, 2023	Monday, May 15, 2023	0	0.0	0.0	0.0
		Thursday, May 18, 2023	3	4.0	4.4	4.6
		Monday, May 22, 2023	7	5.1	5.7	5.7
		Monday, May 29, 2023	14	8.3	9.2	9.1
		Monday, June 5, 2023	21	12.9	12.8	13.3
		Monday, June 12, 2023	28	16.1	16.5	16.7
		Monday, June 19, 2023	35	19.2	21.5	20.3
		Monday, June 26, 2023	42	24.5	25.6	26.7
		Monday, July 3, 2023	49	24.7	26.4	26.8
		Monday, July 10, 2023	56	26.8	27.3	27.5
		Monday, July 17, 2023	63	28.5	27.9	28.1
		Monday, July 24, 2023	70	29.4	28.7	27.4
		Monday, July 31, 2023	77	29.3	28.3	27.6
		Monday, August 7, 2023	84	27.5	28.4	26.8
		Thursday, August 24, 2023	101	28.4	31.1	25.3
		Friday, September 15, 2023	123	29.1	31.5	30.5

Table A- 100 Bulk Resistivity --- 20% RFA 1

RFA 1	Monday, May 15, 2023	Monday, May 15, 2023	0	0.0	0.0	0.0
		Thursday, May 18, 2023	3	4.2	4.4	4.2
		Monday, May 22, 2023	7	5.2	4.6	5.0
		Monday, May 29, 2023	14	5.9	5.5	5.4
		Monday, June 5, 2023	21	6.9	6.3	6.3
		Monday, June 12, 2023	28	8.6	7.5	7.9
		Monday, June 19, 2023	35	10.0	8.8	9.3
		Monday, June 26, 2023	42	13.1	13.6	12.5
		Monday, July 3, 2023	49	12.9	12.8	13.0
		Monday, July 10, 2023	56	14.5	14.9	15.0
		Monday, July 17, 2023	63	16.5	16.7	16.1
		Monday, July 24, 2023	70	17.6	16.5	18.0
		Monday, July 31, 2023	77	17.5	18.5	19.6
		Monday, August 7, 2023	84	18.0	19.6	21.2
		Thursday, August 24, 2023	101	21.2	23.1	23.1
		Friday, September 15, 2023	123	22.3	27.3	27.2

Table A- 101 Bulk Resistivity --- 20% RFA 2

RFA 2	Monday, May 15, 2023	Monday, May 15, 2023	0	0.0	0.0	0.0
		Thursday, May 18, 2023	3	3.2	3.7	3.8
		Monday, May 22, 2023	7	4.2	4.5	4.2
		Monday, May 29, 2023	14	6.2	5.9	6.2
		Monday, June 5, 2023	21	8.4	8.1	8.4
		Monday, June 12, 2023	28	11.0	11.1	11.5
		Monday, June 19, 2023	35	13.1	13.7	13.9
		Monday, June 26, 2023	42	17.2	18.0	17.4
		Monday, July 3, 2023	49	17.9	18.0	17.8
		Monday, July 10, 2023	56	20.5	20.2	20.5
		Monday, July 17, 2023	63	21.7	21.6	21.3
		Monday, July 24, 2023	70	24.3	23.3	22.0
		Monday, July 31, 2023	77	24.8	25.3	23.0
		Monday, August 7, 2023	84	25.5	26.5	24.5
		Thursday, August 24, 2023	101	31.8	32.2	28.8
		Friday, September 15, 2023	123	34.3	33.5	29.8